Dissertation

submitted to the

Combined Faculties for the Natural Sciences and for Mathematics

of the Ruperto-Carola University of Heidelberg, Germany

for the degree of

Doctor of Natural Sciences

Presented by

M.Sc. Ina Krasimirova Simeonova

Born in Sofia, Bulgaria

Oral-examination: 21.12.2016

Generation of Defined Astrocytic Phenotypes from Human Pluripotent Stem Cells for Transplantation after Spinal Cord Injury

Referees: Prof. Dr. Hilmar Bading

Prof. Dr. Armin Blesch

Dedication

I would like to dedicate my dissertation to Prof. Dr. Armin Blesch and Dr. Francesca Ciccolini. Through their trust and support they turned the shy, scared and clueless young student that I was into the scientist and the person that I have become.

In addition, I would like to dedicate my dissertation to the Gertrud Reemtsma Stiftung, which believes in young neuroscientists and supports their first steps towards a scientific career.

Acknowledgements

Hereby I would like to acknowledge all the people that supported my through my scientific and personal development.

First of all, I would like to thank my parents Radoslava Simeonova and Krasimir Simeonov, my brother Martin Simeonov and my grandparents Efrosina Chobanova, Sasho Chobanov, Toni Simeonova and Alexi Simeonov, for their immense love and support even if they did not agree with my life decisions. Particularly, I would like to thank my mother for convincing me to learn German instead of Spanish in high-school: if it weren't so I would not be here.

I would like to thank my boyfriend Raphael Steinfeld for 8 years of trust and love, although I have been emotional, moody, aggressive, screaming, hurtful, difficult and stubborn. During good times and bad times he always knew the perfect words to wake me up, cheer me up or let me come back to reality.

I would like to thank my best friend Nenja Krüger for 7 years of trust and love, for the good and the bad times, for making me feel part of her family, for the almost sleepless nights shared in a 12 m^2 room and for the perfect girl's weekends.

I would like to thank my best friend Nina Tonn for 5 years of trust and love, for being a patient listener, for being a wise life-advisor, for her beautiful smile which always cheered me up and for the wonderful time together in Ziegelhausen.

I would like to thank my friend and colleague LaShae Nicholson for her immense support and for sharing extremely intense experiences.

I would like to thank my friend and neighbor Lara Jung for giving me positive energy during this last phase of my Ph.D.

I would like to thank Dr. Francesca Ciccolini for the trust she had in me when I was nothing but a scared student. She not only supervised me, but guided me through my development, believed in me, allowed me to be independent, taught me scientific thinking talking presenting and writing, gave me the opportunity to turn ideas into experiments, involved me in brain-storming and experimental planning and much more. She helped me to turn into the scientist that I am today. I would also like to thank my former colleagues Claudia Mandl and Gaby Hölzl-Wenig for the great time spent together and for the long and interesting conversations.

I would like to thank the supervisor of my Ph.D. thesis, Prof. Armin Blesch, who not only had trust in me, but gave me full freedom to express myself scientifically and personally. Out of a simple idea that I got during his 2-hour lecture, we developed together a huge and extremely exciting project. Although we had no protocols, no materials and no clue, it is through his trust and support that we were able to turn ideas into reality. He taught me that the meaning of science as well as of life is to believe in your own ideas, find ways and solutions and have the courage to turn them into reality even if you have to risk something. Only through courage there is innovation, only through innovation there is progress. I have to say, however, that I'm still mad at him for moving back to the USA.

I would like to thank the Gertrud Reemtsma Stiftung for putting trust into my ideas and initiative and providing the financial basis for my Ph.D. thesis. In addition, I would like to thank the advisory board for the productive discussions and the supporting feedback during my progress reports.

I would like to thank Prof. Dr. Beate Winner, Dr. Steven Havlicek and Holger Wend for providing the pluripotent stem cell lines and teaching me neural induction, as well as Prof. Dr. Hilmar Bading, Dr. Anna Hagenston-Hertle and Dr. Peter Bengtson for providing the calcium imaging material and for teaching me the technique.

I would like to thank Prof. Dr. Norbert Weidner, who as director of the Spinal Cord Injury Center supported my work from the beginning to the end. I would like to thank him for the productive and challenging discussions, as well as for the fun and sporty moments.

I would like to thank Dr. Radhika Puttagunta for her precious support during a very difficult phase of my Ph.D. Sometimes just a bright smile can make a day much better.

I would like to thank the graduate school HBIGS and the graduate school of the IZN for offering an extremely interesting and diverse program, which gives students the possibility to gain further qualifications and skills.

Last but not least I would like to thank all my colleagues, who shared this intense experience with me: LaShae Nicholson for teaching me molecular biology techniques; Beatrice Sandner and Melanie Motsch for supporting my animal experiments; Ioana Goganau for teaching me DRG isolation and culturing as well as for 4 years of love-and-fight-and-love-and-fight; Shengwen Liu for performing the ELISA experiments; Christopher Sliwinski and Thomas Schackel for being my wonderful students at the beginning and my nightmare at the end, for pulling my hair, for hiding my stuff, for locking me in or out of rooms, for constantly making fun of me, for spraying me with ddH_2O, for trying to trap me in the autoclave trash bin, for scaring me while I'm concentrating and for making me feel like a desperate older sister.

Abbreviations

3D	Three dimensional
A	Anterior
AAV	Adeno-associated virus
AD	Alzheimer's disease
AIS	American Spinal Injury Association Impairment Scale
ALDH1L1	Aldehyde dehydrogenase 1 family member L1
AldoC	Aldolase C
ALS	Amyotrophic lateral sclerosis
AMD	Age-related macular degeneration
ANOVA	Analysis of variance
AQP	Aquaporin
ATP	Adenosine triphosphate
BBB	Blood brain barrier
BDNF	Brain-derived neurotrophic factor
B/W	Black and white
bHLH	Basic helix-loop-helix
BMP	Bone morphogenetic protein
bNM	Basic neural medium
BSA	Bovine serum albumin
C4	Cervical segment 4 of the spinal cord
cAMP	Cyclic adenosine monophosphate
ChABC	Chondroitinase ABC
Chl1	Close homolog of adhesion molecule L1
CNS	Central nervous system
CNTF	Ciliary neurotrophic factor
CRE	Causes Recombination
CREB	cAMP response element binding protein
CSPG	Chondroitin sulphate proteoglycan
CST	Corticospinal tract
CX43	Connexin 43
D	Dorsal
DAPI	4',6-Diamidine-2'-phenylindole dihydrochloride
DC	Dorsal column
DCX	Doublecortin
DEPC	Diethylpyrocarbonat
DIV	Day *in vitro*
dk	Donkey
DMSO	Dimethyl sulfoxide
DNA	Deoxyribonucleic acid
dNTP	Deoxynucleoside triphosphate
DREZ	Dorsal root entry zone
DRG	Dorsal root ganglion
DT	Diphtheria-toxin
DTT	1,4-Dithiothreitol
EAAT	Excitatory amino acid transporter
EB	Embryoid body
ECM	Extracellular matrix
EDTA	Ethylenediaminetetraacetic acid
EGF	Epidermal growth factor
ELISA	Enzyme-linked immunosorbent assay
EMSCI	European multicenter study about spinal cord injury
ESC	Embryonic stem cells
FACS	Fluorescence-activated cell sorting
FBS	Fetal bovine serum
FGF	Fibroblast growth factor
GABA	Gamma-Aminobutyric acid
GAG	Glycosaminoglycan

GAT	GABA transporter
GDNF	Glial cell line-derived neurotrophic factor
GDP	Good documentation practice
GF	Growth factor
GFAP	Glial fibrillary acidic protein
GlyT	Glycine transporter
GMP	Good manufacturing practice
GRP	Glial restricted precursor
gt	Goat
HDAC	Histone deacetylase
HEPES	4-(2-hydroxyethyl)-1-piperazine-ethanesulfonic acid
HGF	Hepatocyte growth factor
HIV	Human immunodeficiency virus
HLA	Human leukocyte antigen
hNUC	Human NUC
HSPG	Heparin sulphate proteoglycan
HUES	Harvard university embryonic stem cell
ICC	Immunocytochemistry
ICM	Inner cell mass
ID	Integrated density
Ig	Immunoglobulin
IGF	Insulin-like growth factor
IHC	Immunohistochemistry
IL	Interleukin
iN	Induced neurons
INF	Interferon
iPSC	Induced pluripotent stem cell
L	Lateral or left
LIF	Leukemia inhibitory factor
M	Medial
MAG	Myelin-associated glycoprotein
MAP	Microtubule-associated protein
MBP	Myelin-binding protein
mGluR	Metabotropic glutamate receptor
MMLV	Moloney murine leukemia virus
MPZ	Myelin protein zero
ms	Mouse
MS	Multiple sclerosis
MSC	Mesenchymal stem cell
mTOR	Mechanistic target of rapamycin
N or N	Number
NEAA	Non-essential amino acids
NFIA	Nuclear factor I-A
NFIX	Nuclear factor I-X
NFH	Neurofilament-H
NG2	Neuron-glial antigen 2
NGF	Nerve growth factor
NgR	Nogo receptor
NMDAR	N-methyl-D-aspartate receptor
NOD/ SCID	Non-obese diabetic Severe combined immunodeficiency
NR	Neural rosette
NSC	Neural stem cell
NT	Neurotrophin
OD	Optic density
OEC	Olfactory ensheathing cells
OMgp	Oligodendrocyte-myelin glycoprotein
OPC	Oligodendrocyte precursor cell
OPDA	O-phenylenediamine
p	P-value or calculated probability
P	Posterior
PBS	Phosphate-buffered saline
PCR	Polymerase chain reaction
PD	Parkinson’s disease
PDGF	Platelet-derived growth factor
PDGFR	Platelet-derived growth factor receptor
PDE	Phosphodiesterase
PET	Positron emission tomography
PFA	Paraformaldehyde
PLO	Poly-L-ornithine

PLP	Proteolipid protein
PNN	Perineuronal net
PNS	Peripheral nervous system
PMP	Peripheral myelin protein
PMSF	Phenylmethylsulfonylfluorid
PTEN	Phosphatase and tensin homolog
PSA-NCAM	Polysialylated-neural cell adhesion molecule
PSC	Pluripotent stem cell
R	Right
RA	Retinoic acid
RAG	Regeneration associated genes
rb	Rabbit
RNA	Ribonucleic acid
ROCK	Rho associated protein kinase
ROS	Reactive oxygen species
rpm	Rounds per minute
rt	Rat
RT	Room temperature
RT-PCR	Reverse transcription polymerase chain reaction
S100ß	S100 calcium-binding protein ß
SC	Spinal cord
SCI	Spinal cord injury
SHH	Sonic hedgehog
STEMCCA	Stem cell cassette
TAE	TRIS-acetate-EDTA
TBI	Traumatic brain injury
TBS	TRIS-buffered saline
TCS	Tissue collecting solution
TM	Trademark
TNF	Tumor necrosis factor
TRIS	Tris(hydroxymethyl)-amino-methan
UV	Ultra violet
VEGF	Vascular Endothelial Growth Factor
V	Ventral
VPA	Valproic acid
WGA	Wheat germ agglutinin
WHO	World health organization

Table of contents

1. Abstract of the dissertation

Spinal cord injury (SCI) is characterized by axonal damage, neural degeneration, formation of cystic cavities, and upregulation of a plethora of inhibitory as well as inflammatory molecules. To protect the surrounding tissue from further damage, fibroblasts and reactive astrocytes form an impenetrable barrier lining the lesion site. This environment impedes endogenous regeneration of axotomized neurons and glial cells. In addition to being exposed to extrinsic inhibitors of axonal regeneration after SCI, neurons in the mammalian central nervous system (CNS) intrinsically lack the capacity for spontaneous axonal regeneration. To restore neural tissue integrity and provide a favorable environment for injured axons to regenerate, an appropriate substrate is needed. An optimal substrate for neuroregeneration should have a neural identity and fulfill several functions including physical support and guidance, trophic and metabolic support, maintenance of tissue homeostasis, and modulation of neuronal outgrowth and network activity. Astrocytes represent the most suitable cell population to fulfill this task. Induced pluripotent stem cells (iPSCs), which show many homologies to embryonic stem cells (ESCs), represent an ethically acceptable means to obtain large amounts of astrocytes *in vitro* for autologous transplantation.

In the present study, populations of immature astrocytes with caudal identity were generated from three human pluripotent stem cell (PSC) lines, whereby terminal *in vitro* differentiation was performed according to previously published studies using the inductors of astrocytic maturation CNTF, BMP2/4 and FGF1 to allow for comparative analysis of specific astrocytic subtypes and for selection of a pro-regenerative cell population.

In accordance with previously published findings, morphological and functional differences among astrocytic populations were observed in the present study. Compared to astrocytes differentiated with FBS only, astrocytes differentiated with BMP2/4 exhibited a significantly increased cell size and a complex cytoarchitecture, decreased expression of the NSC marker Sox2, increased production of potentially growth-inhibitory extracellular matrix (ECM) components and of the growth-promoting neurotrophic factor BDNF, and limited ability to induce neurite outgrowth in co-cultures with primary dorsal root ganglion (DRG) neurons. Astrocytes differentiated with FGF1 were, in contrast, significantly smaller, mainly had a bipolar morphology and retained expression of the NSC marker Sox2, indicative of a rather immature phenotype. On the other side, differentiation with FBS alone or in combination with CNTF led to astrocytes that produced the pro-regenerative ECM component laminin, which was reflected in a strong growth-promoting effect on primary DRG neurons. Importantly, clear differences across the three used pluripotent stem cell (PSC) lines were observed; in particular, differences in the electrophysiological response pattern elicited by stimulation with adenosine triphosphate (ATP) indicated that astrocytic lines with a similar phenotypic profile have distinct characteristics. After transplantation into the intact and injured spinal cord of Fischer 344 rats,

some of these phenotypical characteristics observed *in vitro* were maintained *in vivo*. This is indicative of a stable phenotype of pre-differentiated astrocytes, which allows the selection of an astrocytic subtype *in vitro* to maximize the pro-regenerative effect of cell transplantation after SCI. However, the present study also sheds light on the risks associated with the use of human iPSCs as appreciable cell survival in the injured spinal cord was associated with a predisposition of grafted cells to form tumors. This was particularly evident in the intact spinal cord.

In summary, the present study provides a comparative overview over astrocytic features and pinpoints inclusion or exclusion criteria for transplantation after SCI. These criteria can be used to estimate the pro-regenerative ability of astrocytic populations and to predict the potential of PSC-derived progeny to form tumors.

1. Zusammenfassung der Dissertation

Traumatische Verletzungen des Rückenmarks führen zu axonalem Schäden, Verlust von neuralem Gewebe, zur Entstehung von Zysten und zur Hochregulierung von zahlreichen inhibitorischen und inflammatorischen Molekülen. Um das umliegende Gewebe vor zusätzlichen bzw. sekundären Schäden zu schützen bilden Fibroblasten und reaktive Astrozyten eine undurchdringliche Barriere um die Läsionsstelle herum. Dieses Milieu erschwert die endogene Regeneration beschädigter Neurone und glialen Zellen. In der Folge der Verletzung sind beschädigte Neurone des zentralen Nervensystems (ZNS) von Säugetieren extrinsischen Inhibitoren axonaler Regeneration ausgesetzt. Darüber hinaus fehlt den Neuronen die intrinsische Fähigkeit spontan zu regenerieren. Um die Integrität des neuralen Gewebes wiederherzustellen und um die Regeneration von beschädigten Neuronen durch ein Wachstumsförderndes Milieus zu begünstigen ist die Unterstützung durch ein entsprechendes Substrat notwendig. Ein optimales Substrat für die Neuroregeneration sollte einen neuralen Phänotyp aufweisen und verschiedene Funktionen, wie die physische, trophische und metabolische Unterstützung, die Regulierung axonaler Wegfindung, die Aufrechterhaltung der Gewebe-Homöostase sowie die Modulierung von neuronalem Wachstum und Netzwerk-Aktivität, erfüllen. Aufgrund dieser Anforderungen stellen Astrozyten eine optimale Zellpopulation dar, um diese Aufgaben zu erfüllen. Induzierte pluripotente Stammzellen (iPSZ), die zahlreiche Gemeinsamkeiten mit embryonalen Stammzellen (ESZ) aufweisen, stellen eine ethisch vertretbare Möglichkeit dar, Astrozyten für autologe Transplantation in ausreichender Zahl *in vitro* zu generieren.

Basierend auf bereits veröffentlichten Studien wurden hier Populationen von Astrozyten mit kaudalem Phänotyp aus drei humanen pluripotenten Stammzell- (PSZ)-Linien generiert. Ihre *in vitro* End-Differenzierung wurde dabei mit den Induktoren der astrozytären Reifung CNTF, BMP2/4 und FGF1 durchgeführt. Dadurch ergibt sich die Möglichkeit eines komparativen Vergleiches der daraus entstandenen astrozytären Subtypen und der Selektion einer pro-regenerativen Zellpopulation.

In Einklang mit der vorhandenen Fachliteratur wurden morphologische und funktionelle Unterschiede beobachtet. Astrozyten die mit BMP2/4 differenziert wurden zeigten signifikant erhöhte Zellgröße und komplexere Zytoarchitektur, niedrigere Expression des neuralen Stammzell (NSZ) Markers Sox2, erhöhte Produktion von potentiell wachstumshemmenden Komponenten der extrazellulären Matrix (EZM) und des wachstumsfördernden neurotrophen Faktors BDNF, so wie eine beschränkte Fähigkeit, Neuritenwachstum in co-Kulturen mit primären Spinalganglion Neuronen zu fördern. Mit FGF1 differenzierte Astrozyten waren demgegenüber signifikant kleiner, bipolar in ihrer Morphologie und zeigten Expression den NSZ Markers Sox2, was auf einen nicht ausdifferenzierten Phänotyp hinweist. Differenzierung mit FBS alleine oder in Kombination mit CNTF, wiederum, führte zu Astrozyten, welche die pro-

regenerative EZM Komponente Laminin produzierten, was sich in einem starken wachstumsfördernden Effekt widerspiegelte. Zwischen den drei pluripotenten Stammzell- (PSZ) Linien wurden signifikante Unterschiede beobachtet, vor allem in Bezug auf ihre elektrophysiologischen Reaktionen auf Stimulation mit Adenosintriphosphat (ATP). Diese Diskrepanzen deuten darauf hin, dass astrozytäre Linien trotz eines ähnlichen phänotypischen Profils einen individuellen elektrophysiologischen Charakter aufweisen. Nach Transplantation in das intakte und verletzte Rückenmark von Fischer 344 Ratten wurden einige der *in vitro* beobachteten Eigenschaften beibehalten, was darauf hinweist, dass prä-differenzierte Astrozyten einen stabilen Phänotyp haben. Diese Eigenschaft ermöglicht die frühe Selektion eines geeigneten astrozytären Subtyps *in vitro*, der den pro-regenerativen Effekt der Zelltransplantation infolge eines Rückenmarktraume maximieren kann. Auf der anderen Seite bestätigt diese Studie auch Risiken, die im Zusammenhang mit der Anwendung von iPSZ stehen. Ein beträchtliches Zellüberleben im verletzten Rückenmark korrelierte demnach mit der Prädisposition der transplantierten Zellen, Tumore zu erzeugen. Dieser Zusammenhang war vor allem im intakten Rückenmark deutlich ausgeprägt.

Zusammenfassend verschafft diese Studie einen komparativen Überblick über astrozytäre Eigenschaften und über Einschluss-/Ausschlusskriterien für Transplantation nach Rückenmarktrauma. Diese Kriterien sind geeignet, die wachstumsfördernde Fähigkeit von astrozytäre Subtypen einzuschätzen und das tumorigene Potential von PSZ Tochterzellen vorherzusehen/zu prognostizieren.

2. Introduction

2.1. Spinal cord injury: clinical state

2.1.1. Injury of the spinal cord

Injury of the spinal cord can be caused by compression, contusion or penetration of the spinal cord and leads to massive degeneration of neural tissue, formation of liquid-filled cysts and cavities, and the accumulation of cellular debris and inflammatory cells. Degeneration of neurons and glia and the disruption of ascending, descending and intraspinal projections result in the loss of sensory, motor and autonomic function [1]. Under these conditions functional recovery is only possible if spared projections take over the function of degenerated axons by creating new connections. This process is called regeneration if new connections are formed by an injured neuron, which extends an axon from its cut end, from its shaft (formation of new branches) or from a non-injured branch, while sprouting refers to new connections formed by non-injured neurons [2]. Sprouting is a compensatory mechanism which occurs in response to injury of other axons. To protect the surrounding tissue from further damage infiltrating meningeal cells and reactive astrocytes form an impenetrable barrier lining the lesion site [3]. The formation of liquid-filled cysts, the upregulation of inflammatory and inhibitory molecules and the confinement of the lesion environment by the glial scar represent an impermeable environment that prevents endogenous regeneration of axotomized neurons and lost glial cells [4].

2.1.2. Incidence of spinal cord injury and impact on society

Spinal cord injury (SCI) mostly results from a traumatic event, commonly traffic / motor vehicle crashes, falls, sports accidents and violence. The resulting disruption of sensory, motor and autonomic function has a high impact on the patient's quality of life, as it affects both the physical and the psychological well-being. In addition, it represents a substantial financial burden for patients, their family and the community. No treatment is currently available to fully restore function, therefore health care resources are needed on a long-term or even life-long basis, including hospitalization, rehabilitation, prevention or care of secondary complications, medication and personal assistance [5-8]. A 2013 World Health Organization (WHO) report estimated that global non-traumatic and traumatic SCI incidence is likely to be between 40 and 80 cases per million, which means a yearly world-wide incidence of 250,000 to 500,000 patients [8]. Comparative studies throughoutly analyzing the world-wide economic impact of SCI are currently not available, however an estimation of mean costs that a SCI patient has to cover in the USA amounts to $138,000-476,000 within the first year and $38,000-169,000 in following

years depending on location and severity of injury. Accordingly, as an example, lifetime health care of a 25 year old and of a 50 year old SCI patients amounts up to $3 million and up to $1,7 million, respectively [7, 9]. Interestingly, SCI incidence has decreased or been stable in developed countries, likely due to development of preventive strategies based on epidemiology, whereas it has increased in developing and middle to low-income countries, where there is lack of information about SCI epidemiology [5].

2.1.3. Current state of clinical intervention

To date, no therapeutical approach is available for the full restoration of sensorimotor and autonomic dysfunction after SCI. After complete SCI, sensorimotor and autonomic function controlled by spinal cord segments below the lesion site is irreversibly lost. In incomplete SCI, spontaneous and/or compensatory functional recovery can be partially addressed by rehabilitation procedures. Rehabilitation is meant to train the body to "re-learn" to perform a specific task either by stimulating the restoration of former circuits or inducing novel circuits or by adaptive or compensatory mechanisms. The former are based on plasticity of the nervous system, which is capable of re-organizing after injury both at a physiological and at a morphological level. For incomplete SCI patients, rehabilitative training is the most effective approach to direct and enhance plasticity, thereby inducing some sensorimotor recovery. Such training uses specific tasks to stimulate and facilitate neuroplasticity specifically related to a lost function (e.g. treadmill training for walking; reach & grasp training for everyday hand use). Rehabilitative training is only undertaken after examination of the patient to assess if certain physiological requirements are met, i.e. if the basis for functional improvement is provided. Rehabilitation is, however, costly: long-term training with a high amount of movement-repetitions is intensive both for the patient and for the physiotherapists, and complex robotic devices, which are necessary for standardized training paradigms, are expensive and generally not available for everyday use [10]. In addition, rehabilitation has no effect on irreversibly injured circuits.

Pre-clinical and clinical research has therefore been focusing on understanding why CNS function is irreversibly lost and on designing approaches to enhance CNS regeneration.

2.2. Failure in central nervous system regeneration: key players

The peripheral nervous system (PNS) retains the ability to regenerate axons after injury, whereas central nervous system axons (CNS) do not regenerate. At the beginning of the 20th century it was generally assumed that CNS neurons are completely unable to regenerate [11]. However, subsequent studies demonstrated that the CNS branches of dorsal root ganglion (DRG) neurons were capable of intraspinal regenerative sprouting after partial denervation of

the spinal cord in cats [12]. Nevertheless, CNS regeneration remained controversial for several decades [13], until it was demonstrated that transected CNS axons are able to re-grow into bridges of peripheral nerves transplanted into the rodent spinal cord [14, 15]. This led to the hypothesis that the inhibitory nature of the CNS environment is responsible for the failure of CNS neurons to regenerate [16]. However, CNS neurons display a lower growth potential than PNS neurons on a permissive substrate [17], suggesting that cell-intrinsic mechanisms and the inhibitory CNS environment both represent a barrier to CNS regeneration. It is now generally accepted that cell-intrinsic and extrinsic properties account for the differences in the capacity to regenerate between CNS and PNS neurons.

2.2.1. Extrinsic inhibitors of axonal regeneration

Axonal regeneration and plasticity in the CNS are hampered by a whole range of soluble growth-inhibitory molecules, which accumulate at the site of injury, including CNS-myelin-derived inhibitors, ephrins, semaphorins and proteoglycans [4, 18, 19]. The cellular and molecular responses that contribute to the inhibitory environment after CNS injury have been subject of numerous investigations, and means to overcome growth-inhibition have moved from *in vitro* neurite-growth assays to several pre-clinical and clinical studies to date.

2.2.1.1. Fibroglial scar and proteoglycans

Immediately upon SCI, a sealing cellular barrier composed of reactive fibroblasts, macrophages and hypertrophic astrocytes arises within and at the edge of the injury site. This results in stabilization of the injured CNS tissue by restoration of physical and chemical integrity and by limiting the breakdown of the blood brain barrier (BBB) to impede further infiltration of non-CNS cells/molecules and infections and excessive subsequent secondary tissue damage [3, 20]. In fact, ablation of glial scar formation results in invasion of inflammatory cells into the lesion site, an increase in lesion volume, decreased neuroregeneration and functional deterioration [21-25]. However, the fibroglial scar constitutes a physical and molecular obstacle to regenerating axons due to the upregulation of a growth-inhibitory extracellular matrix (ECM). One class of molecules strongly upregulated in the ECM of CNS injury sites are chondroitin-sulphate-proteoglycans (CSPGs) [26-28]. In the 90's, *in vitro* studies in which non-growth-permissive astrocytic lines were treated with inhibitors of proteoglycan synthesis established a clear link between CSPG secretion and inhibition of neurite growth [29, 30], whereas *in vivo* studies demonstrated that upregulation of CSPGs in the scar tissue contribute to failure of axonal regeneration [31, 32]. In concomitance, digestion of glycosaminoglycan (GAG) side chains of CSPGs with the bacterial enzyme chondroitinase ABC (ChABC) attenuated their growth-inhibitory activity both *in vitro* and *in vivo* [33, 34], suggesting that CSPG digestion could be of therapeutic value.

2.2.1.2. Modulation of the extracellular matrix: chondroitinase ABC

Early pre-clinical studies performed in rodents demonstrated that administration of ChABC after SCI promotes regeneration of ascending and descending lesioned projections, enhances sprouting and connectivity of spared pathways, modulates the immune response and neuroprotection and leads to partial recovery of sensorimotor function [35-45]. Few studies were performed in cats and squirrel monkeys [46, 47], however studies in larger animals are necessary to assess safety, efficacy and dosage of the treatment before moving to a clinical setting. In addition, clinical translation of ChABC treatment remains challenging due to the rapid loss of enzymatic activity at body temperature and consequent lack of appropriate delivery methods [48].

2.2.1.3. Myelin-associated inhibitors

CNS myelin was identified as potent inhibitor of neurite growth more than 30 years ago, when it was shown that CNS axons can regenerate in peripheral nerve transplants [14, 15], whereas PNS neurons displayed more limited neurite extension when exposed to CNS myelin [16, 49]. Nogo-A was identified as one myelin component, which largely accounts for its inhibitory activity [50, 51]. However, myelin-associated glycoprotein (MAG), oligodendrocyte-myelin glycoprotein (OMgp) and the CNS myelin lipid sulfatide also have potent inhibitory activity. All myelin inhibitors bind to a common receptor (NgR) in a complex with Lingo-1 and TROY or p75. Activation of NgR induces axonal cytoskeletal rearrangements and exerts further inhibitory functions via a signaling pathway involving the small Rho GTPase RhoA and the Rho associated protein kinase (ROCK) [4].

2.2.1.4. Pre-clinical and clinical trials targeting Nogo-A

In 1988 the monoclonal antibody IN-1, raised against the two inhibitory antigens (NI-35 and NI-250) known as Nogo-A, was applied intratechally after SCI in rats, leading to enhanced sprouting and longitudinal axonal elongation [16]. Subsequent studies targeted Nogo-A *in vivo* by means of different anti-Nogo antibodies, the NgR blocking peptide NEP1-40, soluble NgR fusion proteins (NgR-Fc) or by genetic ablation, confirming across different animal species including non-human primates enhanced sprouting, some regeneration and functional recovery [52-63]. Based on this solid and very promising pre-clinical evidence, Nogo-A antibodies were produced by Novartis and applied in a Phase I clinical study which started in 2006 within the European Multicenter Study about Spinal Cord Injury (EMSCI) (clinicaltrials.gov ID: NCT00406016). However, results from this clinical study are not published yet. Anti-Nogo-A, also known as Ozanezumab, was also applied in more recent Phase I clinical trials targeting amyotrophic lateral

sclerosis (ALS) patients [64], multiple sclerosis (MS) patients (clinicaltrials.gov ID: NCT01435993; clinicaltrials.gov ID: NCT01424423) and patients with traumatic brain injury (TBI) (clinicaltrials.gov ID: NCT02229643), results have not been published and Phase II trials are yet to be started.

2.2.1.5. Inhibitory molecules

In addition to CSPGs and CNS myelin-associated inhibitory molecules, other classes of potent growth-inhibitory molecules are upregulated after SCI within and around the lesion site, which are known to be crucial axon guidance cues during neurodevelopment: semaphorins, ephrins and Eph receptor tyrosine kinase family members, Wnts and Netrins [65-68]. Members of the Ephrin and Eph receptor families are expressed at the injury site by reactive astrocytes, fibroblasts and oligodendrocytes, indicating that no single cell type accounts for the inhibitory lesion environment, and were shown to affect cell survival and restrict axonal growth and regeneration after SCI [63, 69-74]. Inhibition of the ephrin/Eph receptor signaling by fusion proteins or blocking peptides was shown to promote axonal regeneration [72, 75]. Semaphorins, on the other side are expressed by infiltrating meningeal fibroblasts [76]. Inhibition of Sema3A resulted in improved regeneration, preservation of injured axons, Schwann-cell mediated myelination, decrease in apoptosis and functional recovery after SCI [77, 78].

Based on these pre-clinical results, modulation of the lesion environment, i.e. modulation of proteoglycans, myelin-associated molecules and developmentally relevant growth-inhibitory molecules, represents a promising therapeutical approach to increase regeneration after SCI.

2.2.1.6. Delivery of neurotrophic factors to promote regeneration and sprouting

Besides the growth-inhibitory environment of the injured spinal cord, absence of a permissive growth-substrate or growth-stimulating cues contribute the regenerative failure. Therefore, besides manipulating the extracellular environment of the injured CNS to reduce its inhibitory effect, chemoattractive cues, which promote axon-growth, are necessary to induce robust regeneration.

Both during neurodevelopment and after injury of the PNS, neurotrophic factors play an important role in neuronal survival, axonal growth and target innervation. Several families of trophic factors including members of the neurotrophin family (nerve growth factor, NGF; brain-derived neurotrophic factor, BDNF; neurotrophin-3, NT-3; neurotrophin-4/5, NT-4/5), GDNF-family ligands (Glial cell line-derived neurotrophic factor, GDNF; neurturin, NRTN; artemin; persephin), neuropoietic cytokines (ciliary neurotrophic factor, CNTF; leukemia inhibitory factor,

LIF) and others have therefore been investigated for their influence on neuronal survival and axon growth after SCI.

After injury of the spinal cord, BDNF and NT-3 have been shown to counteract atrophy of injured tracts and to support cell survival [79-81]. In addition, they encourage growth of injured axons [82-84]. Numerous pre-clinical studies used genetically modified cells such as fibroblasts [84-94], Schwann cells [82, 95], bone marrow stromal cells [96, 97], olfactory ensheathing cells [98-100], neural precursor cells [91, 101] or peripheral nerve grafts [102] as "biological mini-pumps" to continuously produce the desired neurotrophic factors, such as BDNF and NT-3, after transplantation to the injured spinal cord. Although these studies showed robust axonal growth into the lesion site filled with neurotrophic factor producing cells, axons rarely exited the graft to extend into the host spinal cord due to the inhospitable environment and lack of chemoattractive cues. Only in the presence of a growth stimulus distal to the cell graft axons extend beyond the lesion site. Using virus-based *in vivo* gene delivery (lentivirus or adeno-associated virus, AAV), neurotrophic factor gradients can be generated within the distal host tissue, allowing for bridging axonal regeneration [103-106].

Although neurotrophic factor delivery represents a promising means to boost neuroregeneration, appropriate and safe techniques for localized and regulatable delivery have to be developed to allow for clinical translation.

2.2.2. Intrinsic factors regulating axonal regeneration

Injured CNS axons are incapable of regenerating not only due to environmental cues, but also due to their intrinsic properties. The growth capacity of CNS axons declines during development as connections mature and synapses are formed. This decline is accompanied by the down-regulation of growth-associated genes. Transcriptional and epigenetic mechanisms, local protein translation, retrograde and anterograde axonal transport and cytoskeletal dynamics have been identified as intrinsic key regulators of axon regeneration.

2.2.2.1. Calcium transients and activation of cAMP

After axonal injury, influx of calcium into the axoplasm is one of the first consequences. This transient intracellular calcium wave propagating from the injured axon to the cell soma seems to be crucial for resealing the axonal membrane, protein synthesis, cytoskeleton rearrangement, assembly of the growth cone and the activation of intracellular signaling cascades. Calcium influx lead to increased cyclic cAMP levels, which promote growth cone assembly [107] and to activate signaling pathways to overcome myelin-associated signals [108-110]. In fact, injection of a cell-permeable cyclic adenosine monophosphate (cAMP) analogue (dibutyryl-cAMP; db-cAMP) into DRG neurons enhanced the regeneration of injured dorsal

column axons [111-113]. An alternative method to enhance cAMP levels is subcutaneous application of the BBB-permeable drug Rolipram, an inhibitor of the cAMP-degrading enzyme phosphodiesterase (PDE) 4. Delivery of Rolipram after injury of the spinal cord led to enhanced regeneration, attenuation of the glial scar and significant increase in functional recovery in several pre-clinical studies [114-118], however clinical trials are still not reported.

2.2.2.2. Epigenetic regulation of regeneration-associated genes

When calcium waves reach the soma of DRG neurons, it leads to activation of PKCμ and consequent export of histone deacetylase 5 (HDAC5) from the nucleus. As a result, increased histone acetylation contributes to the activation of pro-regenerative gene expression in DRG neurons. In particular, increased acetylation of histone 4 (H4) in promoter regions of regeneration-associated genes (RAGs) leads to their increased expression. Several transcription factors including JUN, KLF4, KLF5, c-Fos, ATF3 and Gadd45g, as well as Smad1, Sprr1, Galanin, NPY and VIP, which have been associated with the injury-induced response and axon growth, have been found to be HDAC5-regulated [119, 120]. Independently, the histone acetyltransferase CBP/p300 regulates RAG expression via histone 3 (H3) acetylation of p53, GAP-43 and Sprr1 [121]. These findings suggest that epigenetic regulation of RAG expression may be targeted to promote regeneration after CNS trauma.

2.2.2.3. Growth cone and microtubule dynamics

Injured PNS neurons maintain stable microtubuli at the backbone and have dynamic microtubuli at the tip of their growth cone, whereas injured CNS axons form a retraction bulb with a disorganized network of microtubuli, a rather static structure that can persist for years after spinal cord injury [122]. After nuclear export, HDAC5-mediated deacetylation of microtubuli at the axon tip of DRG neurons increases their dynamics and reorganization. This is a prerequisite for the formation and motility of a growth cone, which are necessary for growth initiation and axonal extension [119, 123]. On the other side, selective inhibition of HDAC6 and the consequent increase in acetylated, stable microtubuli enhanced survival after oxidative stress and growth of CNS neurons on non-permissive substrate [124], indicating that microtubule stability might have divergent effects on axon regeneration. Nevertheless, some efforts have been made to pharmacologically stabilize microtubuli and promote growth cone formation and dynamics via administration of Taxol, an approved and commercially available drug. Moderate stabilization of microtubuli via application of low doses of Taxol prevented the formation of retraction bulbs, decrease axonal degeneration *in vivo* and enable CNS neurons to overcome the growth inhibitory effect of myelin in vitro [125]. *In vivo*, Taxol-mediated stabilization of the microtubule network led to a reduction of the fibrotic scar and of CSPG levels, and to moderate

increase in regeneration and functional recovery [126], which was partially replicated in a subsequent study [127]. Delivery of a Taxol derivative, Epothilone B, led to a decrease in glial scarring, and promoted regeneration and functional recovery [122]. Taken together, despite some convincing pre-clinical evidence, additional studies are needed to define the dose, time window of treatment and maximum benefit before moving towards clinical translation.

2.2.2.4. Transcriptional networks and other signaling cascades

Because CNS neurons fail to effectively activate RAGs [128], means to promote CNS axon growth by gene-delivery of RAGs or by manipulating pathways that lead to the upregulation of RAGs have been explored in numerous studies. The pro-regenerative potential of transcription factors that might have a broad effects by influencing expression of several genes have been studied including SMAD1 [129], CREB [130], STAT3/SOCS3 [131], ATF3 [132] and c-JUN [133]. Among these, STAT3 and c-JUN are perhaps the ones with the strongest indication for a pro-regenerative effect; however none of these experiments promoted extensive long-distance regeneration in the spinal cord.

Besides positive regulators of gene expression, intrinsic inhibitors of axon growth which negatively influence protein translation contribute to the CNS regenerative failure. The activity of mechanistic target of rapamycin (mTOR), a regulator of protein translation, is strongly influenced by phosphatase and tensin homolog (PTEN). Elimination of the tumor suppressor gene PTEN induced robust axon growth of retinal ganglion neurons [134]. Further investigations demonstrated that mTOR activity also regulates sprouting of corticospinal tract (CST) neurons after injury. Conditional deletion of PTEN attenuated injury-induced loss of mTOR activity in CST neurons, and enhanced sprouting and regenerative growth indicating that this signaling pathway represents a promising approach to target the intrinsic regenerative capacity of neurons after SCI [135-137]. Combining PTEN deletion with the activation of the STAT3 pathway showed even more remarkable growth after an optic nerve crush injury [138].

2.2.2.5. What lessons can we learn from the peripheral nervous system?

The ability of peripheral neurons to mount a regenerative program after PNS injury has been a major focus in identifying genes and signaling cascades important for axon regeneration. On one side, intrinsic properties of PNS neurons confer them the ability to regenerate on a life-long basis. On the other side, there is a striking difference in the structural proteins that make up the myelin of the CNS and the PNS. For instance, CNS myelin produced by oligodendrocytes is compact and rich in glycolipids, sulfolipid-sulfatides, proteolipid protein (PLP) and myelin-associated inhibitors such as OMgp. In contrast, myelin protein zero (P0/MPZ) and peripheral myelin protein 22 (PMP22) constitute characteristic structural proteins of peripheral myelin

[139]. Importantly, the inhibitory myelin components MAG, OMgp, p75 and NgR are not absent in the PNS. Rather, after injury they are rapidly cleared by macrophages and Schwann cells. In addition, Schwann cells de-differentiate in order to down-regulate inhibitory myelin proteins. Unlike Schwann cells, CNS oligodendrocytes do not down-regulate myelin components and do not clear myelin debris after injury [140].

DRG neurons can be used to study mechanisms of regeneration in both the PNS and CNS, due to their unique nature: their cell soma is located in the dorsal root ganglia at each side of the spinal cord and they extend two axonal branches, one into the PNS and one into the CNS. The peripheral branch retains its ability to regenerate, whereas the central branch fails. Due to this fascinating property, they have been extensively used to perform basic research on neuroregeneration *in vitro* and *in vivo*.

2.2.2.6. The conditioning lesion effect

Sensory neurons of the DRG are pseudobipolar neurons which extend two axonal branches: the peripheral one, which innervates sensory organs in the skin, joints, muscles and tendons, and the central projection, which crosses the dorsal root entry zone (DREZ) to enter the spinal cord and either form connections with spinal cord interneurons residing in the gray matter or proceed via the white matter to brainstem nuclei to innervate their CNS targets. In 1969, experiments performed with DRG neurons of monkeys revealed a differential response to injury of their peripheral versus their central branches [141], a phenomenon, which had already been observed by Ramón y Cajal during his extensive examinations of the nervous system [142]. Upon damage to axons of the peripheral nerve, genetic and molecular programs are activated, which lead to a state of axonal growth [143]. After the growth program is initiated, axonal elongation is supported by the growth-permissive PNS environment, by tubes of Schwann cell basal lamina, as well as growth-permissive ECM and neurotrophic factor mediated chemoattraction [144]. Most intriguing is the ability of a peripheral lesion to elicit regeneration of the CNS branch of DRG neurons, which was observed more than 30 years ago. However, in this first study a peripheral nerve graft was used as growth substrate [145]. Regeneration of CNS branches in the absence of a permissive PNS substrate was demonstrated 15 years later, were a conditioning lesion of the sciatic nerve one-two weeks before a dorsal column lesion was shown to elicit regeneration of CNS projections beyond the lesion site [146]. Subsequent studies attributed the conditioning lesion effect to the elevation of cAMP levels 24 hours after PNS injury, which persisted for one week before returning to baseline levels; intra-ganglionic injections of db-cAMP could in fact increase neurite outgrowth [111]. cAMP elevation, in turn, is able to promote gene expression and regeneration via activation of the transcription factor cAMP response element binding protein (CREB) [130]. However, subsequent studies demonstrated that conditioning lesions activate a greater and more long-lasting genetic

response than cAMP administration [147], suggesting that cAMP is one but not the only key player accounting for the conditioning lesion effect. Extensive studies investigating the mechanisms behind the conditioning lesion effect might identify promising therapeutical approaches based on the regenerative program activated by peripheral nerve injury.

2.3. Cell transplantation to promote neuroregeneration

The therapeutical approaches reviewed above aimed at enhancing regenerative axon outgrowth and/or sprouting of injured and spared projections by targeting their extrinsic or intrinsic properties. The regenerative capacity of endogenous projections remains, however, still very limited and outgrowing axons only extend for modest distances. Considering the long distances that regenerating axons need to cover in the human body, robust target reinnervation after severe spinal trauma might be utopic. Moreover, boosting endogenous regeneration alone does not lead to restoration of neural tissue integrity and function. Neuroregenerative approaches might therefore become fully effective only in combination with cell replacement strategies, which promote anatomical and functional repair. Cell transplantation should ideally (1) provide a permissive physical and molecular substrate for axon growth, perhaps in concomitance with secretion of pro-regenerative soluble factors, (2) provide for trophic support and remyelination, (3) replace damaged neurons or introduce neurons that can serve as "relays" (a cellular bridge). In cell transplantation experiments, these three aspects were addressed separately, some of them even in a clinical context. However, we are very far from the application of the "perfect" cell transplant covering all these functions. In addition, transplanted cells are heterogeneous in terms of age and gender of the donor, organ of source, culturing conditions across laboratories, method of delivery and other characteristics. Thus, both pre-clinical and clinical studies might report diverging outcomes.

2.3.1. Regeneration versus "relay" formation

Cell replacement strategies can address three main aspects of neural tissue restoration, which will be briefly described hereafter.

Restoration of tissue integrity and regeneration

Non-neural cells or glial cells can be used to provide physical guidance, as well as trophic and metabolic support. They can produce growth-permissive ECM, secrete neurotrophic or chemoattractive factors and interact with endogenous glial scar forming or inflammatory cells, thereby counteracting the extrinsic factors, which influence the regenerative potential of injured neurons. However, they hardly have influence on the intrinsic growth potential, which is very limited in CNS neurons. Nevertheless, they are crucial for restoration of tissue integrity and

homeostasis, support of elongating axons and modulation of network activity (figure 2.1., A). To restore the original neural tissue integrity and function, a CNS-residing cell type would be ideal.

Remyelination

Glial cells, specifically Schwann cells, olfactory ensheathing cells (OECs) or oligodendrocytes are capable of myelinating axonal projections: either by re-myelinating spared axons or by myelinating regenerating axons. Re-/myelination ensures fast transmission of neuronal information and balanced neural network activity. If regenerated axonal projections are not myelinated, they will only have a limited capacity to contribute to functional recovery. In addition, oligodendrocytes provide trophic and metabolic support to axons. Understanding the pathways involved in myelination and in axon-glia communication, and how these pathways may influence axonal growth responses after injury, is crucial for developing regenerative therapies after CNS injury.

The concept of neuronal “relay”

Classic intervention / repair strategies for SCI have aimed at boosting the endogenous regenerative potential of injured axons, which would extend across the lesion site back into the adjacent host spinal cord and beyond to re-innervate their targets. Currently, very few studies demonstrate substantial growth of injured axons into and beyond the injury site. In some cases, few axons have been identified which re-enter the intact spinal cord but only for a short distance. Therefore, in recent years the concept of neuronal „relay“ has gained attention and may represent an alternative strategy to reconstruct damaged neuronal networks. Transplanted neuronal precursors or immature neurons would differentiate and build a “cellular bridge” which receives information from sensory ascending or motor descending projections and convey it either by local connectivity with interneurons or by extending towards and re-innervating original targets (figure 2.1., B).

This concept has been addressed in recent studies [148, 149], which showed robust axonal extension from transplanted dissociated fetal tissue as well as from pluripotent stem cell (PSC)-derived neural stem cells (NSCs). In addition, these studies reported electrophysiological activity of transplanted cells, confirming the functional relevance of this newly formed network, as well as partial recovery of hindlimb / motor function. However, additional pre-clinical studies are needed to assess the impact and the contribution of the neuronal “relay” to functional recovery.

Generally, regeneration and “relay” formation need to be addressed at the same time. While transplantation of a pro-regenerative substrate, f.i. a glial-cell substrate, might not be enough to boost robust endogenous regeneration, it might guide axotomized projections towards “relay” forming cells. The latter on the other side might take advantage of a glial-cell substrate, as this might support their survival and maturation.

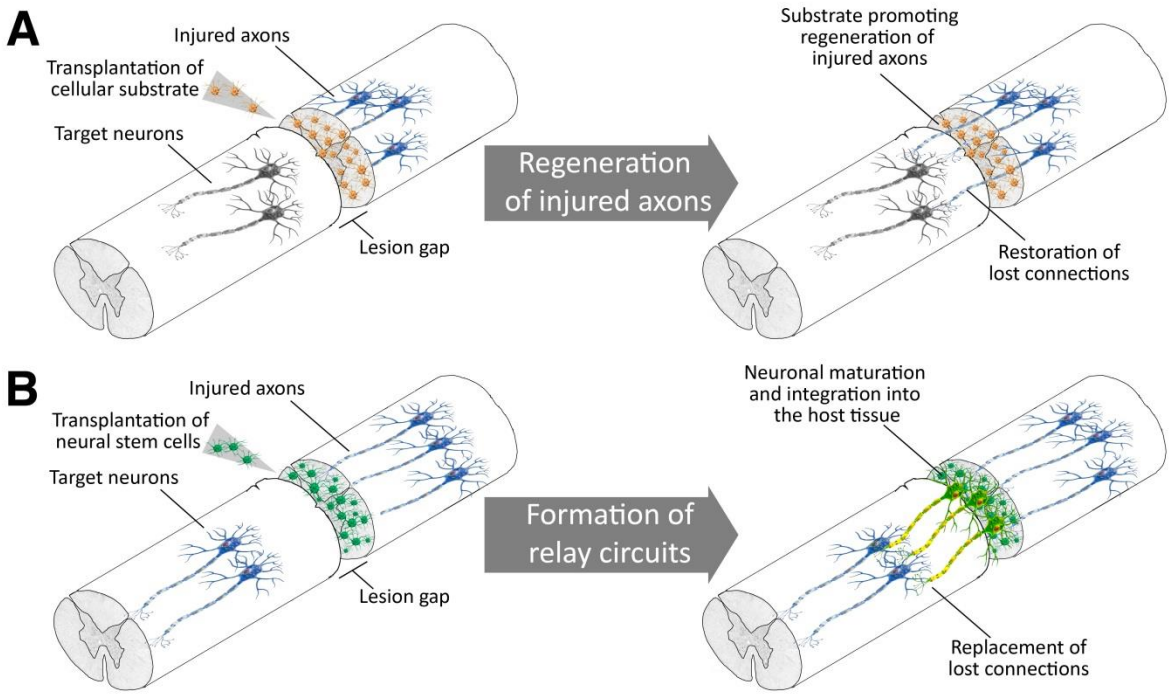

Figure 2.1 Cell replacement after SCI: regeneration versus neuronal „relay" formation.
Transplantation of a cellular substrate after SCI can address three major aspects: **(A)** the cellular substrate provided the optimal conditions for injured neurons to regenerate axons and connect with their original targets to restore function, **(B)** the stem cell substrate gives origin to neurons, which receive the signal from axotomized host neurons and extend projections towards denervated targets, thereby mediating communication and restoring function, and **(C)** re-myelination of de-myelinated spared projections, which can only be addressed if these are present.

2.3.2. Transplantation of non-CNS cells

2.3.2.1. Mesenchymal stem cells

Mesenchymal stromal or stem cells (MSCs) have been extensively used for transplantation into the CNS. These self-renewing / multipotent stem cells, isolated from the bone marrow, can differentiate into osteoblasts, adipocytes and chondroblasts, as well as putative neural cells and myoblasts *in vitro* [150]. MSCs represent a very attractive and promising cell source for tissue repair because they can be easily obtained from autologous bone marrow, cryopreserved and expanded in a relatively short period of time [151]. In addition, they are well tolerated and there are no reports of adverse reactions in both autologous and allogeneic transplantations.
MSCs have been reported to have anti-inflammatory, neuroprotective and pro-regenerative effects by decreasing demyelination and scar formation, promoting regeneration and guiding axons [152, 153]. Improvements of locomotor, sensory and autonomic function, as well as

reduction of neuropathic pain were observed in some studies in different animal models [154, 155]. However, beneficial effects on functional recovery in well-conducted preclinical studies were modest. Nevertheless, a number of ongoing and completed clinical trials have assessed safety and potential beneficial effects of MSC transplantation after SCI. Most of these trials only enrolled a small number of patients and are therefore unable to draw conclusions about clinical efficacy [156, 157].
Taken together, although MSCs can be easily harvested and cultured for transplantation, their non-neural nature might lead to a disappointing outcome in terms of functional recovery.

2.3.2.2. Stimulated macrophages

Despite the detrimental role of the immune response after CNS injury, inflammation can also be beneficial after SCI. Macrophages are crucial for clearing ECM as well as cellular debris and secrete growth factors which facilitate remyelination and axon growth. In the late 1990s, transplantation of non-activated blood-born macrophages after transection of the spinal cord in rodents led to enhanced regeneration and recovery of motor function [158], as well as decreased expression of the axon-growth-inhibitory myelin protein MAG, increased angiogenesis and Schwann cell infiltration [159]. In a later study, a skin biopsy was used as the source to activate autologous macrophages that were administered 8-9 days after a rat spinal cord contusion. This resulted in less pronounced syringomyelia and improved motor function [160]. In subsequent clinical trials, autologous macrophages activated by incubation with autologous skin biopsies were injected into the spinal cord caudal to the lesion [161-163]. In both clinical trials, transplantation was performed in American Spinal Injury Association Impairment Scale (AIS)-A patients within 14 days after injury. While the macrophage cell therapy was well tolerated, no significant difference in primary outcomes (conversion from AIS A to B or C) between treated and control group was detected. While these are very crude clinical outcome measures, stimulated macrophages might not represent a suitable cell source for transplantation after SCI.

2.3.2.3. Schwann cells

Schwann cells are responsible for the myelination of PNS axons, but they are also able to myelinate CNS axons. They play a central role in PNS regeneration, express neurotrophic factors, provide a favorable ECM and guide axons across a lesion after PNS injury [144]. In addition, Schwann cells can be relatively easily obtained from peripheral nerve biopsies and expanded in culture. In the context of SCI, they have been used for over 30 years [164], not only due to their ability to re-/myelinate, but also because they represent a permissive substrate for regenerating axons.

Although several pre-clinical studies demonstrated that Schwann cells promote axon regeneration, other studies pointed out that they are not sufficient to induce bridging of the lesion site, as regenerating axons were not able to exit the graft and grow into the host tissue [165, 166]. In contusion SCI animal models, only few studies reported significant improvement of motor function when adult rodent Schwann cells were transplanted alone [167-169]. In one positive study, functional recovery was induced in mice after compression of the spinal cord, however way more efficiently with genetically engineered Schwann cells which overexpressed Polysialylated-neural cell adhesion molecule (PSA-NCAM) [170]. Only few pre-clinical studies were performed using human Schwann cells. Modest but significant beneficial effects were observed; however Schwann cells were transplanted in a combinatorial treatment [171, 172].

Based on the preclinical evidence, three clinical studies have been conducted to date in which Schwann cells were transplanted in SCI patients. From the first two completed studies, only limited conclusions about efficacy can be drawn, but the transplantation procedure appeared to be safe [173-175]. Supported by safety and toxicity studies in rodents, mini-pigs and primates, a FDA-approved phase I study transplanting autologous Schwann cells in patients with subacute neurologically complete thoracic SCI was recently initiated, which is still ongoing [176] (clinicaltrials.gov ID: NCT01739023). Future clinical application will have to cope with some challenges: (1) autologous isolation of Schwann cells requires sacrificing a peripheral nerve, thus an alternative source needs to be found; (2) expansion of nerve-derived Schwann cells or induction of Schwann cell differentiation from MSCs might take several weeks [177, 178]; (3) when transplanted alone without further intervention, Schwann cells led to limited functional recovery; (4) cell survival following transplantation is rather low similar to other transplanted cells.

Nevertheless, Schwann cells remain a reasonable treatment approach for SCI. While current clinical studies might not show meaningful clinical benefit, the results could provide the basis for future studies combining Schwann cell transplants with other treatments that have shown promise in animal models.

2.3.2.4. Olfactory ensheathing cells

OECs were first described in the 19th century by Golgi [179] and Blanes [180] as specialized glial cells exclusively located in the olfactory nerve and glomerular layers, one region of the CNS where axonal regeneration is possible throughout adulthood. They ensheat and isolate olfactory axons from the growth-inhibitory CNS environment, enabling axonal growth from the olfactory epithelium (PNS) towards targets in the olfactory bulbs (CNS) [181]. The unique axonal growth promoting properties of OECs were confirmed *in vitro* and *in vivo* after dorsal root transections [182] and complete thoracic transections [183]. In the following years, the pro-regenerative and neuroprotective effects of OECs were investigated in various rodent models of SCI [184, 185].

OECs did not only promote axonal regeneration in the injured CNS, but also functional reconnection of injured axons, remyelination, formation of blood vessels, and re-organization of the glial scar [185, 186]. However, other studies which compared OECs and Schwann cells showed only limited beneficial advantages [167, 168, 187]. This might be at least partially attributable to the source of the transplanted cells, culturing conditions, number of passages and the site of injection [184, 188, 189].

The pre-clinical evidence encouraged the initiation of several clinical studies. In Australia OECs isolated from nasal biopsies were transplanted in patients with chronic SCI. These studies confirmed the feasibility and safety of the approach. While functional improvement was not detected, the studies with 3 - 6 patients were too small to draw definitive conclusions [190, 191]. Two subsequent clinical trials reported functional improvement [192, 193], but again, a limited number of patients was included. Larger clinical trials are needed to confirm the safety and efficacy of OECs for the treatment of SCI.

2.3.3. Neural stem cells: sources, transplantation and application in clinical trials

The cell sources described in paragraph 2.3.2. had some beneficial effects when transplanted in pre-clinical and clinical SCI studies. They had neuroprotective and immunomodulatory effects, enhanced remyelination and / or promoted regeneration. However, none of these are native to the CNS and can therefore only partially restore tissue integrity, but not fulfill all tasks normally fulfilled by CNS neurons and glia. Full restoration of damaged CNS tissue may only be achieved by transplanting CNS-NSCs which can give origin to appropriate neuronal and glial phenotypes. CNS astrocytes and oligodendrocytes can provide physical, trophic and metabolic support, and re-/myelinate axonal projections, while neurons might serve as a “relay”, as mentioned in paragraph 2.3.1.

NSCs can be obtained from different sources: adult NSCs can be isolated from the postnatal forebrain subependymal zone or from the spinal cord [194-196] and fetal NSCs from the fetal brain or spinal cord [197-201]; on the other side, NSCs and their progeny can be obtained via differentiation from embryonic or induced pluripotent stem cells (ESCs, iPSCs) [202-213] or from somatic cells via direct fate conversion [214-218]. In comparison to non-CNS cell types described above, NSCs are more difficult to obtain and their generation and expansion takes several weeks to months. Human adult NSCs isolated during surgery or *post mortem* [196, 219], fetal NSCs cannot be used for autologous transplantation and their use is moreover subject to ethical considerations. On the other hand, NSCs obtained from PSCs or generated by fate conversion can be tumorigenic due to genetic or epigenetic abnormalities [220]. Therefore, although they are a highly promising cell source for SCI repair, NSCs derived from either source have to be used with caution.

Numerous pre-clinical SCI studies have examined the potential of NSCs to mediate functional recovery after SCI. In general, a portion of the transplanted NSCs survive, adopt mature neural phenotypes and can integrate into the host tissue. Transplanted NSCs can provide a substrate for regenerating axons [221-223], serve as a "relay" [148, 149, 224], re-myelinate spared projections [200, 201, 210, 225-227] or can be neuroprotective [228]. More recent studies have also reported that human iPSC-derived NSC can promote functional recovery [148, 149, 229-231].

The first NSC transplantation studies which were translated into a clinical setting were based on the generation of oligodendrocyte precursor cells (OPCs) from human ESCs (hESCs) to re-myelinate spared axons and to promote functional recovery [211, 212]. A Phase I "first-ever" clinical study using human ESCs was initiated in 2009 by the Geron Corporation (Menlo Park, California, USA) to evaluate safety and efficacy of human ESC transplantation in acute SCI [232]. After five patients, the clinical trial was suddenly discontinued in 2011, apparently due to financial concerns [233]. Asterias Biotherapeutics Inc. (Fremont, California, USA) has recently initiated a Phase I/IIa trial using ESC-derived OPCs in subacute cervical SCI (clinicaltrials.gov ID: NCT02302157), which will be completed in 2018. Prior to this clinical trial, the ESC-derived OPC line AST-OPC1 was evaluated for pre-/clinical safety in a rodent animal model [234].

Two further clinical trials in SCI were conducted with fetal NSCs isolated from the brain and from the spinal cord, respectively. Stem Cells Inc. (Newark, California, USA) sponsored one phase I/II clinical trial conducted in Canada and Switzerland from 2011 to 2015 (clinicaltrials.gov ID: NCT01321333), in which human spinal cord derived cells (HuCNS-SC cells) were delivered via intramedullary transplantation in patients with thoracic SCI. Prior to this clinical trial, the HuCNS-SC® cell line, which was purified and expanded by the company Stem Cell Inc., was evaluated for pre-/clinical safety in rodent animal models [235]. Whereas no safety concerns have arisen during the clinical trial, recovery of sensory function was observed in 3 out of 12 patients [235]. From 2014 to 2016 safety of human spinal cord stem cells was assessed in a second phase I clinical trial in patients with complete SCI, which was sponsored by Neuralstem Inc. (Germantown, Maryland, USA) (clinicaltrials.gov ID: NCT01772810). This specific cell line (HSSC) was also tested in a multi-centric phase I/II clinical trial in ALS patients. Adverse events were observed, however they were not related to the transplanted cells [236].

Recent pre-clinical studies demonstrated that NSCs isolated from embryonic day 14 (E14) or differentiated from the ESC lines HUES7 and 566RSC as well as from iPSCs are able to extend long-distance axons into the injured spinal cord and form synaptic connections, thereby possibly acting a "relay" [148, 149]. However, two subsequent replication studies reported ectopic growth of transplanted cells in CNS regions distant from the lesion site [237] and no locomotor recovery [238], drawing attention to the necessity to further assess safety and effect of both fetal and PSC-derived NSCs.

2.4. Tissue engineering: the promise of pluripotent stem cells

The major advantage of transplanting dissociated fetal spinal cord derived NSCs without further *in vitro* manipulation is that these NSCs display characteristics of a naturally defined developmental stage and bear a low risk to form tumors – although ectopic colony formation is quite alarming [237]. At this stage NSCs are already patterned and committed to differentiation lineages, but are still malleable and resistant to stress, therefore they are likely to survive in the injured host tissue. However, obtaining the appropriate amount of day 40 human fetal tissue (corresponding to the rat E14 developmental stage) from abortions may not be trivial. Isolation of primary tissue is subject to batch-to-batch variability, and the isolated fetal tissue may not be enough to fill the lesion site (quantity).

Fetal spinal cord derived cell lines (i.e. HuCNS-SC® and HSSC), which were described in paragraph 2.3.3., overcome potential batch-to-batch variability issues and have been expanded to obtain the appropriate quantity needed for clinical studies. They have been tested in several pre-clinical and clinical studies and are therefore "ready-to-go". However, due to extensive propagation *in vitro*, these cell lines may have acquired "artificial" properties.

Both primary fetal spinal cord tissue and fetal spinal cord derived NSC lines are subject to ethical implications and their transplantation has to be accompanied by immunosuppressive treatments to avoid graft rejection. In addition, both cell sources are committed to specific NSC lineages, therefore limiting the degree of freedom to select specific NSC populations, such as OPCs.

In this context, ESCs and ESC-homologue iPSCs represent means to obtain large amounts of any cell type of the human body, however only iPSCs allow for autologous transplantation without ethical implications. Both cell sources will be briefly reviewed hereafter.

2.4.1. Embryonic stem cells and induced pluripotent stem cells

The term "pluripotent" describes in a broader sense a cell that can generate cell types of each of the three germ layers: endoderm, mesoderm and ectoderm. On the other side, a totipotent stem cell has the ability to generate any cell within an organism. ESCs are obtained from the inner cell mass (ICM) of blastocysts and are therefore not totipotent: they can give origin to any cell type of an organism but not to trophoblasts, which constitute the envelope surrounding the ICM.

Human ESCs have been successfully isolated from blastocysts about 20 years ago [239], leading to the optimistic idea that they represent an unlimited source of any cell type for future basic research, drug screenings and cell transplantation. However isolation of ESCs from human blastomeres led to vehement public debate, although a method was published to generate hESC

lines without embryo destruction [240]. Ethical concerns about the morality of the use of human embryos for research purposes led to the prohibition or tight regulation of their use. Nevertheless numerous hESC lines were established and patented world-wide, including several clinical grade hESC lines which have been derived following Good Manufacturing Practice (GMP) guidelines and throughoutly genomically characterized [241-243]. Unfortunately, these lines did not gain the popularity of previously established hESC lines, such as the HUES6, HUES7, HUES9 (Harvard University Embryonic Stem Cell) lines, and were never used in clinical trials [244]. Although derivation of hESCs is standardized and although they express similar markers at the undifferentiated state, hESCs do not have an equal developmental potential. The differentiation propensity of HUES lines 1-17 was compared following spontaneous as well as specific / directed differentiation at early and late passages to assess dependency of differentiation propensity on hESC senescence. While senescence did not affect predisposition for specific differentiation lineages, significant differences were observed across HUES lines. Some lines were committed to the mesodermal lineage (f.i. HUES1, HUES4, HUES8) and to the endodermal lineage (HUES4, HUES8), whereas others were inclined towards ectodermal / neural lineages (HUES6, HUES9) [245]. Altogether, hESCs represent an extremely powerful tool for regenerative medicine and *in vitro* disease modeling, as they are a virtually unlimited source of any cell type of the human body. However, their use is tightly regulated and accurate testing is necessary to assess their differentiation potential. On the other side, their genomic integrity has been throughoutly characterized and the existence of clinical grade hESCs enables faster and safer transfer into a clinical setting.

A decade ago, Kazutoshi Takahashi and Shinya Yamanaka reported the successful development of an unimaginable and incredible technique, which opened up infinite possibilities for development and disease modeling as well as for regenerative medicine: by retroviral introduction of four factors - today known as Yamanaka factors - Oct3/4, Sox2, c-Myc and Klf4 into somatic cells, the authors were able to obtain cells which had lost their somatic identity and assumed morphology, gene expression and growth properties of ESCs. In addition, reprogrammed somatic cells were able to give origin to all three germ layers and to contribute to development when introduced into a blastocyst [213, 246-249]. These cells were named induced pluripotent stem cells (iPSCs) and represent, similarly to ESCs, an unlimited source of all cell types of the human body. The discovery of iPSCs was a breakthrough, had a huge impact on the scientific community world-wide and was awarded with a Nobel Prize in Physiology and Medicine in 2012, only 6 years after the first publication.

The impact of iPSCs in the field of regenerative medicine is remarkable: somatic cells can be harvested through minimally invasive or non-invasive methods, reprogrammed into a pluripotent state and used to obtain any desired cell type for autologous transplantation. Therefore iPSCs represent a unique and non-controversial tool for personalized and autologous therapeutic intervention.

The following paragraphs will be dedicated to the generation and differentiation of iPSCs, as well as their application. Lastly, the emerging field of direct fate conversion will be briefly reviewed.

2.4.1.1. Generation and safety of induced pluripotent stem cells

Conversion of somatic cells to a pluripotent state was first achieved by retroviral introduction of either combination of four transcription factors into fibroblasts: Oct3/4, Sox2, c-Myc and Klf4 (Yamanaka factors) or Oct3/4, Sox2, Nanog and Lin28 [250]. Within only two years after the first publication, several laboratories world-wide published high-impact studies where a variety of somatic cell sources and transcription factor combinations were used to obtain iPSCs, including fibroblasts, blood cells, cord blood cells, liver cells, stomach cells, pancreatic cells, adult NSCs and keratinocytes. These studies proved the reproducibility and reliability of the novel technique [251-262].

Delivery of the Yamanaka factors into somatic cells was originally achieved using moloney murine leukemia virus (MMLV)-derived retroviruses containing the pMX vector and the transcription factors of interest. Each viral vector contained one transcription factor; therefore each transcription factor was delivered separately to somatic cells within a viral cocktail [213, 246]. Reprogramming efficiencies were very low, about 0.01% for human fibroblasts. Moreover, the fact that each reprogramming factor is delivered separately may lead to highly variable expression levels of each factor in each target cells, which in turn may lead to an extremely heterogeneous resulting iPSC population.

Within the past decade, several alternative reprogramming methods were developed to enhance efficiency of reprogramming and address biosafety issues, which are summarized in figure 2.2.

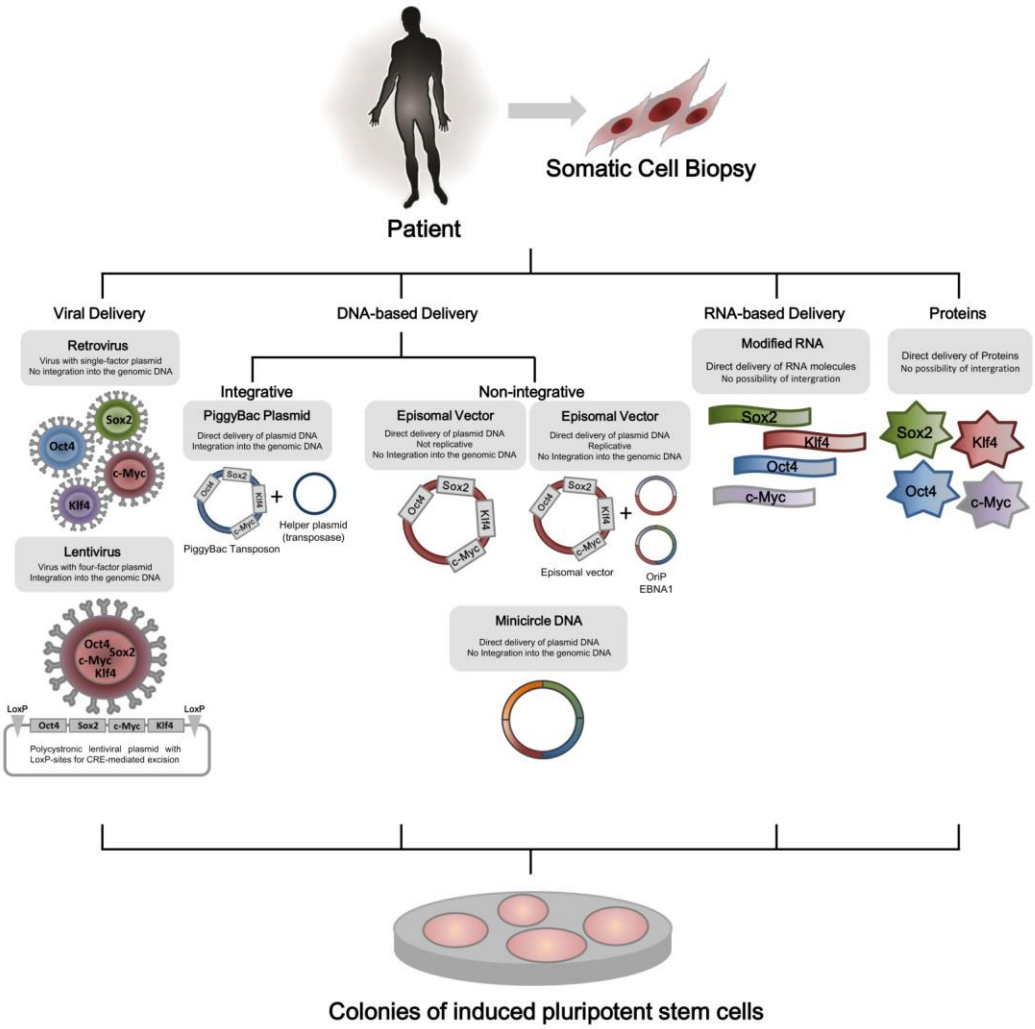

Figure 2.2 Generation of induced pluripotent stem cells.
Numerous techniques for the generation of iPSCs have been developed in the past decade to avoid the necessity of viral delivery of the four reprogramming factors and potential mutagenesis in de-differentiated somatic cells. Viral delivery was first replaced by DNA-based delivery, which however, in the case of integrative DNA fragments, still bares the risk for mutagenesis. RNA-based and protein-based introduction of the four reprogramming factors are the safest reprogramming methods, although their efficiency is still very low.

In fact, when germline competence of retrovirally-reprogrammed iPSCs was tested, about 20% of the chimeric progeny developed tumors, probably due to reactivation of the viral transgenes [249]. In addition, integration of the reprogramming factors into the genome may as well result in tumor formation. Therefore, two studies tested an adenovirus-mediated delivery system [258, 263], as the genetic material of adenoviruses is neither integrated into the host genome nor replicated during cell division: after its release into the host cell, the double-stranded DNA is transcribed and degraded [258]. This reduces the efficiency of reprogramming, which was not

successful when the four reprogramming factors were delivered separately, even if adenoviruses were delivered repeatedly [263]. In one of the studies, reprogramming via plasmid transfection was tested; however, reprogramming efficiency was very low and integration of the plasmid into the genome was detected [263]. To improve reprogramming efficiencies and activate/deactivate the reprogramming factors in a controlled manner, polycistronic lentiviral vectors which contain all transcription factors in a single cassette were developed, whereby gene expression was either regulated by tetracycline (i.e. doxycycline) presence/absence or silenced by Causes Recombination (CRE)-mediated excision of the expression cassette [264-266]. These lentiviral vectors were named STEMCCA ("STEM Cell Cassette") and are now commercially available (Millipore, #SCR548, #SCR518, #SCR513, #SCR512). A subsequent study published by the STEMCCA developers stressed the importance of eliminating residual transgene expression from iPSC lines [267]. However, due to integration of the expression cassette into the genome and to the possibility that activation/deactivation of the oncogenes may not be completely reliable, tumor formation cannot be excluded when using lentiviral STEMCCA plasmids for reprogramming. Therefore, non-viral multiprotein expression cassettes were developed and delivered to somatic cells within a PiggyBac transposon containing a tetracycline trans-activator [268]. A "transposon" is a mobile (=transposable) genetic element: it can change its position within the genome via a non-replicative "cut & paste" or a replicative "copy & paste" mechanism. Long after their discovery, which was awarded with a Nobel Prize in Physiology and Medicine in 1983, transposons were instrumentalized as non-viral gene delivery system [269]. In addition, CRE-mediated factor excision can be used to ensure elimination of the oncogenes from iPSCs [268]. The system seems to represent a reliable means to generate non-genetically modified iPSCs without viral delivery.

Non-integrative reprogramming methods were also developed to bypass the potential and permanent genetic modifications resulting from integration of retroviral and lentiviral vectors, as well as of transposons. Non-replicative as well as replicative episomal (=extra-chromosomal) vectors were used for DNA-based, non-viral and non-integrative reprogramming [270-272]. Episomes are commercially available (ThermoFisher Scientific #A14703) plasmids which can be introduced into somatic cells without viral-mediated delivery and persist as well as replicate in the cytoplasm during the host cell cycle. In absence of a selection drug, plasmid replication does not occur and the episomal DNA is not passed on to the progeny during cell division. Transgene-free progeny can therefore be selected for further use. However, since Episomes in general can persist in the cytoplasm as well as get integrated into chromosomal DNA, a screening is necessary to identify integration-free cell progeny.

Last but not least, two reprogramming methods have been developed, which are not based on DNA delivery and thereby completely bypass the risk for genetic alterations due to insertional mutagenesis: RNA-based and protein-based delivery of reprogramming factors. The first method is based on repeated delivery of a synthetic mRNA molecule which was designed to

overcome immediate degradation by the cell's antiviral response and to be efficiently translated. In addition, the reprogramming efficiencies were very high - however the methodology is relatively complex: RNA engineering, optimization of delivery methods, treatment with soluble interferon to counteract immediate degradation and optimization of cell culture conditions (culture media, feeder cell types, amount of oxygen) were necessary to obtain the desired outcome [273]. In the second study, Oct4, Sox2, Klf4 and c-Myc recombinant proteins containing a poly-arginine (11R) protein transduction domain were generated and transduced into fibroblasts, where they readily entered the nucleus. Repeated transduction as well as the HDAC inhibitor valproic acid (VPA) were used to enhance reprogramming efficiency [274]. Generation of iPSCs using protein transduction is very promising as it relies on a safer, faster and simpler reprogramming method.

Altogether, generation of iPSCs has been performed world-wide using diverse reprogramming techniques and donor cells from several mammalian species and tissues. Although the end-result, i.e. characteristics of the reprogrammed progeny, is generally reproducible, the necessity to define a standardized reprogramming method to reduce laboratory-to-laboratory batch-variability needs to be addressed. In addition, most commonly used reprogramming methods introduce genetic mutations into the donor cells, and reprogramming, as well as characterization of the resulting iPSC line are very time-consuming.

2.4.1.2. Induced pluripotent stem cells for regenerative medicine

Currently, clinical application of PSC-derived progeny comprises five fields: age-related macular degeneration (AMD), Parkinson's disease (PD), SCI, type I Diabetes and myocardial infarction [275]. One clinical trial using iPSCs was started in Japan in an individual with AMD. The outcome was satisfactory, as the patient's vision has stopped deteriorating [276]. However, when the second patient was about to receive the treatment, the presence of potentially dangerous genetic mutations were detected in the iPSC line, leading to the termination of the trial and to critical considerations about the use of iPSCs in a clinical setting [275]. A feasibility clinical trial for the production of autologous retinal pigment epithelial cells from iPSCs was initiated in 2015 to assess the safety and efficacy of the differentiation protocol prior to application in AMD (clinicaltrials.gov ID: NCT02464956). However, there are no reports about the outcome of the study. This example shows that although iPSCs are a highly promising source of any cell type for autologous cell therapy, they are still very far from routine clinical use and have to be used with caution.

One reason behind this is the lack of a standardized production and quality control procedure. While commercially available ESC are well-characterized and have been used for decades of research, iPSCs still remain heterogeneous in terms of reprogramming method adopted, donor tissue, genetic and epigenetic profile, and more importantly of quality. Therefore, while the

potential of iPSCs in the field of regenerative medicine is enormous, as big is the risk of a fragmented development of their application.

Nowadays it becomes more and more common that iPSCs are generated in a core facility, such as the iPSC core facility of the Helmholtz-Center in Munich, Germany (https://www.helmholtz-muenchen.de/ipsc/index.html). The idea behind is to have a central "bank" of iPSC lines, which are generated following highly standardized protocols and throughoutly characterized. In particular, the generation of standardized iPSCs for pre-clinical and clinical use should comply with GMP guidelines.
GMP is a world-wide guideline for ensuring that products, such as f.i. food and pharmaceutical products, are produced and controlled according to quality standards. The guidelines indicate the "minimum requirements" that a manufacturer must meet to make sure that the products are of high quality and of no risk to the customer or patient. GMP fundamentals and a full GMP manual, as well as numerous books about production, validation, quality management and regulations, are published by Maas and Peither GMP Publishing (https://www.gmp-publishing.com/en/gmp-home.html) and cover a whole range of topics including structure and hygienic conditions of manufacturing facilities, environmental conditions, manufacturing processes, manufacturing documentation (Good Documentation Practice, GDP), qualification of operators, product distribution.

GMP regulatory guidelines for "iPSCs as a product" include the type and method for the procurement of somatic donor cells; the derivation, expansion and cryopreservation of iPSC lines; the characterization of their properties, including genetic and epigenetic profile; monitoring of absence/presence of pathogens; monitoring of phenotypical stability over prolonged passaging or storage. Importantly, similar guidelines should be applied to the differentiation procedure.

An ideal pre-requisite for a transfer of iPSCs into routine clinical use would be the establishment of a global "GMP iPSC haplobank" [277]. In fact, while on one side it seems utopic to generate iPSC lines and differentiate them to match any type of target tissue for autologous transplantation *ad hoc* in a timely manner, a haplobank would represent a core storage facility, in which iPSCs are generated in a standardized manner from selected donors, whose profiles matches the widest possible amount of recipients world-wide. For instance, donors would have blood group 0 and would be homozygous for common human leukocyte antigens (HLA), thereby reducing the risk of rejection by the recipient(s). This would reduce the necessity for local GMP compliant iPSC production and reduce global variability of iPSC sources.

Altogether, it is becoming clear that iPSC production and application should be tightly regulated by globally accepted guidelines prior to a transition into the clinic.

2.4.1.3. Differentiation of pluripotent stem cells into neural phenotypes

The relevance of PSCs for regenerative medicine has been extensively discussed above; however neural tissue engineering would not be possible without deep knowledge of the neurodevelopmental mechanisms which underlie the formation of mature neurons and glia and the establishment of neural networks, both in health and disease. Corticogenesis and the complex mechanisms of CNS development have been investigated and recapitulated *in vitro* using PSCs [278], significantly contributing to our understanding of neurodevelopmental processes as well as of neurological disorders. Due to the complexity and inaccessibility of the human brain for experimental investigation, animal models have traditionally been utilized to study embryonic and postnatal CNS development. The advent of PSCs, and especially of iPSCs, opened up the possibility to study human neural development in health and disease [279], culminating in the establishment of 3D *in vitro* cultures, in which differentiating cells self-organize to form complex structures. The latter have been referred to as "organoids". Organoids contain the neural phenotypes normally present in the CNS, and these are in addition self-organized to recapitulate both tissue and organ structure [280-282].

Soon after the discovery of iPSCs, protocols for their differentiation into specific neural lineages have been established, based on early or more recent knowledge gained from ESC *in vitro* differentiation [283-290].

The most common *in vitro* neural induction procedure for hPSCs [288, 291] starts with exposure of free-floating PSC colonies, referred to as embryoid bodies (EBs), to a basic neural medium. Cells acquire a neural plate - homologue neuroepithelial identity and, once plated on a substrate, they self-organize in multi-layered concentric structures, which mimic the closure and stratification of the neural tube and are referred to as neural rosettes (NRs). During neural development, patterning or lineage specification of neural tube progenitors is mediated by exposure to soluble factors called morphogens. For instance, bone morphogenetic proteins (BMPs) and sonic hedgehog (SHH) are released dorsally from the roof plate and ventrally from the notochord, respectively. Neural tube progenitors are exposed to gradients of morphogens, and this in turn leads to their commitment to a specific cell fate: for example, ventrally patterned neural progenitors will give origin to ventral motor neurons. On the other side, exposure to retinoic acid (RA) confers them a caudal or spinal cord phenotype [292-294]. Similarly, NR progenitors are most sensitive to *in vitro* patterning, and commitment to a specific fate is maintained in later stages [288]. After patterning, NRs are manually picked and cultured either at low-adhesion (neurospheres) or on substrate (adherent monolayer) in the presence of the growth factors basic fibroblast growth factor (FGF) 2 and epidermal growth factor (EGF). During this step, neuroepithelial progenitors become tri-potent NSCs and their differentiation will give origin to astrocytes, oligodendrocytes and neurons.

Within the past decade, neural differentiation protocols have been optimized for the directed differentiation of PSCs into a nearly pure desired cell population, such as OPCs [208, 211, 212, 285, 295], astrocytes [205, 296, 297] and neurons. In the latter case, protocols for neuronal differentiation have been additionally fine-tailored in order not to obtain a randomly mixed population [288], but neurons with a defined neurotransmitter-phenotype, including pyramidal neurons [298], midbrain dopaminergic neurons [299-302], spinal motor neurons [206, 303, 304] and serotonergic neurons [207]. Phenotypical specification offers the possibility to investigate or manipulate mechanisms of development or disease progression in a cell population of interest. For instance, iPSC-derived dopaminergic neurons can be useful to investigate molecular mechanisms underlying neurodegeneration in PD. In addition, the healthy neuronal cell population can be engrafted to substitute diseased neurons: healthy dopaminergic neurons can be transplanted in individuals affected by PD. Similarly, neuronal precursors which have been patterned towards a spinal cord phenotype will be more suitable to substitute damaged neurons after SCI than non-spinal cord-residing dopaminergic neurons.
It has to be said, however, that although protocols for directed differentiation of PSCs are very promising, they hardly lead to pure populations without additional selection procedures, such as fluorescence-activated cell sorting (FACS)-mediated purification. In addition, they are not easily reproducible, partially due to the variability of the PSC line used. Thus, these protocols are still not sufficiently robust.

In summary, PSCs are a useful tool for the investigation and recapitulation of neural development, which constitutes the basis for tissue engineering (figure xx). Based on broad knowledge of neurodevelopmental mechanisms, protocols for the directed differentiation of PSC into specific neural phenotypes have been established, however these methods are not easy to reproduce.

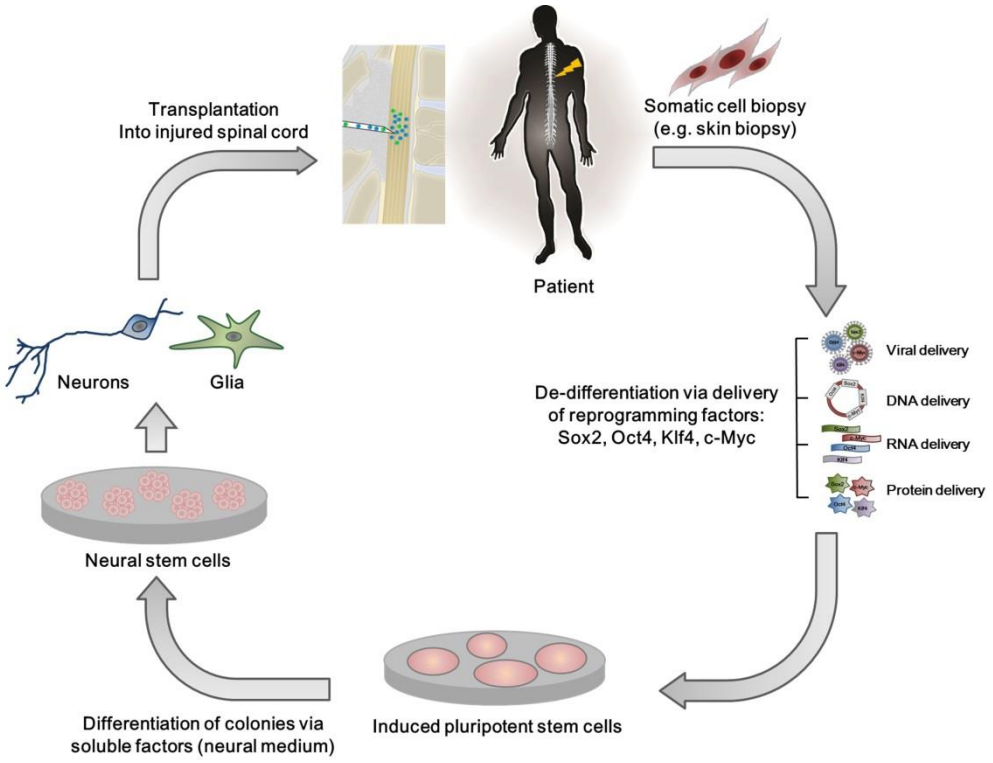

Figure 2.3 Induced pluripotent stem cells for tissue engineering.
Somatic cells, for instance skin cells, can be obtained from any patient in a minimally invasive way. Using viral or non-viral mediated delivery of the four reprogramming factors, somatic cells can be de-differentiated to a ESC-like pluripotent state. Thereafter, by applying soluble factors, they can be guided towards any desired cell fate. For instance, via incubation with basic neural medium, their differentiation into NSCs is promoted. These can in turn give origin to neurons and glia and promote tissue repair, restoration of neural network function and functional recovery after spinal cord injury.

2.4.2. Direct fate conversion of somatic cells into neuronal phenotypes

While one advantage of hPSCs is the high degree of freedom regarding the progeny that can be obtained, a big disadvantage is that most of the differentiation procedures are extremely time-consuming [205]. Moreover, each step of neural induction may introduce additional laboratory-to-laboratory or batch-to-batch variability and strongly influence the outcome of differentiation. For example, both size and density of EBs, NRs and neurospheres or adherent progenitors may affect their sensitivity to a certain soluble factor necessary for directed differentiation. In addition, iPSCs still bear the risk of incomplete differentiation *in vivo* and consequent tumor formation.
In order to shorten the duration of differentiation and to minimize variability, as well as the risk of tumor formation, forced expression of lineage-specific factors has been used to directly

switch the phenotype of somatic cells - this process is called trans-differentiation or direct fate conversion. In 2010/2011 first evidence was published, that combinatorial (forced) expression of neural-lineage-specific transcription factors can efficiently convert fibroblasts into functional neurons *in vitro*, which are referred to as induced neurons (iN) [305, 306]. Mouse iNs not only expressed the neuronal markers ß-III-tubulin, NeuN and microtubule-associated protein 2 (MAP2), but also synapsin, indicative of functional synapses; in addition, electrophysiological recordings demonstrated that they are functional [305]. Using the same transcription factors, human iNs were generated, however these were not electrophysiologically active. Expression of an additional transcription factor and extended culturing time were necessary for neurons to assume mature features [306]. In both studies GABAergic and glutamatergic neuronal phenotypes were predominant. One later study published by the same group demonstrated that one single pro-neural transcription factor, achete-scute family bHLH transcription factor 1 (ASCL1), was sufficient to convert both mouse and gamma-Aminobutyric acid human fibroblasts into functional iNs, which however required a longer maturation process [215]. Subsequently, rodent fibroblasts were trans-differentiated into GABAergic interneurons [307], into OPCs which were able to mature and ensheat axons both *in vitro* and *in vivo* [308], as well as into functional astrocytes [309], demonstrating that fate conversion can be used to obtain a desired neural phenotype without an intermediate pluripotent state.

Altogether, direct fate conversion represents a faster and safer method for the generation of a desired cell phenotype for disease modeling or tissue engineering. However, it is still not clear if the phenotype of trans-differentiated cells is stable for longer time-frames and, similarly to iPSC-derived cells, the limited availability of a human cell population which can be used as a reference makes it difficult to assess how close the phenotype of trans-differentiated cells matches the phenotype of native cells. The progeny obtained by direct fate conversion has low or no proliferation potential and can therefore not be expanded, for instance for transplantation purposes. In addition, in contrast to differentiation of PSCs, only one cell type at the time can be obtained by trans-differentiation. Last but not least, fate conversion is to date induced by viral - mainly lentiviral - delivery of lineage specific transcription factors [215, 305, 308, 309]. As mentioned in 2.4.1.1., viral delivery and genomic integration of the expression cassette are potentially mutagenic. Therefore, although trans-differentiation does not necessarily include a pluripotent stage, the risk for tumor formation cannot be ruled out.

2.4.3. Pluripotent stem cell - derived neural stem cells in pre-clinical studies of spinal cord injury

Soon after the advent of iPSCs and the establishment of neural differentiation protocols, the therapeutic potential of iPSC-derived NSCs for spinal cord injury repair was investigated in rodent models of SCI. The first goals of these studies were to assess safety, survival, differentiation and integration of iPSC-derived NSCs. First, safety of iPSC-derived neurospheres was evaluated by transplantation into the brain of non-obese diabetic / severe combined immunodeficiency (NOD/SCID) mice [229]. Transplantation into the intact CNS is in fact necessary to assess the properties and behavior of iPSC-derived NSCs in a physiologically healthy environment. iPSC-derived NSCs, which did not lead to tumor formation were considered to be safe and were thereafter transplanted into the spinal cord of mice after a contusion injury. Transplanted NSCs differentiated into functional oligodendrocytes, astrocytes and neurons and promoted functional recovery. Myelin-binding protein $(MBP)^+$ myelin produced by oligodendrocytes, BDNF and NT3 likely released by astrocytes, tissue sparing and the presence of $5\text{-}HT^+$ fibers in close proximity to the graft were considered to be potential mechanisms contributing to functional recovery [229]. Next, the therapeutic potential of human iPSC-derived NSCs was examined in NOD/SCID mice after contusive SCI. NSCs differentiated into the three neural lineages, promoted angiogenesis, axonal regeneration and myelination, and formed synapses with host cells. Functional recovery persisted for several months after transplantation [230]. Pro-active contribution of grafted iPSC-derived NSCs, which were expanded in monolayer cultures to enhance homogeneity, to functional recovery was confirmed in a subsequent study by diphtheria-toxin (DT)-mediated selective ablation. This study also for the first time addressed the concept of “neuronal relay” in the context of iPSC-derived NSC transplantation. To this end, WGA-expressing adenoviruses were injected into the motor cortex of spinal cord injured mice. Wheat germ agglutinin or WGA, a plant lectin, which can be passed to second or third-order neurons across synapses, was detected caudally to the injury site. In addition, synapses between transplanted and host cells were detected by immunohistochemistry. Altogether, this study suggested that transplanted iPSC-derived NSC can give rise to functional neurons, which form synaptic connections with descending motor neuron projections as well as with caudal targets, therefore serving as “neuronal relay” and possibly accounting for the observed functional recovery [231]. These three studies addressed relevant questions in clinically relevant contusive SCI models. However, several aspects remained to be addressed. In fact, iPSC-derived NSCs were not patterned to assume spinal cord identities / phenotypes, therefore their efficacy to serve a functional relay in a spinal cord environment might not reach an optimal level. In addition, transplantations were performed acutely or sub-acutely after SCI, raising the question if their therapeutical potential can be exploited in a chronic injury environment. Both these issues were addressed next. Caudalized human iPSC-derived NSCs were transplanted into an “early chronic” model of SCI, four weeks after contusive

injury. In this study, iPSC-derived NSCs were found to differentiate into the three neural lineages, but no functional recovery was detected [310]. This suggests that iPSC-derived NSC transplantation approaches might need to be adapted to be effective in chronic SCI models, but it might also suggest that they might not be effective at all. Lastly, a very impressive study showed robust long-distance axonal outgrowth of transplanted human iPSC-derived NSCs three months after lateral hemisection of the rat spinal cord. Not only axonal outgrowth was remarkable, but extended axons also formed synapses with endogenous neurons. In addition to graft axonal-outgrowth, host axonal-ingrowth was detected, whereby host serotonergic axons penetrated the graft and formed synapses with grafted cells, suggesting the formation of a functional neuronal "relay". However, no functional recovery was detected in this study. Alarmingly, human iPSC-derived axonal terminals were detected in the cortex, olfactory bulb and cerebellum of rats which received transplantation, and iPSC-derived NSCs were detected in the spinal cord central canal distally from the lesion site. More alarmingly, ectopic colony formation was observed in replication studies after transplantation of fetal-derived NSCs into the rat spinal cord, up to the brain stem and 4^{th} ventricle (hindbrain). Ectopic colonies moreover expressed the proliferation marker Ki67 [237, 311, 312]. These findings indicate that although robust survival, differentiation and integration of NSC grafts into the host spinal cord are promising for tissue regeneration, they may also lead to undesired and potentially deleterious outcome.

All in all, the presented studies addressed key aspects of iPSC-derived NSC transplantation after SCI. Transplanted cells are able to differentiate and integrate into the host spinal cord by functionally interacting with host cells, as well as to contribute to functional recovery. However, functional recovery was not observed throughout all studies, possibly due to the batch-to-batch variability of transplanted cells or of the adopted experimental procedure. In addition, although synapse formation was detected, whether these synaptic connections are electrophysiologically active was not demonstrated.

In general, several mechanisms of action of iPSC-derived NSCs have been identified (myelination, production of neurotrophic factors, "relay" formation) as potential contributors to functional recovery. Still, to date it is not clear which role they play and the extent or necessity of their contribution needs to be determined. One reason behind this issue is the mixed phenotypical identity of iPSC-derived differentiated NSCs. Batch-to-batch NSC variability may lead to differentiated progeny with variable compositions of neurons and glia. The latter, in turn, fulfill very specialized tasks in the healthy and injured CNS. For instance, a true spinal cord "relay" mechanism can only be mediated by neurons, which receive an excitatory signal and convey it to the next neuron, such as glutamatergic neurons. In this case, forebrain GABAergic inhibitory or midbrain dopaminergic neurons are most likely of no use. On the other side, astrocytes produce ECM molecules and secrete neurotrophic factors such as BDNF, GDNF, NT-3 and VEGF, which can promote axonal regeneration. Therefore, variable extent of astrocytic

differentiation in independent studies might lead to differential endogenous regeneration. In order to address mechanisms of tissue repair and promote functional recovery in a more controlled way, it is necessary to transplant well-characterized cells with a tailored phenotype.

2.5. Astrocytes for tissue replacement after spinal cord injury

Glial cells constitute about 90% of cell of the human brain [313], and are often being referred to as the "brain glue" due to their multiple roles in brain physiology, metabolism, development and disease, as well as response to traumatic injury. Astrocytes, which account for 20-40% of the total cells in the mammalian brain [314], regulate blood flow, homeostasis of water, ions, neurotransmitters, sugars and metabolites, secrete ECM components, regulate synapse formation and neurotrophins and modulate neuronal network activity. Therefore, they are crucial for brain function in health and disease.

In a broad sense, astrocytes are glial cells of typically stellate morphology, characterized by extension of some big processes and numerous small processes. Astrocyte have been subdivided into two main categories based on their morphologies: protoplasmic astrocytes are located in the gray matter and have numerous short highly branched processes, whereas fibrous astrocytes are located in the white matter and have long sparsely branched processes. However, the astrocytic population is extremely heterogeneous: glial progenitors are subject to developmental patterning, leading to morphological und functional diversity, which is not well characterized and under investigation [315, 316].
It has been shown that astrocytes are organized in individual spatial domains: spatial overlap between two adjoining astrocytes amounts approximately 5% of their volume and only involves the outer portion of their processes, whereas the core region is never penetrated by other astrocytes [317, 318]. Within each domain, a single astrocyte can regulate the function of 10^5 synapses in the rodent cortex and hippocampus and likely more than 10^6 in the human cortex [319]. Moreover, at least one astrocytic end-foot surrounds blood vessels [320]. Accordingly, each astrocyte plays a role in the regulation of both neural network and neurovascular function.

From a neurodevelopmental point of view, specification and maturation of astrocytes has been extensively investigated but remains confusing, especially in terms of marker expression [321]. Initiation of astrogliogenesis or specification from an $A2B5^+$ glial restricted precursor (GRP) [322] has been attributed to the transcription factors Sox9 and nuclear factor I-A (NFIA), which act synergistically to regulate genes involved in glial specification [323]. Following the gliogenic switch, NFIA induces expression of excitatory amino acid transporter 1 (EAAT1 also known as GLAST) in astroglial precursors, one of the two major astrocytic glutamate transporters [324]. Thereafter, maturing astrocytes are characterized by expression of the canonical astrocytic marker glial fibrillary acidic protein (GFAP), as well as by expression of S100 calcium-binding protein ß (S100ß), aldehyde dehydrogenase 1 family member L1 (Aldh1l1), the cell surface

marker CD44, the water channel aquaporin 4 (Aqp4), the astrocytic gap junction component connexin 43 (Cx43), aldolase C (AldoC) and the glutamate transporter EAAT2 (also known as GLT1), the latter four being associated with mature astrocytes [325-331]. However, timing of astrocytic marker expression is still not throughoutly clear. For instance, although Aqp4 is considered to be a hallmark of mature astrocytes [332], it is also expressed in subventricular zone-residing postnatal NSCs [333]. In addition, expression of the cytoskeletal filament marker vimentin has been associated with immature as well as with reactive astrocytes [334-336].

Hereafter, the roles of astrocytes in the healthy as well as damaged CNS will be briefly reviewed.

2.5.1. Role of astrocytes in the healthy central nervous system

2.5.1.1. Cerebrovascular regulation of water, ion and sugar homeostasis

Neural activity is a complex process, which demands a lot of energy. Therefore, the CNS is extremely dependent on continuous supply of energy sources, such as lactate, ATP and glucose, through the blood flow. It has been shown that the distribution of the cerebral blood flow is regulated according to the functional activity of different brain regions in time: when the activity of a certain brain region increases, also the blood flow in this region is increased. This mechanisms is called hyperaemia and is responsible for adequate delivery of energy sources to meet the needs of different tissues under physiological and pathological conditions [337]. Adjustments in blood circulation at a micro-environmental level are regulated by neurovascular units, which comprise endothelial cells (blood vessels), pericytes, a neuronal process and an astrocytic end-foot, as well as microglia and smooth muscle cells. Neurovascular units are not only important for modulating cerebral blood flow, but also play a big role in the regulation of the BBB [338-340]. Astrocytic end-feet almost completely enwrap blood capillaries; here, through the water channel Aqp4, multiple types of K^+ channels and purinergic P2Y receptors [320], astrocytes regulate water and ion homeostasis and respond to purinergic signals (ATP).
Importantly, extracellular K^+ ion concentrations play crucial role in synaptic transmission: maintenance of a constant level of K^+ during neuronal activity is a pre-requisite to maintain neuronal excitability [341].
On the other side, astrocytes release ATP in response to neurotransmitters through connexin hemichannels linking adjacent astrocytic processes in order to activate their own purinergic receptors. These results in intracellular Ca^{2+} fluctuations which propagate from one astrocyte to adjacent astrocytes, process referred to as $Ca2^+$ wave. In addition, ATP's catabolic end-product adenosine, which is released by astrocytes in the neurovascular unit, leads to vasodilation [342] and consequently to a decrease in vascular resistance and an increase in local blood flow. Therefore, through their role in the neurovascular unit, astrocytes are potent regulators of cerebral blood flow and therefore of energy supply.

Glucose is the metabolite which provides most of the energy needed in the brain. One very prominent human brain imaging technique, positron emission tomography or PET, is based on detection of 2-deoxyglucose in functionally and therefore metabolically active brain regions [343]. Interestingly, astrocytes respond to enhanced neuronal activity, particularly to the neurotransmitter glutamate, with increased production of glucose and with enhanced aerobic glycolysis. As a metabolic result, astrocytes produce and release lactate, which is taken up by neurons and used as alternative source of energy [343-345]. Hence, astrocytes serve as providers of energy for neurons.

2.5.1.2. Regulation of neurotransmitter homeostasis

In addition to K^+, extracellular and intracellular concentrations of Na^+ ions are of pivotal importance for neuronal and glial physiology. In the CNS, Na^+ concentrations are crucial for the regulation of neurotransmitter homeostasis: most astrocytic neurotransmitter transporters are dependent on trans-membrane Na^+ gradients to regulate extracellular neurotransmitter concentrations. Specifically, the glutamate (EAAT1 und EAAT2), GABA (GATs) and glycine (GlyT1 and GlyT2) transporters require co-transport of Na^+ ions to the intracellular space for an efficient uptake of the corresponding neurotransmitters. Stimulation of neuronal fibers leads to elevation of intracellular Na^+ concentrations in astrocytes, which is coupled to neurotransmitter clearance [346]. The latter is crucial to ensure neuronal network activity: when glutamate is released from excitatory synapses, only rapid removal from the extracellular space will allow continuous neurotransmission. In addition, glutamate can be excitotoxic by leading to neuronal overstimulation, which results in neuronal degeneration. Under pathological conditions, such as traumatic injury of the CNS, excessive synaptic release, decreased clearance and leakage of glutamate from damaged cells contribute to an increase in extracellular glutamate concentrations. This in turn results in a secondary degeneration cascade [347]. The astrocytic transporters EAAT1 and EAAT2 maintain low extracellular concentrations of glutamate; in particular, EAAT2 accounts for more than 90% of the total glutamate uptake in the brain [347, 348]. Therefore, defects in astrocytic glutamate transporter function might have a deleterious impact in the CNS. For example, expression of a defective splice variant of EAAT2 has been associated with Alzheimer's disease (AD), although it is not clear if this is causal or consequential [349-352]. Once taken up by astrocytes, glutamate is metabolized to glutamine by the enzyme glutamine synthetase. Thereafter, glutamine is transported back into neurons, where it can be used as substrate for the synthesis of glutamate [346].

In summary, Na^+-dependent glutamate uptake and metabolism by astrocytes is crucial for the maintenance of neuronal network activity.

2.5.1.3. Modulation of neural network activity

As mentioned above, a single astrocyte can contact potentially more than 10^6 synapses in the human brain. Accordingly, one single astrocyte is able to sense, modulate and integrate information from several neighboring neurons at once [353]. Since astrocytes are organized in non-overlapping spatial domains [317, 318], the activity of a particular synapse is regulated by one astrocyte only. Astrocytes are able to sense neurotransmitters and react with intracellular Ca^{2+} fluctuations, phenomenon which is referred to as non-electrical excitability [353] and which allows them to monitor synaptic activity and react accordingly. In fact, astrocytes do not only sense but also release neuromodulators, termed "gliotransmitters". These include ATP, adenosine, D-serine and glutamate [353]. For instance, in response to stimulation, Ca^{2+} is released from endoplasmic reticulum stores into the cytoplasm of astrocytes, which in turn may trigger release of glutamate into the extracellular space. Glutamate can here bind to pre-/ or post-synaptic glutamate receptors (mGluR and NMDARs) and regulate neuronal glutamate release and synaptic transmission. Astrocyte-released glutamate has been shown to modulate short-term plasticity of excitatory synapses by increasing (facilitation) or decreasing (depression) their strength [354, 355]. Interestingly, spatial localization and kinetics of glutamate-induced Ca^{2+} fluctuations are dependent on the concentration and duration of extracellular glutamate application: low concentrations of glutamate induce asynchronous Ca^{2+} fluctuations in single astrocytes or even in micro-domains within astrocytic processes without propagation to the soma; in contrast high concentrations of glutamate induce a global intracellular Ca^{2+} increase, which can propagate between adjacent astrocytes [355-357]. These so called astrocytic "Ca^{2+} waves" are considered to be one key mechanism of long-range modulation of neuronal network activity. The recognition of this bi-directional communication between neurons mediated by neurotransmitters led to the concept of "tri-partite synapse". In this model a pre-synaptic terminal, as post-synaptic dendritic spine and an astrocytic process converge to form a functional unit [355].

In summary, astrocytes are able to sense neuronal activity at a micro-domain and at a global level and can modulate synaptic transmission via fluctuations of intracellular Ca^{2+} concentrations and release of gliotransmitters.

2.5.1.4. Production of extracellular matrix

Among their functions, astrocytes are able to shape the extracellular environment to provide a stable milieu for neuronal activity: both neurons and astrocytes synthetize ECM components to support formation, maintenance and function of synapses [358]. Interestingly, ECM components are expressed in dynamic patterns during development and in the adult CNS [359], suggesting that they tightly regulate developmental processes as well as postnatal CNS function [360]. In

addition, the ECM is altered after traumatic injury of the CNS [28], in brain aging [361], as well as in several diseases of the nervous system [362-364].

The ECM is an ensemble of glycoproteins and proteoglycans which form a highly organized environment embedding cells and regulating their interactions with molecular ligands or with other cells. ECM glycoproteins include laminin, tenascins and thrombospondins; proteoglycans, on the other side, can be subdivided into two major classes based on the type of GAG covalently linked to the core protein: heparin sulphate proteoglycans (HSPGs) and CSPGs [358].

The neuronal soma, their proximal dendrites and the initial segment of the axon are enwrapped by a condensed and specialized ECM which is referred to as “perineuronal net” (PNN) and was first described by Camillo Golgi in 1882. The main components of the PNN are tenascin-R, hyaluronan (HA), CSPGs and link proteins, which stabilize the interaction between the latter two. On the other side, the C-terminal domain of CSPGs binds to trimeres of Tenascin-R [365, 366]. The function of the PNN has not been fully understood yet, however it has been suggested to ensheat and thereby support highly active neurons, especially in terms of synapse formation and synaptic activity/plasticity. In fact, development of new synapses is coupled to the emergence of the PNN. On the other side, the negative charge of GAGs might serve as cation buffering agent, controlling the diffusion of K^+, Na^+ and Ca^{2+} ions and therefore neuronal activity [366].

Again, the role of astrocytes is crucial: they are able to secrete relevant ECM components, such as collagen, fibronectin, laminin, tenascin-C, thrombospondins, decorin, HSPGs such as glypican and syndecan and CSPGs such as versican, brevican, neurocan and phosphacan. Therefore, they contribute to the PNN, as well as to healthy CNS ECM and ECM alterations in CNS disease and after traumatic injury [28].

2.5.1.5. Astrocytic secretome

Via exocytosis, diffusion through trans-membrane pores and active trans-membrane transport, astrocytes also serve as CNS secretory cells: they secrete diverse substances which contribute to CNS development and homeostasis, synaptogenesis and neuronal network function [367]. This secretory network has been termed “gliocrine system” [368].

Components of the astrocytic secretome are neuro-/gliotransmitters, neuromodulators, hormones and peptides, metabolic substrates, scavengers of reactive oxygen species (ROS), inflammatory factors and, last but not least, growth factors and neurotrophic factors [368]. One prominent example is BDNF, a powerful regulator of dendritic and axonal growth during development and of their maintenance in the mature CNS [369]. BDNF is produced both by neurons and by astrocytes [370] and has two main forms: pro-BDNF, which binds to the neurotrophin receptor p75, and mature or mBDNF, which binds to TrkB receptors.

Interestingly, neurons usually release pro-BDNF which is taken up and processed by astrocytes to its mature form prior to release into the extracellular space [371]. While mature BDNF promotes survival, differentiation, synaptic long-term potentiation and neurite outgrowth as well as arborization through cytoskeleton remodeling, pro-BDNF is involved in the regulation of apoptosis, long-term depression, as well as neurite pruning and retraction, [369, 372]. Therefore, a well-balanced ratio of neuronally produced pro-BDNF and astrocytically secreted mature BDNF is crucial for an appropriate maintenance of neuronal circuit connectivity and activity.

Both neurons and astrocytes also secrete GDNF, a potent neurotrophic factor which predominantly has trophic and neuroprotective effects on dopaminergic neurons [373] as well as noradrenergic, serotonergic and peripheral motor and sensory neurons [374]. Due to its trophic effect on dopaminergic neurons, GDNF has been under investigation as possible target for the treatment of PD and has been already applied in clinical trials [375-378]. In addition, a neurodevelopmental role has been attributed to GDNF in the pre-/ and postnatal regulation of primary sensory and motor neuron development [379].

NGF, also secreted by astrocytes [380], was the first nerve growth promoting factor discovered [381, 382] and supports survival and maintenance of several types of neurons in the CNS and PNS. Similarly to BDNF, NGF can have two forms: a less active pro-NGF form and a mature or ß-NGF form. When secreted, NGF binds to its receptor TrkA prior to uptake into neurons, where it exerts functions in survival, differentiation and growth of cholinergic, sympathetic and sensory neurons. It has been shown that NGF signaling plays a big role in the development of neuropathies, including diabetes and HIV-associated neuropathy, as well as in neuroprotection of cholinergic neurons in the basal forebrain complex, which is highly affected in AD. Based on this rationale, both pre-clinical and clinical studies have been conducted, where NGF was delivered to address neuropathies and neurodegenerative CNS diseases [383].

Altogether, both neurons and astrocytes secrete neurotrophic factors which regulate neurodevelopment, neuronal survival, differentiation, growth and arborization, pruning and retraction as well as neuronal network activity.

2.5.2. Reactive astrogliosis and glial scar formation

One hallmark of CNS pathologies is reactive astrogliosis, a process in which astrocytes undergo morphological and functional changes in reaction to the altered CNS environment. Astrocytes respond to several forms of CNS insult, including infection, ischemia, neurodegenerative disease and traumatic injury [384], thereby significantly influencing pathobiology. Reactive astrogliosis is however a highly complex and still not throughoutly understood phenomenon.

Several molecular mediators leaking from the disrupted BBB or released by neurons, oligodendrocytes, microglia, endothelial cells, leukocytes or other astrocytes in response to insult have been shown to trigger aspects of reactive astrogliosis. These include cytokines and growth factors, such as LIF, CNTF, tumor necrosis factor (TNF) α, interferon (INF) γ, interleukin (IL) 6 and IL10; neurotransmitters, such as glutamate and noradrenalin; ATP; nitric oxide and ROS; Amyloid-ß; hypoxia and glucose deprivation. As a consequence, astrocytes (I) undergo hypertrophy or structural changes, particularly concerning the expression of intermediate filaments (GFAP, vimentin, nestin), (II) increase proliferation and migration rates, (III) act in a pro-inflammatory or anti-inflammatory manner, (IV) regulate extracellular homeostasis and (V) contribute to the formation of a glial scar [384].

After traumatic injury of the CNS, tissue remodeling leads to the formation of a mature lesion, in which three major components can be identified: the lesion core, compact astrocytic scars and perilesion perimeters. The lesion core is characterized by a fluid-filled cyst of variable size or by a permanent fibrotic scar containing non-neural cells and ECM, as well as cellular debris, inflammatory and inhibitory molecules. The astrocytic scar is initiated by proliferation and migration of astrocytes to the lesion site to form a dense cellular barrier surrounding the lesion core [385], with packing densities up to double than in healthy tissue [24]. The perilesion perimeter is constituted by neural cell types, including neurons, oligodendrocytes and astrocytes which exhibit gradually decreasing reactive phenotypes with increasing distance from the lesion core [385].

As major component of the glial scar, astrocytes exert diverging effects after injury: on one side they are neuroprotective by confining the lesion core in order to prevent diffusion of injury-induced signals and consequent secondary damage; on the other side they represent an impediment to axon regeneration by expressing growth inhibitory molecules, including growth inhibitory ECM [24, 28, 385]. As mentioned above, CSPGs are upregulated in glial scar forming astrocytes and significantly contribute to the non-permissive environment leading to regenerative failure [28, 48]. Digestion of CSPGs with chondroitinase ABC has been extensively exploited in pre-clinical SCI studies in order to reduce the growth-inhibitory lesion environment and pave the way for regenerating axonal projections.

Although the astrocytic scar has been widely regarded as one major impediment to neuroregeneration, its disruption does not have pro-regenerative effects, but the exact opposite. One recent study throughoutly addressed this issue in a rodent SCI model by a triple approach: (I) loss-of-function strategies to ablate scar-forming astrocytes, (II) genetic attenuation of scar-forming astrocytes and (III) ablation of chronic astrocytic scars. Interestingly, transgenic ablation or disruption of the glial scar did not lead to a significant reduction in CSPG expression in the lesion core or in adjacent regions, indicating that non-astrocytic scar-forming cells produce considerable amounts of CSPG. Next, although regeneration of injured axons was boosted by conditioning lesions of by neurotrophic factor delivery, regeneration was not

augmented but instead completely prevented in mice with defective glial scar. At a mechanistic level, the study showed that scar-forming astrocytes are able to up-regulate growth supportive CSPGs and laminin [25]. In conclusion, the study challenges the dogma which sees astrocytic scar formation as principle cause of CNS regenerative failure by demonstrating that glial scar disruption does not rescue but exacerbate it.

In summary, astrocytes play a major role in the response of the CNS to traumatic injury by integrating several environmental signals and undergoing morphological and functional changes (figure 2.4).

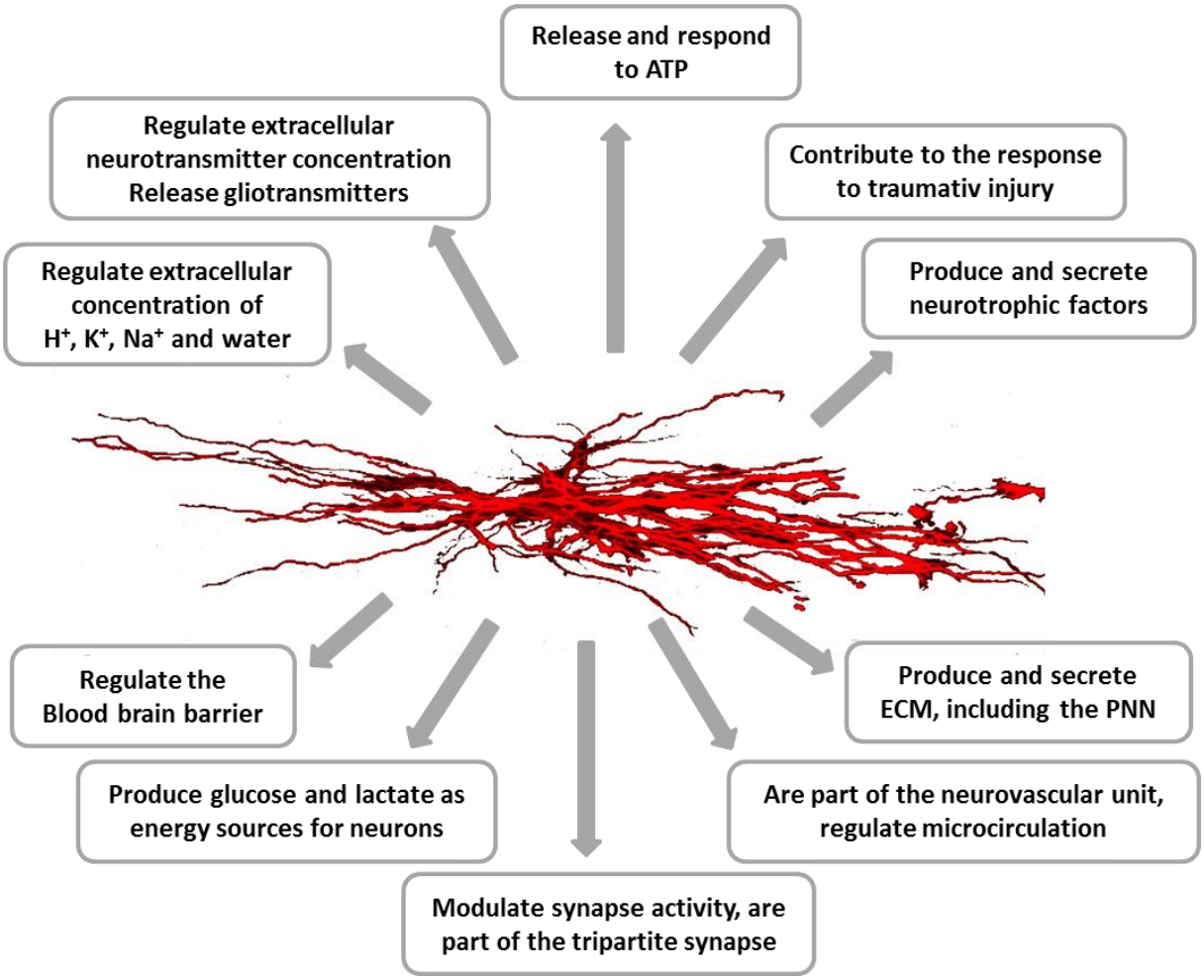

Figure 2.4 Astrocytes have a crucial role in the healthy and diseased CNS.
Astrocytes are a key component of the CNS: they regulate homeostasis of water, ions, metabolites and neurotransmitters; they produce ECM components and neurotrophic factors; they regulate the BBB and contribute to the response to traumatic injury; they regulate synapse formation and function. These are only selected features of astrocytes: their contribution to neural network development and function as well as to the response to injury is indispensable.

2.5.3. Transplantation of astrocytes following central nervous system trauma

Due to the multiple and crucial roles of astrocytes in the CNS both under physiological and under pathological conditions, they represent a very attractive cell source for transplantation after SCI. They can contribute to restoration of tissue integrity by filling the lesion site and providing physical, trophic and metabolic support to damaged or sprouting axons. Through production of a permissive ECM or PNN-specific ECM, as well as through release of neurotrophic factors, they can influence neuronal growth and neural network connectivity. Through neurovascular units, they can regulate exchange of water and sugar between the vascular system and neurons, thereby ensuring adequate supply of energy to meet the neural network's requirements. In addition, through regulation of ions and neurotransmitter homeostasis, they regulate neuronal activity. Therefore, reconstitution of damaged neural tissue may not be possible without an astrocytic scaffold.

Several pre-clinical SCI studies have been conducted, in which astrocytes have been transplanted into the lesion site as substrate for repair. In transection as well as dorsal column injuries of the rat spinal cord, astrocytes differentiated from rat embryonic GRPs were found to promote robust axon growth and recovery of locomotor function. After unilateral dorsal column lesion, transplanted astrocytes were able to fill the lesion site, counteract endogenous astrogliosis and delay the expression of growth-inhibitory ECM components, thereby contributing to axon-growth into as well as beyond the lesion site. When performing in a grid walk test, rats which received astrocytic transplants performed significantly better than lesioned rats [222]. In a subsequent study, the authors compared rat embryonic GRP-derived astrocytes which were differentiated in the presence of either CNTF or BMPs. Both factors contribute to the commitment of multipotent CNS precursors to an astrocytic fate [386]. Morphological differences between the two astrocytic populations were detected, as BMP-treated GRPs gave origin to big, flat astrocytes, whereas astrocytes differentiated with CNTF where rather small, thin and bipolar. Once transplanted after dorsal column lesion of the rat spinal cord, CNTF-astrocytes survived well at the lesion site, but produced inhibitory CSPGs and were not able to induce axonal regeneration or functional recovery. In contrast, BMP-astrocytes did not express inhibitory CSPGs and promoted axon growth and locomotor recovery [387]. This study addressed, for the first time, the question whether some astrocytic subtypes may be more suitable than others to promote repair after SCI. The authors confirmed this hypothesis with astrocytes derived from human 9-week old fetuses in the presence of either CNTF or BMP. Supporting their previous findings, they demonstrated that astrocytes treated with BMP were more suitable to promote regeneration after SCI [388]. However, other studies showed that there was no difference between the two astrocytic populations in the pro-regenerative

capacity after transplantation into the rat injured dorsal column, and functional improvement promoted by BMP-treated astrocytes could not be reproduced [389, 390].
Further pre-clinical studies addressed more in detail astrocytic mechanisms of action underlying their beneficial effects after CNS trauma. In particular, the authors focused on the ability of astrocytes to clear extracellular glutamate, which may accumulate at the injury site due to primary damage and in turn induce secondary damage. In fact, the astrocytic glutamate transporter EAAT2 (also known as GLT-1) is lost at the lesion core after SCI and newly generated astrocytes lack EAAT2 expression [391]; as a consequence, defective clearance of glutamate and its accumulation in the extracellular space may result in susceptibility of the CNS tissue to further damage. To test their hypothesis that astrocytic glutamate clearance is relevant for spinal cord neuroprotection and repair, the authors transplanted mouse glial progenitors overexpressing EAAT2 into the spinal cord of rats which were subject to hemi-contusion of the spinal cord. Indeed, lesion size was reduced in rats which received EAAT2-overexpressing astrocytes; in addition, transplanted cells preserved phrenic motor neurons and consequently diaphragm function [392]. By AAV-mediated overexpression of EAAT2 in endogenous astrocytes of the injured cervical dorsal horn in mice, the authors also demonstrated that defective glutamate clearance may underlie the development of neuropathic pain after SCI, which can be reversed by restoration of astrocytic EAAT2 function [393].

Altogether, this first set of pre-clinical evidence demonstrates the relevance of astrocytes for spinal cord neuroprotection and repair. However, astrocyte transplantation has not been sufficiently investigated to date.

2.5.4. Generation of astrocytes from pluripotent stem cells

In the above mentioned studies, morphologically and functionally distinct astrocytic populations were differentiated from fetally-derived murine or human GRPs. However, these do not represent a suitable cell source for autologous transplantation and always have to face ethical implications relative to the use of fetuses for experimental and clinical research. On the other side, although the generation of safe, non-tumorigenic iPSCs is still being addressed world-wide for future applications, iPSCs represent a cell source of unlimited potential and protocols for their efficient differentiation have been established. While most efforts have been focused on the generation of specific neuronal populations, little attention has been dedicated to the generation of transplantable astrocytes.

Commitment of neural precursors to the astrocytic phenotype can be induced in multiple ways. Two decades ago it was shown that the cytokine LIF and the neurotrophic factor CNTF, which act through the same receptor/signaling system (gp130), are potent inductors of astrocytic fate commitment: CNTF was able to induce astrocytic differentiation in more than 98% of precursors isolated from the fetal murine brain [386, 394]. At the same time, BMP4 and BMP2 were found

to induce commitment of subventricular zone-residing NSCs and bipotent oligodendroglial-astroglial cortical progenitor cells to the astroglial cell fate, respectively [386, 395, 396]. Interestingly, CNTF and BMP4 exerted their astrocyte-inductive effects by distinct pathways [386], suggesting that they might drive specification of phenotypically distinct astrocytes. Indeed, when directly compared, astrocytes differentiated from GRPs with either CNTF or BMPs had distinct properties [387, 389], although their phenotypical properties could be reversed by interchanging the treatment. While $A2B5^+$ GRPs treated with fetal bovine serum (FBS) or BMP gave origin to flat, stellate $A2B5^-/GFAP^+$ astrocytes, CNTF treatment led to intermediate $A2B5^+/GFAP^+$ with long processes; phenotypical properties were not reflected in a different pro-regenerative potential *in vivo* [389]. In addition to CNTF and BMP4, fetal serum was found to be a potent inductor of astrocytic maturation *in vitro* [335], and is currently used in astrocytic cultures, despite its not well characterized composition.

The first published protocols for the efficient generation of astrocytes from PSCs [205, 397] were based on prolonged culturing of neurospheres in minimal neural medium at low adhesion conditions: the authors postulated that, while early neurospheres are neurogenic, neurospheres cultured at least until day *in vitro* (DIV) 180 under these conditions become gliogenic due to a natural commitment-switch of neural precursors to the astrocytic lineage. After the gliogenic switch, progenitors were plated on a laminin substrate and their maturation was induced by treatment with CNTF. Using this simple approach, the authors were able to obtain nearly pure $GFAP^+$ astrocytic populations which were: (I) regionally patterned, following treatment of NRs with the caudalizing agent RA, with the anteriorizing agent FGF8 and with the ventralizing agent SHH; (II) functionally active, as demonstrated by electrophysiological measurements of glutamate uptake and Ca^{2+} waves. Although the results of this study are convincing, the generation of pure astrocytic populations using this extremely simple protocol seems unrealistic. In addition, the fact that six months are required for completion is a major drawback from a clinical point of view.

While the above mentioned protocol relies on GFAP expression as a hallmark of astrocytic identity, another study addressed the complexity of astrocytic maturation and the phenotypical diversity of mature astrocytes. For instance, it has been shown that protoplasmic astrocytes are rather mature/quiescent and express low levels of GFAP but high levels of EAAT2, whereas fibrous astrocytes are rather reactive and express high levels of GFAP but low levels of EAAT2 [296]. Using dual-SMAD-inhibition-based induction of iPSC neural differentiation and exposure of neural progenitors to 1% FBS, the authors obtained nearly pure populations of maturing astrocytes within DIV 90. To induce maturation of astrocytes, instead of using the canonical CNTF treatment, the authors treated the cultures with FGF1 after FBS withdrawal. As a consequence, expression of GFAP, as well as the early astrocytic markers NFIA and connexin 43 were down-regulated, while glutamate uptake was increased – hallmark of a mature/quiescent astrocytic phenotype. However, this seemed to underlie increased expression of EAAT1, but not

EAAT2. In contrast, exposure of progenitors to TNFα led to a reactive astrocytic population, characterized by significant increase in chemokine expression.

As previously mentioned, the importance of astrocyte-mediated glutamate clearance was investigated in a rodent model of SCI [392]. The same group examined the efficacy of human iPSC-derived astrocytes in this respect. Neural progenitors with a caudal phenotype were obtained by dual-SMAD-inhibition and exposure to RA. Subsequently, exposure to neural medium supplemented with FBS for 60 DIV was used to induce astrocytic differentiation. Prior to transplantation, overexpression of EAAT2 in iPSC-derived astrocytes was induced lentivirally, as regular iPSC-derived astrocytes expressed little-to-no EAAT2. Astrocytes were injected immediately after C4 unilateral contusion in mice; EAAT2 expressing astrocytes led to reduced lesion size, as well as preservation of diaphragm innervation by phrenic motor neurons and of diaphragm function [398]. This study demonstrated the potential benefits of iPSC-derived astrocyte transplantation after SCI. However, the use of a lentiviral vector for the induction of EAAT2 expression may lead to mutagenesis. Ideally, EAAT2 expressing, glutamate sequestering astrocytes should be generated without genetic modifications.

To date, no study has used a comparative approach to identify iPSC-derived astrocytes suitable for transplantation after SCI.

2.6. Rationale and Hypotheses

Previous studies have demonstrated that transplantation of astrocytes with specific characteristics can be beneficial after SCI [222, 387, 388, 392, 393]. In particular, Davies et al. directly compared two astrocytic subtypes derived from murine or human glial restricted precursors upon terminal differentiation with FBS in combination with either CNTF or BMPs. Davies et al. pointed out that different astrocytic subtypes exhibit a more or less pronounced ability to serve as pro-regenerative substrate in the injured spinal cord [222, 387, 388]. On the other side, Falnikar et al. and Li et al. demonstrated the beneficial effect of astrocytes overexpressing the glutamate transporter EAAT2, also known as GLT-1, in an animal model of cervical SCI [392, 393]. Thus, selection of astrocytes with a distinct phenotypical and functional profile might increase the efficacy of this therapeutical approach. Generation of large amounts of astrocytes from human iPSCs for autologous transplantation is not subject to ethical debate and was achieved in independent laboratories [205, 296, 397, 399, 400]. These protocols were used as a reference to generate astrocytes from two iPSC lines and one well-characterized commercially available ESC line, which was used as a control.

Hypothesis 1:
Astrocytes can be generated from human ESCs and iPSCs by replication of previously published protocols. Astrocytes obtained following the same procedure will exhibit a similar profile.

Hypothesis 2:
Astrocytes terminally differentiated with CNTF, BMP2/4 or FGF1 are phenotypically different. The phenotypical profile acquired *in vitro* is at least partially maintained *in vivo* and therefore extensive *in vitro* characterization allows the selection of an astrocytic population which is more suitable to support neuroregeneration *in vivo*.

Hypothesis 3:
Pre-differentiated astrocytes survive after transplantation into the spinal cord, mature into their final phenotype and are able to restore tissue integrity as well as to promote regeneration of damaged neuronal projections.

The experimental goal of this thesis was the generation and extensive *in vitro* as well as *in vivo* characterization of astrocytes to define the characteristics of an astrocytic substrate suitable to promote regeneration after SCI.

To test hypothesis 1, I partially replicated and modified previously published protocols [205, 397], whereby terminal differentiation was performed not only with CNTF, but also with BMP2/4 and FGF1. Authenticity of the astrocytic phenotype was assessed by calcium imaging in

response to ATP stimulation, as responsiveness to ATP is a peculiar property of mature astrocytes [401].

To test hypothesis 2, I analyzed the morphological and functional profile of astrocytes differentiated for two weeks. This included (1) cell size and basic morphology, (2) expression of astrocytic markers, (3) expression of NSC markers and proliferation markers, (4) expression and secretion of ECM components and of the neurotrophic factor BDNF and (5) direct influence on neurite elongation in co-cultures with primary DRG neurons. To test if their phenotype was stable and maintained *in vivo*, their expression profile was analyzed after transplantation into the spinal cord of Fischer 344 rats.

To test hypothesis 3 pre-differentiated astrocytes were transplanted into the spinal cord of Fischer 344 rats after a dorsal column wire knife lesion at level C4.

3. Materials and methods

3.1. Materials

3.1.1. Chemicals, reagents and kits

Chemical	Company
Adenosine triphosphate (ATP)	Sigma Aldrich
Aprotinin	Sigma Aldrich
ß-Mercaptoethanol	Roth
Bovine serum albumin (BSA)	Sigma Aldrich
$CaCl_2 \cdot 2H_2O$	Roth
D(+)-Sucrose	Roth
Ethylenediaminetetraacetic acid (EDTA)	Roth
Ethanol 99.8% (denatured)	Roth
Ethylene glycol	Roth
Donkey serum	Biochrome
Fluoromount-G	SouthernBiotech
Fura-2-acetoxymethyl ester (Fura-2)	Sigma Aldrich
Glacial acetic acid	Roth
Glucose	NeoLab
Glycine	Sigma Aldrich
HCl	VWR
4-(2-hydroxyethyl)-1-piperazineethanesulfonic acid (HEPES)	Roth
Isopropanol	Roth
KCl	NeoLab
Methanol (MeOH)	Roth
$MgCl_2 \cdot 6H_2O$	NeoLab
Na_2CO_3	NeoLab
$NaHCO_3$	NeoLab
Na_2HPO_4	Roth
Na_3PO_4	Roth
NaCl	VWR
NaH_2PO_4	Roth
NaOH 10 N solution	Roth

Chemical	Company
Na-Pyruvate 100 mM solution	Thermo Fisher Scientific
O-phenylenediamine (OPDA)	Sigma Aldrich
Paraformaldehyde	Roth
Phenylmethylsulfonylfluorid (PMSF)	Sigma Aldrich
ROTIPURAN® Glycerol	Roth
Sodium azide	Roth
Tissue-Tek O.C.T. ™ compound	Sakura
Tris(hydroxymethyl)-aminomethan (TRIS) base	NeoLab
Tris(hydroxymethyl)-aminomethan (TRIS) hydrochloride	NeoLab
Triton X-100	NeoLab

3.1.2. Reagents and kits for RNA isolation, cDNA synthesis and RT-PCR

Reagents and Enzymes	Company
1,4-Dithiothreitol (DTT)	Roth
6x loading dye	Fermentas
DNA ladder, 2log (1 mg/mL)	New England Biolabs
DNase I (100 Kunitz units/mL)	Cellsystems
Diethylpyrocarbonat (DEPC)	Roth
Deoxynucleoside triphosphate (dNTP)s (10mM)	Promega
Ethidium bromide (EtBr)	NeoLab
MMLV 5x reaction buffer	Promega
MMLV reverse transcriptase (200U/µL)	Promega
Oligo d(T) primers (500 µg/mL)	Promega
RNase A (20 mg/mL)	Thermo Fisher Scientific
RNAsin (40U/µL)	Promega
UltraPure™ Agarose	Thermo Fisher Scientific

Kits	Company
RNeasy Mini Kit	Qiagen
RNase-Free DNase Set	Qiagen
5-PRIME RT-PCR reaction mix	VWR

3.1.3. Solutions and buffers

3.1.3.1. General

TRIS-buffered saline (TBS), pH 7.4

Reagent	For 1.0 Liter solution
TRIS base	1.94 g
TRIS hydrochloride	13.22 g
NaCl	9.0 g
ddH_2O	1.0 L

0.25 M monobasic sodium phosphate solution

Reagent	For 1.0 Liter solution
NaH_2PO_4	27.60 g
ddH_2O	1.0 L

0.4 M dibasic sodium phosphate solution

Reagent	For 1.0 Liter solution
Na_2HPO_4	28.51 g
ddH_2O	1.0 L

0.2 M phosphate buffer, pH 7.3

Reagent	Final concentration	For 1.0 L solution
NaH_2PO_4	0.2 M	230 mL
Na_2HPO_4	0.2 M	770 mL

To prepare 0.2 M phosphate buffer (pH 7.3), solutions of monobasic and dibasic sodium phosphate are prepared separately. When both salts are completely dissolved in ddH_2O, the solutions are mixed and the pH verified using a pH meter.

0.1 M phosphate buffered saline (PBS)

Reagent	Final concentration	For 1.0 L solution
NaCl	-	9.0 g
Phosphate buffer, 0.2 M	0.1 M	500 mL
ddH_2O	-	500 mL

3.1.3.2. Calcium Imaging

Buffered saline (SGG) for Ca^{2+} imaging

Reagent	Final concentration	For 1.0 L solution
$CaCl_2 \cdot 2H_2O$	2 mM	0.29 g
Glucose	35.6 mM	6.305 g
Glycine	1 mM	0.075 g
HEPES	10 mM	2.3 g
KCl	2.5 mM	0.186 g
$MgCl_2 \cdot 6H_2O$	1 mM	0.203 g
NaCl	140 mM	8.18 g
Na-pyruvate 100 mM solution	0.5 mM	5 mL

3.1.3.3. Enzyme-Linked Immunosorbent Assay (ELISA)

Coating buffer, pH 9.6

Reagent	Final concentration	For 250 mL solution
Na_2CO_3	-	397 mg
$NaHCO_3$	-	733 mg
ddH_2O	-	250 mL

Washing buffer

Reagent	Final concentration	For 1.0 L solution
NaCl	-	14.36 g
Triton-X-100, 100%	0.05%	500 µL
PBS	-	500 mL

Blocking buffer

Reagent	Final concentration	For 100 mL solution
BSA	-	3.0 g
PBS	-	100 mL

Homogenization buffer

Reagent	Final concentration	For 250 mL solution
BSA	-	1.25 g
NaCl	-	3.6 g
EDTA, 0.5 M	5 mM	2.5 mL
Triton-X-100, 100%	0.1%	250 µL
PBS	-	500 mL

These two components are added immediately prior to use:

Reagent	Final concentration	For 100 mL solution
Aprotinin	-	228 µL
PMSF, 0.2 M in MeOH	-	125 µL

Peroxidase buffer

Reagent	Final concentration	For 100 mL solution
BSA	-	0.1 g
Triton-X-100, 100%	0.25%	250 µL
PBS	-	100 mL

Citric acid solution

Reagent	Final concentration	For 100 mL solution
Citric acid	-	1.91 g
ddH_2O	-	100 mL

OPDA buffer, pH 5.0-5.4

Reagent	Final concentration	For 100 mL solution
Citric acid, 0.1 M	15mM	16.5 mL
Dibasic sodium phosphate solution, 0.4 M	30 mM	8.3 mL
ddH_2O	-	66.0 mL
OPDA	-	50 mg

10% sulfuric acid solution

Reagent	Final concentration	For 100 mL solution
H_2SO_4, 2N	-	12 mL
ddH_2O	-	88 mL

3.1.3.4. Gel electrophoresis

50x TRIS-acetate-EDTA (TAE) buffer for gel electrophoresis

Reagent	Final concentration	For 1.0 Liter solution
Trizma Base	-	242.0 g
Glacial Acetic Acid	-	57.10 mL
EDTA, 0.5 M	50 mM	100 mL
ddH_2O	-	fill up to 1.0 L

3.1.3.5. Immunocyto- and histochemistry

Immunofluorescence blocking buffer for immunocytochemistry

Reagent	Final concentration	For 100 mL solution
Donkey serum	1%	1.0 mL
Triton-X-100, 10%	0.1%	1.0 mL
TBS	-	fill up to 100 mL

4% Paraformaldehyde (PFA) / 0.1 M phosphate buffer

Reagent	Final concentration	For 100 mL solution
Paraformaldehyde	-	40.0 g
Phosphate buffer, 0.2 M	0.1 M	500 mL
NaOH 10 N	-	4 drops
ddH_2O	-	500 mL

ddH_2O is heated to 65°C under constant stirring. Paraformaldehyde is carefully added, then NaOH is added drop-wise. The solution is cooled down to 40°C under constant stirring. After the paraformaldehyde has completely dissolved, the solution is filtered through a Whatman filter-paper into 0.2 M phosphate buffer (1:1). Until used, the paraformaldehyde is stored at 4°C.

30% Sucrose solution

Reagent	Final concentration	For 1.0 L solution
D(+)-Sucrose	-	300.00 g
Phosphate buffer, 0.2 M	0.1 M	350.00 mL
ddH_2O	-	350.00 mL

Tissue collecting solution (TCS)

Reagent	Final concentration	For 1.05 Liter solution
Glycerol	-	250 mL
Ethylene glycol	-	300 mL
Phosphate buffer, 0.2 M	0.1 M	250 mL
ddH_2O	-	250 mL

Immunofluorescence blocking buffer for immunohistochemistry

Reagent	Concentration	For 100 mL solution
Donkey serum	5%	5 mL
Triton-X-100	0.25%	250 µL
TBS	-	fill up to 100 mL

3.1.4. Antibodies

3.1.4.1. Primary antibodies (ICC, IHC)

Epitope	Species	Isotype	Type	Dilution	Company
B-III-tubulin	ms	IgG	monoclonal	1:1000	Promega
CS-56	ms	IgM	monoclonal	1:300	Sigma Aldrich
DCX	gt	igG	polyclonal	1:500	Santa Cruz
GFAP	rb	IgG	polyclonal	1:1000	Dako
hGFAP	ms	IgG1	monoclonal	1:1000	Stem Cells Inc.
HoxB4	rt	IgG2a	monoclonal	1:10	DSHB
Human Ki67	rb	IgG	monoclonal	1:500	Cell signaling
Laminin	rb	IgG	polyclonal	1:800	Sigma Aldrich
Nestin	ms	IgG1	monoclonal	1:1000	Merck Millipore
Neurofilament-H (NFH)	rb	IgG	Polyclonal	1:500	Merck Millipore
Human NUC (hNUC)	ms	IgG1	monoclonal	1:1000	Merck Millipore
Sox2	gt	IgG	polyclonal	1:200	Santa Cruz
Vimentin	ms	IgG1	monoclonal	1:1000	Merck Millipore

3.1.4.2. Secondary antibodies

Epitope	Species	Isotype	Dilution	Company
Alexa Fluor 488 α-ms	dk	IgG (H+L)	1:1000	Thermo Fisher Scientific
Alexa Fluor 488 α-rb	dk	IgG (H+L)	1:1000	Thermo Fisher Scientific
Alexa Fluor 488 α-gt	dk	IgG (H+L)	1:1000	Thermo Fisher Scientific
Alexa Fluor 488 α-rt	dk	IgG (H+L)	1:1000	Thermo Fisher Scientific
Alexa Fluor 594 α-ms	dk	IgG (H+L)	1:300	Thermo Fisher Scientific
Alexa Fluor 594 α-rb	dk	IgG (H+L)	1:300	Thermo Fisher Scientific
Alexa Fluor 594 α-gt	dk	IgG (H+L)	1:300	Thermo Fisher Scientific
Cy5 α-ms	dk	IgG (H+L)	1:500	Dianova
Cy5 α-rb	dk	IgG (H+L)	1:500	Dianova
FITC α-ms	dk	IgM (H+L)	1:500	Thermo Fisher Scientific
4’,6-Diamidine-2’-phenylindole dihydrochloride (DAPI)			1:1000	Sigma Aldrich

3.1.4.3. Primary antibodies (ELISA)

Epitope	Species	Isotype	Type	Dilution	Company
BDNF	rb	IgG	polyclonal	1:2000	Acris
BDNF	ch	IgY	polyclonal	1:2500	Promega

3.1.4.4. Secondary antibodies (ELISA)

Epitope	Species	Isotype	Dilution	Company
Peroxidase-conjugated α-ch	rb	IgY (H+L)	1:1000	Promega

3.1.5. Primers for RT-PCR

Primer	5'-3' sequence	Annealing °C	Company
Aqp4 fwd	GGAATTTCTGGCCATGCTTA	53-54	Eurofins MWG Operon
Aqp4 rev	AGACTTGGCGATGCTGATCT		Eurofins MWG Operon
Chl1 fwd	ATGGAGCCGCTTTTACTTGGA	54-55	Eurofins MWG Operon
Chl1 rev	GGCAACTTGGACTTTTGACTGT		Eurofins MWG Operon
EAAT1 fwd	ATCCTTGGATTTACCCTCCGA	54-55	Eurofins MWG Operon
EAAT1 rev	CGCCATTCCTGTGACAAGAC		Eurofins MWG Operon
FoxG1 fwd	AGGAGGGCGAGAAGAAGAAC	55-56	Eurofins MWG Operon
FoxG1 rev	TCACGAAGCACTTGTTGAGG		Eurofins MWG Operon
GAPDH fwd	CCTTCATTGACCTCAACTAC	55	Eurofins MWG Operon
GAPDH rev	GGAAGGCCATGCCAGTGAGC		Eurofins MWG Operon
HoxA5 fwd	CCGGAGAATGAAGTGGAAAA	53-54	Eurofins MWG Operon
HoxA5 rev	ACGAGAACAGGGCTTCTTCA		Eurofins MWG Operon
HoxB4 fwd	ACACCCGCTAACAAATGAGG	55	Eurofins MWG Operon
HoxB4 rev	GCAGCAAAGATGAGGGAGAG		Eurofins MWG Operon
Isl1 fwd	AAACAGGAGCTCCAGCAAAA	53	Eurofins MWG Operon
Isl1 rev	AGCTACAGGACAGGCCAAGA		Eurofins MWG Operon
NFIA fwd	ACAGGTGGGGTTCCTCAATC	54-55	Eurofins MWG Operon
NFIA rev	GTGGGACGCTGCAACTTTT		Eurofins MWG Operon
NFIX fwd	ATGTACTCCCCGTACTGCCTC	55-56	Eurofins MWG Operon
NFIX rev	ACATCCGCTTTTCATGCTTCTT		Eurofins MWG Operon
NG2 fwd	GTCTTTTGAGGCTGCCTGTC	54-55	Eurofins MWG Operon
NG2 rev	CTGTGTGACCTGGAAGAGCA		Eurofins MWG Operon
Nkx2.1 fwd	CGCATCCAATCTCAAGGAAT	53	Eurofins MWG Operon
Nkx2.1 rev	TGTGCCCAGAGTGAAGTTTG		Eurofins MWG Operon
Nkx2.2 fwd	TGCCTCTCCTTCTGAACCTTGG	55-56	Eurofins MWG Operon
Nkx2.2 rev	GCGAAATCTGCCACCAGTTG		Eurofins MWG Operon
Nkx6.1 fwd	ACACGAGACCCACTTTTTCCG	56-58	Eurofins MWG Operon
Nkx6.1 rev	TGCTGGACTTGTGCTTCTTCAAC		Eurofins MWG Operon
Olig1 fwd	TTGCATCCAGTGTTCCCGATTTAC	56-58	Eurofins MWG Operon
Olig1 rev	TGCCAGTTAAATTCGGCTACTACC		Eurofins MWG Operon
Olig2 fwd	CAGAAGCGCTGATGGTCATA	53	Eurofins MWG Operon
Olig2 rev	TCGGCAGTTTTGGGTTATTC		Eurofins MWG Operon
Pax3 fwd	GAACACGTTCGACAAAAGCA	52-53	Eurofins MWG Operon
Pax3 rev	GCACACAAGCAAATGGAATG		Eurofins MWG Operon
PDGF-R fwd	CTATCCACACTGTCAAACAGGTTG	56-58	Eurofins MWG Operon
PDGF-R rev	TCTGCTGGACTGAGAAGTTTCATC		Eurofins MWG Operon
S100ß fwd	AAAGAGCAGGAGGTTGTGGA	53	Eurofins MWG Operon
S100ß rev	AGGAAAGGTTTGGCTGCTTT		Eurofins MWG Operon

3.1.6. Cell culture

3.1.6.1. Cell lines and primary cell cultures

Name	Type	Source	Background
Skin fibroblasts	Primary	Strain: Fischer344 rats Age: 9 - 13 weeks old Gender: female Weight: 140 - 180 g Direct source: Charles River Laboratories, Harlan Laboratories (Envigo) or in-house breeding	Wild type
DRG neurons	Primary	Strain: Fischer344 rats Age: 9 - 13 weeks old Gender: male Weight: 140 - 180 g Direct source: Charles River Laboratories, Harlan Laboratories (Envigo) or in-house breeding	Wild type
HUES6 PSCs	Cell line	Human embryonic inner cell mass Cell line established at Harvard University Passage number: 39 Direct source: Laboratory of Prof. Dr. Beate Winner, Friedrich-Alexander Universität Erlangen-Nürnberg	Wild type
iPSC #1	Cell line	Human Skin Biopsy iPSC clone name: 21E6 Passage number: 46 Direct source: Laboratory of Prof. Dr. Beate Winner, Friedrich-Alexander Universität Erlangen-Nürnberg	Wild type
iPSC #2	Cell line	Human Skin Biopsy iPSC clone name: 19-23 Passage number: 34 Direct source: Laboratory of Prof. Dr. Beate Winner, Friedrich-Alexander Universität Erlangen-Nürnberg	Wild type

3.1.6.2. Basic media, enzymes and supplements

Chemical/Reagent	Company
2.5% Trypsin/EDTA	Life Technologies
B27-Supplement (50x)	Thermo Fisher Scientific
Calpain Inhibitor	Calbiochem
Collagenase XI (10 mg/mL)	Sigma Aldrich
Dispase I (10 mg/mL)	Worthington
Destilled water	Thermo Fisher Scientific
DMEM/F12	Thermo Fisher Scientific
Dimethyl sulfoxide (DMSO)	NeoLab
DPBS (1x)	Thermo Fisher Scientific
Fibrinogen (100 mg/mL)	Sigma Aldrich
Gentamicin (10 mg/mL)	Thermo Fisher Scientific
Hanks' Salt Solution	Biochrome
Heparin	Sigma Aldrich
Hibernate®-A	Thermo Fisher Scientific
L-Glutamine (100x)	Thermo Fisher Scientific
Laminin (1 mg/mL)	Sigma Aldrich
Non-essential amino acids (NEAA) (100x)	Thermo Fisher Scientific
N2-Supplement (100x)	Thermo Fisher Scientific
PAA Gold fetal bovine serum (FBS)	Biochrome
Penicillin / Streptomycin (10,000 Units/mL)	Thermo Fisher Scientific
Poly-L-ornithine (PLO) (10 mg/mL)	Sigma Aldrich
Retinoic Acid (RA)	Sigma Aldrich
Thrombin (100 U/mL in 10 mM $CaCl_2$)	Sigma Aldrich
TrypLE™ Express (1x)	Thermo Fisher Scientific

3.1.6.3. Growth factors and cytokines

Factor (Cell culture)	Factor (Additional for surgery)	Company
Recombinant hEGF	Recombinant hGDNF	PeproTech
Recombinant hFGF1	Recombinant hHGF	PeproTech
Recombinant hFGF2	Recombinant hIGF	PeproTech
Recombinant hBDNF (ELISA)	Recombinant hNT-3	PeproTech
Recombinant hBMP2	Recombinant hPDGF	PeproTech
Recombinant hBMP4		PeproTech
Recombinant hCNTF		PeproTech

3.1.6.4. Cell culture media composition

Basic neural medium (bNM)

Reagent	Concentration of stock	Final concentration
DMEM/F12	-	-
NEAA	100x	1x
N2-Supplement	100x	1x
B27-Supplement	50x	1x
Heparin	2 mg/mL	2 µg/mL
Penicillin/Streptomycin	10,000 U/mL	100 U/mL
Gentamicin	10 mg/mL	1 µg/mL

Proliferation medium for HUES6/iPSC-derived neurospheres

Reagent	Concentration of stock	Final concentration
bNM	-	-
Recombinant hEGF	100 µg/mL	20 ng/mL
Recombinant hFGF2	100 µg/mL	20 ng/mL

Proliferation medium for HUES6/iPSC-derived adherent NSCs

Reagent	Concentration of stock	Final concentration
bNM	-	-
FBS	100%	1%
Recombinant hEGF	100 µg/mL	20 ng/mL
Recombinant hFGF2	100 µg/mL	20 ng/mL

Differentiation medium for HUES6/iPSC-derived adherent NSCs:

Treatment	Reagent	Concentration of stock	Final concentration
	bNM	-	-
	FBS	100%	1%
No factors	-	-	-
BMP	Recombinant hBMP2 + hBMP4	200 µg/mL	10 ng/mL each
CNTF	Recombinant hCNTF	200 µg/mL	20 ng/mL
FGF1	Recombinant hFGF1	200 µg/mL	20 ng/mL

Maintenance medium for primary DRG neurons

Reagent	Concentration of stock	Final concentration
DMEM/F12	-	-
Penicillin/Streptomycin	10,000 U/mL	100 U/mL
L-glutamine	100x	1x
B27 supplement	100x	1x

3.1.7. Animals

All primary culture preparation as well as animal experiments were carried out with 9-13 week old male or female Fischer344 rats weighing 140 to 180 g. Direct source: Charles River Laboratories, Harlan Laboratories (Envigo) or in-house breed. Animal experiments were carried out in compliance with national guidelines for animal care and use in accordance with the European Union Directive (2010/63/EU). All animal protocols were reviewed and approved by the local authorities and animal ethics committee. Animals had free access to food and water.

3.1.7.1. Anesthesia mixture

Drug Name	Active substance	Dosage	Company
Ketamine 10%	Ketamine	62.5 mg/kg	HFW Bremer Pharma GmbH
Vetranquil® 1%	Acepromacine	0.625 mg/kg	Ceva
Xylariem®	Xylacine	3.175 mg/kg	Ecuphar
NaCl 0.9%	-	-	Braun

3.1.7.2. Post-surgical animal care

Drug Name	Active substance	Dosage	Company
Ampicillin-ratiopharm®	Ampicillin	25 - 50 mg/kg	Ratiopharm
Bepanthen®	Dexpanthenol	-	Bayer
Fresubin	-	-	Fresenius Kabi
NaCl 0.9%	-	-	Braun
Rimadyl®	Carprofen	4 - 5 mg/kg	Pfizer
Ringer solution	-	-	Braun
Temgesic®	Burprenophine	0.03 - 0.05 mg/kg	Reckitt Benckiser
Sandimmun®	Cyclosporine A	10 mg/kg	Novartis

3.1.8. Laboratory equipment and disposables

Item	Company
Glas bottles	NeoLab
0.5 mL Eppendorf tubes	Greiner Bio-one
1.5 mL Eppendorf tubes	Greiner Bio-one
10 mL disposable pipette tip	Greiner Bio-one
12-well cell culture plates	Greiner Bio-one
15 mL Falcons	Greiner Bio-one
24-well cell culture plates	Greiner Bio-one
24 x 60mm cover glasses	Roth
25 mL disposable pipette tip	Corning, Inc.
2 mL Eppendorf tubes	Greiner Bio-one
4- and 8-well chamber slides	Nunc
50 mL Falcons	Greiner Bio-one
5 mL disposable pipette tip	Greiner Bio-one
6-well cell culture plates	Greiner Bio-one
96-well plate (ELISA)	Greiner Bio-one
AQUAline AL25 water bath	Lauda
1 mL Cryotubes	Greiner Bio-one
Disposable pipette tips: 10 µL, 20 µL, 200 µL, 1000µL	VWR
Disposable pipette tips w/ filter: 10 µL, 20 µL, 200 µL, 1000µL	Greiner Bio-one
DOS-20S shaker	NeoLab
Eppendorf research plus 8-channel pipet	Eppendorf
Feather® disposable scalpels: no. 11, no. 15	Feather
Friedman-Pearson rongeur	Fine Science Tools
Gel electrophoresis chamber	NeoLab
Gel electrophoresis power source	Peqlab, VWR
Glas cover slips, round, 13 mm	VWR
Hamilton microliter syringe: 2µL, 5 µL, 10 µL	Hamilton
HERAcell 240i CO2 incubator	Thermo Fisher Scientific
HM 550 cryostate	Zeiss
Superfrost Plus™ microscope slides	Thermo Fisher Scientific
MSC-Advantage sterile hood	Thermo Fisher Scientific

Item	Company
NanoDrop	VWR
Neubauers' cell counting chamber	Supe-Rior Marienfeld
Olympus CKX41 fluorescence microscope	Olympus
Parafilm	NeoLab
Pasteur capillary pipettes	WU Mainz
Peristaltic pump (perfusion)	Ismatec
PB-11 pH-meter	Sartorius
PCR reaction tubes	Roth
Picospritzer® II microinjector	Science Products
PIPETBOY acu2	INTEGRA Bioscience
Pipettes	VWR
Power source 250V	VWR
Precision balance	Kern
Thermometer	NeoLab
Whatman® filter paper	Sigma Aldrich
Surgical retractor	Roboz
RH basic 2 heating/stirring plates	IKA
Rotina 380R cell culture centrifuge	Hettich Zentrifugen
Silkam® silk suture with micro-lancet needle	Braun
Small animal stereotaxic instrument	Kopf
Sterilizer tray	World precision instruments
Straight and curved surgical forceps	Fine Science Tools
Suture clips	Fine Science Tools
Suture Tying forceps	Fine Science Tools
T175 cell culture flasks	Greiner Bio-one
T25 cell culture flasks	Greiner Bio-one
T75 cell culture flasks	Greiner Bio-one
Thermocycler (PCR)	BioRad
Ultra-Low Adhesion T75 Flasks	Sigmal Aldrich
Vortex mixer	NeoLab
Wire knife and retractable wire knife carrier	Mc Hugh Milieux
Wound clip remover	Fine Science Tools

3.1.9. Imaging Equipment

Imaging equipment	Company
Tecan sunrise 96-well microplate reader (ELISA)	Tecan
BX53 fluorescence microscope	Olympus
BX61 confocal laser-scanning microscope	Olympus
CKX41 bright field microscope (cell culture)	Olympus
IX81 motorized inverted fluorescence microscope	Olympus
UV gel capture chamber	Peqlab
BX51W1 upright fluorescence microscope	Olympus

3.1.10. Software

Software	Company	Application
Adobe Illustrator CS6	Adobe	Image creation and processing
Adobe Photoshop CS6	Adobe	Image processing
BioCapt™	Bio-Budget	Gel imaging (UV)
Cell-F	Olympus	Fluorescence imaging
Cell-P	Olympus	Fluorescence imaging
Cell-R	Olympus	Fluorescence imaging (Calcium Imaging)
Endnote X7	Thomson Reuters	Reference management
Fluoview 2.1.c	Olympus	Confocal laser scanning imaging
ImageJ	RSB	Image processing and evaluation
Magellan6™	Tecan	ELISA: detection
Microsoft Office	Microsoft	Data analysis
Prims 6 Graphpad	Graphpad	Data anaylsis, statistics, representation

3.2. Methods

3.2.1. Maintenance of human pluripotent stem cells

HUES6 (Harvard University embryonic stem cell line 6) and human iPSC lines were obtained from the laboratory of Prof. Dr. Beate Winner, Friedrich-Alexander Universität Erlangen-Nürnberg. Human iPSCs were generated via retroviral delivery of the OSKM factors and thoroughly characterized. After clonal expansion until passage 10 - 11, good/stable iPSC clones per donor were selected and further expanded until passage 30 - 40. Hereby, PSCs were cultured on Matrigel™-coated (BD Biosciences) 6-well plates (Nunc®) in mTeSR medium (Stemcell™ Technologies) and differentiating cells, which may appear at the edges of growing PSC colonies, were mechanically removed every day or every other day. Our collaborators prepared PSC cultures, so that neural induction could be performed upon arrival.

3.2.2. Neural induction of human pluripotent stem cells

3.2.2.1. Day *in vitro* 0: generation of embryoid bodies

Laboratory of Prof. Dr. Beate Winner, Friedrich-Alexander Universität Erlangen-Nürnberg

PSC cultures were mechanically cleaned to eliminate differentiating contaminating cells. PSC colonies were then gently lifted with a cell scraper (Corning®). Homogeneous medium-sized colony fragments were transferred to ultra-low adhesion 6-well plates (Stemcell™ Technologies) and cultured overnight in mTeSR medium. Resulting free-floating colonies are called EBs due to their capacity to give origin to progeny of all three germ layers.

3.2.2.2. Day *in vitro* 1: neural induction

Laboratory of Prof. Dr. Beate Winner, Friedrich-Alexander Universität Erlangen-Nürnberg

Without further dissociation, EBs were centrifuged at 800 - 1000 rpm for 5 minutes and the mTeSR medium was replaced with bNM. Free-floating cultures were transferred to T25 or T75 flasks to be transported to the Spinal Cord Injury Center, Ruprecht-Karls Universität Heidelberg.

3.2.2.3. Day *in vitro* 3 to 7: maintenance of embryoid bodies

On DIV 3, 5 and 7 EBs were centrifuged at 800 - 1000 rpm for 5 minutes and 50-75% of the bNM was replaced. If adherent colonies were observed, EBs were transferred to a new T25 or T75 flask to prevent adherent colonies from undergoing spontaneous differentiation and releasing differentiation signals.

Single EBs tend to fuse and form clumps. To maintain a homogeneous culture and to ensure that all EBs are exposed to the same gradient of nutrients from the culturing medium, EB-clumps or unusually big EBs were allowed to settle down by gravity in 50 mL falcon tube and mechanically fragmented.

3.2.2.4. Day *in vitro* 8 (to 12): generation of neural rosettes

Depending on the size of EBs, they might be kept for longer as free-floating suspension (up to DIV 12), especially if caudalization with RA is planned. RA has some toxicity for EB colonies, therefore very small colonies will die back entirely.
Prior to plating, 6-well plates were coated with PLO (20 µg/mL in ice-cold water for 1 hour at 37°C), rinsed and coated with laminin (10 µg/mL in ice-cold water for 2 hours at 37°C). If present, EB-clumps or big EBs were mechanically fragmented. EBs were allowed to settle down in a 50 mL falcon tube by gravity or by centrifugation at 600 rpm for 5 minutes. Small EBs still present in the supernatant were discarded, as they do not survive during the RA treatment. 40 to 50 medium-sized EBs were plated per well of a PLO/laminin coated 6-well plate and cultured in bNM. The next day, the medium was replaced to eliminate debris and dead cells.

3.2.2.5. Day *in vitro* 11: caudalization with retinoic acid

At DIV 11, neural rosettes (NRs) are visible within attached aggregates as multilayered circular structure resembling the closed neural tube. Several NRs were present within one NR aggregate.
At this point, the medium was replaced with fresh bNM medium containing 0.1 - 0.5 µm RA to induce caudalization. If no morphogen was added at this stage, the default phenotype of the progeny would be rostral (forebrain). RA and RA-containing medium were used in the dark, as RA is light sensitive and unstable. The medium was replaced on DIV 12 and 14 to provide fresh RA.

3.2.2.6. Days *in vitro* 15 - 22: picking of early NRs to initiate free-floating cultures

According to published protocols [205, 397] and to induce a glial phenotype, NRs and the resulting neurospheres need to be cultured as free-floating spheres, as attachment might trigger a neurogenic phenotype.
NRs were selected based on their overall morphology, mechanically picked with a 200 µL pipet and transferred to a T25 or T75 flask without being fragmented to initiate the formation of neurospheres (early NSCs). Here it was particularly important to collect as many NRs as possible

in one T25 flask: the density of the initial culture will influence the proliferation potential of the derived NSCs; if initial densities were too low, resulting NSCs were not well expandable.
75% of the medium was replaced every 2nd day to provide fresh RA until DIV 22. Importantly, NRs were not fragmented or dissociated.

3.2.2.7. Day *in vitro* 23: dissociation of free-floating late NRs and expansion

At DIV 23, RA treatment was completed. Late NRs were mechanically gently dissociated to smaller fragments (not single cells) and, from this day on, cultured in proliferation medium for neurospheres.

3.2.2.8. Days *in vitro* 23 - 180: expansion and freezing of neurospheres

From DIV 23 on, 75% of the proliferation medium was replaced twice per week. In order not to expose early neurospheres to stressful conditions, they were allowed to settle down by gravity and only 75% of the supernatants was centrifuged at 1000 rpm for 5 minutes. Until day 60, neurospheres grew very slowly. Although medium was changed twice a week, passaging was performed only every 2 weeks. During the first 60 - 80 days of expansion, neurospheres were transferred to a new T25 flask if adherent colonies were observed, as neurosphere adhesion augments their neurogenic potential. When neurospheres reached a sufficiently high density, they were transferred to low-adhesion T75 flasks for further expansion until DIV 180.
Density permitting, but generally once a week, neurospheres were frozen. Neurospheres were centrifuged at 1000 rpm for 5 minutes, gently resuspended in 900 µL of bNM without dissociation and transferred to 1 mL cryotubes. 100 µL DMSO was added immediately prior freezing, cryotubes were inverted a few times and then stored at -80°C for maximum 1 week before being transferred to the liquid nitrogen storage unit.

3.2.2.9. Days *in vitro* ~ 40, 50, 65, 80, 90, 100, 180: immunocytochemical analysis of neurospheres

Early and late neurospheres were plated on PLO/laminin coated chamber slides or 24-well plates and fixed for at least 10 minutes with a 4% PFA solution 2 hours later. After 3 washing steps with TBS for 5 minutes and incubation with blocking buffer for 30 minutes at RT, neurospheres were incubated overnight at 4°C with antibodies to Sox2, nestin (NSC markers), vimentin (NSC and early astrocyte marker) and HoxB4 (a transcription factor expressed in the developing spinal cord), respectively diluted in blocking buffer. The next day, after 3 washing steps with TBS for 5 minutes, neurospheres were incubated for 2 hours at RT with fluorescent secondary antibodies and DAPI diluted in blocking buffer. After 3 additional washing steps,

neurospheres were stored at 4°C / in the dark. The % of immunopositive cells was calculated by microscopy and cell counting.

3.2.2.10. Days *in vitro* 80 - 180: maturation of astrocyte precursors without FBS

According to the original publication [205, 397], from day 80 up to day 180 precursor cells increasingly commit to the astrocytic lineage. At this point, neurospheres can be dissociated, plated at low density ($5*10^3$ to $2*10^4$ cells per well of a 24 well plate) on PLO/laminin and differentiation can be started 1 - 3 days later. Differentiation was induced by withdrawal of proliferation factors and stimulation with the pro-astrocytic factor CNTF for 1 week [205, 397].
Importantly, CNTF-containing bNM was entirely replaced every other day, as CNTF is chemically unstable. After 1 and 2 weeks of differentiation, differentiating precursors were fixed and immunolabeled as described above. Differentiation was assessed by quantifying expression of vimentin, GFAP (early and later astrocytic markers) and ß-III-tubulin (neuronal marker), and stemness and proliferation by quantifying expression of Sox2 (NSC marker) and Ki67 (proliferation marker). The % of immunopositive cells was calculated by microscopy and cell counting.
Both early (DIV ~100) and late (DIV ~180) neurospheres were not differentiating to form homogeneous astrocytic cultures. Therefore, the differentiation protocol was adjusted as follows.

3.2.2.11. Days *in vitro* 80 - 180: maturation of "astrocyte precursors" with FBS

From DIV 80 - 90, dissociated neurospheres were plated on PLO/laminin at a (low) density of $1.5*10^5$ per T75 flask. After a short acclimatization phase, 1% FBS was added to the proliferation medium and administered until the end of differentiation. NSCs were cultured as low-density monolayers for at least 2 weeks prior to differentiation. Following advantages were observed: dead cells were removed from the culture before differentiation; small aggregates were dissociated into single differentiating cells; single cells acquired a flat, astrocyte-like morphology. Whenever necessary, astrocytic precursors were passaged by adding 2.5 mL TripLE™ Express to each T75 flask after removing the bNM. After a 3-minute incubation at 37°C, cells were resuspended in bNM, centrifuged at 1000 rpm for 5 minutes, counted using a haemocytometer and replated in a new PLO/laminin coated T75 flask ($1.5*10^5$). After an initial phase at low density for 1-2 passages, cells were allowed to reach confluence at each passage.

3.2.2.12. Days in vitro ~100 - 160: maturation of astrocyte precursors with CNTF, BMP2/4 and FGF1

After at least 2 weeks of FBS treatment at low density, monolayer NSCs were plated at a density of $5*10^3$ to 10^4 cells per well of a 24-well plate. The next day or at latest 3 DIV later differentiation was initiated by incubation with differentiation medium containing FBS and no additional factor or either CNTF, BMP2/4 or FGF1 (concentration: 20 ng, 10 ng each, 20 ng). Importantly, differentiation medium was entirely replaced every other day, as CNTF is chemically unstable. In addition, BMP2/4 treatment led to some NSC death, therefore an initial cell density of 10^4 per well of a 24-well plate was required.
After 2 weeks of differentiation, differentiating precursors were fixed and immunolabeled as described above. Differentiation was assessed by quantifying expression of vimentin, GFAP (early and later astrocytic markers) and ß-III-tubulin (neuronal marker), whereas residual proliferation by quantifying expression of Sox2 (NSC marker) and Ki67 (proliferation marker). The % of immunopositive cells was calculated by microscopy and cell counting. In addition, production of ECM was assessed by immunolabeling for CS-56 and laminin. ECM production was analyzed by microscopy, conversion of the fluorescence signal to a binary (B/W) signal and calculation of the area fraction per cell covered by each ECM component. Whenever possible, for each immunocytochemical analysis 3 - 6 fields of 3 wells of 1 - 3 independent differentiations were analyzed. Each well represents an individual microenvironment and is considered as n = 1.

3.2.3. RNA extraction

For RNA extraction, neurospheres were centrifuged at 1000 rpm for 5 minutes, resuspended directly in 250 µL lysis buffer (1% ß-mercaptoethanol in RLT buffer, RNeasy Mini Kit) and vortexed before immediate use or storage at -80°C. Total RNA was extracted using the RNeasy Mini Kit (Qiagen) and following the manufacturer's instructions.

3.2.4. cDNA synthesis

RNA was reverse-transcribed to the first-strand cDNA using oligo (dT) primers and M-MLV Reverse Transcriptase and according the following scheme:

Reagents solution I	**Amount**	**BioRad thermocycler protocol**
RNA probe	4.0 µL	80°C for 3 min
Oligo (dT) primers	1.0 µL	4°C for ∞

Reagents solution II	Amount	BioRad thermocycler protocol
5x MMLV reaction buffer	3.0 µL	42°C for 1 hour
MMLV reverse transcriptase, 200 U/µL	1.0 µL	80°C for 10 minutes
dNTPs, 10 mM	0.75 µL	4°C for ∞
RNAsin, 40 U/µL	0.35 µL	
DTT, 100 mM in H_2O	1.5 µL	
DEPC-treated H2O	3.4 µL	

3.2.5. PCR and gel electrophoresis

The expression profile of neurospheres was assessed by PCR amplification of genes of interest either associated with positional identity or associated with glial specification, as following:

Reagents	Amount	BioRad thermocycler protocol
2.5x 5-PRIME RT-PCR reaction mix	4.0 µL	95°C for 2 minutes once
10 µM fwd primer	0.25 µL	35 cycles of: 95°C for 30 seconds 55°C for 1 minute * 72°C for 1 minute
10 µM rev primer	0.25 µL	
ddH_2O	4.5 µL	
cDNA (30 ng)	1 µL	
		72°C for 8 minutes once 4°C for ∞

* Annealing temperatures were calculated and adjusted for each primer.

3.2.5.1. Gel electrophoresis

1.5 g of UltraPure™ agarose were dissolved in 150 mL of 1x TAE buffer at boiling temperature. The agarose solution was allowed to cool down under constant stirring, and 1.5 µL EtBr were was added. Afterwards, the solution was poured into a gel chamber and let solidify at RT. 2 µL 6x loading dye were added to the PCR reaction probe, and loaded for gel electrophoresis. 2-log DNA ladder was used to estimate amplicon lenghts, but not amplicon amounts. Electrophoresis was performed at 100 V for at least one hour.

3.2.6. Calcium imaging of maturing astrocytes

3.2.6.1. Imaging procedure

Laboratory of Prof. Dr. Hilmar Bading, Ruprecht-Karls-Universität Heidelberg

To perform Ca^{2+} imaging, 2-week differentiated astrocyte cultures were differentiated for 2 weeks on round 13 mm cover slips in 24-well plates. These were pre-treated with HCl at 65°C overnight and stored in isopropanol, then dried and coated with PLO/laminin (100 µg/mL und 10 µg/mL) immediately prior to use. Due to a less efficient attachment on glass than on plastic surfaces, NSCs were plated at higher densities prior to differentiation ($8*10^4$ cells per cover slip). Two-three days prior to Ca^{2+} imaging, plates were transported to the laboratory of Prof. Hilmar Bading, Ruprecht-Karls-Universität Heidelberg, where the set-up was located, and allowed to acclimatize.

On the day of imaging, few cover slips at one time were transferred to an empty 24-well plate, washed with SGG buffer and incubated with Fura-2 (1:1000 in SGG buffer) for 30-45 minutes at RT. After an additional washing step with SGG buffer, differentiating cells were incubated with SGG buffer for at least 30 minutes at RT. At this point, cover slips were placed into the imaging set-up's chamber under a 40x objective and covered with 1 mL SGG buffer. Up to 13 ROIs corresponding to a single cell each were set. Using the Cell-R imaging software, one-frame-per-second recordings were started at 340 nm and 380 nm in parallel, since Fura-2 is a ratiometric fluorophore.

Resting Ca^{2+} levels were recorded for 60 seconds, then 1 mL of 200 µM ATP in SGG buffer was very carefully pipetted into the chamber in order to expose astrocytes to 100 µM ATP. One-frame-per-second recordings were performed for up to 5 minutes after ATP application.

3.2.6.2. Analysis

The area and integrated density (ID) of 3 empty ROIs (background / noise signal) and up to 13 ROIs per cover slip were calculated as numerical / arbitrary values per frame using ImageJ (ROI manager), both for 340 nm and 380 nm recordings. The total ID per frame of the 3 empty ROIs was subtracted from each ROIs' ID per frame, both for 340 nm and 380 nm recordings. Thereafter, a 340 nm/380 nm ID ratio per frame was calculated for each ROI. The resulting values were plotted as curves using Prims 6 Graphpad and represent Ca^{2+} fluctuations over time.

3.2.7. BDNF Enzyme-Linked Immunosorbent Assay

All ELISA experiments were performed together with Shengwen Liu, a medical doctor working in our research laboratory.
Differentiation of PSC-derived NSCs into astrocytes was performed in PLO/laminin coated 24-well plates with the differentiation factor of interest. FBS-containing differentiation medium was replaced 48 hours prior to ELISA measurements with differentiation medium without FBS (500 µL/well).
On day 2 of the ELISA protocol supernatants were collected and immediately used. Cells were counted to determine the amount of BDNF produced by a defined number of cells.

3.2.7.1. Day 1: coating of 96-well plates

Rabbit anti-BDNF primary antibody was diluted in coating buffer (1:2000) and distributed into the 96-well plate (50 µL / well). Control wells were incubated with rabbit serum (1:4000 in coating buffer). Plates were incubated overnight at 4 °C in a humid chamber and on a horizontal shaker.

3.2.7.2. Day 2: washing, blocking and incubation with cell supernatants

Unbound antibody was removed by washing the wells twice with ELISA washing buffer for 10 - 30 minutes at RT, thereafter wells were incubated with ELISA blocking buffer for one hour at RT and washed again twice. During this time, a purified human BDNF stock solution is diluted in ELISA homogenization buffer to obtain 12 solutions with a range of concentrations [pg/well: 100 / 66.6 / 44.4 / 29.6 / 19.8 / 13.17 / 8.78 / 5.85 / 3.9 / 2.6 / 1.73 / 0] as standard/reference curve to calculate BDNF concentrations of cell supernatants. Cell supernatants were diluted 1:2 in homogenization buffer.
Purified BDNF solutions and diluted supernatants were added to the wells of the 96-well plate and incubated overnight at 4°C in a humid chamber on a horizontal shaker.

3.2.7.3. Day 3: Incubation with anti-BDNF

Samples were removed and wells were washed with ELISA washing buffer at least 4 times for 15 minutes at RT. Chicken anti-BDNF antibody (1:2500 in ELISA homogenization buffer) was then added to each well. The 96-well plate and incubated O/N at 4°C in a humid chamber on a horizontal shaker.

3.2.7.4. Day 4: incubation with peroxidase-conjugated secondary antibody

Chicken anti-BDNF antibody was removed and wells were washed with ELISA washing buffer at least 4 times for 15 minutes at RT. Peroxidase-conjugated anti-chicken IgY antibody (1:1000 in ELISA peroxidase buffer) was added to each well. The 96-well plate and incubated overnight at 4°C in a humid chamber on a horizontal shaker.

3.2.7.5. Day 5: measurement of optic densities

Peroxidase-conjugated anti-chicken IgY antibody was removed and wells were washed twice with ELISA washing buffer and twice with PBS for 15 minutes at RT. To 16 mL ELISA OPDA per 96-well plate 8 mg OPDA and 11 µL 30% H_2O_2 were added immediately prior to use. 150 µL of this solution were added to each well. After an incubation of 5 - 30 minutes until the solution turned bright yellow, 50 µL of a 10% H_2SO_4 solution were added to stop the reaction.
Optic densities were measured with a Tecan sunrise 96-well microplate reader at 490 nm.

3.2.8. Isolation of dorsal root ganglion neurons and co-culture with maturing astrocytes

Differentiation of PSC-derived NSCs into astrocytes was performed in PLO/laminin coated 6-well plates or 12-well plates with the differentiation factor of interest. Differentiation medium was replaced 2 hours prior to co-culturing with differentiation medium without FBS or any differentiation factor, as these might have an effect on neurite growth. Only confluent and homogeneous cultures of astrocytes were used for co-culturing experiments.

3.2.8.1. DRG isolation

10 - 13-week old Fischer344 rats were deeply anesthetized. The spinal column was dissected and the spinal cord wash flushed out through injection of Hank's salt solution into the spinal canal. Two spine halves were obtained by gently cutting dorsally and ventrally. By gently pulling the intra-spinal nerve endings with forceps and gently removing the *dura mater* surrounding them, DRGs were isolated from each segment of the spine along the rostro-caudal axis, collected into 1.5 mL Eppendorf tubes and kept on ice in Hibernate A medium.

3.2.8.2. DRG digestion and plating of isolated neurons

When all DRGs were collected, Hibernate A medium was removed and DRGs were washed with ice cold Hank's salt solution. 500 µL of a 1:1 collagenase XI:DispaseI solutions were added and

incubated for 30 minutes at 37°C. To ensure that all DRGs are equally exposed to the enzymatic solution, Eppendorf tubes were gently turned every 10 minutes. Enzymatic digestion was stopped by incubation with warm DMEM/F12 medium containing 10% FBS for a few seconds. The FBS-containing medium was then removed and DRGs were washed with warm serum-free DMEM/F12 medium. Finally, DRGs are resuspended in DRG maintenance medium and mechanically dissociated by pipetting up-and-down through a fire-polished glass pipet. The total number of DRG cells, including neurons and glia, was counted and cells were plated onto PLO/laminin coated 6-well plates. Importantly, only 0.5 µg/mL laminin were used, since high concentrations of laminin lead to extensive neurite growth of dissociated DRG neurons, which was not needed here. Plated DRG neurons were kept in DRG maintenance medium at 37°C overnight and re-plated after 24 hours: thereby cellular debris and inhibitory ECM components such as myelin were washed away prior to plating onto differentiating astrocytes. To this end, DRG neurons were gently washed with warm DPBS, incubated with trypsin (0.125% in warm DPBS) for 2-3 minutes at 37°C, resuspended in DRG maintenance medium containing 10% FBS, counted and centrifuged at 1000 rpm for 5 minutes. After determining the cell number using a haemocytometer, up to $1.25*10^4$ and $2.5*10^4$ cells per well of a 12-well or 6-well plate respectively were plated onto differentiating astrocytes.

3.2.9. Transplantation of neural stem cells and astrocytes into the rat spinal cord

3.2.9.1. Preparation of NSCs and differentiating astrocytes

Either NSCs or differentiating astrocytes were transplanted into the intact or injured spinal cord of fischer344 rats.

NSCs were cultured as free floating neurospheres in proliferation medium and mechanically fragmented by pipetting up-and-down prior to transplantation. Importantly, they were not dissociated into single cells, since previous studies [228] reported higher survival of transplanted cells when neurospheres were transplanted as small fragments.

Differentiation of PSC-derived NSCs into astrocytes was performed in PLO/laminin coated 6-well plates or 12-well plates with the differentiation factor of interest. Differentiation medium was replaced 2 hours prior to co-culturing with differentiation medium without FBS or any differentiation factor, as these might have an effect on neurite growth.

On the day of transplantation, cells were resuspended, counted and centrifuged at 1000 rpm for 5 minutes. The pellet was rinsed once with DPBS, and then the DPBS solution was removed completely until the pellet was nearly dry. The volume of the pellet was estimated and the remaining volume of a PBS/1% glucose solution was added to reach a concentration of $2.5*10^5$ to $5*10^5$ cells/µL. Concentration of the cell solution strongly depended on cell size, since NSCs, especially if cultured as neurospheres, were generally very small, whereas differentiating

astrocytes were bigger: when resuspending astrocytes it was physically not possible to obtain a concentration of $5*10^5$ cells/µL. Immediately prior to transplantation, the cell solution was diluted 1:2 either in PBS/1% glucose or in a cocktail of Calpain inhibitor (Stock 100 µM, final 25 µM) and either 9 growth/neurotrophic factors (BDNF and NT-3: stock for surgery 100 µg/mL, final 25 µg/mL; EGF, FGF1, FGF2, GDNF, HGF, IGF, PDGF: stock for surgery 20 µg/mL, final 5 µg/mL) or only the differentiation factor used to induce astrocytic maturation (CNTF, BMP2/4, FGF1: stock for surgery 20 µg/mL, final 5 µg/mL). The stock growth factor cocktail itself was diluted 1:2 either in PBS/1% glucose or with fibrinogen (stock for surgery 100 mg/mL, final 25 mg/mL) or thrombin (stock for surgery 100U/mL, final 25 U/mL), as well immediately prior to cell injection.

3.2.9.2. Anesthesia and exposure of the C4 segment of the rat the spinal cord

Female 12 to 14-week old Fischer344 rats weighing 140 - 180g were immunosuppressed 24 hours before surgery by a subcutaneous injection of Sandimmun® (10 mg/kg body weight). Sandimmun® was administered daily until the end of the experiment. After surgery, rats received subcutaneous injections of Temgesic®, ampicillin and Ringer solution twice a day for two days. On the day of surgery, rats were deeply anesthetized, shaved at the dorso-cervical level and the skin was rinsed with Braunol. Animals were fixed on a stereotaxic setup. A midline skin cut from C2 to C5 was done with a scalpel to expose the musculature, then the paraspinous musculature was gently pushed aside with forceps to expose the C4 spinal cord segment and the opening was fixed by insertion of a retractor. The C4 segment of the spinal cord was thereafter exposed by laminectomy and the *dura mater* was disrupted either by a small cut (scalpel) or a small hole (syringe tip).

3.2.9.3. Hemisection of the spinal cord

After laminectomy and disruption of the *dura mater* by a small longitudinal cut, the right half of the spinal cord was completely sectioned using surgical microscissors. The exposed spinal cord segment was covered with a cut-to-fit thin 1% agarose film, thereafter the muscles were sutured with a sterile silk thread and the skin was clipped with suture clips.

3.2.9.4. Wire knife injury of the spinal cord

A retractable wire knife carrier was fixed on the stereotactic arm, then the stereotactic arm was fixed on the stereotactic setup. Prior to lesioning, the wire knife was carefully extruded from its holder in order to position it in the middle of the C4 segment (both on the rostro-caudal and on

a medio-lateral axis), whereby the wire knife had to be as accurately as possible perpendicular to the rostro-caudal axis. After insertion into the spinal cord through the hole previously punched into the *dura mater*, the depth of the wire knife carrier along the dorso-ventral axis was adjusted and the wire knife was slowly extruded. The extruded wire knife was slowly pulled towards the dorsal edge of the spinal cord, while the spinal cord was at the same time gently pressed towards the knife with a blunt stab in order to transect the dorsal column projections. This procedure was repeated until the full-length wire knife was visible underneath the *dura mater*, indicative of successful transection of the dorsal column. The wire knife was slowly retracted and pulled out. A representative picture of the lesion was taken to better identify it one week later, when cells were transplanted into the injury site. The exposed spinal cord segment was covered with a cut-to-fit thin 1% agarose film, thereafter the muscles were sutured with a sterile silk thread and the skin was clipped with suture clips.

3.2.9.5. Re-exposure of the spinal cord and cell injection

One week after transection of the dorsal column, the C4 segment was re-exposed as described above. Using the picture of the lesion, the site for injection was identified.

The previously prepared cell solution was pipetted into a pulled glass micropipette (100 µm diameter), which was fixed on the stereotactic arm and connected to a Picospritzer. After punching a hole into the *dura mater*, the glass needle was carefully inserted into the spinal cord at the lesion site, as well as rostrally and caudally to it. Respectively ~1 µL and ~0.35 µL of the cell solution were injected into each site twice: ~$1.25*10^5$ cells/µL diluted in a cocktail of Calpain inhibitor (final concentration: 25 µM), a specific growth/neurotrophic factor combination (final concentrations ranging from 5 µg/mL to 25 µg/mL) and either fibrinogen (final concentration: 25 mg/mL) or thrombin (final concentration 25 U/mL) respectively, for a total of 2 µL injection volume into the lesion epicenter and 0.7 µL injection volume rostrally and caudally. If PSC-derived NSCs or astrocytes were co-grafted with fibroblasts, they were cultured and resuspended separately at a concentration of ~$2.0*10^5$ cells/µL and $6*10^4$ cells/µL in a growth factor cocktail or PBS/1% glucose respectively, then mixed 1:1 immediately prior to transplantation. No fibrinogen or thrombin were applied in fibroblast co-transplantation experiments.

By application of 20 PSI for 5 ms, cells were injected into the lesion site at a depth of 0.8 mm, while the glass needle was slowly pulled upwards. When the defined volume of cell solution was injected, the glass needle was pulled out after a short break to avoid reflux of injected cells. The muscles were sutured with a sterile silk thread and the skin was stapled with suture clips.

3.2.9.6. Transplantation of differentiating astrocytes into the intact spinal cord

After exposure of the C4 spinal segment as described above, ~1 µL of a ~1.25*10^5 cells/µL solution pre-diluted in a cocktail of Calpain inhibitor and a specific growth/neurotrophic factor combination (CNTF, BMP2/4, FGF1 or EGF/FGF2: stock for surgery 20 µg/mL, final 5 µg/mL) was injected directly into the intact spinal cord at a depth of 1 mm. When the defined volume of cell solution was injected, the glass needle was pulled out after a short break to avoid reflux of injected cells. The muscles were sutured with a sterile silk thread and the skin was clipped with suture clips.

3.2.10. Perfusion and tissue analysis

3.2.10.1. Perfusion

Either 2 or 4 weeks after cell transplantation, rats were sacrificed and perfused.
Prior to perfusion, rats were deeply anesthetized and fixed on a grid placed on a plastic vessel. Their belly was sprayed with 70% EtOH and a 1 cm transversal cut at the level of the sternum was done. A further, deeper small cut was done under the sternum. After cutting the diaphragm and opening a hole into the rib cage, the pericardium was opened up to expose the heart. A butterfly needle was then inserted into the left heart ventricle (1 - 2 mm depth), with particular care in order not to damage the septum. The right atrium was truncated by a scissor to allow the blood to flow out. Using a peristaltic pump, ice-cold PBS was pumped into the heart and consequently into the blood circulation for approximately 10 minutes. Thereby the blood was completely washed out and ice-cold 4% PFA was pumped into the blood circulation in order to fix the tissue for approximately 15 minutes. During the whole procedure particular attention was paid to avoid flow of air bubbles in the perfusion pipes, as their introduction into the blood circulation hampers the efficiency of perfusion. The brain and spinal cord were isolated and stored in 4% PFA at 4°C overnight. The next day the PFA was substituted with 30% sucrose, to avoid ice-crystal mediated damage the tissue, when the latter is frozen for cryosectioning. The brains and spinal cords were stored at 4°C for them to sink, ranging from 2 to 4 days at least.

3.2.10.2. Cryosectioning and immunohistochemistry

Once the brains and spinal cords were sunk, they were cryosectioned.
The C2-C5 portion of the spinal cord was embedded in Tissue-Tek™, the spinal cord fragment was frozen by exposure to -50/-53°C. Sagittal, 35 µm thick tissue sections were obtained using a cryostat and stored at in TCS-filled 24-well plates (free-floating) at 4°C until further use.

The staining procedure began with 3 washing steps with TBS for 10 minutes and incubation with blocking buffer for 1 hour at RT. Tissue sections were then incubated overnight at 4°C and on a horizontal shaker with the following antibodies: hGFAP or hNUC (Human-specific markers) in combination with Ki67, Sox2, vimentin, GFAP, DCX, Neurofilament-H (NFH), CS-56 and laminin, respectively diluted in blocking buffer. The next day, after 3 washing steps with TBS for 10 minutes, tissue sections were incubated for 2.5 hours at RT with fluorescent secondary antibodies and DAPI diluted in blocking buffer. After 3 additional washing steps, tissue sections were mounted on glass slides and covered with Fluoromount-G mounting solution and a glas coverslip, and thereafter stored at RT / in the dark. The % of immunopositive cells was calculated by microscopy and cell counting. To this end, whenever cell survival was high enough 3 - 6 fields from 3 spinal cord slices from 3 animals were analyzed, for a total number of individual cells of $x > 1000$, and this was considered $n = 3$. However, this was not possible for all experiments.

3.2.11. Statistics

Statistical analysis was performed with Prims 6 Graphpad. No statistical analysis was performed if $n < 3$. When $n \geq 3$, either a one-way or a two-way ANOVA statistical tests were performed, followed by post hoc testing either without correction or with a correction for multiple comparisons. In particular, when 3 treatment groups were compared to the 'no factors' control group within a single cell line (closed system, 3 direct comparisons), a one-way ANOVA followed by Fisher's LSD post hoc test was performed. When 4 treatment groups were compared across cell lines (multiple comparisons), two-way ANOVA followed by Tukey's post hoc test was used.

4. Results

4.1. Generation of astrocytes from human pluripotent stem cells

4.1.1. Neural induction and differentiation protocol

To generate astrocytes from human PSCs, recently published protocols were compared [205, 296, 397, 399, 400] and neural induction and differentiation were first performed according to the protocol published by Krencik et al. (Figure 4.1, left timeline) [397].

The first attempt to replicate the protocol did not succeed. Neurospheres were expanded in the presence of EGF and FGF2 in bNM without B27. Under these conditions, neurospheres did not proliferate and each medium change or passaging attempt led to progressive loss of neurospheres until the culture was depleted (data not shown). The second attempt to replicate the protocol was performed in the presence of B27 in the bNM culture medium and led to expandable neurosphere cultures. Neurospheres were generated from four PSC lines: one human ESC line, the well-characterized HUES6 line, and three human iPSC lines, either without or with caudalizing RA treatment (data not shown). Of all available PSC-derived NSC lines, three caudalized NSC lines, referred to as HUES6, iPSC #1 and iPSC #2 were used for further experiments.

4.1.2. Characterization and differentiation of pluripotent stem cell derived neurospheres

At DIV 60 - 90, neurospheres were characterized by immunocytochemistry and RT-PCR (Figure 4.2.1 A, B). Neurospheres were homogeneously immunolabeled for the NSC markers Sox2 and nestin, the NSC / early astrocytic marker vimentin, as well as the transcription factor HoxB4, which is expressed in the developing spinal cord, indicating successful caudalization of neuroepithelial cells (Figure 4.2.1 A) [205, 288]. Along this line, RT-PCR showed low or no expression of the forebrain transcription factor FoxG1, but appreciable expression of the caudal/spinal transcription factors HoxB4, HoxA5 and Isl1 (Figure 4.2.1 B) [288]. Since neural rosettes (NRs) were not treated with dorsalizing or ventralizing agents, NSCs expressed both dorsal (Pax3) and ventral (Nkx2.1, Nkx2.2, Nkx6.1) transcription factors [288]. Importantly, NSCs expressed a broad range of markers associated with the glial lineage, including the oligodendrocyte markers Nkx2.2, NG2, Olig1, Olig2 and PDGFR and the astrocyte-specification markers NFIA, NFIX, S100ß, Aqp4, Chl1 and EAAT1, also known as GLAST (Figure 4.2.1, B).
At an early (DIV 65 - 95, passage 3 - 4) and a late (DIV 170 - 180) time-point, neurospheres were gently dissociated, plated on PLO/laminin and exposed to CNTF in the absence of EGF and FGF2. Based on the original protocol [205, 397], cells were exposed to CNTF for one week, but this

time was insufficient to induce astrocytic maturation. After one week, none of the differentiated NSC lines gave rise to a considerable amount of $GFAP^+$ positive astrocytes (data not shown). Therefore differentiation was extended to two weeks throughout all remaining experiments. After two weeks of differentiation, neither early neurospheres (Figure 4.2.2 A) nor late neurospheres (Figure 4.2.2 B) gave rise to homogeneous astrocytic cultures as expected [205, 397], although they homogeneously expressed the early astrocytic marker vimentin. The $GFAP^+$ population amounted to about 10% in HUES6- and iPSC #2-derived differentiated NSCs and did not exceed 30% of total differentiating cells in iPSC #1-derived NSCs (Figure 4.2.3 A). In contrast to previously published data [205, 397], both early and late NSCs from all lines generated up to 15% ß-III-tubulin$^+$ neurons (Figure 4.2.3 B) and the overall differentiation potential of late neurospheres was significantly decreased (Figure 4.2.2, A, B) in both iPSC-derived NSC lines. Surprisingly, iPSC #1-derived late neurospheres did not differentiate into $GFAP^+$ astrocytes or into ß-III-tubulin$^+$ neurons at all.

Expression of the NSC marker Sox2 was significantly increased in DIV 170 - 180 HUES6- and iPSC #2-derived NSCs differentiated with CNTF (Figure 4.2.3 C), suggesting that extensively passaged neurospheres have a lower capacity of terminally differentiating. Expression of the proliferation marker Ki67 did not exceed 40% in any line and at both time points (Figure 4.2.3 D). iPSC #1-derived late neurospheres exhibited decreased expression of Sox2 and Ki67 (Figure 4.2.3 C, D), but maintained homogeneous vimentin expression. Importantly, differentiating neurospheres did not consistently give rise to homogeneous monolayer cultures, but also included patches of tightly-packed $Sox2^+$ colonies (Figure 4.2.2 A, B).

Taken together, these results show that the original differentiation protocol by Krencik et al. does not lead pure astrocytic cultures under similar experimental conditions with any of the three different PSC lines.

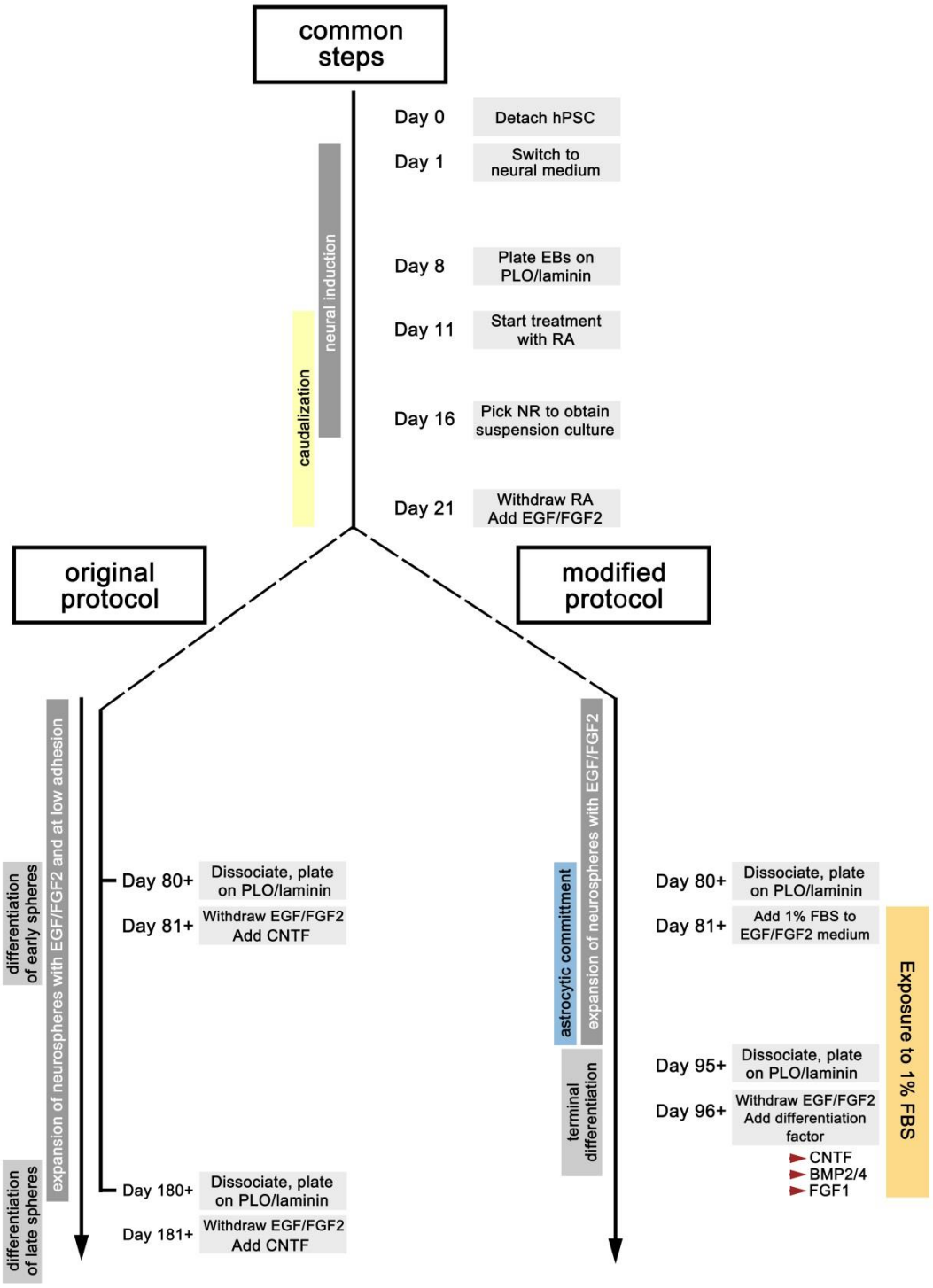

Figure 4.1: Differentiation of PSCs into astrocytes.

Schematic representation of the protocols to differentiate PSCs into astrocytes. First, the protocol by Krencik et al. was replicated (left). Due to insufficient purity of the resulting cultures, the protocol was modified (right): on DIV ~80 free-floating neurospheres were plated at low density on PLO/laminin and exposed to 1% FBS for at least two weeks prior to differentiation. Maturation of NSCs into astrocytes was induced by treatment with CNTF, BMP2/4 or FGF1 in addition to FBS.

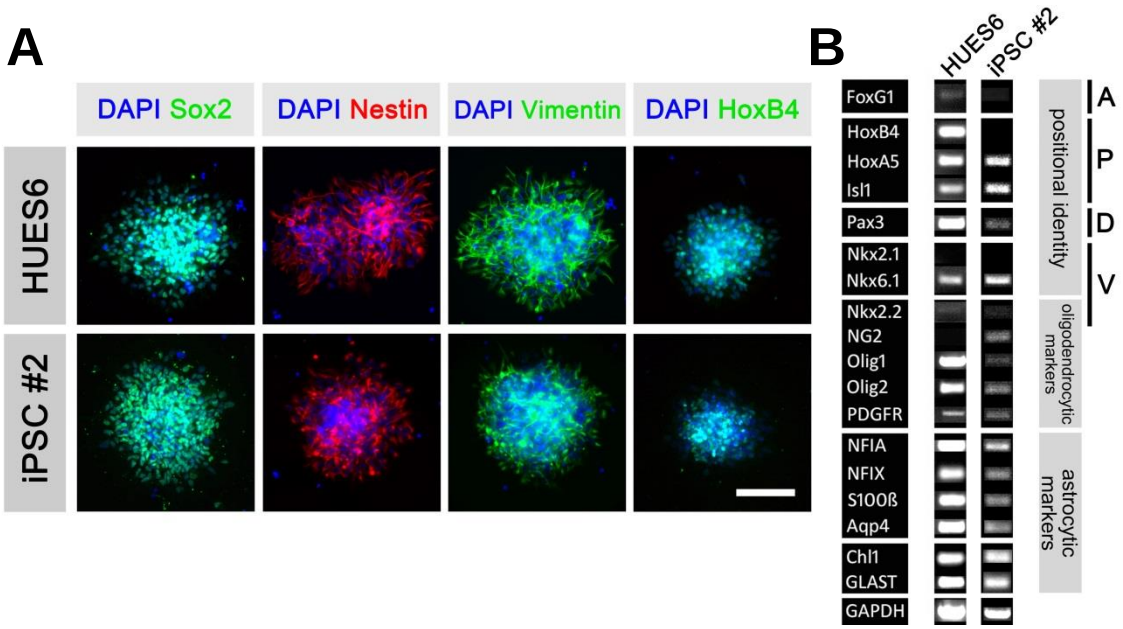

Figure 4.2.1: PSC-derived neurospheres express markers associated with a glial lineage.

(A) Representative photomicrographs of early neurospheres (DIV 60 - 80) expressing the NSC markers Sox2 and nestin, the NSC / early astrocytic marker vimentin and the transcription factor HoxB4, which is expressed by caudal/spinal precursors during neurodevelopment. **(B)** Total RNA was isolated from neurospheres to analyze expression of genes associated with positional identity (FoxG1, HoxB4, HoxA5, Isl1, Pax3, Nkx2.1, Nkx6.1) and glial specification (oligodendrocytic: Nkx2.2, NG2, Olig1, Olig2, PDGFR; astrocytic: NFIA, NFIX, S100ß, Aqp4, Chl1, GLAST) by RT-PCR. HUES6- and iPSC #2-derived neurospheres are shown as representative examples of successful neural induction and caudalization.
Scale bar: 20 µm. A: anterior; P: posterior; D: dorsal; V: ventral.

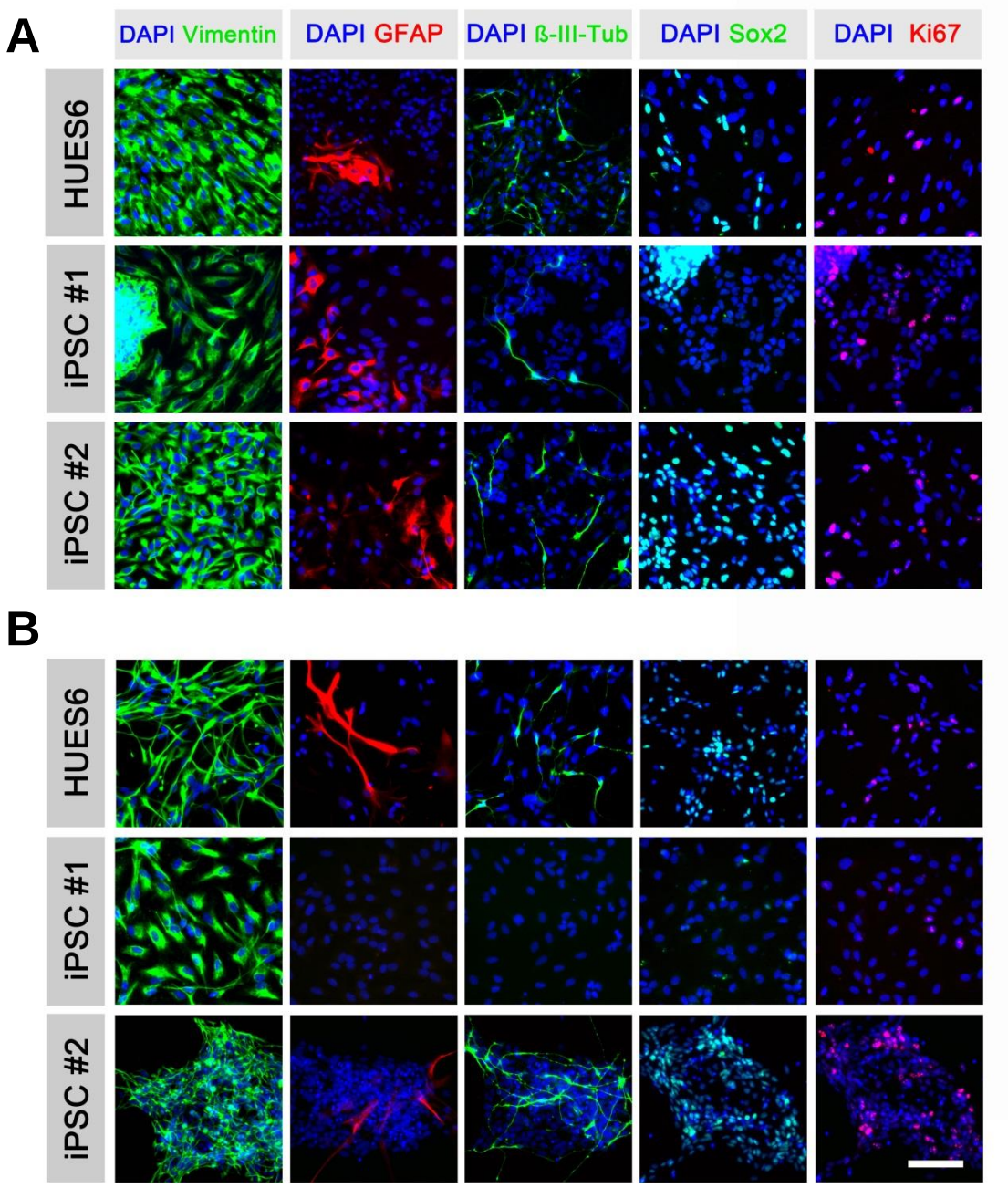

Figure 4.2.2: Differentiation of PSC-derived neurospheres with CNTF for two weeks results in mixed cultures of astrocytes and neurons.

Representative photomicrographs of PSC-derived **(A)** DIV 75 - 95 early neurospheres and **(B)** DIV 170 - 180 late neurospheres after differentiation with CNTF for two weeks. Differentiated cells expressed the early astrocytic marker vimentin, the astrocytic marker GFAP, the neuronal marker ß-III-tubulin, the NSC marker Sox2 and the proliferation marker Ki67. Surprisingly, iPSC #1-derived late precursors did not differentiate into astrocytes or neurons, and showed little Sox2 and Ki67 expression.
Scale bar: 20 µm.

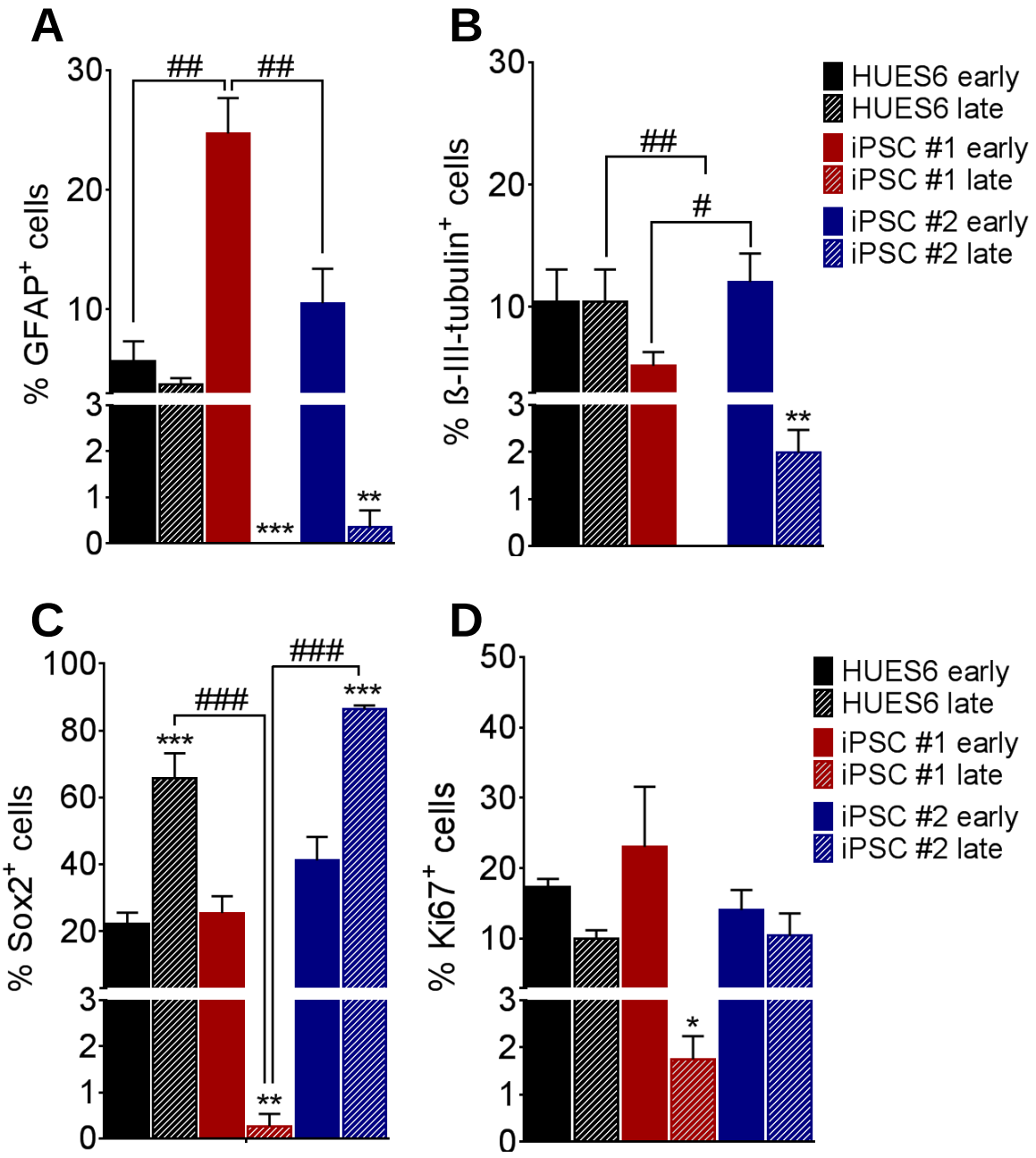

Figure 4.2.3: Quantitative analysis of differentiation and proliferation in PSC-derived neurospheres differentiated with CNTF for two weeks.

Quantitative analysis of marker expression in DIV 75 - 95 early neurospheres (solid bars) and DIV 170 - 180 late neurospheres (striped bars) after two weeks of differentiation with CNTF. Cells expressed **(A)** the astrocytic marker GFAP, **(B)** the neuronal marker ß-III-tubulin, **(C)** the NSC marker Sox2 and **(D)** the proliferation marker Ki67. Marker expression in differentiating HUES6-derived **(black)**, iPSC #1-derived **(red)** and iPSC #2-derived **(blue)** cells was quantified as % of $DAPI^+$ nuclei. n = 3 - 6 wells / condition; asterisks indicate significant differences between early and late neurospheres, hashtags indicate significant differences between cell lines. One-way ANOVA, Fisher's LSD post hoc; * and #: $p < 0.05$, ** and ##: $p < 0.01$, *** and ###: $p < 0.001$.

4.1.3. Transplantation of pluripotent stem cell derived neurospheres into the injured spinal cord

Although differentiation of neurospheres according to the protocol by Krencik et al. [205, 397] (Figure 4.1, left timeline) did not result in pure astrocytic cultures *in vitro* (Figure 4.2.2 and 4.2.3), transplanted cells are exposed to signaling cues from the host environment and survival and differentiation can be drastically influenced. Therefore, to assess survival and differentiation in the lesioned spinal cord, HUES6-derived DIV ~130 neurospheres were transplanted one week after C4 lateral hemisection or wire knife lesion of the C4 dorsal column (Figure 4.3; Appendix table 4.2 A, B). In addition, to evaluate potential effects of growth factor co-delivery on cell survival and differentiation, HUES6-derived neurospheres were resuspended in a mix of calpain inhibitor and nine growth factors or in PBS/1% glucose at a concentration of $2*10^5 – 2.5*10^5$ cells/µl. ~5 µl were injected into the hemisectioned spinal cord, whereas ~2 µl were injected into the wire knife lesioned spinal cord (Appendix, Table 4.2 A) [148, 149].
Animals received subcutaneous injections of cyclosporine A and were allowed to survive for four weeks as indicated. Accordingly, cell integration into the host tissue and phenotype was analyzed four weeks after grafting.

HUES6-derived neurospheres exhibited moderate survival when transplanted without growth factors and appreciable survival when transplanted with the growth-factor cocktail. As shown in Appendix Table 4.2 A, HUES6-derived cells were detected in all animals that received neurospheres in combination with growth factors, whereas neurospheres administered in PBS/1% glucose survived in 5 out of 6 transplanted animals (+GF = 100% survival, (-)GF = 83% survival). In addition, qualitatively more cells survived when transplanted with the growth factor cocktail (Figure 4.4.1). However, across all animals grafted cells were located mostly at the lesion edge rather than the lesion epicenter. The latter was filled by infiltrating cells, potentially reactive fibroblasts and immune cells such as macrophages.
To determine the phenotype of transplanted PSC-derived cells into glial and neuronal lineages, expression of the astrocytic marker GFAP and of the early neuronal marker DCX was quantified. Across all animals, over 90% of the transplanted cells differentiated into $GFAP^+$ astrocytes, whereas 5-10% expressed the early neuronal marker DCX (Figure 4.4.2). This indicates that, although neurospheres do not fully differentiate into astrocytes *in vitro* (reflected by GFAP expression, Figure 4.2.2 and 4.2.3 A), they are robustly driven to a $GFAP^+$ astrocytic phenotype by the host CNS environment. However, reflecting *in vitro* findings (Figure 4.2.2 and 4.2.3 B), neurospheres retained some neurogenic potential *in vivo*. No significant differences in the differentiation potential of transplanted neurospheres were observed between the PBS/1% glucose control group and the full growth factor cocktail group. Interestingly, $GFAP^+$ astrocytes which were located at the lesion epicenter or at the lesion edge co-expressed vimentin, whereas individual cells which migrated into the surrounding host spinal cord further from the

lesion site only expressed GFAP and exhibited a complex cytoarchitecture (Figure 4.2 A). Since vimentin is expressed in early/immature astrocytes but also in reactive astrocytes, these observations suggest that the microenvironment at and immediately surrounding the lesion epicenter either prevents maturation of HUES6-derived vimentin$^+$ early astrocytes or it stimulates them to acquire a reactive phenotype.

To evaluate whether HUES6-derived astrocytes contribute to the growth-inhibitory fibroglial scar, tissue sections were immunolabeled with human specific GFAP and NFH antibodies. hGFAP$^+$ astrocytes and NFH$^+$ projections were closely associated, suggesting that HUES6-derived astrocytes were not completely growth-inhibitory. However, without appropriate control or comparison group, it is not possible to assess whether transplanted astrocytes were growth-promoting or less growth-inhibitory than endogenous reactive astrocytes.

Since a C4 hemisection of the spinal cord is a rather severe SCI model, HUES6-derived neurospheres were transplanted after wire knife lesion of the C4 dorsal column, a model in which the *dura mater* is only slightly damaged during the surgical procedure. Similar to the above described results, HUES6-derived neurospheres transplanted without additional growth factors exhibited only moderate survival, robust differentiation into astrocytes, but also some differentiation into neurons (Figure 4.5).

Taken together, the neurogenic potential of HUES6-derived neurospheres is maintained *in vivo* independent of the lesion model, but their differentiation into vimentin$^+$ and/or GFAP$^+$ astrocytes is influenced by the injured host spinal cord. Survival is moderate and mostly restricted to the lesion edges.

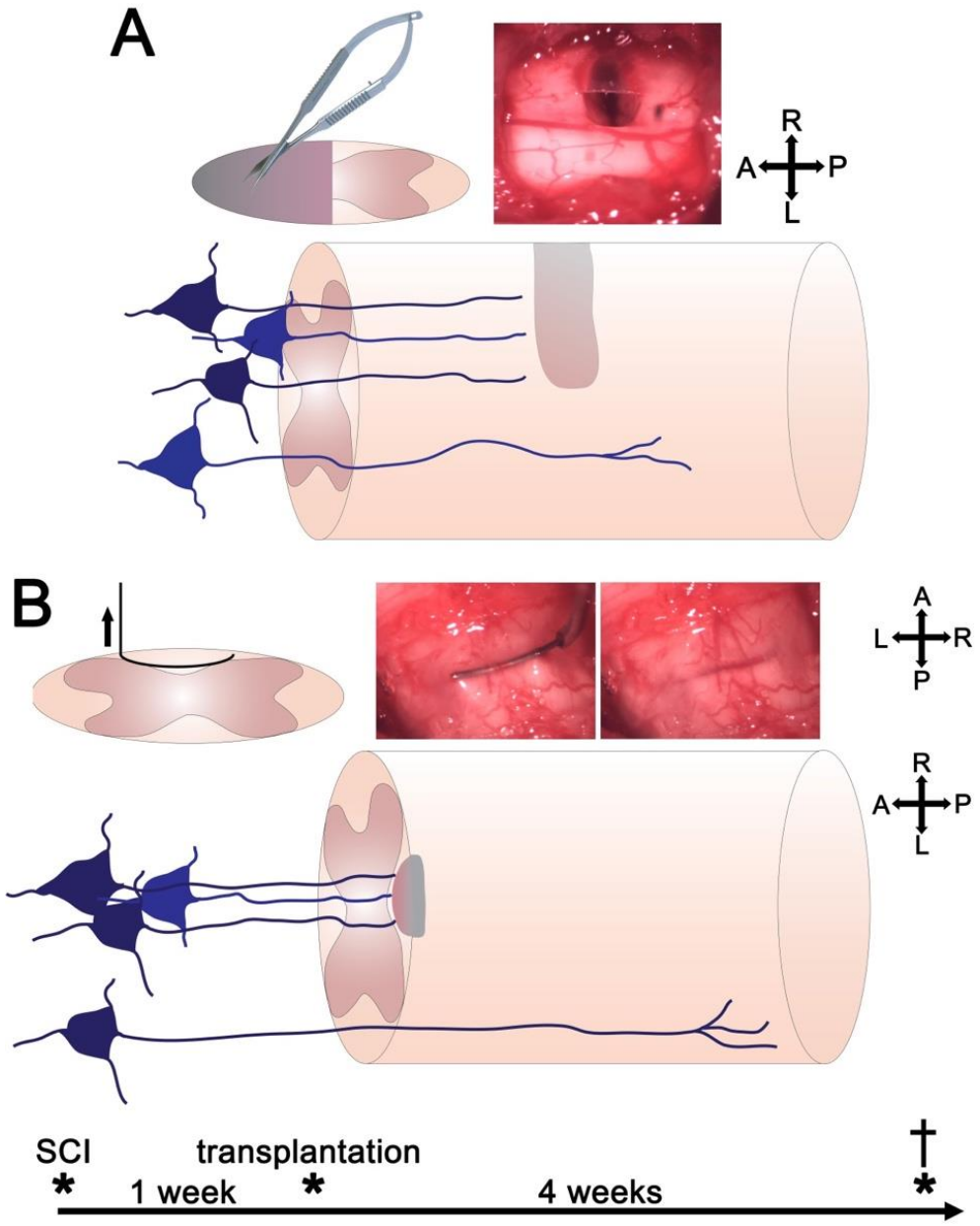

Figure 4.3: Schematic representation of the surgical procedure.
Level C4 of the rat spinal cord was injured either by lateral hemisection using a surgical micro-scissor or by transection of the dorsal column using a wire knife. One week post-injury PSC-derived NSCs were injected into the injury site and four weeks after transplantation animals were sacrificed for tissue analysis.

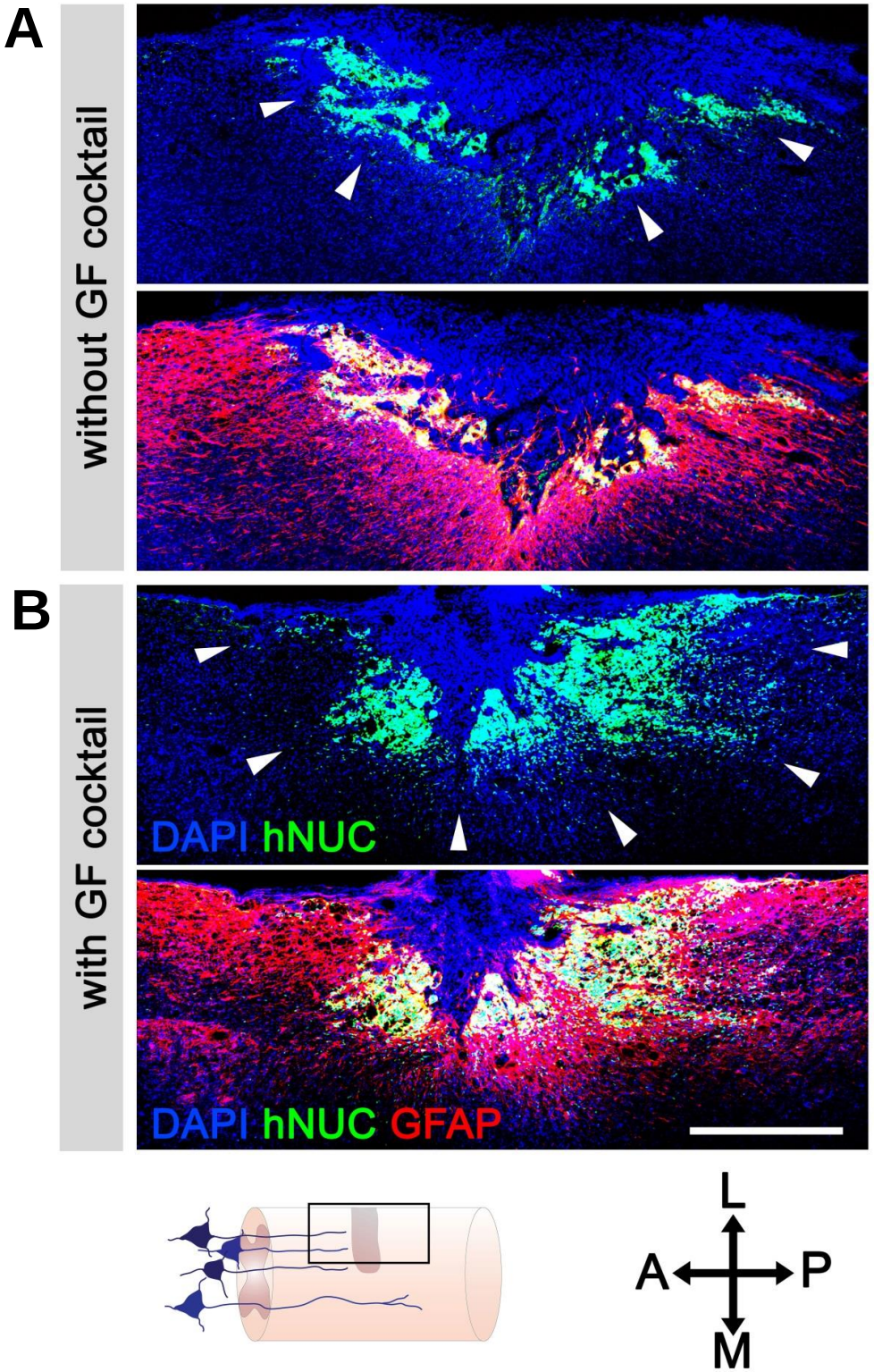

Figure 4.4.1: HUES6-derived neurospheres moderately survive in the injured spinal cord.

Representative photomicrographs of $hNUC^{+}$ HUES6-derived progeny four weeks after C4 hemisection and cell transplantation. HUES6-derived neurospheres were transplanted either **(A)** without additional growth factors or **(B)** were re-suspended in a solution containing calpain inhibitor and nine growth/neurotrophic factors.
Scale bar: 500 µm. GF: growth factor; A: anterior; P: posterior; L: lateral; M: medial.

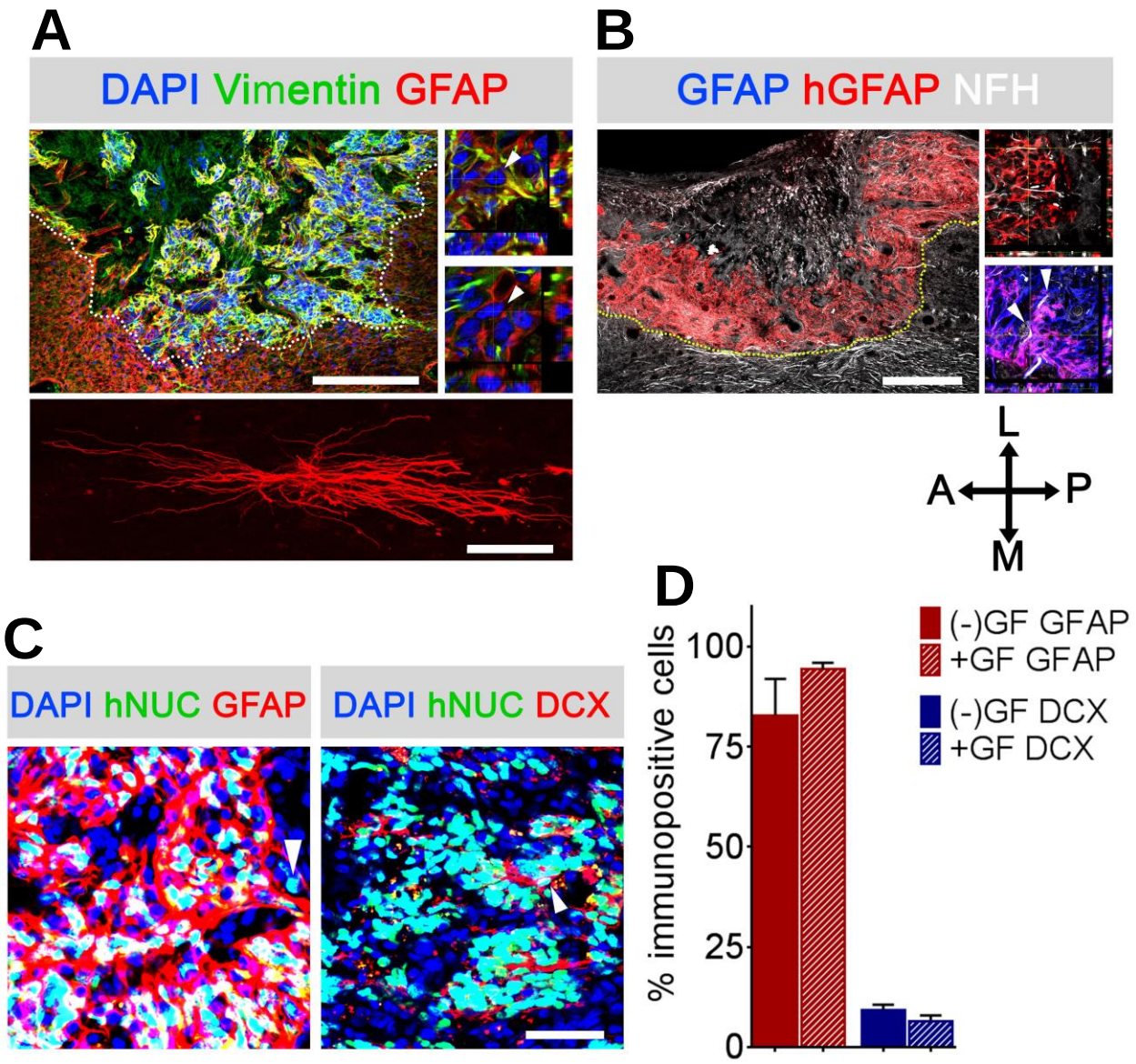

Figure 4.4.2: HUES6-derived neurospheres mainly differentiate into astrocytes in the injured spinal cord.

Representative photomicrographs of HUES6-derived progeny four weeks after C4 hemisection and cell transplantation. HUES6 neurospheres-derived cells expressed **(A, D)** the astrocytic markers vimentin and GFAP and **(C, D)** some cells expressed the early neuronal marker DCX. $GFAP^+$ astrocytes **(B)** co-localized with NFH^+ host neuronal projections.
Scale bars: **(A)** 200 µm und 50 µm, **(B)** 300 µm and **(C)** 100 µm. **(D)** n = 3 - 4 animals per group.
A: anterior; P: posterior; L: lateral; M: medial.

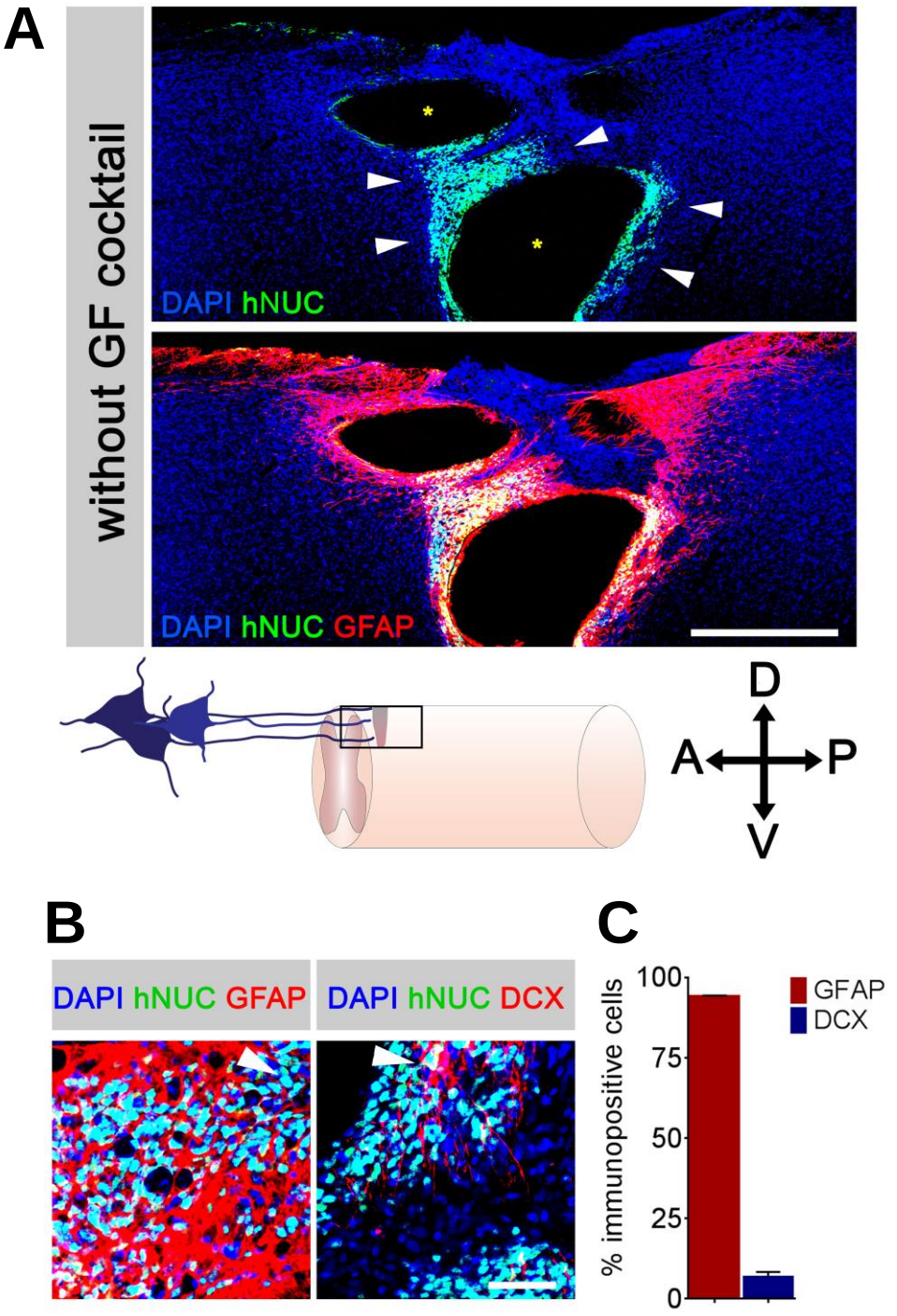

Figure 4.5: HUES6-derived neurospheres moderately survive and mainly differentiate into astrocytes in the injured spinal cord.

(A) Representative photomicrographs of $hNUC^{+}$ HUES6-derived progeny four weeks after wire knife lesion of the C4 dorsal column and transplantation without additional growth factors. Transplanted cells **(B, C)** mainly expressed the astrocytic marker GFAP and some cells expressed the early neuronal marker DCX.
Scale bar: **(A)** 500 µm and **(B)** 100 µm. **(C)** n = 3 animals.
GF: growth factor; A: anterior; P: posterior; D: dorsal; V: ventral.

4.2. In vitro characterization of pluripotent stem cell derived astrocytes

4.2.1. Modified differentiation protocol for the generation of neuron-free astrocytic cultures

In vitro differentiation of NSCs into astrocytes is strongly promoted by exposure to FBS.

As astrospheres differentiated according to the procedure described above did not result in pure astrocytic cultures, early (DIV 80 - 90) neurospheres were dissociated, plated on PLO/laminin and exposed to 1% FBS for at least two weeks prior to differentiation. In addition, to boost astrocytic maturation, NSCs were exposed either to FBS alone or to FBS in combination with CNTF, BMP2/4 or FGF1 in absence of EGF and FGF2 (Figure 4.1, right timeline), as these three factors are considered to be potent modulators of astrocytic maturation (paragraph 2.5.4.). In addition, we aimed to determine whether exposure to these factors influences astrocytic maturation and thereby generating homogeneous astrocytic cultures more suitable for transplantation.

4.2.2. Immunocytochemical analysis and Ca^{2+} imaging of pluripotent stem cell derived astrocytes

NSCs plated at DIV ~80 at low density, pre-treated for at least two weeks with FBS in the presence of EGF/FGF2 and eventually differentiated for two weeks with FBS and CNTF, BMP2/4 or FGF1 (Figure 4.1, right timeline) gave rise to neuron-free (Figure 4.6 B) cultures of maturing astrocytes at any time point after FBS pre-treatment (DIV ≥ 95 + two weeks of differentiation). About 20 - 30% of differentiating cells were $GFAP^+$ (Figure 4.6 A, C). In HUES6-derived cultures, BMP2/4 treatment reduced the number of $GFAP^+$ astrocytes. However, across all lines and indicated treatments, the percentage of $GFAP^+$ astrocytes was not higher than in neurosphere cultures differentiated without FBS (Figure 4.2.2 and 4.2.3).

To further confirm the astrocytic identity of differentiating cells, cellular responses to external stimuli were tested in DIV ≥ 95 cells differentiated with CNTF for two weeks. As previously described [401], *in vitro* stimulation of astrocytes by exposure to ATP leads to increases in nuclear/cytoplasmic Ca^{2+} concentration. Local application of ATP using a Picospritzer leads to single-cell Ca^{2+} fluctuations, which can be transmitted to neighboring astrocytes via gap junctions, generating so called Ca^{2+} waves. After loading with the Ca^{2+} indicator Fura-2 and stimulation with 100 µM ATP (by bath application), increases in nuclear and cytoplasmic Ca^{2+} concentrations were detected as increases in fluorescence intensity (Figure 4.7 A). Fluorescence intensity was measured every second over five minutes and plotted as a continuous intensity-over-time curve (Figure 4.7 B). Differences between cell lines and response patterns were

thereby identified: differentiating astrocytes responded either with an early (< 60 seconds) or late (> 60 seconds) single-peak increase in intracellular Ca^{2+} concentration followed by a decrease towards threshold levels or with early or late oscillatory fluctuations, consisting of more than two consecutive peaks of similar or smaller amplitude. While about 50% of HUES6-derived astrocytes responded to ATP stimulation, up to 80% of iPSC #2-derived astrocytes were responsive. In contrast, iPSC #1-derived astrocytes were generally unresponsive. HUES6-derived astrocytes primarily responded with a single-peak increase in nuclear and cytoplasmic Ca^{2+} concentration whereas iPSC #2-derived astrocytes primarily responded with oscillatory fluctuations (Figure 4.7 C).

The fact that most iPSC #1-derived cells were unresponsive, while about 80% of all iPSC #2-derived stimulated cells responded, yet both lines contain about 20 - 30% were $GFAP^{+}$ cells (Figure 4.6) suggests that GFAP expression alone is insufficient to identify mature and functional astrocytes.

In summary, iPSC #1-derived astrocytes only rarely responded to ATP stimulation, whereas HUES6- and iPSC #2-derived astrocytes exhibited a characteristic response pattern, indicating that, while morphologically similar, astrocytic lines and individual cells have a distinct functional profile.

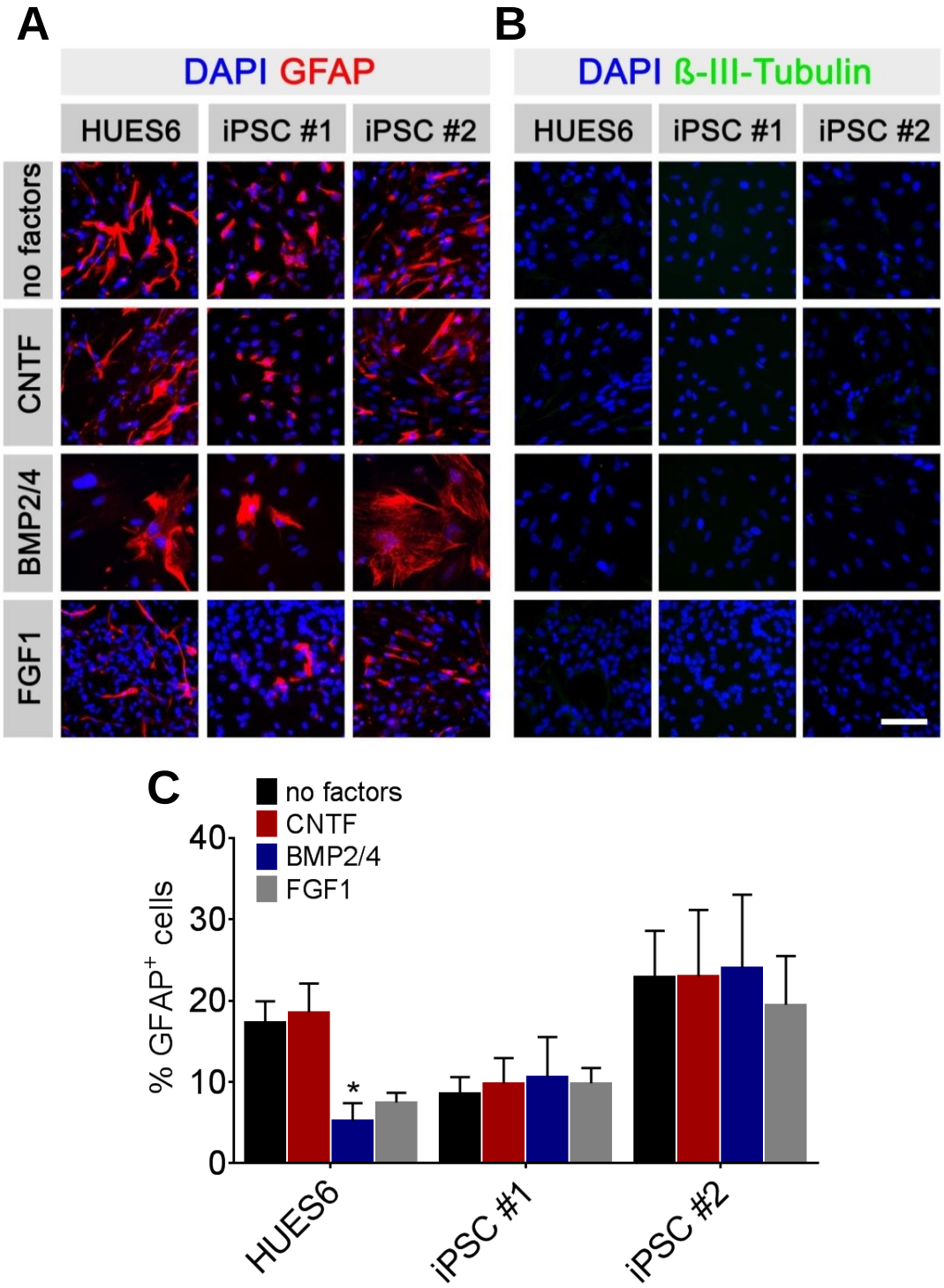

Figure 4.6: Treatment of PSC-derived NSCs with 1% FBS and differentiation with CNTF, BMP2/4 or FGF1 for two weeks leads to neuron-free cultures.

(A-B) Representative photomicrographs of **(A)** GFAP and **(B)** ß-III-tubulin expression after two weeks of NSC-differentiation either with 1% FBS alone or with FBS in combination with the factor indicated. **(B)** NSCs did not differentiate into neurons and **(C)** GFAP expression was detected in ~20 - 30% of the cells.

Scale bar: 20 µm. n = 3 - 6 wells / condition; asterisks indicate significant differences between treatment and the ‚no factors' control. One-way ANOVA, Fisher's LSD post hoc, *: $p < 0.05$.

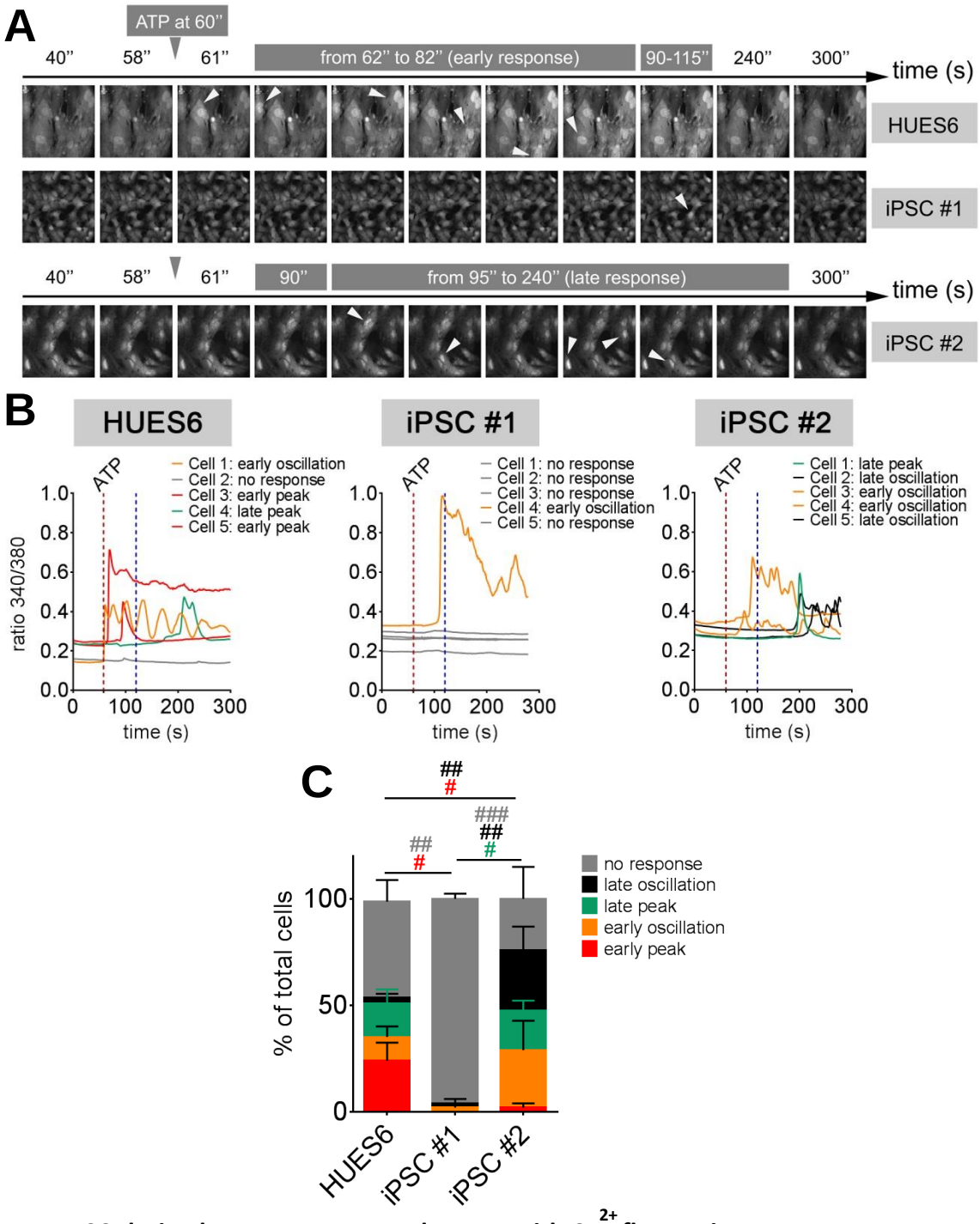

Figure 4.7: PSC-derived astrocytes respond to ATP with Ca^{2+} fluctuations.

(A) Representative photomicrographs and **(B)** graphic representation of Ca^{2+} fluctuations after ATP-mediated stimulation of astrocytes differentiated for two weeks with CNTF. By means of the Ca^{2+} indicator Fura-2, increases in nuclear and cytoplasmic Ca^{2+} concentrations were turned into changes in fluorescence intensity. **(C)** The distribution of „peak“ and „oscillatory“, as well as „early“ and „late“ responses is shown as % of the total number of analyzed cells .

n = 3 independent experiments, n = 48 - 71 individual cells per cell line; hashtags indicate significant differences. One-way ANOVA, Fisher‘s LSD post hoc was performed separately for each response pattern; #: $p < 0.05$, ##: $p < 0.01$, ###: $p < 0.001$.

4.2.3. Astrocytes differentiated in the presence of CNTF, BMP2/4 and FGF1 are morphologically distinct

During differentiation of PSC-derived NSCs with CNTF, BMP2/4 and FGF1, distinct morphological changes in all astrocytic lines were observed. To quantify these qualitative observations, astrocytes were labeled with the early astrocytic marker vimentin, which was expressed in virtually all cells (Table 4.1 and Figure 4.8 A). The perimeters of the cells were traced and the area was measured using ImageJ (Figure 4.8 B). This quantification revealed significant differences in cell size of differentiating astrocytes across treatments: HUES6-derived and iPSC #2-derived astrocytes treated with BMP2/4 were significantly larger, whereas FGF1-treated astrocytes exhibited a trend towards a decrease in cell size. In iPSC #1-derived astrocytes, only a small BMP2/4 treatment-dependent effect was observed suggesting that this line is not only unresponsive to ATP stimulation, but also less sensitive to factors inducing astrocytic maturation. In addition, iPSC #1-derived astrocytes had a rather round and less complex morphology compared to the other two cell lines.

These results indicate that although CNTF, BMP2/4 and FGF1 lead to astrocytic cultures with a similar degree of GFAP expression, they can have a strong effect on cell morphology and may specify distinct astrocytic subtypes, in concert with previously published results [222, 387, 388].

Table 4.1: PSC-derived NSCs differentiated for two weeks homogeneously express vimentin.

	HUES6	iPSC #1	iPSC #2
no factors	99.2 ± 0.6	100 ± 0	98.7 ± 1.3
CNTF	99.1 ± 0.6	100 ± 0	99.2 ± 0.3
BMP2/4	98.8 ± 0.8	99.5 ± 0.5	96.3 ± 1.6
FGF1	99.7 ± 0.3	99.3 ± 0.5	99.8 ± 0.1

Quantitative analysis of vimentin expression in PSC-derived astrocytes differentiated for two weeks. Virtually all cells express vimentin independently of the cell line or culturing conditions.

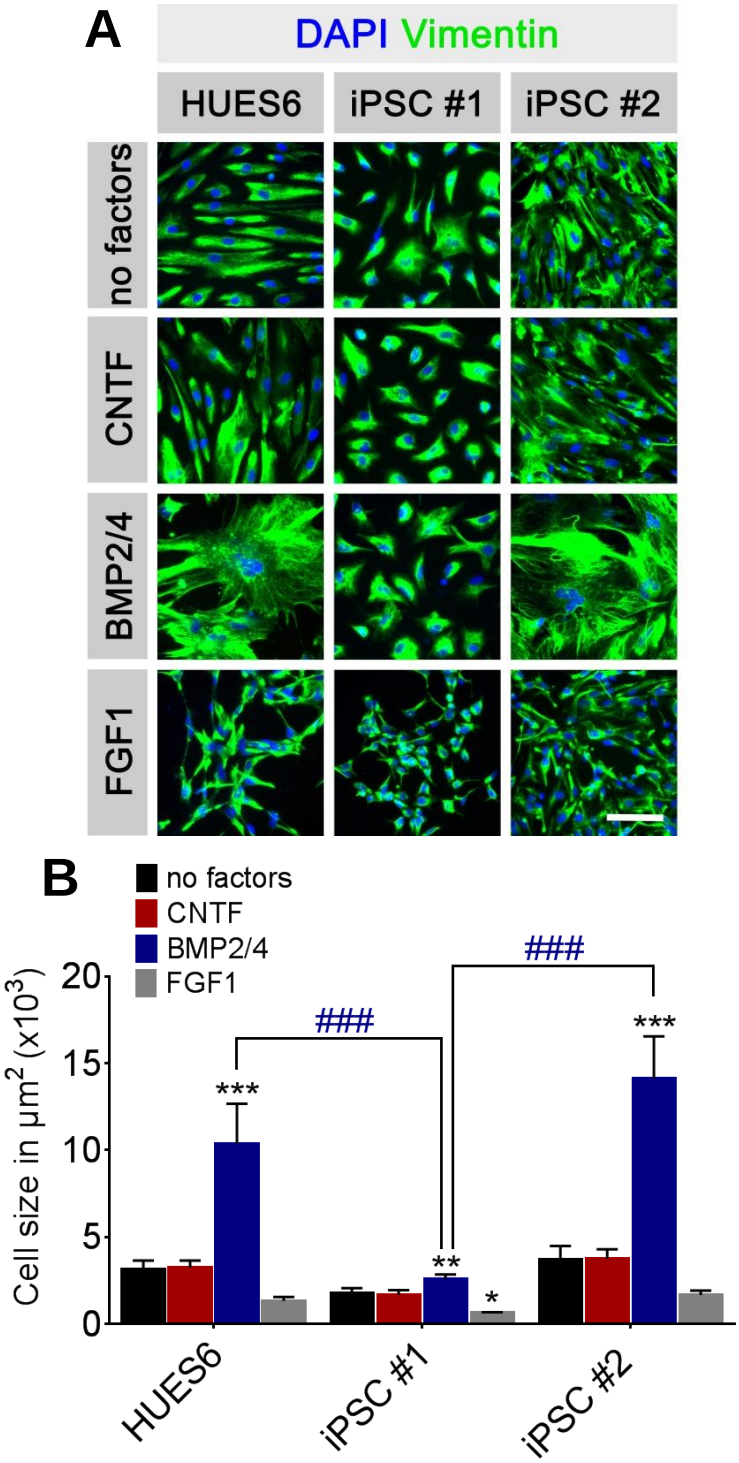

Figure 4.8: BMP2/4 treatment leads to an increase in cell size of PSC-derived astrocytes.

(A) Representative photomicrographs of vimentin expression and **(B)** quantification of the cell size of astrocytes after two weeks of differentiation either with FBS alone or with FBS in combination with the factor indicated. Scale bar: 20 µm. n = 3 - 6 wells / condition; asterisks indicate significant differences between each treatment applied and the ‚no factors' control group, one-way ANOVA, Fisher's LSD post hoc. Hashtags indicate significant differences between cell lines, two-way ANOVA, Tukey's post hoc; * and #: $p < 0.05$, ** and ##: $p < 0.01$, *** and ###: $p < 0.001$.

4.2.4. Pluripotent stem cell derived astrocytes retain Sox2 and Ki67 expression after two weeks of differentiation

As mentioned above, after two weeks of differentiation only about 20 - 30% of all cells were $GFAP^+$ astrocytes.

In order to assess to which degree differentiating cultures were im-/mature, expression of the NSC marker Sox2 was quantified. Across all lines between 20% and 40% of cells were $Sox2^+$ after two weeks; the highest amount - up to about 80% - of $Sox2^+$ cells was observed in FGF1-treated cultures across all lines (Figure 4.9). This suggests that FGF1 does not promote maturation of PSC-derived NSCs into astrocytes. On the other hand, a significant decrease in $Sox2^+$ precursors in HUES6-derived and iPSC #2-derived astrocytes treated with BMP2/4 suggests that these cells are more mature, which is not reflected in increased $GFAP^+$ expression (Figure 4.6).

Maturing HUES6-derived and iPSC #2-derived astrocytic cultures retained a generally low proliferation potential: between 5% and 20% of the cells were immunolabeled for Ki67 (Figure 4.10). HUES6-derived astrocytes were the least proliferative, with a significant increase to about 20% in the FGF1-treated group. Strikingly, in iPSC #1-differentiating cultures about 50% of the cells expressed Ki67, whereby about 90% $Ki67^+$ cells were detected in the FGF1-treated group.

These findings suggest that FGF1 is not a potent inductor of astrocytic maturation for PSC-derived NSCs. In addition, iPSC #1-derived cultures were highly proliferative, indicating that they might be robust, stress-resistant and capable of filling a lesion site after SCI or that they might result in uncontrolled proliferation after transplantation.

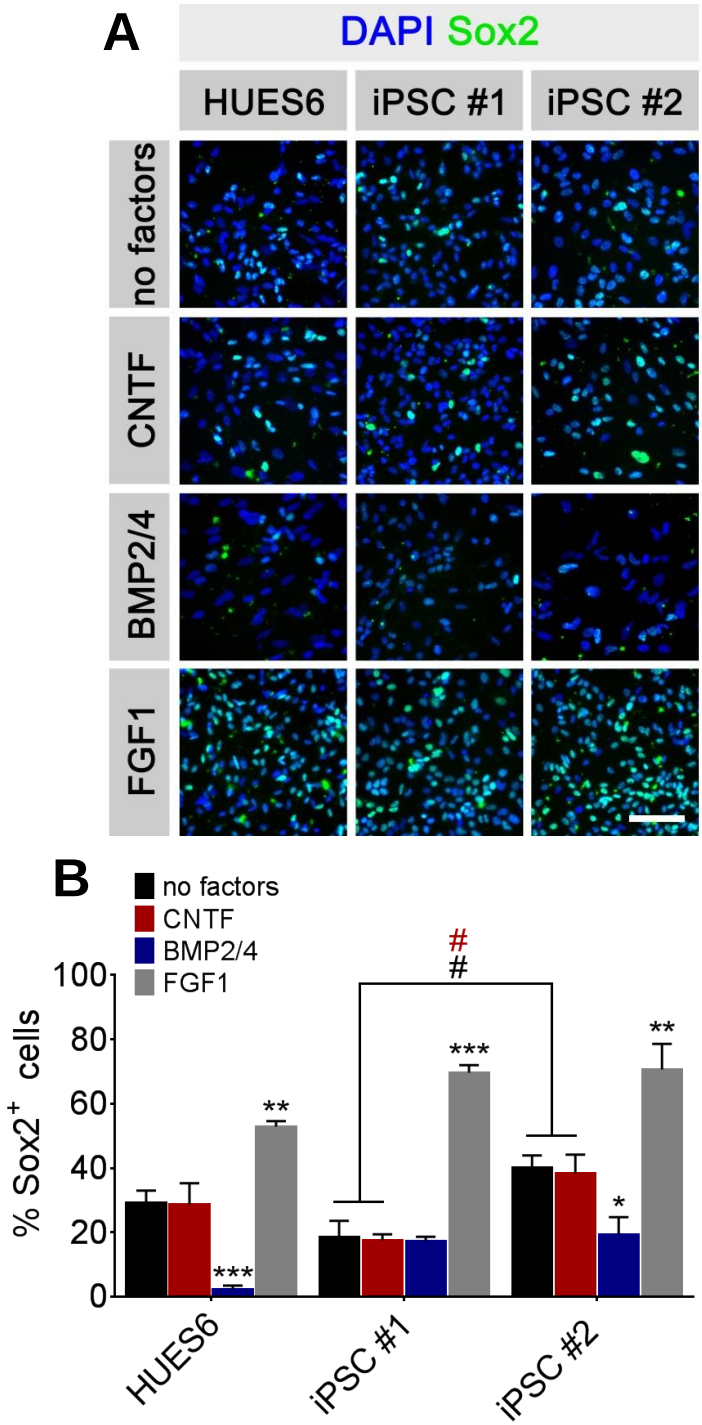

Figure 4.9: FGF1 treatment leads to an increase in Sox2 expression in PSC-derived NSCs.

(A) Representative photomicrographs and **(B)** quantification of Sox2 expression in maturing PSC-derived astrocytes after two weeks of differentiation either with FBS alone or with FBS in combination with the factor indicated.

Scale bar: 20 µm. n = 3 - 6 wells / condition; asterisks indicate significant differences between each treatment applied and the ‚no factors' control group, one-way ANOVA, Fisher's LSD post hoc. Hashtags indicate significant differences between cell lines, two-way ANOVA, Tukey's post hoc; * and #: $p < 0.05$, ** and ##: $p < 0.01$, *** and ###: $p < 0.001$.

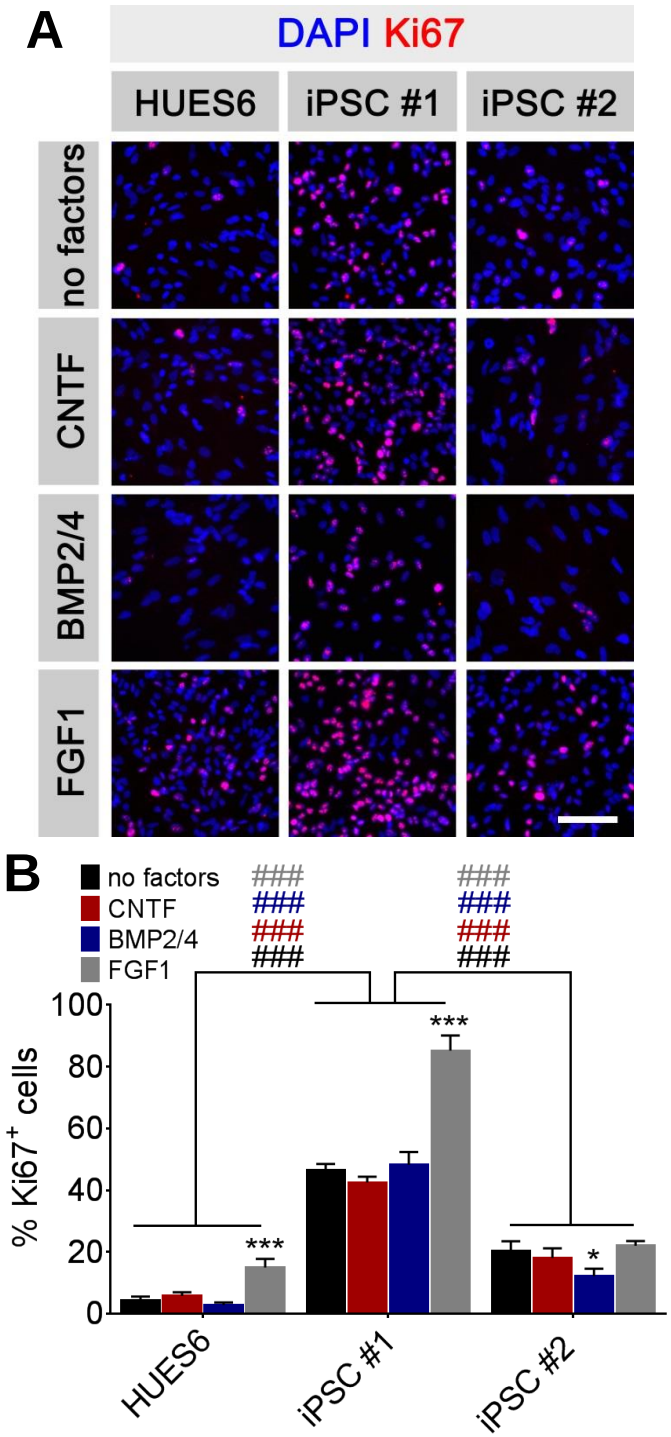

Figure 4.10: iPSC #1-derived astrocytes are highly proliferative.

(A) Representative photomicrographs and **(B)** quantification of Ki67 expression in maturing PSC-derived astrocytes after two weeks of differentiation with FBS alone or with FBS in combination with the factor indicated.

Scale bar: 20 µm. n = 3 - 6 wells / condition; asterisks indicate significant differences between each treatment applied and the ‚no factors' control group, one-way ANOVA, Fisher's LSD post hoc. Hashtags indicate significant differences between cell lines, two-way ANOVA, Tukey's post hoc; * and #: $p < 0.05$, *** and ###: $p < 0.001$.

4.2.5. Pluripotent stem cell derived astrocytes produce extracellular matrix

One function of astrocytes which is highly relevant in the healthy and injured CNS is the production of ECM components. The latter can be growth-promoting or growth-repulsive. As previously mentioned (paragraph 2.5.2.), reactive astrocytes up-regulate CSPGs after injury; of these, some can be growth-repulsive (e.g. CSPG1-3 and 7 also known as Aggrecan, Versican, Neurocan, Brevican, as well as Phosphacan) and some can be growth-promoting (e.g. CSPG4-5 also known as NG2 and Neuroglycan C) [25].

Total CSPG expression in astrocytic cultures was analyzed by immunolabeling of the CSPG core protein CS-56 (Figure 4.11 A, C). To quantify the amount of CSPG, the fluorescence signal was first converted into a binary (black and white) image and the area-fraction covered by CSPG was quantified and divided by the total number of cells per field, to express CSPG levels as % covered area per cell.
Expression of CSPG was significantly higher in astrocytes differentiated for two weeks with BMP2/4 (Figure 4.11 C, D) and decreased in FGF1-treated cultures across all lines. iPSC #1-derived astrocytes produced the lowest amount of CSPG across all treatments, however, due to the fact that they had to be passaged at least once during differentiation, the low amount of CSPG detected might underlie enzymatic digestion of the ECM. Therefore, CSPG production was also analyzed after one week of differentiation, before passaging was necessary (Figure 4.11 A, B). The same expression pattern was observed across treatments and cell lines, and iPSC #1-derived precursors hardly produced any CSPG.

In summary, HUES6-derived and iPSC #2-derived BMP2/4-treated astrocytes produced the highest amount of CSPG both after one week and after two weeks of differentiation. In addition, the highly proliferative and ATP unresponsive iPSC #1-derived cultures were not capable of producing appreciable amounts of CSPG further indicating their limited differentiation potential.

As a second ECM component, laminin expression was examined. Laminin has been associated with axonal growth in the developing CNS and PNS, such as in areas of the adult CNS where regeneration is observed [402, 403], and is used *in vitro* to promote attachment and growth of NSCs as well as their progeny, including neurons.

Laminin expression in maturing astrocyte cultures was mostly restricted to the HUES6-derived line and particularly to FBS only- or CNTF-treated astrocytes (Figure 4.12). iPSC #2-derived astrocytes produced low levels of laminin and in iPSC #1-derived cultures hardly any laminin immunolabeling could be detected.

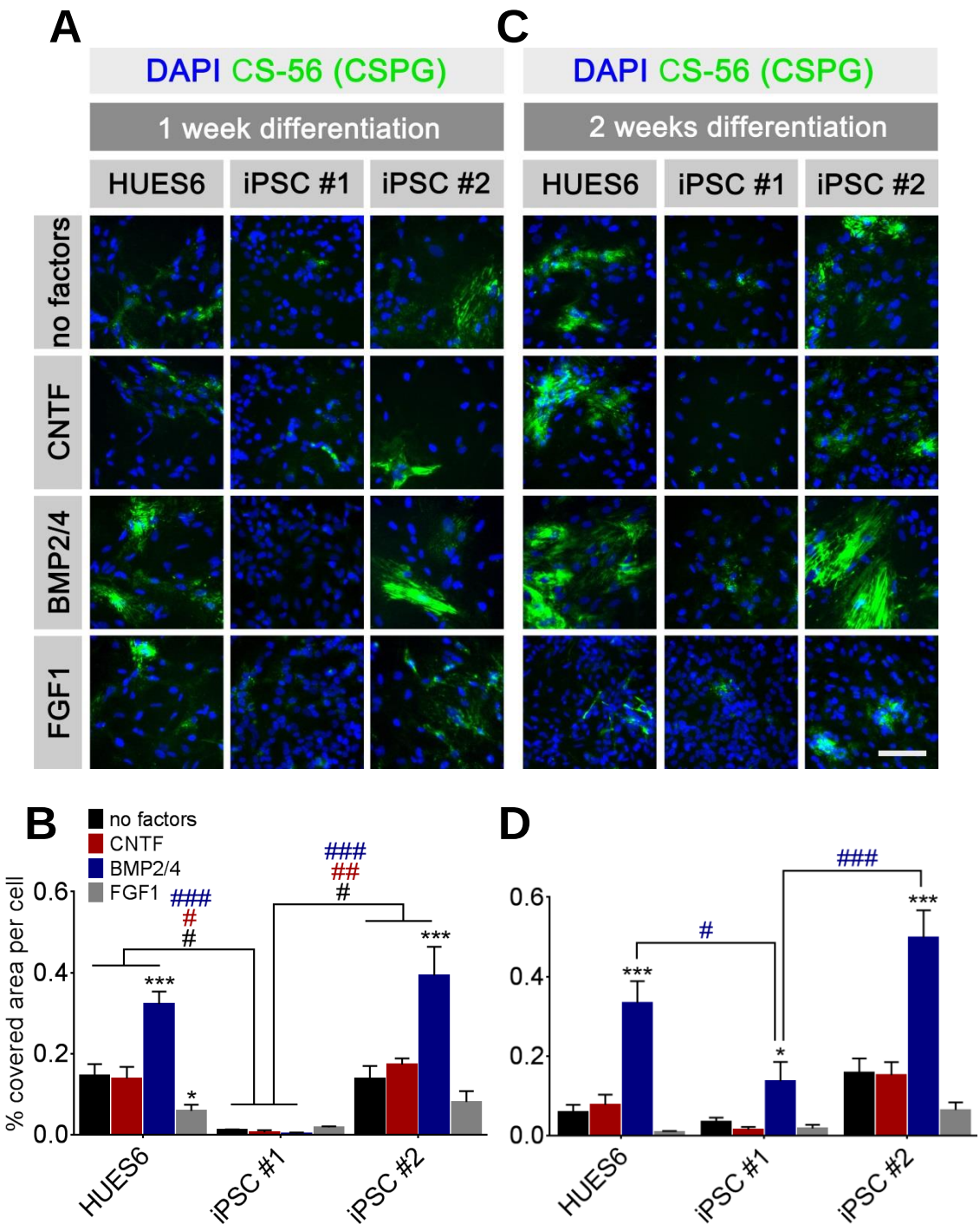

Figure 4.11: BMP2/4 treatment leads to an increase in CSPG production by PSC-derived astrocytes.

(A, C) Representative photomicrographs and **(B, D)** quantitative analysis of CSPG expression in PSC-derived astrocytes after **(A, B)** one week and **(C, D)** two weeks of differentiation with FBS alone or with FBS in combination with the factor indicated.

Scale bar: 20 µm. n = 3 - 6 wells / condition; asterisks indicate significant differences between each treatment applied and the ‚no factors' control group, one-way ANOVA, Fisher's LSD post hoc. Hashtags indicate significant differences between cell lines, two-way ANOVA, Tukey's post hoc; * and #: $p < 0.05$, ** and ##: $p < 0.01$, *** and ###: $p < 0.001$.

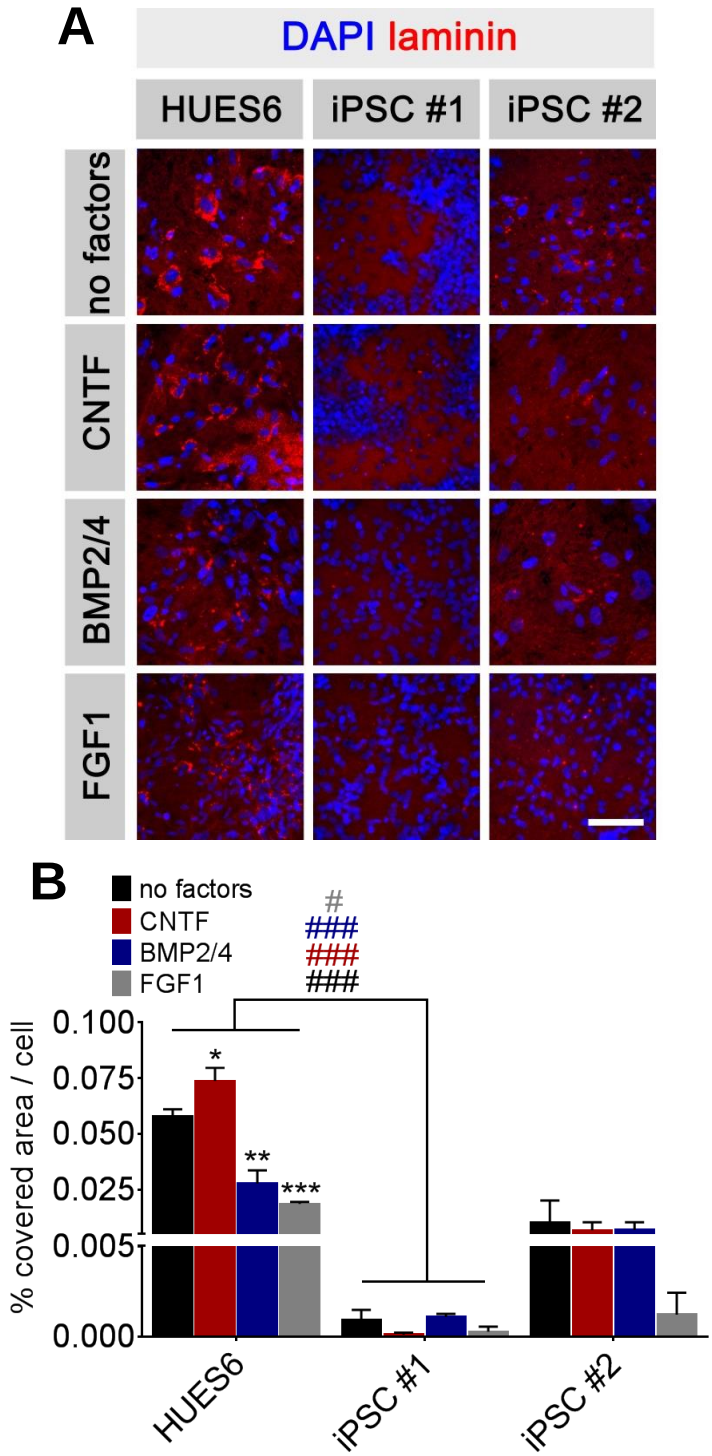

Figure 4.12: Laminin expression is low in PSC-derived astrocytes.

(A) Representative photomicrographs and **(B)** quantitative analysis of laminin expression in PSC-derived astrocytes after two weeks of differentiation either with FBS alone or with FBS in combination with the factor indicated.

Scale bar: 20 µm. n = 3 wells / condition; asterisks indicate significant differences between each treatment applied and the ‚no factors' control group, one-way ANOVA, Fisher's LSD post hoc. Hashtags indicate significant differences between cell lines, two-way ANOVA Tukey's post hoc;

* and #: $p < 0.05$, ** and ##: $p < 0.01$, *** and ###: $p < 0.001$.

4.2.6. Pluripotent stem cell derived astrocytes produce a low amount of BDNF

Astrocytes can exert their neurotrophic and growth-promoting effect by releasing neurotrophic factors including BDNF into the extracellular space (paragraph 2.5.1.5.).

Therefore we analyzed BDNF levels in astrocytic supernatants by ELISA after differentiation for two weeks. The measured absolute amount was divided by the total number of cells per well to calculate the amount of BDNF produced by 10^6 cells under the same conditions (Figure 4.13). Across all lines, up to 300 pg BDNF/10^6 cells/24h was measured, with a significant increase in the BMP2/4 group across all cell lines. iPSC #2-derived BMP2/4-treated astrocytes produced up to 3 ng of BDNF, at least ten-fold more than in all other treatments across all lines.

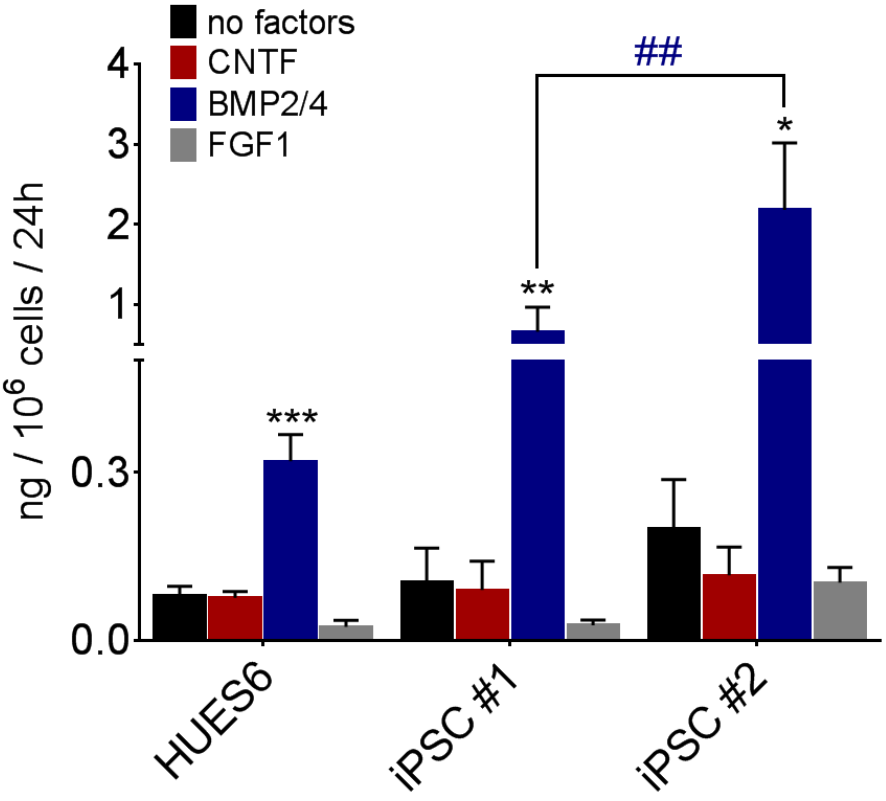

Figure 4.13: BMP2/4 treatment leads to an increase in BDNF production in PSC-derived astrocytes.

BDNF ELISA of supernatants from PSC-derived astrocytes differentiated for two weeks with FBS alone or with FBS in combination with the factor indicated.

n = 3 - 6 wells / condition; asterisks indicate significant differences between each treatment applied and the ‚no factors' control group, one-way ANOVA, Fisher's LSD post hoc. Hashtags indicate significant differences between cell lines, two-way ANOVA Tukey's post hoc; * and #: $p < 0.05$, ** and ##: $p < 0.01$, *** and ###: $p < 0.001$.

4.2.7. Co-culture of two-week differentiated pluripotent stem cell derived astrocytes with rat primary dorsal root ganglion neurons

In order to assess the direct interaction between PSC-derived astrocytes and neurons, PSC-derived NSCs were differentiated for two weeks and then co-cultured with rat primary DRG neurons for 24 hours. To this end, rat primary DRGs were isolated, plated on PLO/laminin-coated 6-well plates and re-plated 24 hours later; immediately prior to re-plating, dead cells and potentially inhibitory debris, such as DRG-derived myelin, were washed out. DRG neurons survived on astrocytic monolayers and extended numerous branched and unbranched neurites within 24 hours (Figure 4.14 A). To quantify the maximal *in vitro* pro-regenerative effect of astrocytic cultures, the longest neurite of each DRG neuron was measured using the NeuronJ plugin of ImageJ. The average length of the longest DRG neurites was significantly higher in HUES6-derived astrocytic co-cultures, especially in the FBS-only and CNTF groups, where neurites with a length of > 2000 µm were measured - a quite impressive length considering the short co-culturing time. FBS-only and CNTF-treated HUES6-derived astrocytes also promoted the highest amount of neurite outgrowth above 500 µm (Figure 4.14 C).
iPSC #1- and iPSC #2-derived astrocytes promoted an average neurite outgrowth of 600 µm, whereby iPSC #1-derived astrocytes were less pro-regenerative (figure 4.14 B).

Although it is not possible to establish a causal relationship between these two findings, a correlation between the laminin expression pattern (figure 4.12) and the extent of neurite outgrowth was observed.

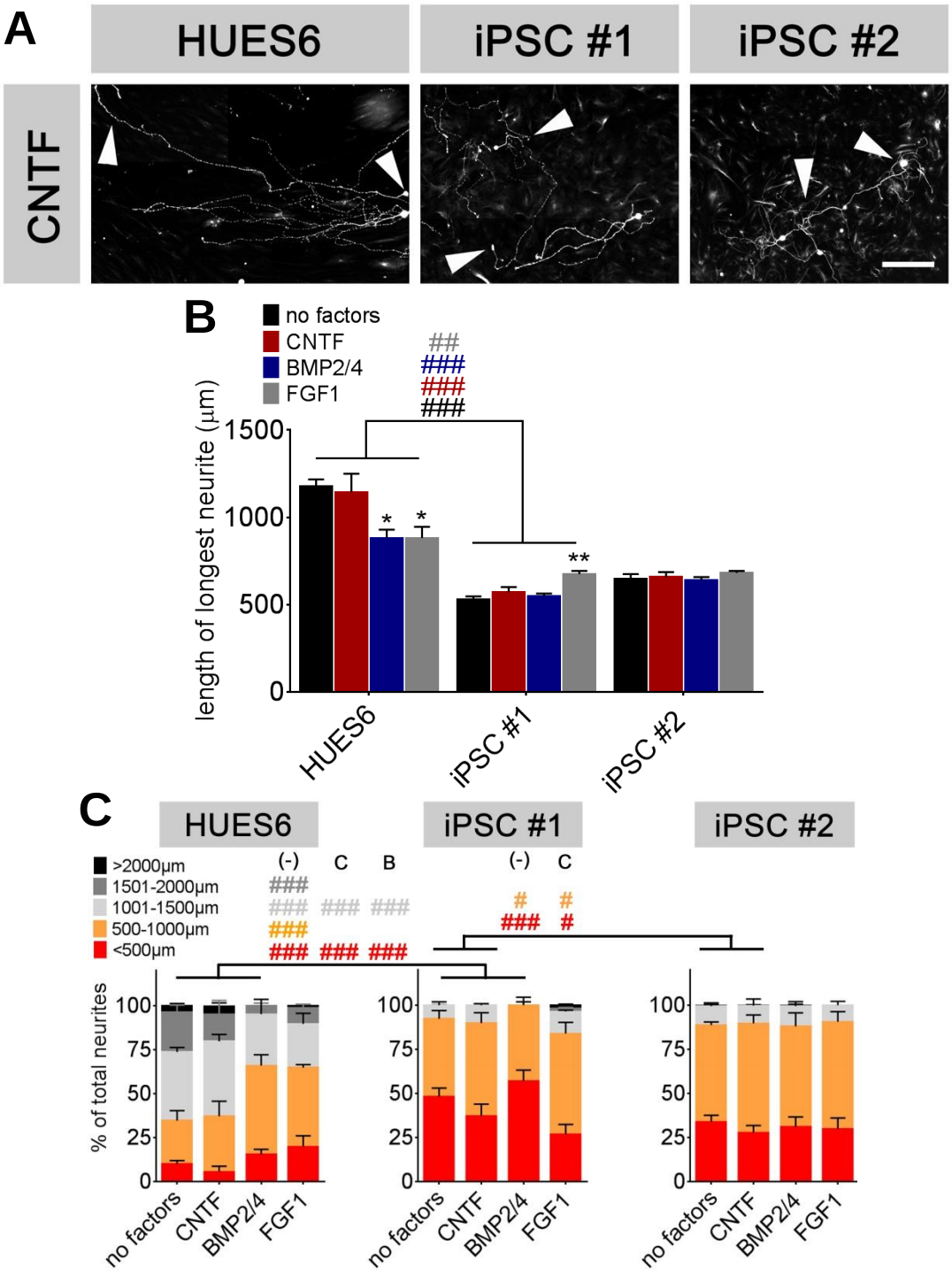

Figure 4.14: Influence of PSC-derived astrocytes on neurite growth of DRG neurons.

(A) Representative photomicrographs of ß-III-tubulin immunolabeled DRG neurons after 24 hours of co-culturing on PSC-derived astrocytes differentiated for two weeks with FBS and CNTF. **(B)** Quantification of the average length of the longest neurite across cell lines and differentiation conditions as indicated. **(C)** Quantification of the incidence of neurite length-ranges across cell lines and differentiation conditions as indicated.

Scale bar: 250 µm. n = 3 wells; Hashtags indicate significant differences between cell lines, two-way ANOVA, Tukey's post hoc; * and #: $p < 0.05$, ** and ##: $p < 0.01$, *** and ###: $p < 0.001$.

4.3. Transplantation of differentiated astrocytes into the intact and lesioned spinal cord

PSC-derived neurospheres differentiated without FBS treatment and transplanted into the injured spinal cord (Figures 4.4.1, 4.4.2 and 4.5) modestly survived and differentiated into astrocytes *in vivo*, but the neurogenic potential observed *in vitro* persisted *in vivo*.

We next aimed at transplanting proliferative NSCs or neuron-free pre-differentiated astrocytes into the injured as well as intact spinal cord to evaluate their survival and whether the set of phenotypical and functional properties acquired *in vitro* are maintained *in vivo* in the host microenvironment, allowing us to choose a pro-regenerative astrocytic subtype.

To minimize the number of animals, only one PSC-line was chosen for the first pilot animal experiment and thereafter only CNTF-treated astrocytes were compared across three lines. Due to their high proliferation rate, we hypothesized that iPSC #1-derived NSCs might be robust enough to fill the lesion site after a dorsal column wire knife lesion.

An overview of experimental groups and survival rates of this pilot experiment can be found in Appendix table 4.2 B. Animals received subcutaneous injections of cyclosporine A and were allowed to survive for two or four weeks as indicated.

4.3.1. iPSC #1-derived neural stem cells hardly survive after transplantation into the injured spinal cord

First, to evaluate the robustness of proliferating iPSC#1-derived NSCs cultured with 1% FBS and EGF/FGF2, we transplanted DIV ~130 - 160 proliferating precursors one week after a wire knife lesion of the spinal cord. To assess which paradigm is more suitable to maximize survival rates, prior to transplantation, PSC-derived NSCs were resuspended in a solution containing calpain inhibitor and either EGF/FGF2 or nine growth factors, or they were co-grafted with adult rat fibroblasts to assess if they can sustain PSC-derived NSCs in the lesion site; either EGF/FGF2 or the full growth factor cocktail were used to resuspend the cell mixture.

In contrast to our hypothesis that proliferating NSCs may be more robust than pre-differentiated cells, proliferating iPSC #1-derived NSCs exhibited poor survival two weeks after transplantation into the injured spinal cord (Figure 4.15 A-D and Appendix Table 4.2 B). Although $hNUC^+$ cells were detected in almost all animals, neither the presence of a growth factor cocktail (Figure 4.15 B, D) nor co-transplantation with rat fibroblasts (Figure 4.15 C, D) resulted in appreciable differences in survival rates.

Although the lesion site was filled in both fibroblast co-transplantation groups, the vast majority of the cells was $hNUC^-$ (Figure 4.15 C, D). In addition, in contrast to HUES6-transplanted neurospheres (Figure 4.5), only few $hNUC^+$ cells expressed GFAP (Figure 4.15 A-D, and

magnifications of boxed areas). In addition, colony-like tightly-packed hNUC$^+$ aggregates were detected in some animals (Figure 4.15 A, left-pointing arrow).

Altogether, these results show that iPSC #1-derived proliferating NSCs did not show superior survival after transplantation into the lesioned spinal cord. Poor differentiation into astrocytes might be due to the short time-frame (two weeks). Therefore, pre-differentiation of astrocytes with CNTF, BMP2/4 or FGF1 might result in a robust astrocytic phenotype *in vivo*.

4.3.2. iPSC #1-derived differentiated neural stem cells survive after transplantation into the injured spinal cord, but do not express GFAP

To evaluate their survival and the stability of their phenotype, astrocytes differentiated for two weeks with FBS and the indicated differentiation factor were transplanted one week after wire knife lesion of the spinal cord.

CNTF, BMP2/4 and FGF1 differentiation groups were included: (1) to assess the effect of the host microenvironment on their phenotype, (2) to evaluate whether differences observed in previous studies between astrocytes treated with CNTF *versus* BMP2/4 [222, 387, 388] were valid for our cultures and (3) to identify a potentially more growth-promoting astrocytic phenotype.
To support growth factor specific differentiation of astrocytic subtypes and to at least initially counteract the influence of the host microenvironment on the phenotype of grafted cells, differentiated astrocytes were re-suspended in a solution containing calpain inhibitor and the differentiation factor (CNTF, BMP2/4 or FGF1) used *in vitro* prior to transplantation.

iPSC #1-derived FGF1-treated NSCs exhibited a similarly low survival rate as proliferating precursors and did not result in decreased cavity formation (Figure 4.16 C and Appendix Table 4.2 B). CNTF- and BMP2/4-treated iPSC #1-derived NSCs on the other side were able to survive both at the edge of the lesion and at the lesion epicenter. Some small cavities were observed, however the lesion site was filled with hNUC$^+$ cells. In addition, hNUC$^+$ cells were found within the host tissue rostral and caudal to the lesion site (Figure 4.16 A, B and Appendix Table 4.2 B).

This result could be positively interpreted, since survival of transplanted cells is one of the major issues in stem cell-based SCI studies. However, hNUC$^+$ cells did not express the astrocytic marker GFAP (Figure 4.16 A-C and magnifications of boxed areas). Considering that they had been pre-differentiated for two weeks, this finding was unexpected.

4.3.3. iPSC #1-derived differentiated neural stem cells are likely tumorigenic, whereas HUES6- and iPSC #2-derived differentiated astrocytes express GFAP and laminin *in vivo*

As mentioned above, proliferative or differentiated iPSC #1-derived NSCs did not differentiate into $GFAP^+$ astrocytes within two weeks after injection into the wire knife lesioned spinal cord. To test whether the duration of the experiment (two weeks) or the host microenvironment underlie this outcome, we transplanted iPSC #1-derived NSCs after two weeks of differentiation into the intact spinal cord and allowed them to differentiate *in vivo* for four weeks (Appendix table 4.2 C).

iPSC #1-derived NSCs gave origin of tumor-like colonies of $hNUC^+$ cells, which expanded in all directions in the intact spinal cord. Colonies were densely packed and confined, with only few $hNUC^+$ cells migrating and integrating into the host tissue (Figure 4.17). This phenomenon was not observed in all animals: as shown in Appendix table 4.2, $hNUC^+$ cells were detected only in 33 - 50% of the animals, suggesting host rejection of transplanted iPSC #1-derived NSCs and clonal expansion of tumor-forming cells. To address this issue we transplanted HUES6- and iPSC #2-derived NSCs differentiated for two weeks with CNTF into the intact spinal cord and, after four weeks, we compared the three lines phenotypically (Figures 4.18.1 and 4.18.2, and Appendix table 4.2 C).
Reflecting the *in vitro* differences between iPSC #1 *versus* HUES6-/iPSC #2-derived differentiated NSCs (Figures 4.7, 4.8, 4.10, 4.11, 4.12 and 4.14), the latter two cell lines did not give origin to tumor-like colonies, and the survival rate was considerably lower (Figure 4.18.1 A, C). Independent on the differentiation factor applied, iPSC #1-derived NSCs pre-differentiated for two weeks were hardly $GFAP^+$ *in vivo* (Figure 4.18.1 B, magnification and figure 4.18.2 A, light blue bars), but ~15 - 25% of the cells were proliferative (Figure 4.18.2 B). Alarmingly, iPSC #1 $hNUC^+$ cells were surrounded by a thick layer of GFAP-expressing host astrocytes, suggesting that they might have induced an astrogliotic reaction. In contrast, HUES6- and iPSC #2-derived NSCs pre-differentiated for two weeks with CNTF *in vitro* homogeneously expressed GFAP (Figure 4.18.1 A, B, magnifications and Figure 4.18.2 A, grey bars). To determine if these astrocytes are functional, we analyzed expression of laminin, which is indicative of their ability to produce ECM. Laminin expression was observed in areas where $hNUC^+$ cells were present, but co-localized both with $hNUC^+$ and $hNUC^-$ host cells (figure 4.18.1 A, C, magnifications). Reflecting the *in vitro* findings (Figure 4.12), HUES6-derived astrocytes produced higher amounts of laminin and/or induced laminin production in host cells (Figure 4.18.2 C).

Altogether, *in vivo* findings reflect *in vitro* observations: phenotypical differences observed between the three lines *in vitro* correlated with phenotypical differences *in vivo*. However, due to the low number of animals and the low survival rate (Appendix table 4.2), these last animal experiments are not sufficient to draw definitive conclusions.

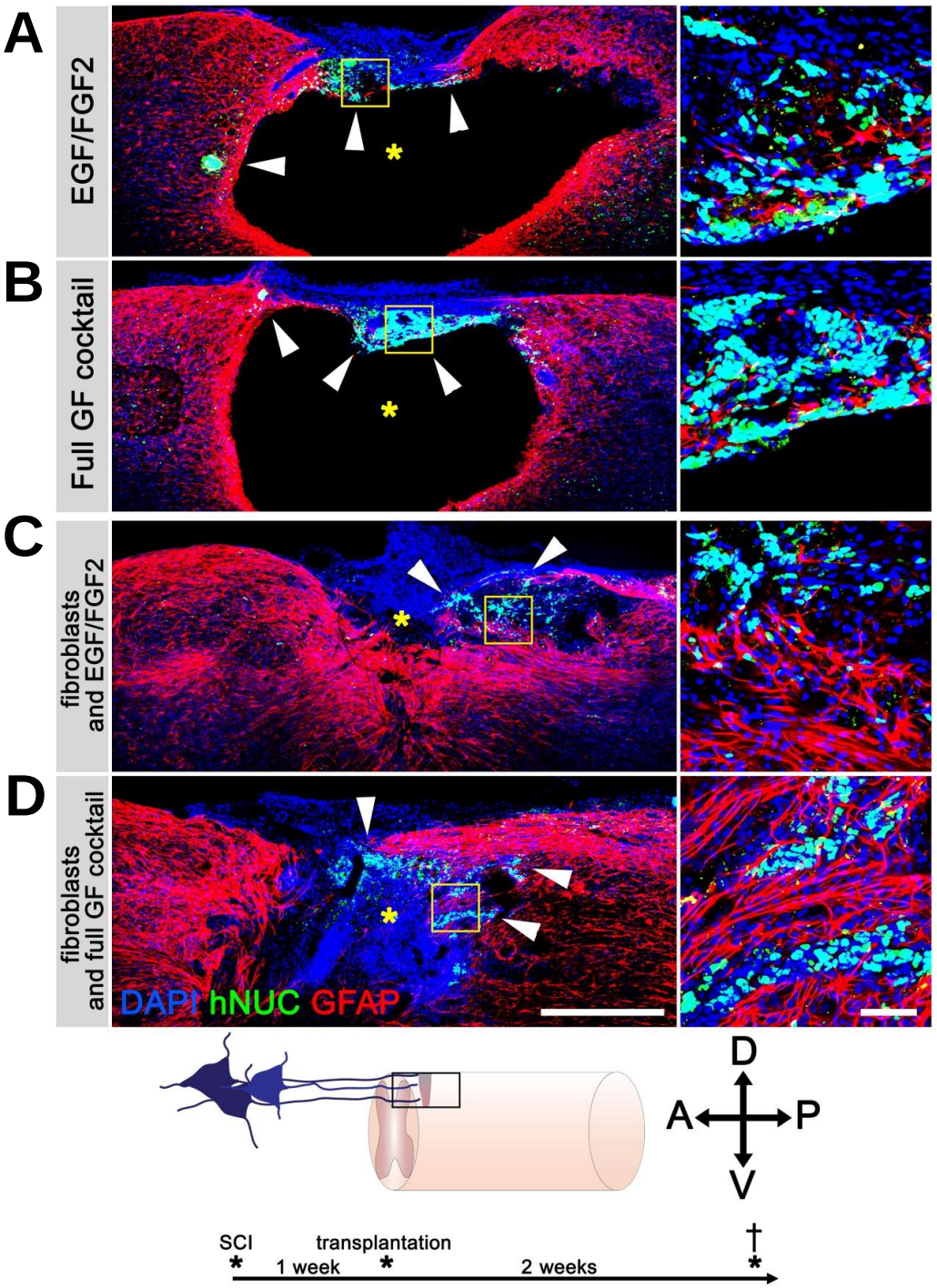

Figure 4.15: iPSC #1-derived NSCs hardly survive in the injured spinal cord and do not differentiate into GFAP$^+$ astrocytes.

Representative photomicrographs of hNUC$^+$ iPSC #1-derived progeny two weeks after transplantation into a C4 wire knife lesion **(A)** with EGF/FGF2, **(B)** with the full growth factor cocktail, **(C)** co-grafted with fibroblast and EGF/FGF2 or **(D)** co-grafted with fibroblast and the full growth factor cocktail. Higher magnification of boxed areas shows that transplanted cells hardly expressed the astrocytic marker GFAP. Scale bar: 500 µm (left panels) and 100 µm (right panels). GF: growth factor; A: anterior; P: posterior; D: dorsal; V: ventral.

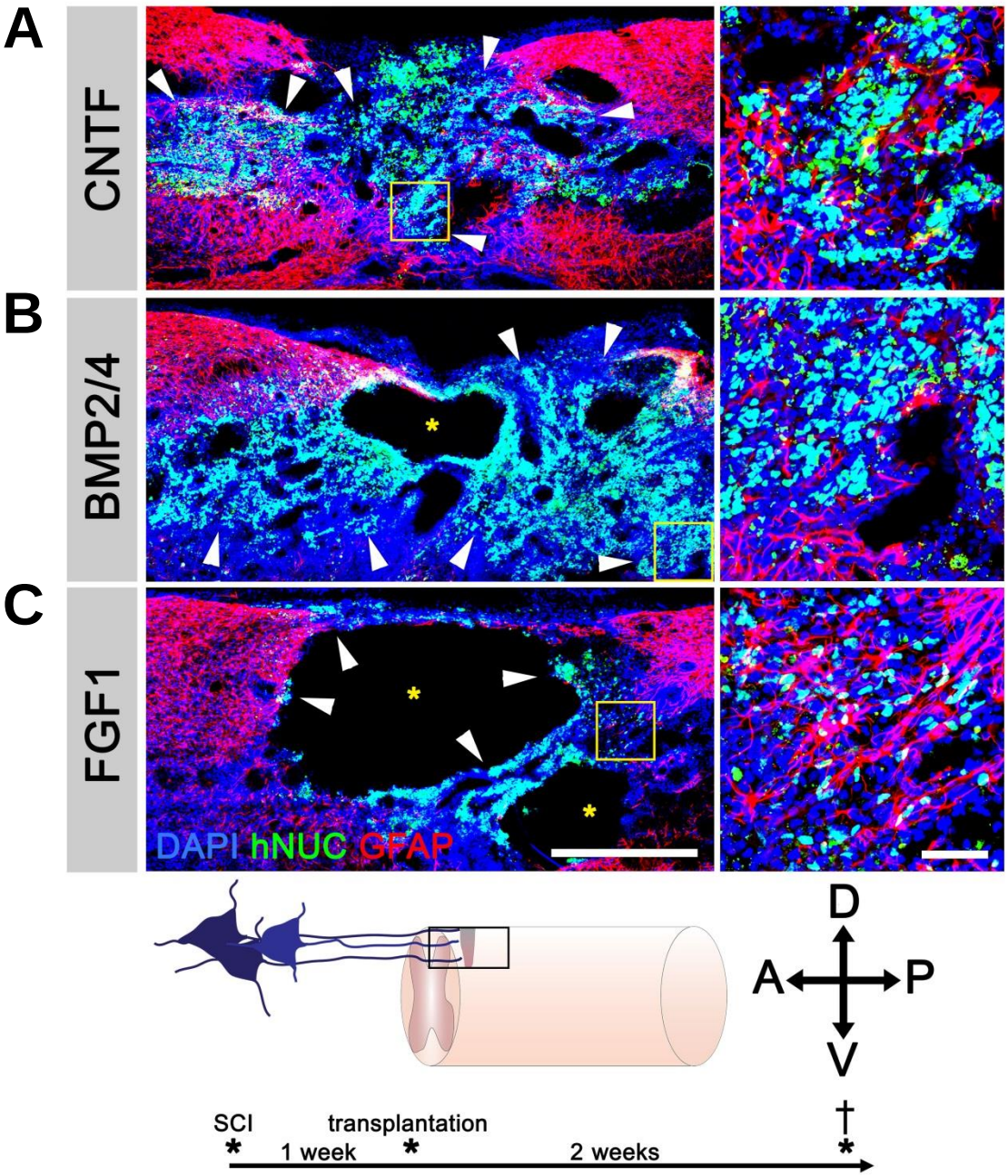

Figure 4.16: iPSC #1-derived NSCs differentiated for two weeks survive in the injured spinal cord but do not express GFAP.

Representative photomicrographs of hNUC^{+} iPSC #1-derived progeny differentiated *in vitro* for two weeks with the factor indicated followed by injection into a C4 wire knife lesion **(A)** with CNTF, **(B)** BMP2/4 or **(C)** FGF1. Higher magnification of boxed areas shows that very few transplanted cells expressed the astrocytic marker GFAP under all conditions.
Scale bar: 500 µm (left panels) and 100 µm (right panels).
A: anterior; P: posterior; D: dorsal; V: ventral.

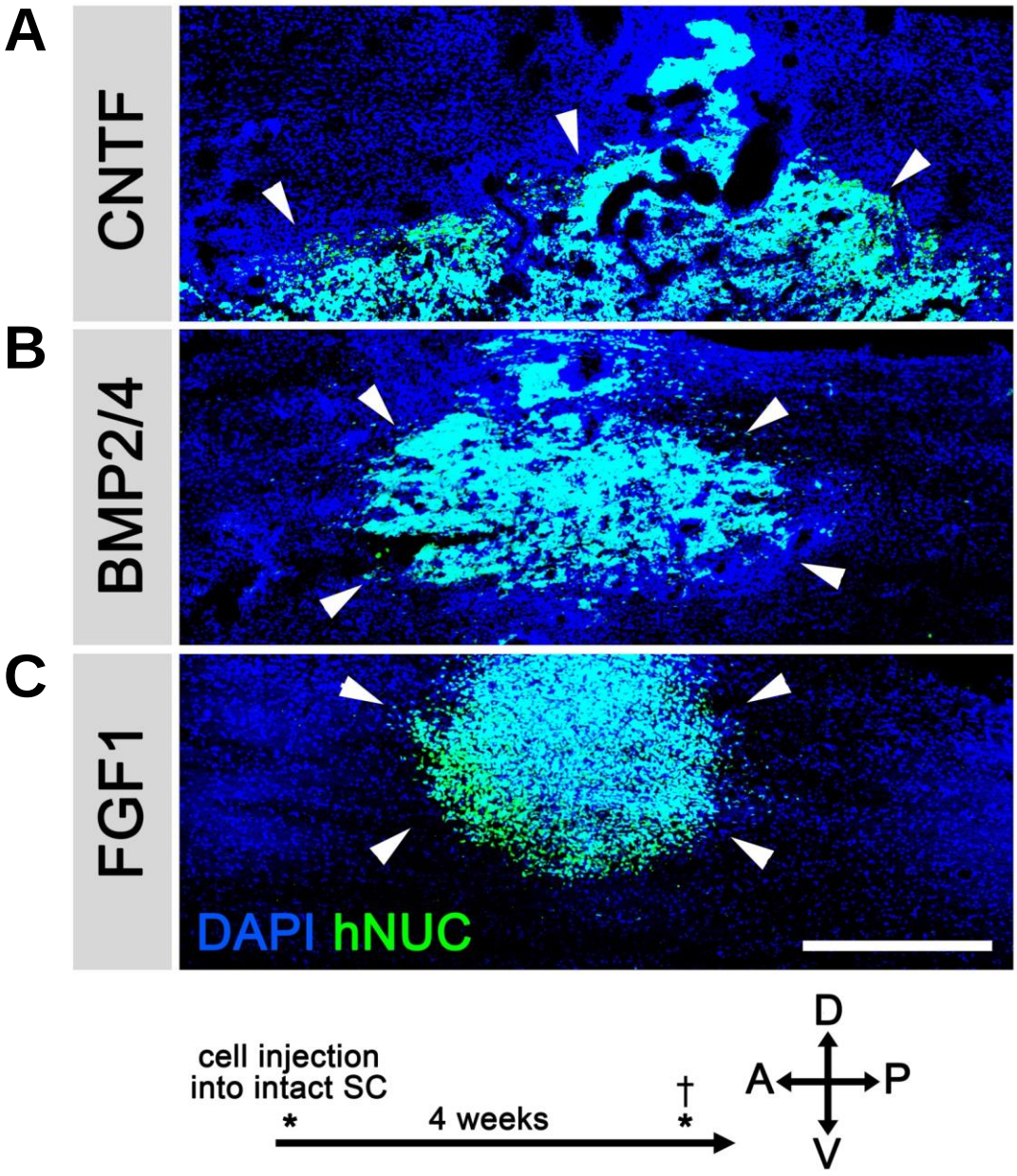

Figure 4.17: iPSC #1-derived NSCs differentiated for two weeks survive in the intact spinal cord but exhibit tumor-like growth.

Representative photomicrographs of hNUC^{+} iPSC #1-derived progeny after two weeks of differentiation with the factor indicated followed by injection into the C4 level of the intact spinal cord **(A)** with CNTF, **(B)** BMP2/4 or **(C)** FGF1.
Scale bar: 500 µm. SC: spinal cord; A: anterior; P: posterior; D: dorsal; V: ventral.

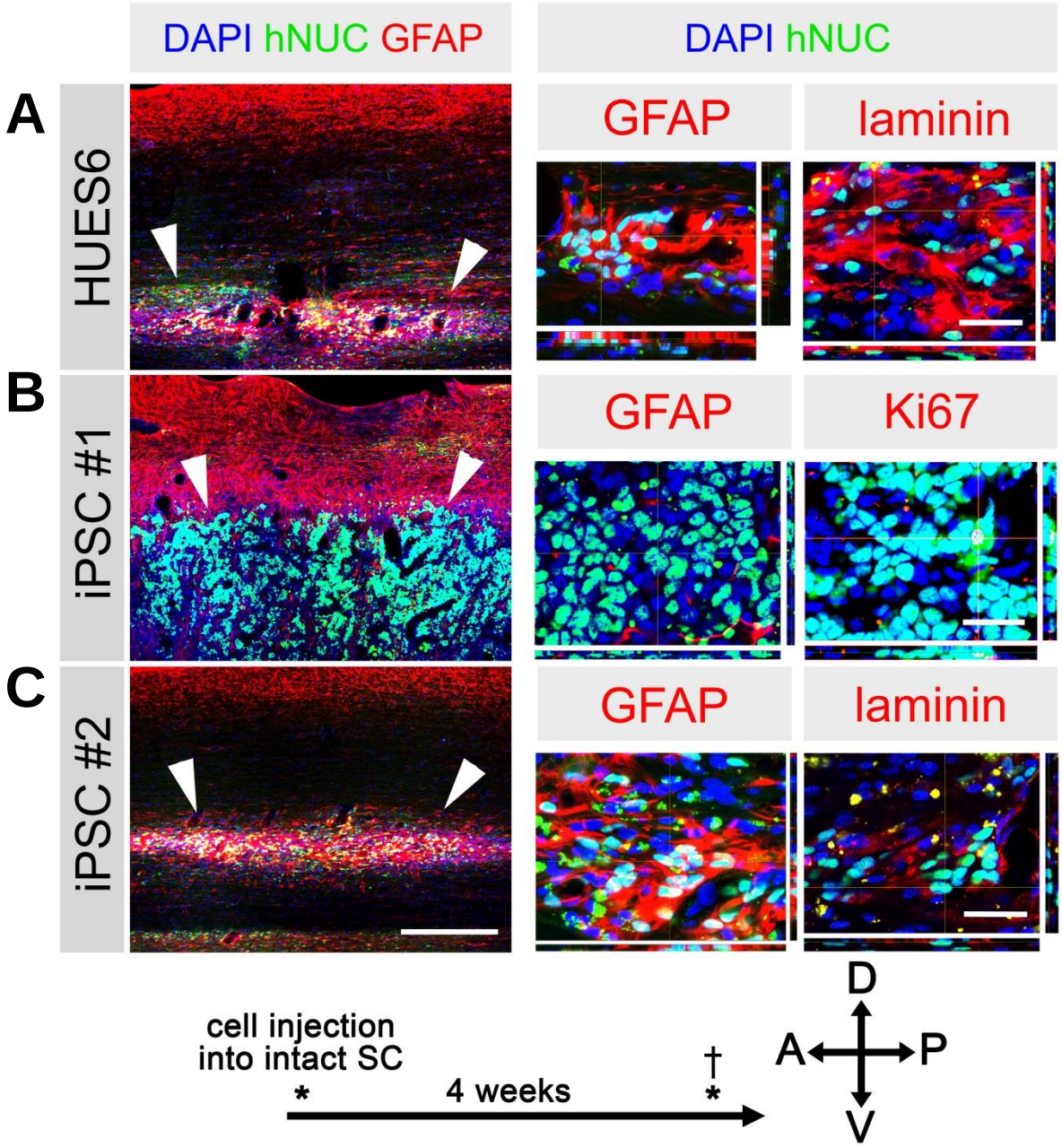

Figure 4.18.1: HUES6- and iPSC #2-derived NSCs differentiated for two weeks with CNTF moderately survive in the intact spinal cord and express GFAP and laminin.

Representative photomicrographs of hNUC^{+} **(A)** HUES6-, **(B)** iPSC #1- and **(C)** iPSC #2-derived progeny after two weeks of differentiation with CNTF followed by injection into the C4 level of the intact spinal cord. Magnifications show that HUES6- and iPSC#2-derived cells which express the astrocytic marker GFAP show immunolabeling for laminin, whereas iPSC #1-derived cells did not differentiate into GFAP^{+} astrocytes, but retained Ki67 expression.
Scale bars: 500 µm and 20 µm. SC: spinal cord; A: anterior; P: posterior; D: dorsal; V: ventral.

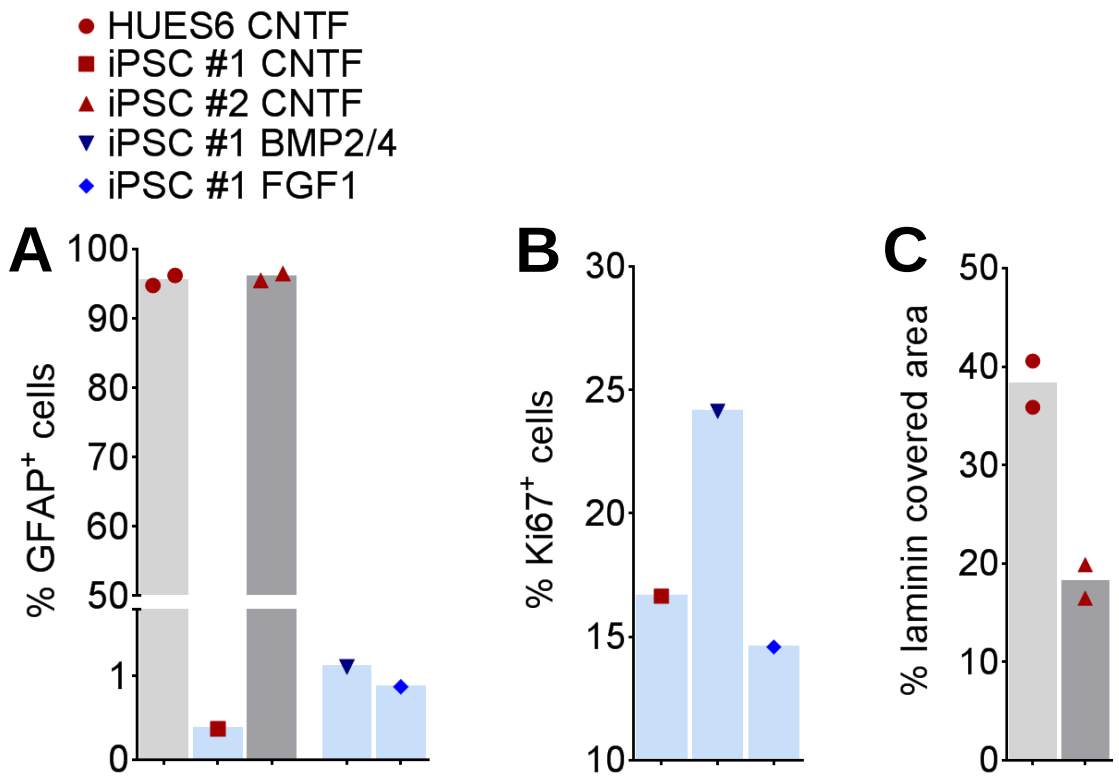

Figure 4.18.2: Quantification of marker expression of PSC-derived NSCs pre-differentiated *in vitro* for two weeks after transplantation into the intact spinal cord.

Quantification of marker expression of hNUC$^+$ cells in **(A, C light grey)** HUES6-, **(A, B light blue)** iPSC #1 and **(A, C dark grey)** iPSC #2-derived progeny pre-differentiated *in vitro* for two weeks with the factor indicated and for four weeks *in vivo* after injection into the intact spinal cord. HUES6- and iPSC#2-derived cells expressed the astrocytic marker GFAP and showed laminin immunolabeling, whereas iPSC #1-derived cells did not differentiate into GFAP$^+$ astrocytes, but retained a higher percentage of Ki67-expressing cells. Symbols represent individual values, bar represent the mean value; n = 1 - 2 as indicated.

Appendix table 4.2: Overview of PSC-derived NSC and astrocyte transplantations into the intact or injured rat spinal cord.

A

Injured spinal cord (hemisection)					
Cell line	Treatment	Transplanted in	Survival detected in		Tumor formation?
		N animals	N animals	%	
HUES6	EGF/FGF2 neurospheres	6	5	83,3	No
HUES6	EGF/FGF2 neurospheres + GF cocktail	5	5	100	No

B

Injured spinal cord (dorsal column lesion)					
Cell line	Treatment	Transplanted in	Survival detected in		Lesion filled?
		N animals	N animals	%	
HUES6	EGF/FGF2 neurospheres	4	3	75	No
iPSC #1	EGF/FGF2	4	4	100	No
iPSC #1	EGF/FGF2 + GF cocktail	3	3	100	No
iPSC #1	EGF/FGF2 + fibroblasts	3	3	100	Yes, but hNUC$^-$ cells
iPSC #1	EGF/FGF2 + fibroblasts + GF cocktail	3	3	100	Yes, but hNUC$^-$ cells
iPSC #1	BMP2/4 differentiation	3	3	100	Yes, partially
iPSC #1	CNTF differentiation	4	3	75	Yes, partially
iPSC #1	FGF1 differentiation	4	3	75	No

C

Intact spinal cord					
Cell line	Treatment	Transplanted in	Survival detected in		Tumor formation?
		N animals	N animals	%	
HUES6	CNTF differentiation	4	2	50,0	No
iPSC #1	EGF/FGF2	3	2	66,7	Yes
iPSC #1	BMP2/4 differentiation	4	2	50,0	Yes
iPSC #1	CNTF differentiation	3	1	33,3	Yes
iPSC #1	FGF1 differentiation	3	1	33,3	Yes
iPSC #2	CNTF differentiation	4	3	75	No

HUES6- and iPSC #1-derived NSCs cultured with EGF and FGF2 were transplanted into the **(A-B)** injured and **(C)** intact spinal cord in the presence or absence of a growth factor (GF) cocktail and with or without fibroblast co-grafting.

iPSC #1-derived cells treated for two weeks with FBS and CNTF, BMP2/4 or FGF1 were transplanted into the **(B)** injured and **(C)** intact spinal cord.

(C) HUES6- and iPSC #2-derived astrocytes treated for two weeks with CNTF were transplanted into the intact spinal cord.

5. Discussion

This study aimed to define and specify a cellular substrate from PSCs which is able to restore tissue integrity after SCI. In particular, the generated cell graft should (1) fill the lesion site, thereby decreasing lesion size and cavitation, (2) take on tasks typical of adjuvant CNS cells such as providing physical, trophic and metabolic support to healthy, injured and spared neurons.

Due to their multiple crucial roles in the developing, healthy and diseased CNS (paragraph 2.5 and figure 2.4), this study focused on the specification of astrocytes.
Human ESCs and iPSCs were chosen as primary cell sources based on their potential in the field of tissue engineering and regenerative medicine. In fact, since the first isolation of mouse ESCs more than three decades ago [404, 405] and the isolation of human ESCs almost two decades ago [239], developmental processes have been not only elucidated at a molecular level, but also recapitulated *in vitro*, culminating in the generation of complex tri-dimensional organoids [279-282]. Our understanding of developmental processes has considerably advanced within the past few decades, allowing us to obtain basically any known/characterized somatic cell from PSCs *in vitro*.
Based on knowledge gained from neurodevelopmental *in vitro* studies, I first aimed at generating astrocytes from human PSCs, which were thereafter transplanted into the intact and injured spinal cord of Fischer344 rats.

5.1. Generation of astrocytes from human pluripotent stem cells

5.1.1. Embryonic neural stem cells: the gliogenic switch

To date, only few studies have focused on the generation of astrocytes from human PSCs [205, 296, 397, 399, 400], since the generation of neuronal subtypes is highly relevant for modeling neurodegenerative diseases and developing therapeutical approaches to counteract the symptoms. For instance, the generation of dopaminergic neurons from PSCs is considered to be a promising means for the treatment of PD [406-408]. Although transplantation of neurons into the injured spinal cord might allow for re-connection of injured neurons and their targets (Paragraph 2.3.1. and Figure 2.1), they cannot survive and efficiently exert their function in the lesion environment without the support of an astrocytic substrate.

The studies published by Krencik et al. in 2011 [205, 397] represented a time consuming but seemingly uncomplicated method to obtain large amounts of pure astrocytic populations from PSCs and was based on the principle of a “gliogenic switch” of developing NSCs.
In the embryo, NSCs arise from neuroepithelial cells after the closure of the neural tube, first produce neuronal progenitors and then start to differentiate into glia: both *in vivo* and during *in vitro* expansion, embryonic NSCs have been shown to switch from an early neurogenic to a late

gliogenic state, which in the mouse embryo culminate at E12 and start at E18 respectively. Unlike astrocytes, which can differentiate from NSCs in several regions of the CNS, oligodendrocytes only arise from specific CNS areas, such as the ventral neural tube [208, 409].
It was suggested that neurons produced by NSCs *in vivo* instruct the latter to switch to a gliogenic phenotype via a negative feedback mechanism [410], which is however not provided during *in vitro* expansion of NSCs. Nevertheless, an increase in gliogenic potential has been observed in NSCs *in vitro* with increasing passaging, leading to the hypothesis of an "inner clock" regulating this cell fate switch [409].

Based on this knowledge and based on observations by Sun et al. about the higher neurogenic potential of NSCs cultured as monolayers compared to NSCs cultured as free-floating spheres [409], Krencik et al. proposed a method in which human PSC-derived NSCs are expanded as neurospheres at low-adhesion serum-free conditions for ~160 days [205, 397] and then differentiated into astrocytes by exposure to CNTF for one week. According to the authors, at this late time point the *in vitro* gliogenic switch had already occurred (paragraph 4.1. and figure 4.1, left timeline).
However, Sun et al. also pointed out that NSCs cultured as neurospheres, especially big-sized ones, can be more heterogeneous than NSCs cultured as monolayers, due to their three-dimensional structure and complex cell-cell interactions. In addition, Sun et al. mentioned that human fetal NSCs can retain their neurogenic potential for over 200 days *in vitro* [409].
Last but not least, we experienced in the laboratory of our collaborator Prof. Dr. Beate Winner, Friedrich-Alexander Universität Erlangen-Nürnberg, that *in vitro* maturation of human PSC-derived NSCs into neurons requires up to eight weeks; therefore, only one week of exposure to CNTF seemed to be a very short time for the *in vitro* maturation of astrocytes.

As a result, in our hands differentiation of human PSCs based on the protocol published by Krencik et al. led to mixed populations of neurons, astrocytes and undifferentiated cells (Figures 4.2.2 and 4.2.3), both in DIV ~80 and in DIV ~180 neurospheres. In addition, DIV ~180 neurospheres differentiated for two weeks had a reduced differentiation potential and expressed a higher % of the NSC marker Sox2 compared to DIV ~80 differentiated neurospheres (figure 4.2.3), suggesting that extensive passaging reduced their ability to differentiate. However, when DIV ~130 HUES6-derived neurospheres were transplanted into the injured rat spinal cord, about 90-95% of the cells differentiated into $GFAP^+$ astrocytes, indicating that neurospheres can give origin to almost pure astrocytic populations when exposed to the complex CNS microenvironment (Figures 4.4.1, 4.4.2 and 4.5).
Thus, *in vitro* differentiation may not provide sufficient cues to induce the maturation of human PSC-derived NSCs.

Reflecting *in vitro* findings (Figures 4.2.2 and 4.2.3), HUES6-derived neurospheres gave origin to 5-10% DCX^+ young neurons *in vivo* (Figure 4.4.2 and 4.5).

In summary, these results do not demonstrate or recapitulate a “gliogenic switch” in PSC-derived NSCs *in vitro*, but highlight the strong influence of the spinal cord lesion environment on the differentiation into astrocytes.

5.1.2. Astrocytic specification by exposure to FBS and selected soluble factors

As mentioned above, neurospheres are composed of a mixed cell population [409]. On the other side, although there is no specific study claiming its absolute necessity, fetal bovine serum has been used to culture astrocytes for almost four decades [335, 411, 412], including fetally derived astrocytes [222, 387, 388] and astrocytes derived from human PSCs [296, 400].

For this reason, and to minimize cell-cell contact and heterogeneity, I dissociated DIV ~80 human PSC-derived neurospheres, plated them at low density on PLO/laminin and exposed them to 1% FBS (paragraph 4.2. and figure 4.1, right timeline) for at least two weeks. Under these conditions, all NSCs had an equal amount of space and were equally exposed to FBS and to the growth factors EGF and FGF2. As a result, their cell size increased and they assumed a flat and more complex morphology (data not shown), possibly indicative of a preliminary astrocytic stage.

When EGF and FGF2 were withdrawn and substituted by the inductors of astrocytic maturation CNTF, BMP2/4 and FGF1 for two weeks, human PSC-derived NSCs gave rise to cultures, which were neuron-free (Paragraph 4.2. and figure 4.6). Although the % of $GFAP^+$ astrocytes was within the same range as in cultures differentiated from neurospheres (Figures 4.2.2 and 4.2.3 *versus* 4.6), astrocytic morphology was more complex in cells exposed to 1% FBS and BMP2/4 than in cells differentiated from neurospheres, which were generally small and bipolar (figure 4.6).

Up to 80-90% of iPSC #2-derived cells differentiated for two weeks with CNTF were electrophysiologically active in response to ATP stimulation (Figure 4.7), a feature typical of mature astrocytes [401, 413, 414], which is relevant for neural network activity [415]. In both HUES6- and iPSC #2-derived “CNTF astrocytes”, responses to ATP were either a peak in intracellular Ca^{2+} concentrations or complex oscillatory responses (Figure 4.7). This indicates that these astrocytes not only expressed functional P2Y ATP-sensitive receptors, but were also able to elicit complex responses, which were independent of their GFAP expression. According to these observations, GFAP expression is not sufficient to determine the amount of mature or functional astrocytes in PSC-derived differentiating astrocytes. On the other side, although ~10% iPSC #1-derived cells expressed GFAP, they were mostly non-responsive, indicative of an immature phenotype.

Interestingly, HUES6- and iPSC #2-derived astrocytes exhibited differences in the distribution of the “preferred” response pattern (figure 4.7), indicating that different astrocytic populations

can have specific characteristics even if they are morphologically similar, which make them unique.

In summary, DIV ~80 PSC-derived NSCs plated at low density, exposed to 1% FBS for at least two weeks (DIV ~95) and differentiated for two weeks with CNTF, BMP2/4 and FGF1 show morphological and functional features of mature astrocytes, whereas neurons were depleted from these cultures.

5.2. Characterization of human pluripotent stem cell derived astrocytes

5.2.1. Diversity of astrocytic subtypes

Although astrocytes are generally depicted as more or less homogeneous cell population characterized by a stellate morphology, it is now clear that astrocytes are actually highly diverse.

Astrocytes are generally subdivided into protoplasmic and fibrous astrocytes, which have been attributed to the grey matter and white matter, respectively; however, it becomes more and more clear that astrocytes are morphologically and functionally at least as diverse as neurons [319]. It seems logical that astrocytic precursors are as sensitive as neurons to morphogens during development and that in response to patterning morphogens they will adopt a phenotype which enables them to fulfill functions specific to the microenvironment they reside in [319]. Accordingly, they will for instance have an appropriate size and express appropriate neurotransmitter receptors, cell-adhesion molecules and ECM.

In order to generate astrocytes with a caudal / spinal identity [293], neuroepithelial cells (NRs) were exposed to RA for 10 days (Figure 4.1) [205, 397]. Expression of the caudal transcription factors HoxA5, HoxB4 and Isl1 was detected in PSC-derived neurospheres, along with the dorsal transcription factor Pax3 and the ventral transcription factors Nkx2.1 and Nkx6.1 (Figure 4.2.1).

In addition, since according to literature LIF/CNTF and BMP2/4 exert their inductive effects on astrocytes via distinct signaling pathways [386] and FGF1 was found to promote differentiation of human PSCs into quiescent astrocytes [296], these three factors are possibly promoting specification of distinct astrocytic subtypes.

Supporting this hypothesis, CNTF-, BMP2/4- and FGF1- treated human PSC-derived cells differentiated for two weeks were morphologically tremendously different (figure 4.8): BMP2/-4 treated astrocytes were 3- to 4-fold larger than CNTF-treated astrocytes, while FGF1-treated astrocytes were smaller and rather bipolar. iPSC #1-derived NSCs seemed to be less responsive to BMP2/4 treatment, as the size of their progeny was not increased after two weeks of differentiation. However, FGF1-treatment led to significantly decreased cell size.

In addition, although cell size differences were consistent across cell lines, differences in the "basic" morphology of astrocytes ("no factors" group) were also observed (Figure 4.8).

Differences in basic morphology as well as in the pattern of response elicited by ATP stimulation (Figure 4.7) are both indicative of the unique character of astrocytic populations. Based on these observations it can be concluded that even when exactly the same differentiation protocol is applied, it is possible to obtain comparable but not even nearly identical progeny from human PSCs. This can be due to a number of factors, including intrinsic factors such as genetic and epigenetic background and extrinsic factors such as slight technical variability, for instance variability in size and density of neurosphere cultures. Considering the amount of external signals that stem cells are exposed to within their microenvironment to acquire the required phenotype, it seems logical that these cells are very sensitive to slight microenvironmental changes *in vitro*.

Astrocytes differentiated from all three human PSC lines by exposure to 1% FBS and CNTF, BMP2/4 and FGF1 were extensively characterized in order to identify an astrocytic subtype which may be more beneficial / regeneration-promoting after transplantation into the injured spinal cord. Based on literature, a difference in pro-regenerative potential has been suggested between CNTF and BMP2/4-treated astrocytes [222, 387, 388].

5.2.2. Astrocytes are proliferative

Unlike other post-mitotic cells including neurons, astrocytes retain the ability to proliferate, a feature which was first observed more than four decades ago [416]. In particular, astrocytes were found to be proliferative in the intact [416, 417] as well as in the injured brain [418]. Proliferation in astrocytes was found to be induced by soluble factors such as EGF, but interestingly also by signals coming directly from adjacent neurons: neuronal removal was shown to induce changes in astrocytic morphology and an increase in their proliferation *in vitro* [419]. In addition, proliferation was found to be one key feature of reactive astrogliosis [420].
On the other side, unlike neurons, astrocytes express the transcription factor Sox2, which is mainly associated with neural progenitors [421]. Astrocytes which express Sox2 might be less mature and to some extent phenotypically flexible.
These two features confer to astrocytes a certain resistance to stressful conditions and a certain ability to adapt to micro-environmental changes, which neurons lack. Herewith, astrocytes are for instance able to readjust in response to injury, a mechanism which is crucial for the prevention of secondary damage.

Thus, I analyzed expression of the NSC marker Sox2 and of the proliferation marker Ki67.

Presence of Sox2 might partially explain why only ~20-40% of PSC-derived astrocytes expressed the astrocytic marker GFAP. After two weeks of differentiation, expression of Sox2 amounted to

~20-40% across all lines, with a significant decrease in HUES6-derived and iPSC #2-derived BMP2/4-treated astrocytes and a significant increase to ~80% in FGF1-treated cells across all PSC lines (Figure 4.9).
These results suggest that expression of Sox2 is a shared feature of different astrocytic lines. Correlating with their increased cell size and complex morphology, PSC-derived BMP2/4-treated astrocytes might be more mature and at the same time less resistant to stressful conditions. In fact, as mentioned in paragraph 3.2.2.12, PSC-derived NSCs differentiated with BMP2/4 had to be seeded at two-fold density prior to differentiation due to their lower survival rate. In contrast, correlating with their decreased cell size and less complex morphology, PSC-derived FGF1-treated astrocytes are likely less mature but possibly more resistant to stressful conditions. This specific finding is in contrast with findings published by Roybon et al., who stated that human PSC-derived FGF1-treated astrocytes have features of mature quiescent astrocytes [296].

Expression of the proliferation marker Ki67 was generally low in HUES6- and iPSC #1-derived astrocytes, reaching about ~20%. Again, Ki67 immunolabeling showed a trend towards and a significant decrease in BMP2/4-treated HUES6- and iPSC #1-derived astrocytes, supporting the hypothesis that these astrocytes are more mature. FGF1 treatment induced a significant increase in Ki67 expression in HUES6- and iPSC #1-derived astrocytes, again in contrast with the hypothesis that FGF1 induces a mature quiescent astrocytic phenotype (Figure 4.10) [296].

Surprisingly and quite astonishingly, proliferation in iPSC #1-derived differentiating cells amounted to ~50-90%, correlating with their lower sensitivity to BMP2/4 (Figure 4.8) treatment and lack of electrophysiological activity in response to ATP (Figure 4.7). This finding may reflect the robustness of this cell line, which may be of advantage after transplantation into the injured spinal cord. However, as it is known that iPSC-derived progeny may rise to tumors, high Ki67 expression might also be indicative of uncontrolled proliferation and propensity to form tumors *in vivo*. Indeed, residual proliferation was detected in iPSC #1-derived NSCs differentiated for two weeks *in vitro* and for four weeks *in vivo* in the intact spinal cord (Figure 4.18.1 and 4.18.2), which likely underlies the resulting formation of tumor-like colonies (figure 4.17).

5.2.3. Astrocytic extracellular matrix in health and injury

The ECM is an ensemble of extracellular molecules which provide not only a physical substrate for attachment and cohesion of cells, but also signaling cues, which can regulate cell survival, proliferation, growth, progression along their lineage and migration. In the CNS, ECM molecules can be produced by endothelial cells, microglia, macrophages, pericytes, oligodendrocytes, neurons and astrocytes. Astrocytes, in particular, are able to secrete a wide range of ECM molecules including agrin, brevican, collagen IV and VIII, decorin, fibronectin, glypican, laminin, neurocan, phosphacan, syndecan, tenascin-C, thrombospondins and versican [28]. Changes in

ECM composition are crucial in the CNS response to traumatic injury: (1) the barrier produced by glial scarring cell is able to confine the lesion environment and to protect the surrounding tissue from secondary damage; (2) signaling ECM cues may serve as attractors for astrocytes, fibroblasts and immune cells; (3) signaling ECM cues promote proliferation, de-differentiation and re-differentiation in cells residing around the injured area.

As members of the CSPG family, aggrecan, versican, neurocan, brevican, known as CSPG1-3 and 7, as well as phosphacan, are upregulated after SCI and represent a growth inhibitory barrier for axon growth. In fact, enzymatic digestion of CSPGs with ChABC has been extensively used in animal models of SCI to promote regeneration [35, 39, 42, 44, 48]. However, complete ablation of the glial scar has been shown to have deleterious effects on the regenerative potential after SCI, pinpointing its importance for recovery after injury. Moreover, not all CSPG family members are growth inhibitory: NG2 and Neuroglycan C, known as CSPG 4 and 5, can be growth promoting [25]. The growth-inhibitory CSPGs neurocan and phosphacan, the growth-promoting CSPG NG2 as well as the above mentioned HSPGs glypican and syndecan have been detected in the ventricular zone of the embryonic brain and have been associated with regulatory functions within the NSC niche and with the formation of neural networks [422]. As an example, a phosphacan short isoform has been associated with neuronal differentiation, myelination and neurite outgrowth of cortical neurons [423].

Laminin, on the other side, is an ECM molecule, which has been associated with axonal growth in the developing CNS and PNS. Developing neurons have been shown to elongate along laminin-expressing cells until the completion of axonal outgrowth, when laminin declines in the extracellular space. In the adult CNS, axonal sprouts were found in close association with laminin expressing astrocytes after SCI, suggesting that laminin does not only play a role in embryogenesis but also in the pro-regenerative response to injury [402]. One decade later it was shown that growth-modulating ECM molecules, such as collagen IV, fibronectin and laminin co-localize with infiltrating Schwann cells, but not with astrocytes in the injured human spinal cord [424]; however laminin co-localizes with $GFAP^+$ glial processes and with regenerating axons in other model systems, such as fish [425]. In addition, laminin is a key player in the regenerative response after PNS injury [426].

Historically, in the astrocytic scar formed after SCI, laminin has been suggested to mediate axon growth, whereas CSPGs have been associated with inhibition of growth [427]. To assess if human PSC-derived astrocytes differentiated for two weeks with 1% FBS and the factors indicated are (1) functional in terms of their ability to produce ECM and (2) potentially growth-promoting or growth-inhibitory, expression of laminin and of the CSPG core protein CS-56 were analyzed.

While the electrophysiologically inactive, highly proliferating iPSC #1 derived differentiating NSCs were generally not able to produce considerable amounts of ECM, HUES6- and iPSC #2-

derived astrocytes produced CSPGs, especially if treated with BMP2/4 (Figure 4.11). These observations (1) indicate that PSC-derived astrocytes exhibit functional properties of mature astrocytes, (2) support the hypothesis that BMP2/4-treated astrocytes are more mature (Paragraph 5.1.2. and Figures 4.9 and 4.10) and (3) suggest that BMP2/4-treated astrocytes are potentially growth-inhibitory.

Laminin expression was detected mainly in HUES6-derived astrocytes, especially in the "no factors" and CNTF groups, and to some extent in iPSC #2-derived astrocytes (Figure 4.12). These observations (1) confirm the ability of PSC-derived astrocytes to produce ECM components relevant for the modulation of axon growth, (2) suggests that HUES6-derived CNTF-treated astrocytes might be growth-supportive and (3) again shows that PSC-derived astrocytic cell lines are functionally comparable but not identical.

Interestingly, the intrinsic capacity of PSC-derived CNTF-treated astrocytes to produce laminin was maintained *in vivo* after transplantation to the intact spinal cord (Figure 4.18.1 and 4.18.2), whereby differences in laminin expression between HUES6-derived *versus* iPSC #2 derived astrocytes *in vivo* reflected the *in vitro* expression pattern. This finding suggests *in vitro* features of PSC-derived astrocytes are intrinsic and can be maintained in a complex microenvironment. Close observation of the laminin expression pattern *in vivo* (Figure 4.18.1) revealed that (1) laminin expression was confined to the region where $hNUC^{+}/GFAP^{+}$ cells were present, but (2) laminin was also expressed in $hNUC^{-}$ host cells within this specific area. This interesting finding suggests potential graft-host cross interactions, whereby transplanted PSC-derived astrocytes are able to induce phenotypical changes in host astrocytes.

Since HUES6- and iPSC #2-derived astrocytes were not transplanted into the injured spinal cord within this thesis and since the exact composition of the CSPG ECM component was not characterized in detail *in vitro* (incidence of growth-inhibitory *versus* growth-promoting CSPGs), it cannot be determined at this point if PSC-derived astrocytes, for instance CSPG-expressing BMP2/4-treated astrocytes *versus* laminin-expressing CNTF-treated astrocytes, differ in their growth-promoting potential.

5.2.4. BDNF-mediated stimulation of axonal extension

As previously described (paragraph 2.5.1.5), astrocytes are able to process the immature form of BDNF, pro-BDNF, to mature BDNF, which promotes axonal outgrowth and dendritic branching [372]. Due to this property, BDNF has been administered in numerous pre-clinical studies of SCI to promote regeneration and sprouting, either by viral delivery or by genetic modification of cells, which served as biological mini-pumps after transplantation into the lesion site [428]. In order to assess if human PSC-derived astrocytes are naturally able to serve as

BDNF-producing mini-pumps without further genetic manipulation, BDNF production was analyzed by ELISA in supernatants of PSC-derived NSCs differentiated for two weeks.

The amount of BDNF produced by PSC-derived astrocytes was relatively low. While across all conditions and cell lines the amount of BDNF was hardly detectable, it reached up to 3 ng produced by one million cells within 24 hours in BMP2/4-treated cells across all lines (figure 4.13).

Again, this might be indicative of a more mature phenotype in PSC-derived cells differentiated with BMP2/4. However, whether such small amounts of BDNF can have effects on axonal outgrowth in vivo remains to be determined, especially considering the low survival rate of PSC-derived NSCs and astrocytes after transplantation (Figures 4.4.1, 4.4.2, 4.5, 4.15, 4.18.1 and Appendix Table 2).

5.2.5. Direct interaction between astrocytes and DRG neurons *in vitro*

All findings mentioned so far are indicative of phenotypical differences among astrocytic subtypes, both dependent on treatment with a specific factor and on the PSC-line of origin; however their predictive value in terms of pro-regenerative potential is only valid if their effect on axonal growth is directly assessed.

To address this issue, their effect on axonal growth was tested in an *in vitro-ex vivo* system: primary DRG neurons, which extend an axonal branch into the PNS and a sensory ascending branch into the CNS, were co-cultured on homogeneous layers of PSC-derived astrocytes. Mirroring the laminin expression pattern, neurite extension was highest in DRG neurons co-cultured on HUES6-derived astrocytes differentiated with 1% FBS alone or in combination with CNTF (figure 4.14). However, whether this correlation is causal has not been demonstrated in this study.

On the other side, CSPG expression did not seem to have a big impact on neurite outgrowth. Lower neurite extension was observed in DRG neurons co-cultured on HUES6-derived BMP2/4 treated astrocytes compared to “no factors”- or CNTF-treated astrocytes, however this was not the case in iPSC #2-derived astrocytes, where neurites reached an average length of 600 µm in all groups.

Although this technique (co-culturing) is the only experiment of this study that directly addresses the interaction between astrocytes and axotomized neurons, it has several limitations. First of all the absence of a “control” condition: a “PLO/laminin control” could not be used due to the fact that our astrocytic cultures are plated on a substrate whose initial laminin concentration is twenty-fold higher than the concentration normally used to culture DRG neurons. Plating DRG neurons on 10 µg/mL laminin does not represent an appropriate control: during the two weeks of differentiation the initial concentration of laminin has likely

decreased due to detachment from the plastic surface and to astrocyte-mediated digestion or it has increased due to astrocyte-mediated deposition. For this reason, only neurites which were on top of astrocytes or astrocytic processes were included in the analysis.
Another possibility would have been to co-culture DRG neurons on another cellular substrate, such as human BMSCs or fibroblast, or rat primary astrocytes. The first two cell types are not of interest, since the aim of this study is not to transplant BMSCs or fibroblasts, but to create a cellular substrate of neural identity. Rat primary astrocytes are, on the other side, obtained from the brain of new born rats and have therefore neither the appropriate age nor the appropriate caudal phenotype.

Therefore, this experiments aims at comparing PSC-derived astrocytic populations in a closed system: it is not possible to say if PSC-derived astrocytes are generally more or less growth-promoting compared to spinal cord-residing astrocytes, but it is possible to select the astrocytic population with the highest pro-regenerative potential among the cell lines and treatments analyzed.

An additional limitation of this experiment is due to the unique character of DRG neurons. It is known that their peripheral branch is able to regenerate after PNS insult, but their central branch has a limited ability to re-grow in response to CNS injury. In this co-culture experiment it is not possible to say if the longest neurite of a DRG neuron is a dendrite or an axonal projection and more importantly it not possible to say if the axonal projection is a central or a peripheral branch. Again, the use of alternative primary neurons would not necessarily have been of advantage; hippocampal neurons, which are relatively easy to isolate, are not spinal neurons or motor neurons and therefore do not represent a target population.

In summary, DRG co-cultures represent a closed system to roughly evaluate the effect of different classes of astrocytic populations on axonal outgrowth of from a more general point of view.

5.3. Transplantation of pluripotent stem cell derived neural stem cells and astrocytes into the spinal cord

5.3.1. Animal models of spinal cord injury

SCI leads to an extremely complex series of molecular and cellular events and his extremely diverse in terms of type and severity of injury as well as of region affected. First animal models of SCI date back to over a century ago [429] and have since then considerably contributed to our understanding of SCI, from molecular mechanisms to neurological outcome.
Obviously, non-human primates constitute the animal model closest to humans; however size and longevity of “old-world” primates is a big limiting factor for pre-clinical studies, as these

only allow small studies, in which few experimental conditions can be tested. On the other extreme, rodents are easy to house and allow large pre-clinical studies. Hereby, mice are a powerful tool for genetic studies due to the availability of thousands of transgenic lines, but rats represent the preferred animal model of SCI due to the functional, electrophysiological and morphological similarities with human SCI [430].

The next question is, which segment of the spinal cord should be injured. Complete transection of the spinal cord at thoracic levels will lead to complete and permanent loss of hindlimb function, as well as of bowel and bladder control. The advantage of this model is that axon growth and functional improvement can only be attributed to true regeneration and not to sprouting or compensatory mechanisms. However, cervical models of SCI, including the models presented in this study, are becoming more and more relevant due to epidemiological data which indicate that more than 50% of SCI patients have injuries in the cervical spine, whereby the most common segments affected are C5, C4 and C6 [431, 432]. Accordingly, throughout this study the injury was applied at cervical segment 4 (Figure 4.3). Lateral hemisection of the spinal cord at C4 is a more severe model of SCI that has been used in previous studies to evaluate transplants of fetal spinal cord tissue or PSC-derived NSCs [148, 149]. Thus, this was the first model of choice for the present study (Figures 4.3, 4.4.1 and 4.4.2). Inspired by the publications by Lu et al., a cocktail of calpain inhibitor and nine growth factors, as well as fibrinogen and thrombin, were used to support the survival of HUES6-derived neurospheres (Figure 4.4.1).

Despite the possibility to directly compare injured and healthy fibers within the same animal, hemisection models are not reflecting human SCI. As an example, to perform a hemisection of the spinal cord, the integrity of the *dura mater* is disrupted but a longitudinal cut of several millimeters, whereas the *dura mater* usually remains intact in human SCI. Other possible models of SCI are contusion, compression, distraction, dislocation, full or partial transection and chemical models [430]. Although contusion would have been a model that is well established in our laboratory and closest to human SCI, wire knife transection of the dorsal column, i.e. transection of CST projections, was chosen for this study (figures 4.3, 4.5, 4.15, 4.16 and appendix table 2). In this animal model, the dura mater is not disrupted during the injury, cysts typical of contusive SCI models develop, a well-characterized neuronal tract is transected, a feature which is useful to address regeneration, and spinal cord injured rats do not exhibit drastic loss of neurological function, which makes post-surgical animal care easier. A big disadvantage of this animal model is that it is more difficult to assess neurological improvements due to the small functional deficits. Nevertheless, since survival and differentiation in the lesioned spinal cord was a first parameter to analyze, the use of a neurologically relevant model of SCI was not a priority.

5.3.2. Survival of pluripotent stem cells derived neural stem cells and astrocytes in the spinal cord

Survival of grafted cells is one of the major issues leading to the current low efficacy of cell transplantation studies in SCI. Although they are robust, proliferative and expandable *in vitro*, once transplanted into the lesioned spinal cord, NSCs or their more differentiated progeny are exposed to a multiplicity of challenging environmental cues (Paragraph 2.2.1.), which they do not have to cope with *in vitro*. These stressful conditions severely reduce their survival rate. To promote survival of PSC-derived NSCs, we therefore provided two additional factors. On one side, cells were resuspended in a solution containing thrombin or fibrinogen immediately prior to injection and delivered separately; known from studies on blood coagulation, thrombin cleaves fibrinogen to fibrin monomers and fibrinopeptides A and B; fibrin protein chains then polymerize and crosslink to establish the framework of a thrombus or blood clot [433]. The consequent gelation provides a physical substrate for the transplanted cells, impeding their dispersion. On the other side, based on studies published by Lu et al. [148, 149], cells were resuspended in a solution containing calpain inhibitor, which counteracts calpain-induced cell injury and death [434, 435], and nine additional growth- and neurotrophic factors.

Indeed, survival of HUES6-derived neurospheres was qualitatively higher if the cells were resuspended in the full growth factor cocktail prior to transplantation (Figure 4.4.1), whereby cells generally did not survive at the lesion epicenter but rather at the edge of the lesion (Figure 4.4.1 and 4.5). After transplantation into the wire knife lesioned spinal cord without additional growth factors, HUES6-derived neurospheres were not able to fill the cyst(s), but survived at the lesion edge or within areas of spared tissue proximal to it, where they could provide a growth-promoting substrate for regenerating or sprouting projections (Figure 4.5). The effects of the growth factor cocktail did not seem to lead to a qualitative improvement in cell survival in later experiments: iPSC #1-derived NSCs cultured as monolayers in the presence of 1% FBS and then transplanted with or without fibroblasts, respectively, or with or without growth factor cocktail were not able to survive in the wire knife-lesioned spinal cord, and qualitative differences in cell survival were not striking (Figure 4.15). In contrast, iPSC #1-derived NSCs differentiated as monolayers in the presence of 1% FBS plus CNTF, BMP2/4 or FGF1 and then resuspended in a solution containing calpain inhibitor and their respective differentiation factor exhibited a much better survival: CNTF- and BMP2/4-treated iPSC #1-derived cells survived at the lesion epicenter and reduced cyst size compared to all other conditions within the same experiment (Figure 4.16 *versus* 4.15), suggesting that the use of the full growth factor cocktail does not necessarily play a major role.

Transplantation into the intact spinal cord led to some unexpected observations. First, survival of HUES6- and iPSC #2-derived astrocytes was generally low although the host environment was less challenging (Figure 4.18.1), and $hNUC^{+}$ cells were detected only in 50-75% of the animals

(Appendix Table 2). Second, while hNUC$^+$ iPSC #1-derived NSCs differentiated for two weeks the factors indicated were observed in 75-100% of all wire knife injured animals, they were detected in only 33-50% of the intact animals (Appendix Table 2). When detected, they led to tumor-like colony formation. One possible explanation is that the host environment is rather capable to reject the xenograft while intact, and that iPSC #1-derived NSCs, which survive this rejection are robust enough to form a tumor via clonal expansion.

Generally, survival of grafted cells in one big issue, which needs to be addressed to improve therapeutical approaches based on cell transplantation. Several options are available, of which few were adopted in this study: (1) delivery of ECM molecules such has fibrin, (2) delivery of inhibitors of cell death, (3) delivery of growth- and neurotrophic factors, (4) co-transplantation with cells which are more robust, such as fibroblasts or BMSCs, (5) inclusion in a stable biomaterial. However, these aspects need to be fine-tailored. For instance, delivery of fibrinogen and thrombin is useful to provide an initial physical substrate for the transplanted cells, but does not provide the supportive signals of CNS ECM. Accordingly, specific CNS ECM compositions could be identified and co-delivered to specifically enhance the survival of transplanted cells or to enhance regeneration of injured projections. Recent studies have started to address this issue by comparing the effect of selected ECM molecules on NSC survival and differentiation [436] and on neurite outgrowth [437, 438]. Although only recently this issue has been addressed in the context of CNS nerve injury [437], ECM-engineering seems worth-while pursuing. However, delivery of ECM molecules and soluble factors is challenged by the rapid degradation *in vivo*, which does not affect biomaterials to the same extent. Co-transplantation of non-CNS cells (fibroblasts), on the other side, did not seem to have a positive effect on the survival of our cells.

In conclusion, survival of grafted cells is a high-priority, which needs to be extensively addressed in order to enhance the efficacy of cell-based therapeutical approaches for SCI.

5.3.3. Differentiation of pluripotent stem cells derived neural stem cells and astrocytes in the spinal cord

When PSC-derived NSCs are transplanted into the injured spinal cord they give rise to mixed populations of mainly neurons and astrocytes - only rarely oligodendrocytes - which vary from batch to batch, from animal model to animal model, as well as from laboratory to laboratory, strongly depending on the experimental paradigm. For instance, Nori et al. in 2011 [230] and Lu et al. in 2014 [148] reported that hiPSC-derived NSCs transplanted into mice and into rats gave rise to 50% and 70% neurons after two and three months, respectively, whereby in the first study only 22% of the total transplanted cells were NeuN$^+$ after two months and in the second study all neurons (70%) were NeuN$^+$ after three months. In both studies ~17% of the transplanted cells gave rise to GFAP$^+$ astrocytes. Although this last finding is consistent, the two

studies are generally hardly comparable: (1) Nori et al. transplanted human iPSC-derived neurospheres into NOD/SCID mice which received a thoracic contusive lesion of the spinal cord without additional factors and analyzed the outcome after two months, whereas (2) Lu et al. transplanted human iPSC-derived NSCs cultured on PLO/laminin into athymic nude rats which received a cervical hemisection with a full growth factor cocktail and analyzed the outcome after three months. In the study by Nori et al., neurons were mostly GABAergic, whereas Lu et al. hardly detected transmitter associated markers and, if so, GABAergic markers were absent.

If such experimental variability exists across laboratories and studies, the phenotype of the transplanted PSC-derived progeny will be as well highly variable and it will be therefore difficult to dissect out the mechanisms, which lead to functional improvement. In contrast, if a specific cell population is transplanted, for instance GRPs / astrocytes [222, 387, 388], genetically modified astrocytes [392] or specific populations of neurons, it is possible to address specific aspects or tissue repair, such as restoration of tissue integrity (astrocytes) or replacement of lost neuronal connections (neurons).

Based on this, the present study aimed at generating specific and well-characterized astrocytic populations with a stable phenotype to provide a favorable substrate for axonal regeneration after SCI. While PSC-derived neurospheres retained the ability to generate neurons *in vitro* and *in vivo* (Figures 4.2.2, 4.2.3, 4.4.2 and 4.5), PSC-derived NSCs treated with 1% FBS led to neuron-free cultures *in vitro* (figure 4.6) and to nearly pure astrocytic populations *in vivo* (figures 4.18.1 and 4.18.2).
The host environment had a clear effect on the differentiation of HUES6-derived neurospheres: within the lesion $hNUC^+$ cells homogeneously expressed vimentin, suggesting that they are either less mature or reactive, whereas they expressed only GFAP once they migrated into the surrounding host tissue (Figure 4.4.2). On the other hand, pre-differentiated PSC-derived astrocytes maintained their intrinsic capacity to produce a low or a high amount of laminin in the host environment (Figures 4.18.1 and 4.18.2), suggesting that some phenotypical characteristics acquired during *in vitro* specification can be maintained *in vivo*. This makes it possible, for instance, to directly compare the pro-regenerative effect of astrocytes, which produce laminin *versus* astrocytes which produce less laminin, thus allowing (1) the identification specific mechanisms which promote axonal outgrowth and (2) the selection of a specific cell population for transplantation experiments. Accordingly, while HUES6 neurosphere-derived astrocytes were generally not growth-repulsive and co-localized with NFH^+ host projections (figure 4.4.2), laminin expressing astrocytes pre-differentiated with CNTF might be more growth-promoting. On the other side, undesired differentiation patterns *in vitro* or *in vivo* can be used as an exclusion criterion.

While this study applied this principle to astrocytes, it is worthwhile to pursue experiments in a similar way with neurons: to form a functional “relay” it is reasonable to transplant neurons or

neuronal precursors which will acquire a glutamatergic phenotype. A mix of undefined, glutamatergic, GABAergic, serotonergic and cholinergic neurons might not be equally effective.

5.4. Safety of induced pluripotent stem cells

5.4.1. Tumor formation of grafted pluripotent stem cells derived neural stem cells

Based on the fact that survival of PSC-derived NSCs is generally limited in the injured spinal cord (Figures 4.4.1 and 4.5), highly proliferative iPSC #1-derived NSCs were chosen for transplantation experiments due to their robustness.
Transplanted iPSC #1-derived NSCs treated with CNTF and BMP2/4 showed promising survival in the wire knife lesioned spinal cord (Figure 4.16), but most $hNUC^{+}$ cells did not express GFAP. In addition, in some animals small tightly-packed colonies of $GFAP^{-}$ cells were observed (Figure 4.15). These alarming findings led to the hypothesis that iPSC #1-derived cells might give rise to tumor-like tissue, which was confirmed once the cells were transplanted into the intact spinal cord (Figure 4.17). Because iPSC #1-derived NSCs differentiated into other lineages (neuronal, oligodendroglial) did not give origin to tumors both in the wire knife lesioned and in the intact spinal cord (data not shown, n = 21 animals), this outcome was actually unexpected. It pinpoints, however, that a simple pre-evaluation of tumorigenicity [229, 439] is not necessarily sufficient to exclude tumor-formation by iPSC-derived progeny. The genetic and epigenetic background of specific iPSC-lines might confer a predisposition to give rise to a tumor, however this ability might be generally "invisible" and only be "waken up" by a specific treatment, for instance incubation with 1% FBS.

This study provides to some extent "predictive" or inclusion/exclusion criteria for transplantation of PSC-derived NSCs/progeny. In almost all parameters analyzed, iPSC #1-derived precursors significantly differed from the other two PSC-lines: they (1) were not responsive to ATP stimulation (Figure 4.7), (2) less responsive to BMP2/4-mediated maturation (Figure 4.8 and 4.9), (3) significantly more proliferative (figure 4.10), (4) hardly produced ECM molecules (Figures 4.11 and 4.12), resulting in (5) low support of axon outgrowth in co-cultures with astrocytes (Figure 4.14). As a consequence, although the fact that they were able to fill cysts resulting from wire knife lesion of the DC, they did not acquire the desired astrocytic phenotype.

The above mentioned observations are likely not universal predictive criteria, but represent exclusion criteria, which can be used in future studies to better select astrocytic populations for transplantation after SCI.

5.4.2. Safe methods for the generation of induced pluripotent stem cells

Despite the major effort which has been made within the past decade to establish reprogramming methods which do not modify the genome of de-differentiated somatic cells, virus mediated reprogramming is still quite commonly used. As an example, in the previously mentioned study by Lu et al., reprogramming was achieved via retroviral delivery of the Yamanaka factors [148], and the same method adopted in the laboratory of our collaborator, Prof. Dr. Beate Winner, Friedrich-Alexander Universität Erlangen-Nürnberg. This is the oldest reprogramming method and is not considered to be safe due to integration into the genomic DNA, which can result in one or more genetic mutations during the integration process. In addition, although retrovirally transduced genes are subject to epigenetic silencing during the reprogramming process, they can be reactivated in vivo by an unknown/unpredictable stimulus and enhance predisposition of iPSC-derived progeny to form tumors [440]. Indeed, one of two human iPSC lines we used gave origin to tumors once *in vivo*.

As mentioned in paragraph 2.4.1.1., the safest methods for reprogramming somatic cells are delivery of the reprogramming factors via (1) RNA delivery and (2) protein delivery. Since these techniques were developed only recently, most laboratories might be resilient to adopt them due to concerns arising from lack of experience and of tools. In addition, in most cell transplantation studies, including this study, the scope is not to establish safe iPSC-lines. Thus, the fastest and more convenient iPSC source is chosen. As this study shows, this leads to undesired outcome, which considerably slows down the progress towards the set goals – in this case the generation of astrocytes for transplantation after SCI.

Therefore, it is worthwhile to fully take into account risks associated with the reprogramming method of choice and to consider alternatives and preventive solutions. In fact, virus-free reprogramming kits are already commercially available: Merck-Millipore recently launched the Simplicon^{TM} RNA Reprogramming Technology, where a single RNA molecule encoding for four transcription factors allows for efficient reprogramming bypassing genomic integration.

6. Conclusions

The present study focused on the generation of astrocytes from human PSCs for transplantation after SCI. Neuron-free astrocytic cultures were successfully generated from two human PSC lines and their morphological as well as functional properties were extensively analyzed to (1) determine if generated astrocytes exhibit features of authentic/mature astrocytes and (2) to estimate their *in vivo* pro-regenerative potential. In particular, potential inclusion/exclusion criteria were defined, which may facilitate the choice of the astrocytic subtype for transplantation studies. The present study also sheds light on the necessity to use iPSC lines

obtained by means of non-integrative reprogramming methods in order to minimize or completely eliminate the risk for tumor formation.

References

1. Thuret, S., L.D. Moon, and F.H. Gage, *Therapeutic interventions after spinal cord injury.* Nat Rev Neurosci, 2006. **7**(8): p. 628-43.
2. Bradbury, E.J. and S.B. McMahon, *Spinal cord repair strategies: why do they work?* Nat Rev Neurosci, 2006. **7**(8): p. 644-53.
3. Silver, J. and J.H. Miller, *Regeneration beyond the glial scar.* Nat Rev Neurosci, 2004. **5**(2): p. 146-56.
4. Yiu, G. and Z. He, *Glial inhibition of CNS axon regeneration.* Nat Rev Neurosci, 2006. **7**(8): p. 617-27.
5. Jazayeri, S.B., et al., *Incidence of traumatic spinal cord injury worldwide: a systematic review.* Eur Spine J, 2015. **24**(5): p. 905-18.
6. Singh, A., et al., *Global prevalence and incidence of traumatic spinal cord injury.* Clin Epidemiol, 2014. **6**: p. 309-31.
7. Priebe, M.M., et al., *Spinal cord injury medicine. 6. Economic and societal issues in spinal cord injury.* Arch Phys Med Rehabil, 2007. **88**(3 Suppl 1): p. S84-8.
8. WHO, *International Perspectives on Spinal Cord Injury*. 2013.
9. Chan, B.M., A.; Mittmann, N.; Teasell, R.; Wolfe, D.L., *Economic Evaluation of Spinal Cord Injury*, in *Spinal Cord Injury Rehabilitation Evidence*. 2014. p. 1-21.
10. Dietz, V. and K. Fouad, *Restoration of sensorimotor functions after spinal cord injury.* Brain, 2014. **137**(Pt 3): p. 654-67.
11. le Gros Clark, W.E., *The problem of neuronal regeneration in the central nervous system: II. The insertion of peripheral nerve stumps into the brain.* J Anat, 1943. **77**(Pt 3): p. 251-9.
12. Liu, C.N. and W.W. Chambers, *Intraspinal sprouting of dorsal root axons; development of new collaterals and preterminals following partial denervation of the spinal cord in the cat.* AMA Arch Neurol Psychiatry, 1958. **79**(1): p. 46-61.
13. Guth, L., *History of central nervous system regeneration research.* Exp Neurol, 1975. **48**(3 pt. 2): p. 3-15.
14. Richardson, P.M., U.M. McGuinness, and A.J. Aguayo, *Axons from CNS neurons regenerate into PNS grafts.* Nature, 1980. **284**(5753): p. 264-5.
15. Aguayo, A.J., S. David, and G.M. Bray, *Influences of the glial environment on the elongation of axons after injury: transplantation studies in adult rodents.* J Exp Biol, 1981. **95**: p. 231-40.
16. Caroni, P. and M.E. Schwab, *Antibody against myelin-associated inhibitor of neurite growth neutralizes nonpermissive substrate properties of CNS white matter.* Neuron, 1988. **1**(1): p. 85-96.
17. Chierzi, S., et al., *The ability of axons to regenerate their growth cones depends on axonal type and age, and is regulated by calcium, cAMP and ERK.* Eur J Neurosci, 2005. **21**(8): p. 2051-62.
18. Carmeliet, P. and M. Tessier-Lavigne, *Common mechanisms of nerve and blood vessel wiring.* Nature, 2005. **436**(7048): p. 193-200.
19. Curinga, G. and G.M. Smith, *Molecular/genetic manipulation of extrinsic axon guidance factors for CNS repair and regeneration.* Exp Neurol, 2008. **209**(2): p. 333-42.
20. Bush, T.G., et al., *Leukocyte infiltration, neuronal degeneration, and neurite outgrowth after ablation of scar-forming, reactive astrocytes in adult transgenic mice.* Neuron, 1999. **23**(2): p. 297-308.
21. Faulkner, J.R., et al., *Reactive astrocytes protect tissue and preserve function after spinal cord injury.* J Neurosci, 2004. **24**(9): p. 2143-55.

22. Okada, S., et al., *Conditional ablation of Stat3 or Socs3 discloses a dual role for reactive astrocytes after spinal cord injury.* Nat Med, 2006. **12**(7): p. 829-34.
23. Herrmann, J.E., et al., *STAT3 is a critical regulator of astrogliosis and scar formation after spinal cord injury.* J Neurosci, 2008. **28**(28): p. 7231-43.
24. Wanner, I.B., et al., *Glial scar borders are formed by newly proliferated, elongated astrocytes that interact to corral inflammatory and fibrotic cells via STAT3-dependent mechanisms after spinal cord injury.* J Neurosci, 2013. **33**(31): p. 12870-86.
25. Anderson, M.A., et al., *Astrocyte scar formation aids central nervous system axon regeneration.* Nature, 2016. **532**(7598): p. 195-200.
26. Jones, L.L., et al., *NG2 is a major chondroitin sulfate proteoglycan produced after spinal cord injury and is expressed by macrophages and oligodendrocyte progenitors.* J Neurosci, 2002. **22**(7): p. 2792-803.
27. Jones, L.L., R.U. Margolis, and M.H. Tuszynski, *The chondroitin sulfate proteoglycans neurocan, brevican, phosphacan, and versican are differentially regulated following spinal cord injury.* Exp Neurol, 2003. **182**(2): p. 399-411.
28. Roll, L. and A. Faissner, *Influence of the extracellular matrix on endogenous and transplanted stem cells after brain damage.* Front Cell Neurosci, 2014. **8**: p. 219.
29. Smith-Thomas, L.C., et al., *An inhibitor of neurite outgrowth produced by astrocytes.* J Cell Sci, 1994. **107 (Pt 6)**: p. 1687-95.
30. Smith-Thomas, L.C., et al., *Increased axon regeneration in astrocytes grown in the presence of proteoglycan synthesis inhibitors.* J Cell Sci, 1995. **108 (Pt 3)**: p. 1307-15.
31. Davies, S.J., et al., *Regeneration of adult axons in white matter tracts of the central nervous system.* Nature, 1997. **390**(6661): p. 680-3.
32. Davies, S.J., et al., *Robust regeneration of adult sensory axons in degenerating white matter of the adult rat spinal cord.* J Neurosci, 1999. **19**(14): p. 5810-22.
33. Bovolenta, P., F. Wandosell, and M. Nieto-Sampedro, *Characterization of a neurite outgrowth inhibitor expressed after CNS injury.* Eur J Neurosci, 1993. **5**(5): p. 454-65.
34. Lemons, M.L., D.R. Howland, and D.K. Anderson, *Chondroitin sulfate proteoglycan immunoreactivity increases following spinal cord injury and transplantation.* Exp Neurol, 1999. **160**(1): p. 51-65.
35. Bradbury, E.J., et al., *Chondroitinase ABC promotes functional recovery after spinal cord injury.* Nature, 2002. **416**(6881): p. 636-40.
36. Yick, L.W., et al., *Axonal regeneration of Clarke's neurons beyond the spinal cord injury scar after treatment with chondroitinase ABC.* Exp Neurol, 2003. **182**(1): p. 160-8.
37. Caggiano, A.O., et al., *Chondroitinase ABCI improves locomotion and bladder function following contusion injury of the rat spinal cord.* J Neurotrauma, 2005. **22**(2): p. 226-39.
38. Shields, L.B., et al., *Benefit of chondroitinase ABC on sensory axon regeneration in a laceration model of spinal cord injury in the rat.* Surg Neurol, 2008. **69**(6): p. 568-77; discussion 577.
39. Barritt, A.W., et al., *Chondroitinase ABC promotes sprouting of intact and injured spinal systems after spinal cord injury.* J Neurosci, 2006. **26**(42): p. 10856-67.
40. Massey, J.M., et al., *Chondroitinase ABC digestion of the perineuronal net promotes functional collateral sprouting in the cuneate nucleus after cervical spinal cord injury.* J Neurosci, 2006. **26**(16): p. 4406-14.
41. Starkey, M.L., et al., *Chondroitinase ABC promotes compensatory sprouting of the intact corticospinal tract and recovery of forelimb function following unilateral pyramidotomy in adult mice.* Eur J Neurosci, 2012. **36**(12): p. 3665-78.
42. Bartus, K., et al., *Large-scale chondroitin sulfate proteoglycan digestion with chondroitinase gene therapy leads to reduced pathology and modulates macrophage phenotype following spinal cord contusion injury.* J Neurosci, 2014. **34**(14): p. 4822-36.

43. Carter, L.M., et al., *The yellow fluorescent protein (YFP-H) mouse reveals neuroprotection as a novel mechanism underlying chondroitinase ABC-mediated repair after spinal cord injury.* J Neurosci, 2008. **28**(52): p. 14107-20.
44. Carter, L.M., S.B. McMahon, and E.J. Bradbury, *Delayed treatment with chondroitinase ABC reverses chronic atrophy of rubrospinal neurons following spinal cord injury.* Exp Neurol, 2011. **228**(1): p. 149-56.
45. James, N.D., et al., *Chondroitinase gene therapy improves upper limb function following cervical contusion injury.* Exp Neurol, 2015. **271**: p. 131-5.
46. Tester, N.J. and D.R. Howland, *Chondroitinase ABC improves basic and skilled locomotion in spinal cord injured cats.* Exp Neurol, 2008. **209**(2): p. 483-96.
47. Bowes, C., et al., *Chondroitinase ABC promotes selective reactivation of somatosensory cortex in squirrel monkeys after a cervical dorsal column lesion.* Proc Natl Acad Sci U S A, 2012. **109**(7): p. 2595-600.
48. Bradbury, E.J. and L.M. Carter, *Manipulating the glial scar: chondroitinase ABC as a therapy for spinal cord injury.* Brain Res Bull, 2011. **84**(4-5): p. 306-16.
49. Fawcett, J.W., J. Rokos, and I. Bakst, *Oligodendrocytes repel axons and cause axonal growth cone collapse.* J Cell Sci, 1989. **92 (Pt 1)**: p. 93-100.
50. Chen, M.S., et al., *Nogo-A is a myelin-associated neurite outgrowth inhibitor and an antigen for monoclonal antibody IN-1.* Nature, 2000. **403**(6768): p. 434-9.
51. GrandPre, T., et al., *Identification of the Nogo inhibitor of axon regeneration as a Reticulon protein.* Nature, 2000. **403**(6768): p. 439-44.
52. Fournier, A.E., et al., *Truncated soluble Nogo receptor binds Nogo-66 and blocks inhibition of axon growth by myelin.* J Neurosci, 2002. **22**(20): p. 8876-83.
53. GrandPre, T., S. Li, and S.M. Strittmatter, *Nogo-66 receptor antagonist peptide promotes axonal regeneration.* Nature, 2002. **417**(6888): p. 547-51.
54. Kim, J.E., et al., *Axon regeneration in young adult mice lacking Nogo-A/B.* Neuron, 2003. **38**(2): p. 187-99.
55. Fouad, K., I. Klusman, and M.E. Schwab, *Regenerating corticospinal fibers in the Marmoset (Callitrix jacchus) after spinal cord lesion and treatment with the anti-Nogo-A antibody IN-1.* Eur J Neurosci, 2004. **20**(9): p. 2479-82.
56. Liebscher, T., et al., *Nogo-A antibody improves regeneration and locomotion of spinal cord-injured rats.* Ann Neurol, 2005. **58**(5): p. 706-19.
57. Freund, P., et al., *Nogo-A-specific antibody treatment enhances sprouting and functional recovery after cervical lesion in adult primates.* Nat Med, 2006. **12**(7): p. 790-2.
58. Freund, P., et al., *Anti-Nogo-A antibody treatment promotes recovery of manual dexterity after unilateral cervical lesion in adult primates--re-examination and extension of behavioral data.* Eur J Neurosci, 2009. **29**(5): p. 983-96.
59. Freund, P., et al., *Anti-Nogo-A antibody treatment enhances sprouting of corticospinal axons rostral to a unilateral cervical spinal cord lesion in adult macaque monkey.* J Comp Neurol, 2007. **502**(4): p. 644-59.
60. Mullner, A., et al., *Lamina-specific restoration of serotonergic projections after Nogo-A antibody treatment of spinal cord injury in rats.* Eur J Neurosci, 2008. **27**(2): p. 326-33.
61. Steward, O., et al., *A re-assessment of the effects of a Nogo-66 receptor antagonist on regenerative growth of axons and locomotor recovery after spinal cord injury in mice.* Exp Neurol, 2008. **209**(2): p. 446-68.
62. Raineteau, O., et al., *Functional switch between motor tracts in the presence of the mAb IN-1 in the adult rat.* Proc Natl Acad Sci U S A, 2001. **98**(12): p. 6929-34.

63. Kempf, A., et al., *Upregulation of axon guidance molecules in the adult central nervous system of Nogo-A knockout mice restricts neuronal growth and regeneration.* Eur J Neurosci, 2013. **38**(11): p. 3567-79.
64. Meininger, V., et al., *Safety, pharmacokinetic, and functional effects of the nogo-a monoclonal antibody in amyotrophic lateral sclerosis: a randomized, first-in-human clinical trial.* PLoS One, 2014. **9**(5): p. e97803.
65. Goldshmit, Y., S. McLenachan, and A. Turnley, *Roles of Eph receptors and ephrins in the normal and damaged adult CNS.* Brain Res Rev, 2006. **52**(2): p. 327-45.
66. Niclou, S.P., E.M. Ehlert, and J. Verhaagen, *Chemorepellent axon guidance molecules in spinal cord injury.* J Neurotrauma, 2006. **23**(3-4): p. 409-21.
67. Giger, R.J., E.R. Hollis, 2nd, and M.H. Tuszynski, *Guidance molecules in axon regeneration.* Cold Spring Harb Perspect Biol, 2010. **2**(7): p. a001867.
68. Onishi, K., E. Hollis, and Y. Zou, *Axon guidance and injury-lessons from Wnts and Wnt signaling.* Curr Opin Neurobiol, 2014. **27**: p. 232-40.
69. Miranda, J.D., et al., *Induction of Eph B3 after spinal cord injury.* Exp Neurol, 1999. **156**(1): p. 218-22.
70. Willson, C.A., et al., *Upregulation of EphA receptor expression in the injured adult rat spinal cord.* Cell Transplant, 2002. **11**(3): p. 229-39.
71. Bundesen, L.Q., et al., *Ephrin-B2 and EphB2 regulation of astrocyte-meningeal fibroblast interactions in response to spinal cord lesions in adult rats.* J Neurosci, 2003. **23**(21): p. 7789-800.
72. Fabes, J., et al., *Regeneration-enhancing effects of EphA4 blocking peptide following corticospinal tract injury in adult rat spinal cord.* Eur J Neurosci, 2007. **26**(9): p. 2496-505.
73. Fan, X.Y., A.J. Mothe, and C.H. Tator, *Ephrin-B3 decreases the survival of adult rat spinal cord-derived neural stem/progenitor cells in vitro and after transplantation into the injured rat spinal cord.* Stem Cells Dev, 2013. **22**(3): p. 359-73.
74. Duffy, P., et al., *Myelin-derived ephrinB3 restricts axonal regeneration and recovery after adult CNS injury.* Proc Natl Acad Sci U S A, 2012. **109**(13): p. 5063-8.
75. Goldshmit, Y., et al., *EphA4 blockers promote axonal regeneration and functional recovery following spinal cord injury in mice.* PLoS One, 2011. **6**(9): p. e24636.
76. Pasterkamp, R.J. and J. Verhaagen, *Semaphorins in axon regeneration: developmental guidance molecules gone wrong?* Philos Trans R Soc Lond B Biol Sci, 2006. **361**(1473): p. 1499-511.
77. Kaneko, S., et al., *A selective Sema3A inhibitor enhances regenerative responses and functional recovery of the injured spinal cord.* Nat Med, 2006. **12**(12): p. 1380-9.
78. Mire, E., et al., *Modulating Sema3A signal with a L1 mimetic peptide is not sufficient to promote motor recovery and axon regeneration after spinal cord injury.* Mol Cell Neurosci, 2008. **37**(2): p. 222-35.
79. Giehl, K.M. and W. Tetzlaff, *BDNF and NT-3, but not NGF, prevent axotomy-induced death of rat corticospinal neurons in vivo.* Eur J Neurosci, 1996. **8**(6): p. 1167-75.
80. Bradbury, E.J., et al., *NT-3, but not BDNF, prevents atrophy and death of axotomized spinal cord projection neurons.* Eur J Neurosci, 1998. **10**(10): p. 3058-68.
81. Shibayama, M., et al., *Neurotrophin-3 prevents death of axotomized Clarke's nucleus neurons in adult rat.* J Comp Neurol, 1998. **390**(1): p. 102-11.
82. Menei, P., et al., *Schwann cells genetically modified to secrete human BDNF promote enhanced axonal regrowth across transected adult rat spinal cord.* Eur J Neurosci, 1998. **10**(2): p. 607-21.
83. Bradbury, E.J., et al., *NT-3 promotes growth of lesioned adult rat sensory axons ascending in the dorsal columns of the spinal cord.* Eur J Neurosci, 1999. **11**(11): p. 3873-83.
84. Jin, Y., et al., *Transplants of fibroblasts genetically modified to express BDNF promote axonal regeneration from supraspinal neurons following chronic spinal cord injury.* Exp Neurol, 2002. **177**(1): p. 265-75.

85. Tuszynski, M.H., E. Mafong, and S. Meyer, *Central infusions of brain-derived neurotrophic factor and neurotrophin-4/5, but not nerve growth factor and neurotrophin-3, prevent loss of the cholinergic phenotype in injured adult motor neurons.* Neuroscience, 1996. **71**(3): p. 761-71.
86. Tuszynski, M.H., et al., *Fibroblasts genetically modified to produce nerve growth factor induce robust neuritic ingrowth after grafting to the spinal cord.* Exp Neurol, 1994. **126**(1): p. 1-14.
87. Nakahara, Y., F.H. Gage, and M.H. Tuszynski, *Grafts of fibroblasts genetically modified to secrete NGF, BDNF, NT-3, or basic FGF elicit differential responses in the adult spinal cord.* Cell Transplant, 1996. **5**(2): p. 191-204.
88. Grill, R., et al., *Cellular delivery of neurotrophin-3 promotes corticospinal axonal growth and partial functional recovery after spinal cord injury.* J Neurosci, 1997. **17**(14): p. 5560-72.
89. Grill, R.J., A. Blesch, and M.H. Tuszynski, *Robust growth of chronically injured spinal cord axons induced by grafts of genetically modified NGF-secreting cells.* Exp Neurol, 1997. **148**(2): p. 444-52.
90. McTigue, D.M., et al., *Neurotrophin-3 and brain-derived neurotrophic factor induce oligodendrocyte proliferation and myelination of regenerating axons in the contused adult rat spinal cord.* J Neurosci, 1998. **18**(14): p. 5354-65.
91. Liu, Y., et al., *Intraspinal delivery of neurotrophin-3 using neural stem cells genetically modified by recombinant retrovirus.* Exp Neurol, 1999. **158**(1): p. 9-26.
92. Jin, Y., et al., *Fibroblasts genetically modified to produce BDNF support regrowth of chronically injured serotonergic axons.* Neurorehabil Neural Repair, 2000. **14**(4): p. 311-7.
93. Himes, B.T., et al., *Transplants of cells genetically modified to express neurotrophin-3 rescue axotomized Clarke's nucleus neurons after spinal cord hemisection in adult rats.* J Neurosci Res, 2001. **65**(6): p. 549-64.
94. Blesch, A., et al., *Axonal responses to cellularly delivered NT-4/5 after spinal cord injury.* Mol Cell Neurosci, 2004. **27**(2): p. 190-201.
95. Weidner, N., et al., *Nerve growth factor-hypersecreting Schwann cell grafts augment and guide spinal cord axonal growth and remyelinate central nervous system axons in a phenotypically appropriate manner that correlates with expression of L1.* J Comp Neurol, 1999. **413**(4): p. 495-506.
96. Lu, P., L.L. Jones, and M.H. Tuszynski, *BDNF-expressing marrow stromal cells support extensive axonal growth at sites of spinal cord injury.* Exp Neurol, 2005. **191**(2): p. 344-60.
97. Lu, P., L.L. Jones, and M.H. Tuszynski, *Axon regeneration through scars and into sites of chronic spinal cord injury.* Exp Neurol, 2007. **203**(1): p. 8-21.
98. Ruitenberg, M.J., et al., *NT-3 expression from engineered olfactory ensheathing glia promotes spinal sparing and regeneration.* Brain, 2005. **128**(Pt 4): p. 839-53.
99. Ruitenberg, M.J., et al., *Ex vivo adenoviral vector-mediated neurotrophin gene transfer to olfactory ensheathing glia: effects on rubrospinal tract regeneration, lesion size, and functional recovery after implantation in the injured rat spinal cord.* J Neurosci, 2003. **23**(18): p. 7045-58.
100. Cao, L., et al., *Olfactory ensheathing cells genetically modified to secrete GDNF to promote spinal cord repair.* Brain, 2004. **127**(Pt 3): p. 535-49.
101. Cao, Q., et al., *Functional recovery in traumatic spinal cord injury after transplantation of multineurotrophin-expressing glial-restricted precursor cells.* J Neurosci, 2005. **25**(30): p. 6947-57.
102. Blits, B., et al., *Intercostal nerve implants transduced with an adenoviral vector encoding neurotrophin-3 promote regrowth of injured rat corticospinal tract fibers and improve hindlimb function.* Exp Neurol, 2000. **164**(1): p. 25-37.
103. Taylor, L., et al., *Neurotrophin-3 gradients established by lentiviral gene delivery promote short-distance axonal bridging beyond cellular grafts in the injured spinal cord.* J Neurosci, 2006. **26**(38): p. 9713-21.

104. Alto, L.T., et al., *Chemotropic guidance facilitates axonal regeneration and synapse formation after spinal cord injury.* Nat Neurosci, 2009. **12**(9): p. 1106-13.
105. Kadoya, K., et al., *Combined intrinsic and extrinsic neuronal mechanisms facilitate bridging axonal regeneration one year after spinal cord injury.* Neuron, 2009. **64**(2): p. 165-72.
106. Lu, P., et al., *Motor axonal regeneration after partial and complete spinal cord transection.* J Neurosci, 2012. **32**(24): p. 8208-18.
107. Ghosh-Roy, A., et al., *Calcium and cyclic AMP promote axonal regeneration in Caenorhabditis elegans and require DLK-1 kinase.* J Neurosci, 2010. **30**(9): p. 3175-83.
108. Ming, G.L., et al., *cAMP-dependent growth cone guidance by netrin-1.* Neuron, 1997. **19**(6): p. 1225-35.
109. Song, H., et al., *Conversion of neuronal growth cone responses from repulsion to attraction by cyclic nucleotides.* Science, 1998. **281**(5382): p. 1515-8.
110. Song, H.J., G.L. Ming, and M.M. Poo, *cAMP-induced switching in turning direction of nerve growth cones.* Nature, 1997. **388**(6639): p. 275-9.
111. Neumann, S., et al., *Regeneration of sensory axons within the injured spinal cord induced by intraganglionic cAMP elevation.* Neuron, 2002. **34**(6): p. 885-93.
112. Qiu, J., et al., *Spinal axon regeneration induced by elevation of cyclic AMP.* Neuron, 2002. **34**(6): p. 895-903.
113. Lu, P., et al., *Combinatorial therapy with neurotrophins and cAMP promotes axonal regeneration beyond sites of spinal cord injury.* J Neurosci, 2004. **24**(28): p. 6402-9.
114. Nikulina, E., et al., *The phosphodiesterase inhibitor rolipram delivered after a spinal cord lesion promotes axonal regeneration and functional recovery.* Proc Natl Acad Sci U S A, 2004. **101**(23): p. 8786-90.
115. Beaumont, E., et al., *Effects of rolipram on adult rat oligodendrocytes and functional recovery after contusive cervical spinal cord injury.* Neuroscience, 2009. **163**(4): p. 985-90.
116. Iannotti, C.A., et al., *A combination immunomodulatory treatment promotes neuroprotection and locomotor recovery after contusion SCI.* Exp Neurol, 2011. **230**(1): p. 3-15.
117. Costa, L.M., et al., *Rolipram promotes functional recovery after contusive thoracic spinal cord injury in rats.* Behav Brain Res, 2013. **243**: p. 66-73.
118. Schaal, S.M., et al., *The therapeutic profile of rolipram, PDE target and mechanism of action as a neuroprotectant following spinal cord injury.* PLoS One, 2012. **7**(9): p. e43634.
119. Cho, Y., et al., *Injury-induced HDAC5 nuclear export is essential for axon regeneration.* Cell, 2013. **155**(4): p. 894-908.
120. Finelli, M.J., J.K. Wong, and H. Zou, *Epigenetic regulation of sensory axon regeneration after spinal cord injury.* J Neurosci, 2013. **33**(50): p. 19664-76.
121. Gaub, P., et al., *The histone acetyltransferase p300 promotes intrinsic axonal regeneration.* Brain, 2011. **134**(Pt 7): p. 2134-48.
122. Ruschel, J., et al., *Axonal regeneration. Systemic administration of epothilone B promotes axon regeneration after spinal cord injury.* Science, 2015. **348**(6232): p. 347-52.
123. Cho, Y. and V. Cavalli, *HDAC5 is a novel injury-regulated tubulin deacetylase controlling axon regeneration.* EMBO J, 2012. **31**(14): p. 3063-78.
124. Rivieccio, M.A., et al., *HDAC6 is a target for protection and regeneration following injury in the nervous system.* Proc Natl Acad Sci U S A, 2009. **106**(46): p. 19599-604.
125. Erturk, A., et al., *Disorganized microtubules underlie the formation of retraction bulbs and the failure of axonal regeneration.* J Neurosci, 2007. **27**(34): p. 9169-80.
126. Hellal, F., et al., *Microtubule stabilization reduces scarring and causes axon regeneration after spinal cord injury.* Science, 2011. **331**(6019): p. 928-31.
127. Popovich, P.G., et al., *Independent evaluation of the anatomical and behavioral effects of Taxol in rat models of spinal cord injury.* Exp Neurol, 2014. **261**: p. 97-108.

128. Fernandes, K.J., et al., *Influence of the axotomy to cell body distance in rat rubrospinal and spinal motoneurons: differential regulation of GAP-43, tubulins, and neurofilament-M.* J Comp Neurol, 1999. **414**(4): p. 495-510.
129. Zou, H., et al., *Axotomy-induced Smad1 activation promotes axonal growth in adult sensory neurons.* J Neurosci, 2009. **29**(22): p. 7116-23.
130. Gao, Y., et al., *Activated CREB is sufficient to overcome inhibitors in myelin and promote spinal axon regeneration in vivo.* Neuron, 2004. **44**(4): p. 609-21.
131. Smith, P.D., et al., *SOCS3 deletion promotes optic nerve regeneration in vivo.* Neuron, 2009. **64**(5): p. 617-23.
132. Seijffers, R., C.D. Mills, and C.J. Woolf, *ATF3 increases the intrinsic growth state of DRG neurons to enhance peripheral nerve regeneration.* J Neurosci, 2007. **27**(30): p. 7911-20.
133. Raivich, G., et al., *The AP-1 transcription factor c-Jun is required for efficient axonal regeneration.* Neuron, 2004. **43**(1): p. 57-67.
134. Park, K.K., et al., *Promoting axon regeneration in the adult CNS by modulation of the PTEN/mTOR pathway.* Science, 2008. **322**(5903): p. 963-6.
135. Liu, K., et al., *PTEN deletion enhances the regenerative ability of adult corticospinal neurons.* Nat Neurosci, 2010. **13**(9): p. 1075-81.
136. Danilov, C.A. and O. Steward, *Conditional genetic deletion of PTEN after a spinal cord injury enhances regenerative growth of CST axons and motor function recovery in mice.* Exp Neurol, 2015. **266**: p. 147-60.
137. Geoffroy, C.G., et al., *Effects of PTEN and Nogo Codeletion on Corticospinal Axon Sprouting and Regeneration in Mice.* J Neurosci, 2015. **35**(16): p. 6413-28.
138. Sun, F., et al., *Sustained axon regeneration induced by co-deletion of PTEN and SOCS3.* Nature, 2011. **480**(7377): p. 372-5.
139. Rao, S.N. and D.D. Pearse, *Regulating Axonal Responses to Injury: The Intersection between Signaling Pathways Involved in Axon Myelination and The Inhibition of Axon Regeneration.* Front Mol Neurosci, 2016. **9**: p. 33.
140. Filbin, M.T., *Myelin-associated inhibitors of axonal regeneration in the adult mammalian CNS.* Nat Rev Neurosci, 2003. **4**(9): p. 703-13.
141. Carmel, P.W. and B.M. Stein, *Cell changes in sensory ganglia following proximal and distal nerve section in the monkey.* J Comp Neurol, 1969. **135**(2): p. 145-66.
142. Ramón y Cajal, S., *Degeneration and Regeneration of the Nervous System* 1928.
143. Abe, N. and V. Cavalli, *Nerve injury signaling.* Curr Opin Neurobiol, 2008. **18**(3): p. 276-83.
144. Scheib, J. and A. Hoke, *Advances in peripheral nerve regeneration.* Nat Rev Neurol, 2013. **9**(12): p. 668-76.
145. Richardson, P.M. and V.M. Issa, *Peripheral injury enhances central regeneration of primary sensory neurones.* Nature, 1984. **309**(5971): p. 791-3.
146. Neumann, S. and C.J. Woolf, *Regeneration of dorsal column fibers into and beyond the lesion site following adult spinal cord injury.* Neuron, 1999. **23**(1): p. 83-91.
147. Blesch, A., et al., *Conditioning lesions before or after spinal cord injury recruit broad genetic mechanisms that sustain axonal regeneration: superiority to camp-mediated effects.* Exp Neurol, 2012. **235**(1): p. 162-73.
148. Lu, P., et al., *Long-distance axonal growth from human induced pluripotent stem cells after spinal cord injury.* Neuron, 2014. **83**(4): p. 789-96.
149. Lu, P., et al., *Long-distance growth and connectivity of neural stem cells after severe spinal cord injury.* Cell, 2012. **150**(6): p. 1264-73.
150. Jiang, Y., et al., *Pluripotency of mesenchymal stem cells derived from adult marrow.* Nature, 2002. **418**(6893): p. 41-9.

151. Sekiya, I., et al., *Expansion of human adult stem cells from bone marrow stroma: conditions that maximize the yields of early progenitors and evaluate their quality.* Stem Cells, 2002. **20**(6): p. 530-41.
152. Malgieri, A., et al., *Bone marrow and umbilical cord blood human mesenchymal stem cells: state of the art.* Int J Clin Exp Med, 2010. **3**(4): p. 248-69.
153. Oliveri, R.S., S. Bello, and F. Biering-Sorensen, *Mesenchymal stem cells improve locomotor recovery in traumatic spinal cord injury: systematic review with meta-analyses of rat models.* Neurobiol Dis, 2014. **62**: p. 338-53.
154. Tetzlaff, W., et al., *A systematic review of cellular transplantation therapies for spinal cord injury.* J Neurotrauma, 2011. **28**(8): p. 1611-82.
155. Li, J. and G. Lepski, *Cell transplantation for spinal cord injury: a systematic review.* Biomed Res Int, 2013. **2013**: p. 786475.
156. Forostyak, S., P. Jendelova, and E. Sykova, *The role of mesenchymal stromal cells in spinal cord injury, regenerative medicine and possible clinical applications.* Biochimie, 2013. **95**(12): p. 2257-70.
157. Vawda, R. and M.G. Fehlings, *Mesenchymal cells in the treatment of spinal cord injury: current & future perspectives.* Curr Stem Cell Res Ther, 2013. **8**(1): p. 25-38.
158. Rapalino, O., et al., *Implantation of stimulated homologous macrophages results in partial recovery of paraplegic rats.* Nat Med, 1998. **4**(7): p. 814-21.
159. Franzen, R., et al., *Effects of macrophage transplantation in the injured adult rat spinal cord: a combined immunocytochemical and biochemical study.* J Neurosci Res, 1998. **51**(3): p. 316-27.
160. Bomstein, Y., et al., *Features of skin-coincubated macrophages that promote recovery from spinal cord injury.* J Neuroimmunol, 2003. **142**(1-2): p. 10-6.
161. Knoller, N., et al., *Clinical experience using incubated autologous macrophages as a treatment for complete spinal cord injury: phase I study results.* J Neurosurg Spine, 2005. **3**(3): p. 173-81.
162. Jones, L.A., et al., *A phase 2 autologous cellular therapy trial in patients with acute, complete spinal cord injury: pragmatics, recruitment, and demographics.* Spinal Cord, 2010. **48**(11): p. 798-807.
163. Lammertse, D.P., et al., *Autologous incubated macrophage therapy in acute, complete spinal cord injury: results of the phase 2 randomized controlled multicenter trial.* Spinal Cord, 2012. **50**(9): p. 661-71.
164. Duncan, I.D., et al., *Transplantation of rat Schwann cells grown in tissue culture into the mouse spinal cord.* J Neurol Sci, 1981. **49**(2): p. 241-52.
165. Xu, X.M., et al., *Bridging Schwann cell transplants promote axonal regeneration from both the rostral and caudal stumps of transected adult rat spinal cord.* J Neurocytol, 1997. **26**(1): p. 1-16.
166. Xu, X.M., et al., *Axonal regeneration into Schwann cell-seeded guidance channels grafted into transected adult rat spinal cord.* J Comp Neurol, 1995. **351**(1): p. 145-60.
167. Takami, T., et al., *Schwann cell but not olfactory ensheathing glia transplants improve hindlimb locomotor performance in the moderately contused adult rat thoracic spinal cord.* J Neurosci, 2002. **22**(15): p. 6670-81.
168. Barakat, D.J., et al., *Survival, integration, and axon growth support of glia transplanted into the chronically contused spinal cord.* Cell Transplant, 2005. **14**(4): p. 225-40.
169. Schaal, S.M., et al., *Schwann cell transplantation improves reticulospinal axon growth and forelimb strength after severe cervical spinal cord contusion.* Cell Transplant, 2007. **16**(3): p. 207-28.
170. Papastefanaki, F., et al., *Grafts of Schwann cells engineered to express PSA-NCAM promote functional recovery after spinal cord injury.* Brain, 2007. **130**(Pt 8): p. 2159-74.
171. Guest, J.D., et al., *Influence of IN-1 antibody and acidic FGF-fibrin glue on the response of injured corticospinal tract axons to human Schwann cell grafts.* J Neurosci Res, 1997. **50**(5): p. 888-905.

172. Guest, J.D., et al., *The ability of human Schwann cell grafts to promote regeneration in the transected nude rat spinal cord.* Exp Neurol, 1997. **148**(2): p. 502-22.
173. Saberi, H., et al., *Safety of intramedullary Schwann cell transplantation for postrehabilitation spinal cord injuries: 2-year follow-up of 33 cases.* J Neurosurg Spine, 2011. **15**(5): p. 515-25.
174. Saberi, H., et al., *Treatment of chronic thoracic spinal cord injury patients with autologous Schwann cell transplantation: an interim report on safety considerations and possible outcomes.* Neurosci Lett, 2008. **443**(1): p. 46-50.
175. Zhou, X.H., et al., *Transplantation of autologous activated Schwann cells in the treatment of spinal cord injury: six cases, more than five years of follow-up.* Cell Transplant, 2012. **21 Suppl 1**: p. S39-47.
176. Guest, J., A.J. Santamaria, and F.D. Benavides, *Clinical translation of autologous Schwann cell transplantation for the treatment of spinal cord injury.* Curr Opin Organ Transplant, 2013. **18**(6): p. 682-9.
177. Kamada, T., et al., *Transplantation of bone marrow stromal cell-derived Schwann cells promotes axonal regeneration and functional recovery after complete transection of adult rat spinal cord.* J Neuropathol Exp Neurol, 2005. **64**(1): p. 37-45.
178. Biernaskie, J., et al., *Skin-derived precursors generate myelinating Schwann cells that promote remyelination and functional recovery after contusion spinal cord injury.* J Neurosci, 2007. **27**(36): p. 9545-59.
179. Golgi, C., *Sulla fina anatomia del bulbi olfattorii.* Rivista Sperimentale di Freniatria, 1875. **1**: p. 403-425.
180. Blanes, T., *Sobre algunos puntos dudosos del la estructura del bulbo olfactorio.* Revista Trimestral Micrográfica, 1898. **3**: p. 99-127.
181. Doucette, R., *PNS-CNS transitional zone of the first cranial nerve.* J Comp Neurol, 1991. **312**(3): p. 451-66.
182. Ramon-Cueto, A. and M. Nieto-Sampedro, *Regeneration into the spinal cord of transected dorsal root axons is promoted by ensheathing glia transplants.* Exp Neurol, 1994. **127**(2): p. 232-44.
183. Ramon-Cueto, A., et al., *Functional recovery of paraplegic rats and motor axon regeneration in their spinal cords by olfactory ensheathing glia.* Neuron, 2000. **25**(2): p. 425-35.
184. Ramon-Cueto, A. and C. Munoz-Quiles, *Clinical application of adult olfactory bulb ensheathing glia for nervous system repair.* Exp Neurol, 2011. **229**(1): p. 181-94.
185. Roet, K.C. and J. Verhaagen, *Understanding the neural repair-promoting properties of olfactory ensheathing cells.* Exp Neurol, 2014. **261C**: p. 594-609.
186. Franssen, E.H., F.M. de Bree, and J. Verhaagen, *Olfactory ensheathing glia: their contribution to primary olfactory nervous system regeneration and their regenerative potential following transplantation into the injured spinal cord.* Brain Res Rev, 2007. **56**(1): p. 236-58.
187. Pearse, D.D., et al., *Transplantation of Schwann cells and/or olfactory ensheathing glia into the contused spinal cord: Survival, migration, axon association, and functional recovery.* Glia, 2007. **55**(9): p. 976-1000.
188. Richter, M.W., et al., *Lamina propria and olfactory bulb ensheathing cells exhibit differential integration and migration and promote differential axon sprouting in the lesioned spinal cord.* J Neurosci, 2005. **25**(46): p. 10700-11.
189. Au, E., et al., *SPARC from olfactory ensheathing cells stimulates Schwann cells to promote neurite outgrowth and enhances spinal cord repair.* J Neurosci, 2007. **27**(27): p. 7208-21.
190. Feron, F., et al., *Autologous olfactory ensheathing cell transplantation in human spinal cord injury.* Brain, 2005. **128**(Pt 12): p. 2951-60.
191. Mackay-Sim, A., et al., *Autologous olfactory ensheathing cell transplantation in human paraplegia: a 3-year clinical trial.* Brain, 2008. **131**(Pt 9): p. 2376-86.

192. Rao, Y., et al., *Long-term outcome of olfactory ensheathing cell transplantation in six patients with chronic complete spinal cord injury.* Cell Transplant, 2013. **22 Suppl 1**: p. S21-5.
193. Tabakow, P., et al., *Transplantation of autologous olfactory ensheathing cells in complete human spinal cord injury.* Cell Transplant, 2013.
194. Weiss, S., et al., *Multipotent CNS stem cells are present in the adult mammalian spinal cord and ventricular neuroaxis.* J Neurosci, 1996. **16**(23): p. 7599-609.
195. Nemati, S.N., et al., *Transplantation of adult monkey neural stem cells into a contusion spinal cord injury model in rhesus macaque monkeys.* Cell J, 2014. **16**(2): p. 117-30.
196. Mothe, A.J., et al., *Neural stem/progenitor cells from the adult human spinal cord are multipotent and self-renewing and differentiate after transplantation.* PLoS One, 2011. **6**(11): p. e27079.
197. Quinn, S.M., et al., *Lineage restriction of neuroepithelial precursor cells from fetal human spinal cord.* J Neurosci Res, 1999. **57**(5): p. 590-602.
198. Vescovi, A.L. and E.Y. Snyder, *Establishment and properties of neural stem cell clones: plasticity in vitro and in vivo.* Brain Pathol, 1999. **9**(3): p. 569-98.
199. Uchida, N., et al., *Direct isolation of human central nervous system stem cells.* Proc Natl Acad Sci U S A, 2000. **97**(26): p. 14720-5.
200. Cummings, B.J., et al., *Human neural stem cell differentiation following transplantation into spinal cord injured mice: association with recovery of locomotor function.* Neurol Res, 2006. **28**(5): p. 474-81.
201. Cummings, B.J., et al., *Human neural stem cells differentiate and promote locomotor recovery in spinal cord-injured mice.* Proc Natl Acad Sci U S A, 2005. **102**(39): p. 14069-74.
202. Tropepe, V., et al., *Direct neural fate specification from embryonic stem cells: a primitive mammalian neural stem cell stage acquired through a default mechanism.* Neuron, 2001. **30**(1): p. 65-78.
203. Thomson, J.A., V.S. Marshall, and J.Q. Trojanowski, *Neural differentiation of rhesus embryonic stem cells.* APMIS, 1998. **106**(1): p. 149-56; discussion 156-7.
204. Gaspard, N., et al., *Generation of cortical neurons from mouse embryonic stem cells.* Nat Protoc, 2009. **4**(10): p. 1454-63.
205. Krencik, R., et al., *Specification of transplantable astroglial subtypes from human pluripotent stem cells.* Nat Biotechnol, 2011. **29**(6): p. 528-34.
206. Du, Z.W., et al., *Generation and expansion of highly pure motor neuron progenitors from human pluripotent stem cells.* Nat Commun, 2015. **6**: p. 6626.
207. Lu, J., et al., *Generation of serotonin neurons from human pluripotent stem cells.* Nat Biotechnol, 2016. **34**(1): p. 89-94.
208. Hu, B.Y., Z.W. Du, and S.C. Zhang, *Differentiation of human oligodendrocytes from pluripotent stem cells.* Nat Protoc, 2009. **4**(11): p. 1614-22.
209. Yuan, S.H., et al., *Cell-surface marker signatures for the isolation of neural stem cells, glia and neurons derived from human pluripotent stem cells.* PLoS One, 2011. **6**(3): p. e17540.
210. Brustle, O., et al., *Embryonic stem cell-derived glial precursors: a source of myelinating transplants.* Science, 1999. **285**(5428): p. 754-6.
211. Keirstead, H.S., et al., *Human embryonic stem cell-derived oligodendrocyte progenitor cell transplants remyelinate and restore locomotion after spinal cord injury.* J Neurosci, 2005. **25**(19): p. 4694-705.
212. Sharp, J., et al., *Human embryonic stem cell-derived oligodendrocyte progenitor cell transplants improve recovery after cervical spinal cord injury.* Stem Cells, 2010. **28**(1): p. 152-63.
213. Takahashi, K., et al., *Induction of pluripotent stem cells from adult human fibroblasts by defined factors.* Cell, 2007. **131**(5): p. 861-72.

214. Thier, M., et al., *Direct conversion of fibroblasts into stably expandable neural stem cells.* Cell Stem Cell, 2012. **10**(4): p. 473-9.
215. Chanda, S., et al., *Generation of induced neuronal cells by the single reprogramming factor ASCL1.* Stem Cell Reports, 2014. **3**(2): p. 282-96.
216. Wapinski, O.L., et al., *Hierarchical mechanisms for direct reprogramming of fibroblasts to neurons.* Cell, 2013. **155**(3): p. 621-35.
217. Bago, J.R., et al., *Therapeutically engineered induced neural stem cells are tumour-homing and inhibit progression of glioblastoma.* Nat Commun, 2016. **7**: p. 10593.
218. Kim, S.M., et al., *Direct conversion of mouse fibroblasts into induced neural stem cells.* Nat Protoc, 2014. **9**(4): p. 871-81.
219. Pfeifer, K., et al., *Autologous adult rodent neural progenitor cell transplantation represents a feasible strategy to promote structural repair in the chronically injured spinal cord.* Regen Med, 2006. **1**(2): p. 255-66.
220. Lee, A.S., et al., *Tumorigenicity as a clinical hurdle for pluripotent stem cell therapies.* Nat Med, 2013. **19**(8): p. 998-1004.
221. Pfeifer, K., et al., *Adult neural progenitor cells provide a permissive guiding substrate for corticospinal axon growth following spinal cord injury.* Eur J Neurosci, 2004. **20**(7): p. 1695-704.
222. Davies, J.E., et al., *Astrocytes derived from glial-restricted precursors promote spinal cord repair.* J Biol, 2006. **5**(3): p. 7.
223. Medalha, C.C., et al., *Transplanting neural progenitors into a complete transection model of spinal cord injury.* J Neurosci Res, 2014. **92**(5): p. 607-18.
224. Bonner, J.F., et al., *Grafted neural progenitors integrate and restore synaptic connectivity across the injured spinal cord.* J Neurosci, 2011. **31**(12): p. 4675-86.
225. Groves, A.K., et al., *Repair of demyelinated lesions by transplantation of purified O-2A progenitor cells.* Nature, 1993. **362**(6419): p. 453-5.
226. McDonald, J.W., et al., *Transplanted embryonic stem cells survive, differentiate and promote recovery in injured rat spinal cord.* Nat Med, 1999. **5**(12): p. 1410-2.
227. Karimi-Abdolrezaee, S., et al., *Delayed transplantation of adult neural precursor cells promotes remyelination and functional neurological recovery after spinal cord injury.* J Neurosci, 2006. **26**(13): p. 3377-89.
228. Emgard, M., et al., *Neuroprotective effects of human spinal cord-derived neural precursor cells after transplantation to the injured spinal cord.* Exp Neurol, 2014. **253**: p. 138-45.
229. Tsuji, O., et al., *Therapeutic potential of appropriately evaluated safe-induced pluripotent stem cells for spinal cord injury.* Proc Natl Acad Sci U S A, 2010. **107**(28): p. 12704-9.
230. Nori, S., et al., *Grafted human-induced pluripotent stem-cell-derived neurospheres promote motor functional recovery after spinal cord injury in mice.* Proc Natl Acad Sci U S A, 2011. **108**(40): p. 16825-30.
231. Fujimoto, Y., et al., *Treatment of a mouse model of spinal cord injury by transplantation of human induced pluripotent stem cell-derived long-term self-renewing neuroepithelial-like stem cells.* Stem Cells, 2012. **30**(6): p. 1163-73.
232. Mayor, S., *First patient enters trial to test safety of stem cells in spinal injury.* BMJ, 2010. **341**: p. c5724.
233. Kaiser, J., *Embryonic stem cells. Researchers mull impact of Geron's sudden exit from field.* Science, 2011. **334**(6059): p. 1043.
234. Priest, C.A., et al., *Preclinical safety of human embryonic stem cell-derived oligodendrocyte progenitors supporting clinical trials in spinal cord injury.* Regen Med, 2015. **10**(8): p. 939-58.
235. Tsukamoto, A., et al., *Clinical translation of human neural stem cells.* Stem Cell Res Ther, 2013. **4**(4): p. 102.

236. Glass, J.D., et al., *Transplantation of spinal cord-derived neural stem cells for ALS: Analysis of phase 1 and 2 trials.* Neurology, 2016.
237. Steward, O., et al., *Characterization of ectopic colonies that form in widespread areas of the nervous system with neural stem cell transplants into the site of a severe spinal cord injury.* J Neurosci, 2014. **34**(42): p. 14013-21.
238. Sharp, K.G., K.M. Yee, and O. Steward, *A re-assessment of long distance growth and connectivity of neural stem cells after severe spinal cord injury.* Exp Neurol, 2014. **257**: p. 186-204.
239. Thomson, J.A., et al., *Embryonic stem cell lines derived from human blastocysts.* Science, 1998. **282**(5391): p. 1145-7.
240. Chung, Y., et al., *Human embryonic stem cell lines generated without embryo destruction.* Cell Stem Cell, 2008. **2**(2): p. 113-7.
241. Crook, J.M., et al., *The generation of six clinical-grade human embryonic stem cell lines.* Cell Stem Cell, 2007. **1**(5): p. 490-4.
242. Funk, W.D., et al., *Evaluating the genomic and sequence integrity of human ES cell lines; comparison to normal genomes.* Stem Cell Res, 2012. **8**(2): p. 154-64.
243. Canham, M.A., et al., *The Molecular Karyotype of 25 Clinical-Grade Human Embryonic Stem Cell Lines.* Sci Rep, 2015. **5**: p. 17258.
244. Ilic, D. and C. Ogilvie, *Human Embryonic Stem Cells-What Have We Done? What Are We Doing? Where Are We Going?* Stem Cells, 2016.
245. Osafune, K., et al., *Marked differences in differentiation propensity among human embryonic stem cell lines.* Nat Biotechnol, 2008. **26**(3): p. 313-5.
246. Takahashi, K. and S. Yamanaka, *Induction of pluripotent stem cells from mouse embryonic and adult fibroblast cultures by defined factors.* Cell, 2006. **126**(4): p. 663-76.
247. Takahashi, K., et al., *Induction of pluripotent stem cells from fibroblast cultures.* Nat Protoc, 2007. **2**(12): p. 3081-9.
248. Nakagawa, M., et al., *Generation of induced pluripotent stem cells without Myc from mouse and human fibroblasts.* Nat Biotechnol, 2008. **26**(1): p. 101-6.
249. Okita, K., T. Ichisaka, and S. Yamanaka, *Generation of germline-competent induced pluripotent stem cells.* Nature, 2007. **448**(7151): p. 313-7.
250. Yu, J., et al., *Induced pluripotent stem cell lines derived from human somatic cells.* Science, 2007. **318**(5858): p. 1917-20.
251. Giorgetti, A., et al., *Generation of induced pluripotent stem cells from human cord blood using OCT4 and SOX2.* Cell Stem Cell, 2009. **5**(4): p. 353-7.
252. Loh, Y.H., et al., *Generation of induced pluripotent stem cells from human blood.* Blood, 2009. **113**(22): p. 5476-9.
253. Park, I.H., et al., *Reprogramming of human somatic cells to pluripotency with defined factors.* Nature, 2008. **451**(7175): p. 141-6.
254. Aoi, T., et al., *Generation of pluripotent stem cells from adult mouse liver and stomach cells.* Science, 2008. **321**(5889): p. 699-702.
255. Lowry, W.E., et al., *Generation of human induced pluripotent stem cells from dermal fibroblasts.* Proc Natl Acad Sci U S A, 2008. **105**(8): p. 2883-8.
256. Stadtfeld, M., K. Brennand, and K. Hochedlinger, *Reprogramming of pancreatic beta cells into induced pluripotent stem cells.* Curr Biol, 2008. **18**(12): p. 890-4.
257. Kim, J.B., et al., *Pluripotent stem cells induced from adult neural stem cells by reprogramming with two factors.* Nature, 2008. **454**(7204): p. 646-50.
258. Eminli, S., et al., *Reprogramming of neural progenitor cells into induced pluripotent stem cells in the absence of exogenous Sox2 expression.* Stem Cells, 2008. **26**(10): p. 2467-74.
259. Aasen, T., et al., *Efficient and rapid generation of induced pluripotent stem cells from human keratinocytes.* Nat Biotechnol, 2008. **26**(11): p. 1276-84.

260. Meissner, A., M. Wernig, and R. Jaenisch, *Direct reprogramming of genetically unmodified fibroblasts into pluripotent stem cells.* Nat Biotechnol, 2007. **25**(10): p. 1177-81.
261. Wernig, M., et al., *c-Myc is dispensable for direct reprogramming of mouse fibroblasts.* Cell Stem Cell, 2008. **2**(1): p. 10-2.
262. Wernig, M., et al., *In vitro reprogramming of fibroblasts into a pluripotent ES-cell-like state.* Nature, 2007. **448**(7151): p. 318-24.
263. Okita, K., et al., *Generation of mouse induced pluripotent stem cells without viral vectors.* Science, 2008. **322**(5903): p. 949-53.
264. Somers, A., et al., *Generation of transgene-free lung disease-specific human induced pluripotent stem cells using a single excisable lentiviral stem cell cassette.* Stem Cells, 2010. **28**(10): p. 1728-40.
265. Sommer, C.A., et al., *Excision of reprogramming transgenes improves the differentiation potential of iPS cells generated with a single excisable vector.* Stem Cells, 2010. **28**(1): p. 64-74.
266. Sommer, C.A., et al., *Induced pluripotent stem cell generation using a single lentiviral stem cell cassette.* Stem Cells, 2009. **27**(3): p. 543-9.
267. Sommer, C.A., et al., *Residual expression of reprogramming factors affects the transcriptional program and epigenetic signatures of induced pluripotent stem cells.* PLoS One, 2012. **7**(12): p. e51711.
268. Kaji, K., et al., *Virus-free induction of pluripotency and subsequent excision of reprogramming factors.* Nature, 2009. **458**(7239): p. 771-5.
269. Wilson, M.H., C.J. Coates, and A.L. George, Jr., *PiggyBac transposon-mediated gene transfer in human cells.* Mol Ther, 2007. **15**(1): p. 139-45.
270. Okita, K., et al., *Generation of mouse-induced pluripotent stem cells with plasmid vectors.* Nat Protoc, 2010. **5**(3): p. 418-28.
271. Jia, F., et al., *A nonviral minicircle vector for deriving human iPS cells.* Nat Methods, 2010. **7**(3): p. 197-9.
272. Yu, J., et al., *Human induced pluripotent stem cells free of vector and transgene sequences.* Science, 2009. **324**(5928): p. 797-801.
273. Warren, L., et al., *Highly efficient reprogramming to pluripotency and directed differentiation of human cells with synthetic modified mRNA.* Cell Stem Cell, 2010. **7**(5): p. 618-30.
274. Zhou, H., et al., *Generation of induced pluripotent stem cells using recombinant proteins.* Cell Stem Cell, 2009. **4**(5): p. 381-4.
275. Trounson, A. and N.D. DeWitt, *Pluripotent stem cells progressing to the clinic.* Nat Rev Mol Cell Biol, 2016. **17**(3): p. 194-200.
276. *First iPS cell transplant patient makes progress one year on.* Japan Times (online), 2015.
277. Barry, J., et al., *Setting Up a Haplobank: Issues and Solutions.* Curr Stem Cell Rep, 2015. **1**(2): p. 110-117.
278. Gaspard, N. and P. Vanderhaeghen, *Mechanisms of neural specification from embryonic stem cells.* Curr Opin Neurobiol, 2010. **20**(1): p. 37-43.
279. Kelava, I. and M.A. Lancaster, *Dishing out mini-brains: Current progress and future prospects in brain organoid research.* Dev Biol, 2016.
280. Lancaster, M.A. and J.A. Knoblich, *Generation of cerebral organoids from human pluripotent stem cells.* Nat Protoc, 2014. **9**(10): p. 2329-40.
281. Lancaster, M.A. and J.A. Knoblich, *Organogenesis in a dish: modeling development and disease using organoid technologies.* Science, 2014. **345**(6194): p. 1247125.
282. Lancaster, M.A., et al., *Cerebral organoids model human brain development and microcephaly.* Nature, 2013. **501**(7467): p. 373-9.
283. Dinsmore, J., et al., *Embryonic stem cells as a model for studying regulation of cellular differentiation.* Theriogenology, 1998. **49**(1): p. 145-51.

284. Kawamorita, M., et al., *In vitro differentiation of mouse embryonic stem cells after activation by retinoic acid.* Hum Cell, 2002. **15**(3): p. 178-82.
285. Glaser, T., et al., *Generation of purified oligodendrocyte progenitors from embryonic stem cells.* FASEB J, 2005. **19**(1): p. 112-4.
286. Dang, L. and V. Tropepe, *Neural induction and neural stem cell development.* Regen Med, 2006. **1**(5): p. 635-52.
287. Dottori, M. and M.F. Pera, *Neural differentiation of human embryonic stem cells.* Methods Mol Biol, 2008. **438**: p. 19-30.
288. Koch, P., et al., *A rosette-type, self-renewing human ES cell-derived neural stem cell with potential for in vitro instruction and synaptic integration.* Proc Natl Acad Sci U S A, 2009. **106**(9): p. 3225-30.
289. Zhang, S.C., et al., *In vitro differentiation of transplantable neural precursors from human embryonic stem cells.* Nat Biotechnol, 2001. **19**(12): p. 1129-33.
290. Gerrard, L., L. Rodgers, and W. Cui, *Differentiation of human embryonic stem cells to neural lineages in adherent culture by blocking bone morphogenetic protein signaling.* Stem Cells, 2005. **23**(9): p. 1234-41.
291. Conti, L. and E. Cattaneo, *Neural stem cell systems: physiological players or in vitro entities?* Nat Rev Neurosci, 2010. **11**(3): p. 176-87.
292. Rowitch, D.H., *Glial specification in the vertebrate neural tube.* Nat Rev Neurosci, 2004. **5**(5): p. 409-19.
293. Harris, W.A., *Specifying motor neurons: up and down and back to front.* Nat Neurosci, 2003. **6**(12): p. 1247-9.
294. Goulding, M., *Circuits controlling vertebrate locomotion: moving in a new direction.* Nat Rev Neurosci, 2009. **10**(7): p. 507-18.
295. Livesey, M.R., et al., *Maturation and electrophysiological properties of human pluripotent stem cell-derived oligodendrocytes.* Stem Cells, 2016. **34**(4): p. 1040-53.
296. Roybon, L., et al., *Human stem cell-derived spinal cord astrocytes with defined mature or reactive phenotypes.* Cell Rep, 2013. **4**(5): p. 1035-48.
297. Holmqvist, S., et al., *Generation of human pluripotent stem cell reporter lines for the isolation of and reporting on astrocytes generated from ventral midbrain and ventral spinal cord neural progenitors.* Stem Cell Res, 2015. **15**(1): p. 203-20.
298. Espuny-Camacho, I., et al., *Pyramidal neurons derived from human pluripotent stem cells integrate efficiently into mouse brain circuits in vivo.* Neuron, 2013. **77**(3): p. 440-56.
299. Chen, Y., et al., *Chemical Control of Grafted Human PSC-Derived Neurons in a Mouse Model of Parkinson's Disease.* Cell Stem Cell, 2016. **18**(6): p. 817-26.
300. Xi, J., et al., *Specification of midbrain dopamine neurons from primate pluripotent stem cells.* Stem Cells, 2012. **30**(8): p. 1655-63.
301. Ma, L., Y. Liu, and S.C. Zhang, *Directed differentiation of dopamine neurons from human pluripotent stem cells.* Methods Mol Biol, 2011. **767**: p. 411-8.
302. Theka, I., et al., *Rapid generation of functional dopaminergic neurons from human induced pluripotent stem cells through a single-step procedure using cell lineage transcription factors.* Stem Cells Transl Med, 2013. **2**(6): p. 473-9.
303. Hu, B.Y. and S.C. Zhang, *Differentiation of spinal motor neurons from pluripotent human stem cells.* Nat Protoc, 2009. **4**(9): p. 1295-304.
304. Sances, S., et al., *Modeling ALS with motor neurons derived from human induced pluripotent stem cells.* Nat Neurosci, 2016. **19**(4): p. 542-53.
305. Vierbuchen, T., et al., *Direct conversion of fibroblasts to functional neurons by defined factors.* Nature, 2010. **463**(7284): p. 1035-41.

306. Pang, Z.P., et al., *Induction of human neuronal cells by defined transcription factors.* Nature, 2011. **476**(7359): p. 220-3.
307. Colasante, G., et al., *Rapid Conversion of Fibroblasts into Functional Forebrain GABAergic Interneurons by Direct Genetic Reprogramming.* Cell Stem Cell, 2015. **17**(6): p. 719-34.
308. Yang, N., et al., *Generation of oligodendroglial cells by direct lineage conversion.* Nat Biotechnol, 2013. **31**(5): p. 434-9.
309. Caiazzo, M., et al., *Direct conversion of fibroblasts into functional astrocytes by defined transcription factors.* Stem Cell Reports, 2015. **4**(1): p. 25-36.
310. Nutt, S.E., et al., *Caudalized human iPSC-derived neural progenitor cells produce neurons and glia but fail to restore function in an early chronic spinal cord injury model.* Exp Neurol, 2013. **248**: p. 491-503.
311. Steward, O., K.G. Sharp, and K. Matsudaira Yee, *Long-distance migration and colonization of transplanted neural stem cells.* Cell, 2014. **156**(3): p. 385-7.
312. Tuszynski, M.H., et al., *Neural stem cell dissemination after grafting to CNS injury sites.* Cell, 2014. **156**(3): p. 388-9.
313. Kandel, E.R.S., J.; Jessell, T., Principles of Neural Science, Fourth Edition, 2000.
314. Herculano-Houzel, S., *The glia/neuron ratio: how it varies uniformly across brain structures and species and what that means for brain physiology and evolution.* Glia, 2014. **62**(9): p. 1377-91.
315. Bayraktar, O.A., et al., *Astrocyte development and heterogeneity.* Cold Spring Harb Perspect Biol, 2015. **7**(1): p. a020362.
316. Schitine, C., et al., *Astrocyte heterogeneity in the brain: from development to disease.* Front Cell Neurosci, 2015. **9**: p. 76.
317. Ogata, K. and T. Kosaka, *Structural and quantitative analysis of astrocytes in the mouse hippocampus.* Neuroscience, 2002. **113**(1): p. 221-33.
318. Bushong, E.A., et al., *Protoplasmic astrocytes in CA1 stratum radiatum occupy separate anatomical domains.* J Neurosci, 2002. **22**(1): p. 183-92.
319. Oberheim, N.A., et al., *Astrocytic complexity distinguishes the human brain.* Trends Neurosci, 2006. **29**(10): p. 547-53.
320. Simard, M., et al., *Signaling at the gliovascular interface.* J Neurosci, 2003. **23**(27): p. 9254-62.
321. Molofsky, A.V. and B. Deneen, *Astrocyte development: A Guide for the Perplexed.* Glia, 2015. **63**(8): p. 1320-9.
322. Behar, T., et al., *Growth and differentiation properties of O-2A progenitors purified from rat cerebral hemispheres.* J Neurosci Res, 1988. **21**(2-4): p. 168-80.
323. Kang, P., et al., *Sox9 and NFIA coordinate a transcriptional regulatory cascade during the initiation of gliogenesis.* Neuron, 2012. **74**(1): p. 79-94.
324. Deneen, B., et al., *The transcription factor NFIA controls the onset of gliogenesis in the developing spinal cord.* Neuron, 2006. **52**(6): p. 953-68.
325. Liu, Y., et al., *CD44 expression identifies astrocyte-restricted precursor cells.* Dev Biol, 2004. **276**(1): p. 31-46.
326. Cahoy, J.D., et al., *A transcriptome database for astrocytes, neurons, and oligodendrocytes: a new resource for understanding brain development and function.* J Neurosci, 2008. **28**(1): p. 264-78.
327. Hubbard, J.A., et al., *Expression of the Astrocyte Water Channel Aquaporin-4 in the Mouse Brain.* ASN Neuro, 2015. **7**(5).
328. Aoyama, M., et al., *Region-specific expression of a water channel protein, aquaporin 4, on brain astrocytes.* J Neurosci Res, 2012. **90**(12): p. 2272-80.
329. Vives, V., et al., *Visualization of S100B-positive neurons and glia in the central nervous system of EGFP transgenic mice.* J Comp Neurol, 2003. **457**(4): p. 404-19.

330. Dermietzel, R., et al., *Gap junctions between cultured astrocytes: immunocytochemical, molecular, and electrophysiological analysis.* J Neurosci, 1991. **11**(5): p. 1421-32.
331. Gegelashvili, G., N.C. Danbolt, and A. Schousboe, *Neuronal soluble factors differentially regulate the expression of the GLT1 and GLAST glutamate transporters in cultured astroglia.* J Neurochem, 1997. **69**(6): p. 2612-5.
332. Molofsky, A.V., et al., *Astrocytes and disease: a neurodevelopmental perspective.* Genes Dev, 2012. **26**(9): p. 891-907.
333. Li, Y., et al., *gamma-Aminobutyric A receptor (GABA(A)R) regulates aquaporin 4 expression in the subependymal zone: relevance to neural precursors and water exchange.* J Biol Chem, 2015. **290**(7): p. 4343-55.
334. Chiu, F.C., W.T. Norton, and K.L. Fields, *The cytoskeleton of primary astrocytes in culture contains actin, glial fibrillary acidic protein, and the fibroblast-type filament protein, vimentin.* J Neurochem, 1981. **37**(1): p. 147-55.
335. Fischer, G., A. Leutz, and M. Schachner, *Cultivation of immature astrocytes of mouse cerebellum in a serum-free, hormonally defined medium. Appearance of the mature astrocyte phenotype after addition of serum.* Neurosci Lett, 1982. **29**(3): p. 297-302.
336. Pixley, S.K. and J. de Vellis, *Transition between immature radial glia and mature astrocytes studied with a monoclonal antibody to vimentin.* Brain Res, 1984. **317**(2): p. 201-9.
337. Bliss, M.R., *Hyperaemia.* J Tissue Viability, 1998. **8**(4): p. 4-13.
338. Abbott, N.J., L. Ronnback, and E. Hansson, *Astrocyte-endothelial interactions at the blood-brain barrier.* Nat Rev Neurosci, 2006. **7**(1): p. 41-53.
339. Iadecola, C., *Neurovascular regulation in the normal brain and in Alzheimer's disease.* Nat Rev Neurosci, 2004. **5**(5): p. 347-60.
340. Neuwelt, E.A., et al., *Engaging neuroscience to advance translational research in brain barrier biology.* Nat Rev Neurosci, 2011. **12**(3): p. 169-82.
341. Koehler, R.C., R.J. Roman, and D.R. Harder, *Astrocytes and the regulation of cerebral blood flow.* Trends Neurosci, 2009. **32**(3): p. 160-9.
342. Iliff, J.J., et al., *Adenosine receptors mediate glutamate-evoked arteriolar dilation in the rat cerebral cortex.* Am J Physiol Heart Circ Physiol, 2003. **284**(5): p. H1631-7.
343. Pellerin, L. and P.J. Magistretti, *Food for thought: challenging the dogmas.* J Cereb Blood Flow Metab, 2003. **23**(11): p. 1282-6.
344. Pellerin, L., *Food for thought: the importance of glucose and other energy substrates for sustaining brain function under varying levels of activity.* Diabetes Metab, 2010. **36 Suppl 3**: p. S59-63.
345. Pellerin, L. and P.J. Magistretti, *Glutamate uptake into astrocytes stimulates aerobic glycolysis: a mechanism coupling neuronal activity to glucose utilization.* Proc Natl Acad Sci U S A, 1994. **91**(22): p. 10625-9.
346. Kirischuk, S., et al., *Astrocyte sodium signaling and the regulation of neurotransmission.* Glia, 2015.
347. Yi, J.H. and A.S. Hazell, *Excitotoxic mechanisms and the role of astrocytic glutamate transporters in traumatic brain injury.* Neurochem Int, 2006. **48**(5): p. 394-403.
348. Rothstein, J.D., et al., *Knockout of glutamate transporters reveals a major role for astroglial transport in excitotoxicity and clearance of glutamate.* Neuron, 1996. **16**(3): p. 675-86.
349. Lee, A. and D.V. Pow, *Astrocytes: Glutamate transport and alternate splicing of transporters.* Int J Biochem Cell Biol, 2010. **42**(12): p. 1901-6.
350. Meeker, K.D., J.S. Meabon, and D.G. Cook, *Partial Loss of the Glutamate Transporter GLT-1 Alters Brain Akt and Insulin Signaling in a Mouse Model of Alzheimer's Disease.* J Alzheimers Dis, 2015. **45**(2): p. 509-20.

351. Scott, H.A., et al., *Glutamate transporter variants reduce glutamate uptake in Alzheimer's disease.* Neurobiol Aging, 2011. **32**(3): p. 553 e1-11.
352. Woltjer, R.L., et al., *Aberrant detergent-insoluble excitatory amino acid transporter 2 accumulates in Alzheimer disease.* J Neuropathol Exp Neurol, 2010. **69**(7): p. 667-76.
353. Allen, N.J., *Astrocyte regulation of synaptic behavior.* Annu Rev Cell Dev Biol, 2014. **30**: p. 439-63.
354. De Pitta, M., et al., *A tale of two stories: astrocyte regulation of synaptic depression and facilitation.* PLoS Comput Biol, 2011. **7**(12): p. e1002293.
355. Agulhon, C., et al., *What is the role of astrocyte calcium in neurophysiology?* Neuron, 2008. **59**(6): p. 932-46.
356. Cornell-Bell, A.H., et al., *Glutamate induces calcium waves in cultured astrocytes: long-range glial signaling.* Science, 1990. **247**(4941): p. 470-3.
357. Panatier, A. and R. Robitaille, *Astrocytic mGluR5 and the tripartite synapse.* Neuroscience, 2016. **323**: p. 29-34.
358. Dzyubenko, E., C. Gottschling, and A. Faissner, *Neuron-Glia Interactions in Neural Plasticity: Contributions of Neural Extracellular Matrix and Perineuronal Nets.* Neural Plast, 2016. **2016**: p. 5214961.
359. Barros, C.S., S.J. Franco, and U. Muller, *Extracellular matrix: functions in the nervous system.* Cold Spring Harb Perspect Biol, 2011. **3**(1): p. a005108.
360. Frischknecht, R. and E.D. Gundelfinger, *The brain's extracellular matrix and its role in synaptic plasticity.* Adv Exp Med Biol, 2012. **970**: p. 153-71.
361. Morawski, M., et al., *ECM in brain aging and dementia.* Prog Brain Res, 2014. **214**: p. 207-27.
362. Pitkanen, A., et al., *Neural ECM and epilepsy.* Prog Brain Res, 2014. **214**: p. 229-62.
363. Lubbers, B.R., et al., *Neural ECM in addiction, schizophrenia, and mood disorder.* Prog Brain Res, 2014. **214**: p. 263-84.
364. Bonneh-Barkay, D. and C.A. Wiley, *Brain extracellular matrix in neurodegeneration.* Brain Pathol, 2009. **19**(4): p. 573-85.
365. Wang, D. and J. Fawcett, *The perineuronal net and the control of CNS plasticity.* Cell Tissue Res, 2012. **349**(1): p. 147-60.
366. Kwok, J.C., et al., *Extracellular matrix and perineuronal nets in CNS repair.* Dev Neurobiol, 2011. **71**(11): p. 1073-89.
367. Verkhratsky, A., et al., *Astrocytes as secretory cells of the central nervous system: idiosyncrasies of vesicular secretion.* EMBO J, 2016. **35**(3): p. 239-57.
368. Vardjan, N. and R. Zorec, *Excitable Astrocytes: Ca(2+)- and cAMP-Regulated Exocytosis.* Neurochem Res, 2015. **40**(12): p. 2414-24.
369. Gonzalez, A., et al., *Cellular and molecular mechanisms regulating neuronal growth by brain-derived neurotrophic factor (BDNF).* Cytoskeleton (Hoboken), 2016.
370. Juric, D.M., D. Loncar, and M. Carman-Krzan, *Noradrenergic stimulation of BDNF synthesis in astrocytes: mediation via alpha1- and beta1/beta2-adrenergic receptors.* Neurochem Int, 2008. **52**(1-2): p. 297-306.
371. Bergami, M., et al., *Uptake and recycling of pro-BDNF for transmitter-induced secretion by cortical astrocytes.* J Cell Biol, 2008. **183**(2): p. 213-21.
372. Deinhardt, K. and M.V. Chao, *Shaping neurons: Long and short range effects of mature and proBDNF signalling upon neuronal structure.* Neuropharmacology, 2014. **76 Pt C**: p. 603-9.
373. Lin, L.F., et al., *GDNF: a glial cell line-derived neurotrophic factor for midbrain dopaminergic neurons.* Science, 1993. **260**(5111): p. 1130-2.
374. Allen, S.J., et al., *GDNF, NGF and BDNF as therapeutic options for neurodegeneration.* Pharmacol Ther, 2013. **138**(2): p. 155-75.

375. d'Anglemont de Tassigny, X., A. Pascual, and J. Lopez-Barneo, *GDNF-based therapies, GDNF-producing interneurons, and trophic support of the dopaminergic nigrostriatal pathway. Implications for Parkinson's disease.* Front Neuroanat, 2015. **9**: p. 10.
376. Kramer, E.R. and B. Liss, *GDNF-Ret signaling in midbrain dopaminergic neurons and its implication for Parkinson disease.* FEBS Lett, 2015. **589**(24 Pt A): p. 3760-72.
377. Lapchak, P.A., *A preclinical development strategy designed to optimize the use of glial cell line-derived neurotrophic factor in the treatment of Parkinson's disease.* Mov Disord, 1998. **13 Suppl 1**: p. 49-54.
378. Patel, N.K. and S.S. Gill, *GDNF delivery for Parkinson's disease.* Acta Neurochir Suppl, 2007. **97**(Pt 2): p. 135-54.
379. Airaksinen, M.S. and M. Saarma, *The GDNF family: signalling, biological functions and therapeutic value.* Nat Rev Neurosci, 2002. **3**(5): p. 383-94.
380. Schwartz, J.P. and N. Nishiyama, *Neurotrophic factor gene expression in astrocytes during development and following injury.* Brain Res Bull, 1994. **35**(5-6): p. 403-7.
381. Levi-Montalcini, R., *Growth regulation of sympathetic nerve cells.* Arch Ital Biol, 1965. **103**(4): p. 832-46.
382. Levi-Montalcini, R., *The nerve growth factor: its mode of action on sensory and sympathetic nerve cells.* Harvey Lect, 1966. **60**: p. 217-59.
383. Aloe, L., et al., *Nerve growth factor: from the early discoveries to the potential clinical use.* J Transl Med, 2012. **10**: p. 239.
384. Sofroniew, M.V., *Molecular dissection of reactive astrogliosis and glial scar formation.* Trends Neurosci, 2009. **32**(12): p. 638-47.
385. Burda, J.E. and M.V. Sofroniew, *Reactive gliosis and the multicellular response to CNS damage and disease.* Neuron, 2014. **81**(2): p. 229-48.
386. Rajan, P. and R.D. McKay, *Multiple routes to astrocytic differentiation in the CNS.* J Neurosci, 1998. **18**(10): p. 3620-9.
387. Davies, J.E., et al., *Transplanted astrocytes derived from BMP- or CNTF-treated glial-restricted precursors have opposite effects on recovery and allodynia after spinal cord injury.* J Biol, 2008. **7**(7): p. 24.
388. Davies, S.J., et al., *Transplantation of specific human astrocytes promotes functional recovery after spinal cord injury.* PLoS One, 2011. **6**(3): p. e17328.
389. Haas, C., et al., *Phenotypic analysis of astrocytes derived from glial restricted precursors and their impact on axon regeneration.* Exp Neurol, 2012. **233**(2): p. 717-32.
390. Jin, Y., et al., *Transplantation of human glial restricted progenitors and derived astrocytes into a contusion model of spinal cord injury.* J Neurotrauma, 2011. **28**(4): p. 579-94.
391. Nicaise, C., et al., *Transplantation of stem cell-derived astrocytes for the treatment of amyotrophic lateral sclerosis and spinal cord injury.* World J Stem Cells, 2015. **7**(2): p. 380-98.
392. Li, K., et al., *Transplantation of glial progenitors that overexpress glutamate transporter GLT1 preserves diaphragm function following cervical SCI.* Mol Ther, 2015. **23**(3): p. 533-48.
393. Falnikar, A., et al., *GLT1 overexpression reverses established neuropathic pain-related behavior and attenuates chronic dorsal horn neuron activation following cervical spinal cord injury.* Glia, 2016. **64**(3): p. 396-406.
394. Johe, K.K., et al., *Single factors direct the differentiation of stem cells from the fetal and adult central nervous system.* Genes Dev, 1996. **10**(24): p. 3129-40.
395. Gross, R.E., et al., *Bone morphogenetic proteins promote astroglial lineage commitment by mammalian subventricular zone progenitor cells.* Neuron, 1996. **17**(4): p. 595-606.
396. Papavasiliou, A.K., et al., *Paracrine regulation of colony-stimulating factor-1 in medulloblastoma: implications for pathogenesis and therapeutic interventions.* Neurosurgery, 1997. **41**(4): p. 916-23.

397. Krencik, R. and S.C. Zhang, *Directed differentiation of functional astroglial subtypes from human pluripotent stem cells.* Nat Protoc, 2011. **6**(11): p. 1710-7.
398. Li, K., et al., *Human iPS cell-derived astrocyte transplants preserve respiratory function after spinal cord injury.* Exp Neurol, 2015. **271**: p. 479-92.
399. Serio, A., et al., *Astrocyte pathology and the absence of non-cell autonomy in an induced pluripotent stem cell model of TDP-43 proteinopathy.* Proc Natl Acad Sci U S A, 2013. **110**(12): p. 4697-702.
400. Shaltouki, A., et al., *Efficient generation of astrocytes from human pluripotent stem cells in defined conditions.* Stem Cells, 2013. **31**(5): p. 941-52.
401. Pires, M., et al., *Modeling the functional network of primary intercellular Ca2+ wave propagation in astrocytes and its application to study drug effects.* J Theor Biol, 2014. **356**: p. 201-12.
402. Frisen, J., et al., *Spinal axons in central nervous system scar tissue are closely related to laminin-immunoreactive astrocytes.* Neuroscience, 1995. **65**(1): p. 293-304.
403. Plantman, S., et al., *Neuronal myosin-X is upregulated after peripheral nerve injury and mediates laminin-induced growth of neurites.* Mol Cell Neurosci, 2013. **56**: p. 96-101.
404. Evans, M.J. and M.H. Kaufman, *Establishment in culture of pluripotential cells from mouse embryos.* Nature, 1981. **292**(5819): p. 154-6.
405. Martin, G.R., *Isolation of a pluripotent cell line from early mouse embryos cultured in medium conditioned by teratocarcinoma stem cells.* Proc Natl Acad Sci U S A, 1981. **78**(12): p. 7634-8.
406. Xiao, B., et al., *Induced pluripotent stem cells in Parkinson's disease: scientific and clinical challenges.* J Neurol Neurosurg Psychiatry, 2016. **87**(7): p. 697-702.
407. Pen, A.E. and U.B. Jensen, *Current status of treating neurodegenerative disease with induced pluripotent stem cells.* Acta Neurol Scand, 2016.
408. Thies, R.S. and C.E. Murry, *The advancement of human pluripotent stem cell-derived therapies into the clinic.* Development, 2015. **142**(18): p. 3077-84.
409. Sun, Y.E., K. Martinowich, and W. Ge, *Making and repairing the mammalian brain--signaling toward neurogenesis and gliogenesis.* Semin Cell Dev Biol, 2003. **14**(3): p. 161-8.
410. Morrow, T., M.R. Song, and A. Ghosh, *Sequential specification of neurons and glia by developmentally regulated extracellular factors.* Development, 2001. **128**(18): p. 3585-94.
411. Sakellaridis, N., D. Mangoura, and A. Vernadakis, *Effects of neuron-conditioned medium and fetal calf serum content on glial growth in dissociated cultures.* Brain Res, 1986. **392**(1-2): p. 31-41.
412. Pettmann, B., et al., *Stimulation of proliferation and maturation of rat astroblasts in serum-free culture by an astroglial growth factor.* J Neurosci Res, 1982. **8**(2-3): p. 463-76.
413. Tang, W., et al., *Stimulation-evoked Ca2+ signals in astrocytic processes at hippocampal CA3-CA1 synapses of adult mice are modulated by glutamate and ATP.* J Neurosci, 2015. **35**(7): p. 3016-21.
414. Hashioka, S., et al., *Purinergic responses of calcium-dependent signaling pathways in cultured adult human astrocytes.* BMC Neurosci, 2014. **15**: p. 18.
415. Verkhratsky, A., J.J. Rodriguez, and V. Parpura, *Calcium signalling in astroglia.* Mol Cell Endocrinol, 2012. **353**(1-2): p. 45-56.
416. Mori, S. and C.P. Leblond, *Electron microscopic features and proliferation of astrocytes in the corpus callosum of the rat.* J Comp Neurol, 1969. **137**(2): p. 197-225.
417. Hajos, F., et al., *Proliferation of astroglia in the embryonic mouse forebrain as revealed by simultaneous immunocytochemistry and autoradiography.* Acta Morphol Acad Sci Hung, 1981. **29**(4): p. 361-4.
418. Cavanagh, J.B., *The proliferation of astrocytes around a needle wound in the rat brain.* J Anat, 1970. **106**(Pt 3): p. 471-87.
419. Nagata, I., G. Keilhauer, and M. Schachner, *Neuronal influence on antigenic marker profile, cell shape and proliferation of cultured astrocytes obtained by microdissection of distinct layers from the early postnatal mouse cerebellum.* Brain Res, 1986. **389**(1-2): p. 217-32.

420. Roessmann, U. and P. Gambetti, *Pathological reaction of astrocytes in perinatal brain injury. Immunohistochemical study.* Acta Neuropathol, 1986. **70**(3-4): p. 302-7.
421. Komitova, M. and P.S. Eriksson, *Sox-2 is expressed by neural progenitors and astroglia in the adult rat brain.* Neurosci Lett, 2004. **369**(1): p. 24-7.
422. Ida, M., et al., *Identification and functions of chondroitin sulfate in the milieu of neural stem cells.* J Biol Chem, 2006. **281**(9): p. 5982-91.
423. Garwood, J., et al., *Phosphacan short isoform, a novel non-proteoglycan variant of phosphacan/receptor protein tyrosine phosphatase-beta, interacts with neuronal receptors and promotes neurite outgrowth.* J Biol Chem, 2003. **278**(26): p. 24164-73.
424. Buss, A., et al., *Growth-modulating molecules are associated with invading Schwann cells and not astrocytes in human traumatic spinal cord injury.* Brain, 2007. **130**(Pt 4): p. 940-53.
425. Takeda, A., et al., *Axonal regeneration through the fibrous scar in lesioned goldfish spinal cord.* Neuroscience, 2015. **284**: p. 134-52.
426. Tucker, B.A. and K.M. Mearow, *Peripheral sensory axon growth: from receptor binding to cellular signaling.* Can J Neurol Sci, 2008. **35**(5): p. 551-66.
427. McKeon, R.J., A. Hoke, and J. Silver, *Injury-induced proteoglycans inhibit the potential for laminin-mediated axon growth on astrocytic scars.* Exp Neurol, 1995. **136**(1): p. 32-43.
428. Harvey, A.R., et al., *Neurotrophic factors for spinal cord repair: Which, where, how and when to apply, and for what period of time?* Brain Res, 2015. **1619**: p. 36-71.
429. Allen, A.R., *Surgery of experimental lesion of spinal cord equivalent to crush injury of fracture dislocation of spinal column a preliminary report.* Journal of the American Medical Association, 1911(57): p. 878-880.
430. Cheriyan, T., et al., *Spinal cord injury models: a review.* Spinal Cord, 2014. **52**(8): p. 588-95.
431. Dunham, K.A., et al., *Characterization of a graded cervical hemicontusion spinal cord injury model in adult male rats.* J Neurotrauma, 2010. **27**(11): p. 2091-106.
432. Doulames, V.M. and G.W. Plant, *Induced Pluripotent Stem Cell Therapies for Cervical Spinal Cord Injury.* Int J Mol Sci, 2016. **17**(4): p. 530.
433. Gustafsson, D., et al., *A new oral anticoagulant: the 50-year challenge.* Nat Rev Drug Discov, 2004. **3**(8): p. 649-59.
434. Carragher, N.O., *Calpain inhibition: a therapeutic strategy targeting multiple disease states.* Curr Pharm Des, 2006. **12**(5): p. 615-38.
435. Cagmat, E.B., et al., *Potential Use of Calpain Inhibitors as Brain Injury Therapy*, in *Brain Neurotrauma: Molecular, Neuropsychological, and Rehabilitation Aspects*, F.H. Kobeissy, Editor. 2015: Boca Raton (FL).
436. Stabenfeldt, S.E., et al., *Biomimetic microenvironment modulates neural stem cell survival, migration, and differentiation.* Tissue Eng Part A, 2010. **16**(12): p. 3747-58.
437. Harris, G.M., et al., *Nerve Guidance by a Decellularized Fibroblast Extracellular Matrix.* Matrix Biol, 2016.
438. Vecino, E., et al., *Influence of extracellular matrix components on the expression of integrins and regeneration of adult retinal ganglion cells.* PLoS One, 2015. **10**(5): p. e0125250.
439. Kobayashi, Y., et al., *Pre-evaluated safe human iPSC-derived neural stem cells promote functional recovery after spinal cord injury in common marmoset without tumorigenicity.* PLoS One, 2012. **7**(12): p. e52787.
440. Seifinejad, A., et al., *Progress and promise towards safe induced pluripotent stem cells for therapy.* Stem Cell Rev, 2010. **6**(2): p. 297-306.